RESERVOIR DELINEATION AND CUMULATIVE IMPACTS

ASSESSMENT IN LARGE RIVER BASINS: A CASE STUDY FOR THE

YANGTZE RIVER BASIN

YANG XIANKUN

NATIONAL UNIVERSITY OF SINGAPORE

2014

RESERVOIR DELINEATION AND CUMULATIVE IMPACTS

ASSESSMENT IN LARGE RIVER BASINS: A CASE STUDY FOR THE

YANGTZE RIVER BASIN

YANG XIANKUN
(M.Sc. Wuhan University)

A THESIS SUBMITTED

FOR THE DEGREE OF DOCTOR OF PHYLOSOPHY
DEPARTMENT OF GEOGRAPHY
NATIONAL UNIVERSITY OF SINGAPORE

2014

Declaration

I hereby declare that this thesis is my original work and it has been written by me in its entirety. I have duly acknowledged all the sources of information which have been used in the thesis.

This thesis has also not been submitted for any degree in any university previously.

_____   _____

Yang Xiankun

7 August, 2014

Acknowledgements

Table of contents

Summary

There are no places left on Earth that are untouched by the consequences of anthropogenic activities; the Yangtze River is no exception. Over the past decades, The Yangtze River has been being dammed at a dazzling pace. Previous studies have reported the impacts of individual dams from different perspectives; but the cumulative impacts of multiple dams/reservoirs have not been well investigated due to lack of needed information on nearly 44,000 dams/reservoirs. Focusing on the fast-damming Yangtze River, this thesis developed a parsimonious approach based on remote sensing techniques to delineate reservoirs in the entire Yangtze River basin. Using the data, this study proposed new models to assess the cumulative impacts of dams/reservoirs on water regulation, sediment retention, river connectivity and river landscape fragmentation.

This study delineated nearly 43,600 reservoirs with a total water storage capacity of approximately 288 km^3 which is equivalent of approximately 30% of the annual runoff of the Yangtze River. Compared to the existing natural lakes with a combined storage volume of only 46 km^3, the artificial reservoirs have undoubtedly become the dominant water bodies in the Yangtze River basin. However, there is considerable geographic variation in the potential surface water impacts of the reservoirs.

The results indicate that annual sediment accumulated in the 43,600 reservoirs is approximately 691 ($\pm$ 94) million tons (Mt), 669 ($\pm$ 89) Mt of which is trapped by 1,358 large and medium-sized reservoirs and 22 ($\pm$ 5) Mt is trapped by smaller reservoirs. The estimated mean annual rate of storage loss is approximately 5.3 x 10^8 m^3 yr^{-1}; but against the world trend, the Yangtze River is now losing reservoir capacity at a rate much lower than new capacity being constructed.

Based on three proposed metrics, the assessments revealed that the Gezhouba Dam and the Three Gorges Dam have the highest impact on river connectivity. The values for weighted dendritic connectivity index (WDCI) and weighted habitat connectivity index for upstream passage (WHCIU) for the whole Yangtze River have decreased from 100 to 34.12 and 33.96, respectively, indicating that the Yangtze has experienced strong alterations over the past decades. The measurement of the weighted river landscape fragmentation index (WRLFI) indicated that the Wu, Min and Jialing tributaries only maintain connectivity among one to three river landscapes. Situation in the middle and lower basin is the highest. Even so, only a small part of the streams still maintains connectivity in 7 out of 12 river landscapes.

This study revealed that previously overlooked small dams can also exert significant impacts in flow regulation and river landscape fragmentation on regional river systems through their sheer number and density. The results indicated that the impacts of small

dams are comparable to large dams for the fourth- and fifth-order streams, or even significantly exceed large dams for the first-, second- and third-streams. Although the impacts of small dams are weaker than large dams for large streams, they do worsen the impacts caused by large dams. Therefore, regional water resources management schemes should be "optimized" by prioritizing the siting of new small dams based on which locations would have the lowest estimated cumulative impacts downstream.

The knowledge obtained in this study is essential to identify environmental risks associated with further impacts on river systems. Also, using this knowledge, it is possible to quantify the potential impacts of incremental dam development on river systems at basin and sub-basin levels in terms of environmental intactness. This knowledge will also make it easier to develop the Yangtze River basin with a relatively lower environmental footprint. Ultimately, this would lead us to a situation where local energy demands are met, and relevant ecosystem processes can be conserved basin-wide.

List of Tables

List of Figures

List of Acronyms and Symbols

A	Catchment area in km^2
a	Specific constant
$Area_G$	Area delineated on Google Earth
$Area_S$	Area delineate on Landsat TM/ETM+ images
AWDD	Area-weighted dam density
b	Specific constant
C	Reservoir storage capacity in km^3
c_i	Cumulative passability for dam i
CWRC	the Changjiang (Yangtze) Water Resources Commission
d	Depth of water stored behind a dam (m)
D	Particle size ranging from 0.046 to 1.0
DAI	Deviation area index
DD	Degree of dissection of terrain
DEM	Digital Elevation Model
DIC	Dendritic connectivity index
DL	Drainage length (km)
DOR_s	Degree of regulation for river section
e	The total number of distinct river landscape classes
ETM+	Landsat Enhanced Thematic Mapper Plus
GIS	Geographic Information Systems
H_{mean}	Mean elevation (m)
H_{min}	Minimum elevation (m)
H_{max}	Maximum elevation (m)
HI	Hypsometric integral
ICOLD	The International Commission on Large Dams
km	Kilometer

l	Stream length (km)
Ln	Natural log
LOG	Logarithm of 10
Mt	Million tons
m	Meter
MWR	Ministry of Water Resources of China
N; *n*	Number
NDVI	Normalized Difference Vegetation Index
NDWI	Normalized Difference Water Index
NDSI	Normalized Difference Snow Index
P	Precipitation (mm)
p_i	Passability of dams in section *i*
Q	Water discharge or runoff ($m^3 \, yr^{-1}$)
R	Basin relief (m)
RO	Mean annual runoff (mm)
RG	Index of basin ruggedness
RR	Ratio of the basin relief and the basin length
R_r	Reservoir rank
R^2	R square
S	Sediment load ($t \, yr^{-1}$)
S_{mean}	Mean slope (degree)
SR	Specific runoff ($km^3 \, km^{-2} \, yr^{-1}$)
SRTM	Shuttle Radar Topographic Mission
SS	Rate of change of elevation with respect to distance proxy to surface runoff velocity
SSY	Specific sediment yield ($t \, km^{-2} \, yr^{-1}$)
SY	Sediment yield ($t \, km^{-2} \, yr^{-1}$)
t	Ton
TE	Trap efficiency

TM	Landsat Thematic Mapper
TGD	the Three Gorges Dam
TGR	the Three Gorges Reservoir
w	Weight
wp$_i$	Weighted percentage of river length for section *i*
WDCI	Weighted dendritic connectivity index
WHCIU	Weighted habitat connectivity index for upstream passage
WRLFI	Weighted river landscape fragmentation index
Yr	Year
%	Percent
$\sum$	Summation

1 Introduction

1.1 General background

The desire and ability to impound water by different civilizations dates back many millennia. Some of the early societies in Mesopotamia, Pakistan and China were termed 'Hydraulic civilizations' and were probably formed specifically to organize the large labor necessary to construct canals and flood embankments. By 1950, Asia had 1,541 large dams, accounting for 30% of the global total; by 1982 that figure had grown to 22,701 (65% of the global total). Most—18,595, or 82%—were in China (Dudgeon, 2000). Absolute numbers of dams have changed over the last several decades, of course, but Asia's proportionate share of the global total of dams remains high. According to the estimates of the International Commission on Large Dams (ICOLD), there are more than 45,000 large dams worldwide – defined as those higher than 15 m – used for water supply, power generation, flood control, navigation and downstream releases. (White, 2000; ICOLD, 2011; Lehner *et al.*, 2011). Their associated impoundments are estimated to have a cumulative storage capacity in the range of 7,000 to 8,300 km^3 (Vörösmarty *et al.*, 2003; Chao *et al.*, 2008). This compares to nearly 10% of the water stored in all natural freshwater lakes in the world, and represents about one-sixth of the total annual river flow into the oceans (Downing *et al.*, 2006; Lehner *et al.*, 2011).

A reservoir operated for water conservation traps irregular flows to make subsequent

deliveries to users at scheduled rates; but operation for hydropower dams seeks to balance two conflicting objectives: to maximize energy yield per unit of water, the pool should be maintained at the highest possible level, yet the pool elevation should be low enough to capture all inflowing flood runoff for energy generation (Morris and Fan, 1998). However, large dams usually generate hydroelectricity and the impacts of dams vary greatly depending on whether a rock or alluvial channel is present. The resultant operation indicates a compromise between high-head and storage requirements. Now, about 20% of cultivated land worldwide is irrigated, about 300 million hectares, which produces about 33% of the worldwide food supply; about 20% of the worldwide generation of electricity is attributable to hydroelectric schemes, which equates to about 7% of worldwide energy usage (White, 2001). Many dams have been built with flood control and storage as the main motivator, e.g., the Hoover dam, the Tennessee Valley dams and some of the more recent dams in China. The benefits attributable to dams and reservoirs, most of which have been built since 1950, are considerable and stored water in reservoirs has improved the quality of life worldwide. Dams and reservoirs play an important role in the control and management of water resources.

On the other hand, dams and reservoirs have adversely affected fluvial processes at global and catchment scales, inducing direct or indirect impacts to biological, chemical and physical properties of rivers and riparian environments, although the impacts of dams and reservoirs vary greatly depending on whether a rock or alluvial

channel is present. Dams hold back sediments that would naturally replenish downstream river systems, leading the flow to become sediment-starved and prone to erode the channel bed and banks, producing channel incision (downcutting), coarsening of bed material, and leading to the loss of spawning gravels for fish species (Kondolf, 1997). Half of all discharge entering large reservoirs shows a local sediment trapping efficiency of 80% or more. Several large basins such as the Colorado and Nile show nearly complete trapping due to large reservoir construction and flow diversion (Vörösmarty *et al.*, 2003). Reservoir construction currently represents the most important influence on land-ocean processes. Due to sediment retention, it has exerted severe influence on land-ocean processes thereby triggering various harmful effects, such as, loss of floodplains and adjacent wetlands (Rosenberg *et al.*, 2000), and deterioration and loss of river deltas and ocean estuaries (Milliman, 1997; Syvitski *et al.*, 2009) in the Nile (Stanley and Warne, 1993), Colorado (Topping *et al.*, 2000), Mississippi (Blum and Roberts, 2009), and Yellow (Wang *et al.*, 2007b) river basins.

Another significant and obvious impact is the transformation upstream of the dam from a free-flowing river ecosystem to an artificial slack-water reservoir habitat. Changes in temperature, chemical composition, dissolved-oxygen levels and the physical properties of a reservoir are often not suitable to the aquatic plants and animals that evolved with a given river system. Dynesius and Nilsson (1994; 2005) concluded that 77% of the total water discharge of the 139 largest river systems in

North America and north Mexico, Europe and the republics of the former Soviet Union is strongly or moderately affected by fragmentation of river channels by large dams. Similar results on Mississippi, Colorado and Mekong rivers were also reported in a recent study (Grill *et al.*, 2014).

Although the oft-heard colloquial wisdom that "the dam building era is over in developed countries" was born since 1980 (Graf, 1999), dam construction in Asia still keeps a strong momentum, especially after the 1990s. Most of the large Asian rivers (such as the Mekong, Indus, Ganges, Yangtze and Yellow rivers) are being dammed at a dazzling pace. Like other countries in different parts of the world, such as, Australia (Callow and Smettem, 2009), Romania (Radoane and Radoane, 2005), Spain (Verstraeten and Poesen, 2000; de Vente *et al.*, 2005), and the United States (Minear and Kondolf, 2009), the formation of an increasingly dense multiple dam system in large Asian river basins has also been observed (Milliman, 1997; Xu and Milliman, 2009; Yang *et al.*, 2011).

Under such a context, it is widespread agreement in the ongoing sustainable reservoir management debate about the importance of better assessing the impacts of dams and reservoirs and of minimizing associated environmental costs while leveraging the benefits in multi-dam river systems. Meanwhile, there have been many new challenges to face, such as, soaring dam development, increased complex interactions between dams and complex fluvial responses, which are coupled with increased

public awareness of associated environmental issues. For example, agencies in the United States have adopted procedures and methods for predicting and assessing the environmental impacts of dams. They define three types of effects: direct, indirect, and cumulative. While federal agencies routinely consider the direct and indirect impacts of dams, almost all agencies say they have difficulty addressing the cumulative effects (Clark, 1994). In order to address these challenges, scientists have been developing novel methods to assess the increasingly complex interactions between dam development and the current and future impacts. As these impacts manifest in a cumulative manner over broad temporal and spatial scales, methods which address these impacts must be developed.

In recent academic literature, cumulative impacts have been defined as "the incremental impacts of a single action assessed in the context of past, present and future actions, regardless of who undertakes the action" (Ma *et al.*, 2009). For the purposes of this thesis, cumulative impacts are several effects associated with multiple dams or reservoirs, which exist over space and persist over time. An impact is defined as "a change" response to multi-dam or multi-reservoir operations and relative to a chosen benchmark determined by comparing temporally or spatially differing points of reference. Cumulative impact assessments are the process of systematically evaluating effects (changes) resulting from incremental, accumulating and interacting multi-dam or multi-reservoir operations.

It is important to assess the cumulative impacts at a basin-wide scale. Historically methods have been criticized for being conducted at too small a spatial scale (Ziemer, 1994). Within each river basin is a branching network of channels. The main, or trunk, channel is fed by numerous small tributaries which join to form progressively larger channels. The development and evolution of drainage networks is influenced by a number of factors, including geology, relief, climate and long-term drainage basin history (Charlton, 2007). Dams are often constructed in the upper stream reaches which have rich water power resources; but dams can also present serious problems downstream, creating sediment-starved flows and disrupting the connectivity of river systems (Graf, 2006). The impacts can even extend to deltas, leading to deterioration and loss of river deltas and ocean estuaries (Stanley and Warne, 1993; Milliman, 1997; Blum and Roberts, 2009; Syvitski *et al.*, 2009) . Therefore, including an assessment of the entire basin (headwaters to mouth) is an important aspect of cumulative impact assessment. In addition, limited spatial magnitudes generally narrow impact analysis to considerations of single dam and simple cause-effect relationships which can be attributed a specific environmental attribute at an individual site. To minimize bias, the spatial scale of the assessment should be defined by the spatial scale of the fluvial processes. This means that many of the impacts that occur can also be attributed natural variations that occur within the whole river system and they should be assessed at a basin-wide scale. For example, sediment retention by dams can cause delta shoreline recession due to insufficient sediment supply; but insufficient

precipitation as a result of climate change and land cover change as a result of human activities can also lead to similar results in the delta area. Incorporating these natural changes will help to differentiate between those impacts that are man-made and those which are not. On the basis then, an assessment for dams should include impacts accumulating along the river continuum. Impacts should also be considered over multiple scales such as reach, catchment, sub-basin and regional landscape (Sindorf and Wickel, 2011; Grill *et al.*, 2014). Obviously, this level of assessment is beyond the capacity of individual dam project proponents to conduct under the existing assessment processes.

As stated above, assessing the cumulative impacts of dams at a basin-wide scale is important, but existing methods are unable to conduct such assessment due to various limitations.

The first limitation is lack of needed dam data. Although many researchers and organizations (ILEC, 1988-1993; Birkett and Mason, 1995; Vörösmarty *et al.*, 1997; MSSL and UNEP, 1998; Lehner and Doll, 2004; ICOLD, 2011; Lehner *et al.*, 2011) have created their own georeferenced, global and regional datasets of dams and reservoirs in previous attempts, these attempts are primarily based on national archives. These datasets usually have incomplete reservoir information for developing countries, especially the countries in Africa, South America and Asia because national inventories of dams are usually unavailable in these countries. In addition, no small or

medium reservoirs are included in current global datasets, making it impossible to assess the cumulative impacts caused by these dams. Therefore, developing a parsimonious approach to rapidly delineate reservoirs in developing countries is a prerequisite for cumulative impact assessment. As an alternative data source, recent developments in remote sensing techniques promise global land cover images in increasing quality and resolution (Gupta *et al.*, 2002; Lehner and Doll, 2004; Gupta and Liew, 2007). Remote sensing techniques could be used as a parsimonious approach to rapidly delineate reservoirs in developing countries where national inventories are unavailable and field survey is laborious and expensive, but few studies have been conducted to obtain reservoirs in all size classes, although delineation of large reservoirs has been done by many researchers.

Secondly, although many previous studies focused on the impacts of dams and reservoirs, these studies have predominantly been focused on the effects of general scour of the main channel below the dams, sediment retention behind individual dams, and changes in water and sediment discharge (Erskine, 1985; Dade *et al.*, 2011; Draut *et al.*, 2011); yet literature is rare concerning the cumulative impacts of reservoirs in a multi-reservoir system. Modeling the impacts in such a multi-reservoir system is still a challenge at present. There are two research challenges in terms of the impact of dams on sediment retention. First, the estimation of surface erosion and sediment yield from a large catchment has large uncertainty due to the spatial variation of rainfall and to great heterogeneity in relief, slope and soil (Williams, 1975). How to calculate more accurate

sediment yield by integrating these factors (such as relief, slope, soil and rainfall) directly determines the success of the following assessment. Second, in a multi-reservoir system, trapping efficiency is insufficient to explain the true sediment retention of a dam, because sediment trapping by upstream reservoirs is also important. By considering the effect of trapping by upstream reservoirs in a multi-reservoir system, the rate of sediment retention in each individual reservoir could be significantly different.

Thirdly, in order to quantify the cumulative impacts on river connectivity and river landscape fragmentation caused by dam construction, various models have been proposed over the past decades in global or catchment scale studies; but most of the models are debatable. For example, serving as a first-level approximation of the potential impact on flow regulation, Dynesius and Nilsson (1994; 2005) used the flow regulation ratio or degree of regulation to investigate fragmentation and flow regulation of the world's large river systems; but these studies are just a very coarse assessment for flow regulation because no reservoir locations were considered. Alternatively, graph-theoretic models started to emerge (Cote *et al.*, 2009; Sindorf and Wickel, 2011; McKay *et al.*, 2013). However, river sizes and stream length between dams are also not considered in these models. To avoid this problem, Grill *et al.* (2014) proposed the river connectivity index (RCI) by simply replacing the 'river length' measure with 'river volume', but the model is somewhat impractical because river volume for each river section is often unknown.

A fourth problem is that the cumulative impacts of numerous small dams are unclear but have been understudied due to lack of needed data for large-scale river basins (Jager and McManamay, 2014). As introduced above, the impacts of large dams have been examined, but few studies have investigated impacts of more ubiquitous small dams. In contrast to large dams, most small dams are constructed on small streams with small catchments. Small hydropower projects are often considered to have fewer environmental impacts than large, main-stem projects (Kibler and Tullos, 2013) because these more moderate changes to streams associated with small dams produce relatively subtle and spatially-limited changes along stream continua (Gangloff *et al.*, 2011). Despite the subtle impacts by individual small dams, the cumulative impacts could be extended unlimitedly with the sharp increase in dam number. However, the cumulative impacts of small dams have not been well investigated.

As stated above, further work is required to provide precise quantitative cumulative impact assessments of dams on fluvial processes at a basin-wide scale. This study, using the Yangtze River basin as a case study, attempts to quantify the cumulative impacts caused by multiple reservoirs on water regulation, sediment retention, river connectivity and river landscape fragmentation at basin and sub-basin scales. It hopes to inform the public about how a river basin-wide assessment provides the ability to evaluate dam development in a multi-dam system in terms of water and sediment transport and environmental intactness, by providing a series of modeling methods on the general siting of dams.

1.2 Justification for the study area

The Yangtze River is one of the typical large rivers in river length, having almost all the important characteristics of fluvial landforms. It flows from the glaciers on the Qinghai-Tibet Plateau, running eastward through a mountainous upper reach, flat middle reach with numerous lakes, and reaching the East China Sea at Shanghai. Its distinctive climatic features, typical hydrological features and comprehensive fluvial landforms make the Yangtze River stand out as an ideal study area.

In addition, the Yangtze has been continuously measured by an extensive hydrological monitoring program cross the entire Yangtze River basin, which was established in the 1950s by the Changjiang (Yangtze) Water Resources Commission (CWRC). The program includes 384 hydrological gauge stations and 163 meteorological stations scattered across the entire basin. The monitoring program includes discharge and suspended load in accordance with national data standards. The original records for each station provide information on station coordinates (latitude and longitude), catchment area, mean monthly and annual water discharge, and the magnitude and date of occurrence of the maximum and minimum daily discharges (Yan *et al.*, 2011). Besides, supplementary data on geological background, spatial heterogeneity of soil erosion intensity and land-change data (e.g. soil conservation programs and reservoir sediment investigation reports in the upper Yangtze reach), are also publicly available for use. These data made it possible to conduct this study on the assessment of

cumulative impacts of dam construction.

The Yangtze River is rich in hydropower resources. The total potential power is estimated to be more than 200 million kilowatts (kW), representing about 40% of the total energy potential of all the rivers of China. China has planned 13 hydropower bases, six of which are in the Yangtze River basin (Huang and Yan, 2009). The Yangtze River and its tributaries are being dammed at a dazzling pace, today reaching 44,000 dams because of a large demand for water caused by a population boom and rapid economic development (Yang and Lu, 2013a). Together with planned developments in the Amazon (Fearnside, 2006) and the Mekong (Lu and Siew, 2006; Kummu *et al.*, 2010), the Yangtze region can be considered to be one of the hotbeds of dam development in the world.

The Yangtze River basin is therefore a potentially incomparable experimental basin for investigating the cumulative impacts by dams. Using the long-term continuous hydrological data covering the entire river basin started before large-scale dam development, the cumulative impacts can be fully investigated at basin and sub-basin scales. In particular, given the development of contiguous cascade dams on the major tributaries, it is an excellent opportunity to integrate a large amount of existing information in a cumulative impact context.

1.3 Objectives and significance

The Yangtze River is a large river experiencing fast reservoir development and associated environmental issues (Stone, 2011). Consequently, it is required to gain better knowledge involving more accurate and highly resolved monitoring of the cumulative impacts of reservoir development over time to meet the challenges caused by reservoir development. As stated in the above section, the Yangtze River basin is an excellent model to carry out assessments of cumulative impacts by dam development because of its typical river-landscape characteristics, fast dam development and public availability of long-term hydrological data. This study offers a unique opportunity to develop these methods to quantify these cumulative impacts in the multi-dam Yangtze River system. Through the cumulative impact assessments this study can be proactive in reservoir management decisions rather than reactive. This will make it easier to develop the Yangtze River basin with a relatively lower environmental footprint. Ultimately, this would lead us to a situation where local energy demands are met, and relevant ecosystem processes could be conserved in the Yangtze River basin.

Four specific objectives of this research were to:

I.   develop a parsimonious method to delineate reservoirs across the entire Yangtze River basin to explore their spatial distribution pattern and cumulative impacts on water regulation;

II. develop a framework to estimate reservoir sedimentation in a multi-dam system to investigate the cumulative impacts on sediment retention by integrating the effects of upstream dams;

III. design novel indices based on Geographic Information System (GIS) to quantify cumulative impacts of large dams on river connectivity and river landscape fragmentation at the basin and sub-basin scales;

IV. quantify the cumulative impacts of numerous small dams on flow regulation and river landscape fragmentation.

Based on the objectives established, this research is based on three assumptions:

a) Water discharge and sediment load within a catchment can be predicted from the interactions between land cover properties, anthropogenic activities (such as, reservoir construction and water diversion) and climate;

b) Reservoir operation usually follows this procedure: reservoirs start to impound water after the wet season in September; stored water is then gradually released to improve conditions for navigation, irrigation and water quality.

c) Environmental factors, such as climate (precipitation, temperature), topography (slope, altitude) and geology (karst geology), can create different river landscapes; the river landscapes can also be classified based on these factors.

1.4 Research questions and framework of the methodology

In order to achieve the research objectives stated above, several questions to be addressed have been proposed:

I.   How reservoirs and their associated dams are spatially distributed in the Yangtze River basin? What is the impact on flow regulation?

II.   Reservoirs are a crucial component in sediment retention, how much sediment is annually trapped in reservoirs? And what is the impact on land-ocean sediment transfer? What contributions have been made by large, medium and small reservoirs, respectively?

III. To what degree has the Yangtze River has been disconnected due to dam development? How does river landscape fragmentation vary in different tributary basins? And what are the implications of the assessment for future dam development?

IV.   There are more numerous small dams built in the Yangtze River basin, what are the cumulative impacts of small dams on flow regulation and river landscape fragmentation? How to quantify the impacts and compare against the impacts caused by large dams?

1.5 Arrangement and structure of the dissertation

To address the questions and to achieve the objectives highlighted in the previous section, the research framework was designed as shown in Figure 1.1. Data used in this study were diverse, including climatological data, geomorphological maps, geological thematic maps, hydrological records, digital elevation model (DEM) data, reports about human activities in the past decades and remotely sensed data (Landsat TM/ETM+ imagery). The climatological data, geomorphological maps, geological thematic maps, hydrological records were also used as parameters to assess the cumulative impacts of dams, such as, providing water discharge and sediment yield at dams. DEM data were used to derive river network, reservoir catchments, and catchment properties, such as, mean slope, mean elevation.

The remotely sensed images were firstly used to delineate reservoirs in Chapter 3. Data for reservoir geographical distribution was the basic information for further analysis; thus, the first is image processing, based on which the impact on water regulation was examined. The historical hydrological and climatological data, DEM data, geological maps were then used to establish a relationship between sediment yield at each dam and these variables in Chapter 4. These variables were further used to classify river landscapes in different classes; the classification map was used as an input for the impact assessment of river landscape fragmentation.
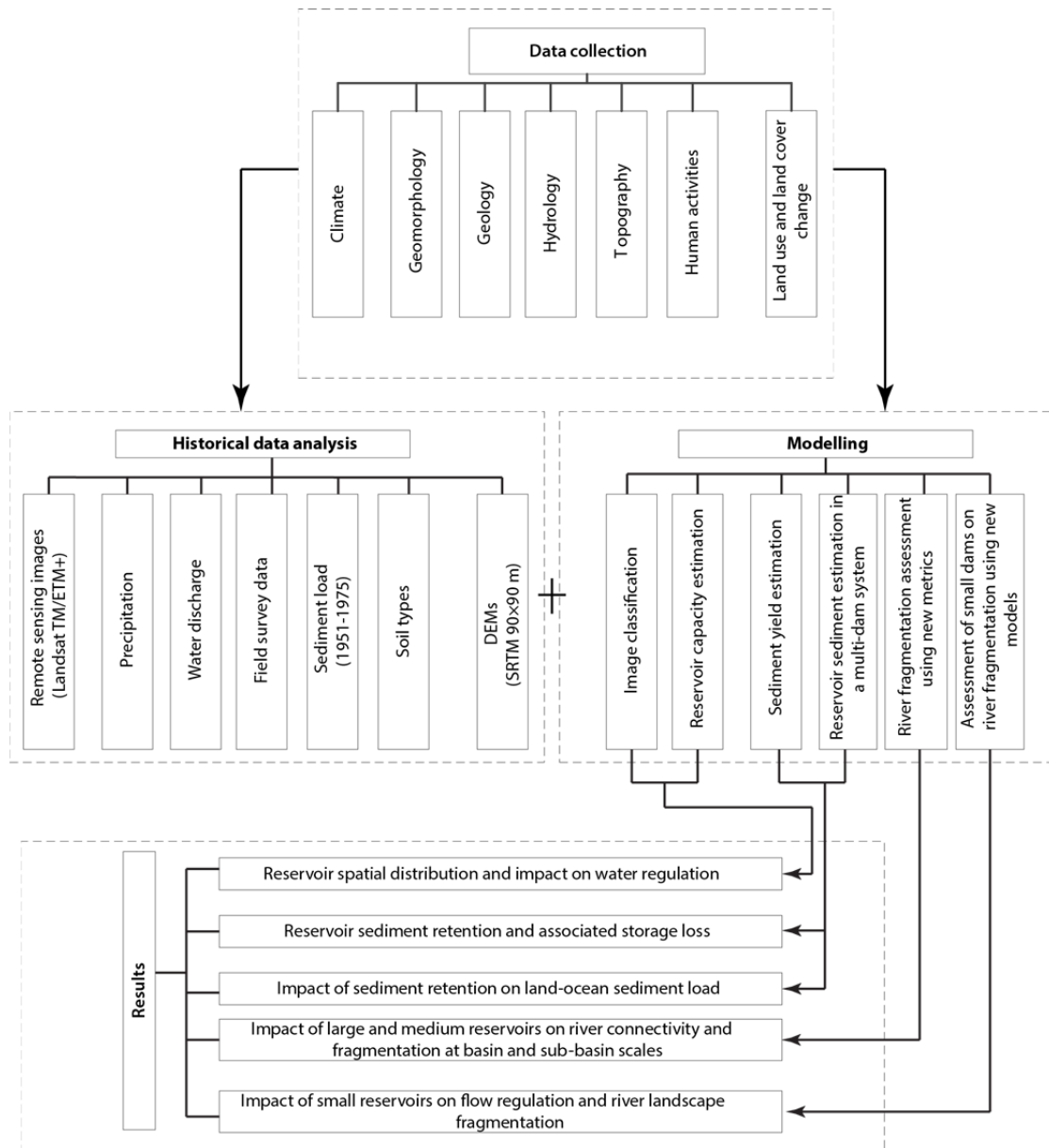
Figure 1.1 Framework of the overall research methodology.

Based on the overall framework, the structure of this thesis and the main content that each chapter covered are briefly described below. To ensure the content flows smoothly, literature reviews for each specific research topic are first provided in Chapter 3, but short separate introductions are provided at the beginning of each chapter before presenting the results. However, some of the chapters have been organized in a

manuscript format when already published in scientific journals. Therefore, there is some repetition of introduction, materials and methods and figures throughout.

Chapter 2 provides brief literature reviews for each specific research topic. Contributions by previous studies are introduced; related research progress, research gaps and challenges are also identified.

Chapter 3 provides overall description about the background information of the Yangtze River, such as, geographic setting, geological context, climate change and human activities in the past six decades.

Chapter 4 provides reservoir delineation and examines the spatial distribution of reservoirs on water regulation at basin and sub-basin scales. Other human activities (such as land reclamation) are also discussed in this chapter.

Chapter 5 presents a new framework to assess the cumulative impacts of dams on sediment retention in the multi-reservoir Yangtze system with respect to upstream sediment trap; the impact of sediment trapping on land-ocean sediment load is also discussed in the chapter.

Chapter 6 illustrates new metrics to quantify the cumulative impacts of large dams on river connectivity and river landscape fragmentation at basin and sub-basin scales. The implications of the metrics are also stated in this chapter.

Chapter 7 shows two new models to assess the cumulative impacts of numerous small dams on flow regulation and river landscape fragmentation; the implications of the models are also shown in this chapter. Some comparisons with large dams are also discussed in this chapter.

Chapter 8 displays some possible projections of the future trends of the Yangtze River in terms of future dam construction, water diversion from Yangtze to North China. Possible impacts on water regulation, sediment retention, river connection and river landscape fragmentation and others are discussed in this chapter.

A summary of the major findings, an evaluation of methods, and suggestions for future work appear in the final chapter.

2 Brief literature review

2.1 Cumulative impacts assessment at a basin-wide scale

The field of geoscience has undergone increased fast expansion and scrutiny in recent years. There have been many new challenges to face, such as climate change and increased human activities (e.g., dam construction, water diversion, irrigation, land reclamation and urban development), which are coupled with increased public awareness of environmental issues. In order to address these challenges, researchers have been developing novel methods which attempt to evaluate the increasingly complex interactions between our environment and the current and future demands of human beings. As these demands manifest in a cumulative manner over broad spatial scales, approaches which address these types of impacts must be developed.

In terms of dam construction, environmental impact assessments (EIAs) have become a fundamental component of the planning process for large dams to characterize and minimize environmental effects associated with proposed dam projects (Tullos, 2009). In the United States, the EIA process was created in 1969 with the passage of the National Environmental Policy Act, which mandated assessment of the environmental outcomes of large dam projects. The EIA process was quickly adopted by governments and legislatures around world, including Japan (1972), Hong Kong (1972), Canada (1973), Australia (1974) and China (1979) (Gilpin, 1995). Under this context, cumulative impact assessments, as an important part of EIA, are required

when a new dam project is proposed. However, there are a number of issues concerning the consideration of cumulative impacts. First, there is no definition of cumulative impacts and no specific requirements as to how cumulative effects could be addressed (Cooper and Sheate, 2002). Second, the guidance to the procedures does not mention methods or frameworks for the assessment of cumulative effects (Department of Environment (DOE), 1989). In addition, these approaches used for cumulative impact assessments have been criticized for being conducted at a too small spatial scale over a too short time period (Ziemer, 1994).

It has recently been recognized that there is a need to shift from local, project scale to broader, basin-wide scale or regional scale assessments to accurately assess cumulative impact assessments (Duinker and Greig, 2006). Consequently, a variety of approaches have been developed at a basin-wide scale. The methods frequently used by researchers to evaluate the cumulative impacts of dams are summarized in Table 2.1. However, it seems that different methods have priorities in coping with different issues caused by dam operation.

When investigating water- and sediment-related issues, such as, reservoir sedimentation, bank erosion, channel dynamics and variation in flow regimes, spatial analysis techniques are commonly adopted. These methods often map geomorphic variations over time using computer-aided models, GIS models or remotely sensed images to demonstrate the spatial changes caused by dam operation. One of the

Table 2.1 Analytical methods for assessing the cumulative impacts of dams

Category	Description	Source
Spatial analysis	Map spatial changes (e.g., variations in river channels, water attributes and water availability) over time using computer-aided models, GIS models or remotely sensed images	Channel erosion: Kondolf and Curry (1986), Kondolf (1997), Brandt (2000), Shields *et al.* (2000), Phillips *et al.* (2005), Hupp *et al.* (2009); sediment retention: Milliman and Meade (1983), Vörösmarty *et al.* (2003), Syvitski *et al.* (2005), Minear and Kondolf (2009), Yang and Lu (2014b); Water availability: Lehner and Doll (2004), Downing *et al.* (2006), Chao *et al.* (2008); changes in water attributes: King *et al.* (1998), Wright *et al.* (2009)
Network analysis	Identify river network structure and interactions of confluences and sections	Benda *et al.* (2004b), Flitcroft (2007), Cote *et al.* (2009), Crook *et al.* (2009), McKay *et al.* (2013)
Biogeographic analysis	Analyze structure and function of river landscape unit	Graf (1999), Chin *et al.* (2008), Sindorf and Wickel (2011)
Observational analysis	Demonstrate changes with before and after dam construction based on actual observations	Watters (1996), Fu *et al.* (2003), Park *et al.* (2003), Keefer *et al.* (2004), Wu *et al.* (2004), Magilligan and Nislow (2005), Graf (2006), Yang *et al.* (2006), Poff *et al.* (2007), Xu and Milliman (2009), Zhang *et al.* (2012b)
Ecological modeling	Model behavior of a river system or river system component (e.g., aquatic animals)	Power *et al.* (1996), Benstead *et al.* (1999), Gowans *et al.* (1999), Coutant and Whitney (2000), Jager *et al.* (2001), Neraas and Spruell (2001), Vinson (2001), Schilt (2007)
Expert option	Problem-solving using professional knowledge	Willis and Griggs (2003), Wu *et al.* (2003), Xie (2003), Dugan *et al.* (2010), Grumbine and Xu (2011), Grumbine and Pandit (2013)

advantages is these methods are efficient and easy-to-implement, as long as spatial data are available. Thus, these methods are often used at basin-wide scale (e.g., Minear and Kondolf, 2009; Yang and Lu, 2013b), national scale (e.g., Kondolf and Curry, 1986; Kondolf, 1997), or even global scale (e.g., Vörösmarty et al., 2003; Syvitski et al., 2005; Chao et al., 2008; Lehner et al, 2011). In addition, these methods can also quantify the impacts; the quantitative evaluation provides some important references for policy-makers. However, the biggest issue for these methods is the heavy dependence on spatial data, but spatial data are often not available or incomplete, especially at a large scale. Data collection for these methods is laborious and expensive.

As an alternative to spatial analysis techniques, network analysis methods are often employed when evaluating the impacts of dams on the entire river network (e.g., river connectivity and river landscape fragmentation). These methods are based on a network dynamics hypothesis that hierarchical and branching river networks interact with dynamic watershed disturbances to impose a spatial and temporal organization on the nonuniform distribution of riverine habitats with consequences for biological diversity (Benda *et al.*, 2004b). When taken in the context of a river network as a population of channels and their confluences, it allows the development of testable predictions about how dams and basin shape, drainage configuration, and network geometry interact to regulate the spatial distribution of physical diversity in channel

and riparian attributes throughout a river basin. Different models based network analysis have been proposed, such as, dendritic connectivity index (Cote et al. 2009), index of longitudinal riverine connectivity (Crook et al. 2009), habitat connectivity index for upstream passage (McKay et al. 2013), patch-based spatial graph (Flitcroft 2007; Erős et al. 2012). However, critics said that these metrics often demonstrate the impacts using single values; they are therefore unable to detect the variation in degree of the impacts caused by dams at regional scale.

Biogeographic analysis and Ecological modeling are often used by ecologist to investigate the impacts of dams on the distribution of aquatic species and ecosystems in river systems based on the change in numbers and types of organisms (Power et al. 1996). These methods have been widespread used by ecologist. Like network analysis, biogeographic analysis and ecological modeling also reveal the impacts of dams on river connectivity and river landscape fragmentation from ecological perspective. A detailed discussion of the methods is beyond the scope this study. Valuable reviews on these methods can be found from Power et al. (1996) and Poff et al. (2007).

Observational analysis has been involved in almost all the issues related to dam operation, such as, water and sediment monitoring, and field investigation of the numbers and types of organisms. It collects firsthand data on the impacts and illustrates the impacts caused by dams based on field investigation results. Although it has been used by numerous researchers (Table 2.1), these investigations are

commonly conducted at small-watershed scale, or incompletely at large scale. It is limited because it focuses on a target species or one specific issue in a specified river section. Thus, it cannot provide an overall result. Another problem is that observational analysis is time-consuming and expensive, which disables the implications at a large scale.

As discussed above, it can be found that the core cumulative impacts caused by dams are water regulation, sediment retention (and related channel dynamics), river connectivity and river landscape fragmentation. In the following sections, detailed literature reviews about research progress, research gaps and challenges on these issues were summarized below.

2.2 Dam spatial configuration and impact on water regulation

Many researchers and organizations (ILEC, 1988-1993; Birkett and Mason, 1995; Vörösmarty *et al.*, 1997; MSSL and UNEP, 1998; Lehner and Doll, 2004; ICOLD, 2011; Lehner *et al.*, 2011) have created their own georeferenced, global and regional datasets of dams and reservoirs in previous attempts. The majority of currently available data sets can be grouped into two categories:

(i)   Databases, registers and inventories that focus on descriptive attributes, such as, Birkett and Mason (1995), Vörösmarty *et al.* (1997), ICOLD (2011), ILEC

(1988-1993), Ryanzhin *et al.* (2001) and Wetlands International (2002) in Table 2.2. These data can supply extensive characterizations for individual lakes or reservoirs; but they generally tend to select only the largest or most important representatives, and they often lack detailed geo-referencing information. For example, Birkett and Mason (1995) represent 13 global and regional lake datasets, which partly include spatial information, the largest of them including 1,755 large lakes and reservoirs. After that, some new datasets were created, including up to 40,000 individual records (Ryanzhin *et al.*, 2001), but all of them provide geo-referencing information only in terms of longitude/latitude point coordinates, instead of shoreline polygons.

(ii)   Analog or digital maps that display lakes, reservoirs in their spatial extent. The digital maps include (1) polygon datasets of global hydrography, i.e. vectorized maps of river, lake and reservoir outlines as derived from various source maps (Table 2.2, Nos. 7–8), and (2) rasterized global land use or land cover characterizations as derived from remote sensing images or other sources.

Both type (1) and (2) data provide information on extent and distribution of lakes and reservoirs, but have limitations when individual attributes, e.g. name or ecological condition, are of interest. An important difference between type (1) and (2) data sets is that remote sensing maps span only the most recent time period, while the polygon datasets are largely based on analog maps which were drawn from local observations

Table 2.2 Overview of existing global and regional datasets of lakes and reservoirs; updated after Lehner and Doll (2004)

No.	Name and citation	Geo-spatial characteristics	Attribute characteristics
1	MSSL Global Lakes database - MGLD; Birkett and Mason (1995)	Global; point coordinates derived from satellite imagery and 1:1 million Operational Navigation Charts (ONC)	Comprises 1,409 large natural lakes and reservoirs with surface areas larger than 100 km^2; attributes include name, and area of lakes
2	Dataset of Large Reservoirs - LRs; Vörösmarty *et al.* (1997)	Global; point coordinates approximated on a global 0.5 × 0.5 degree grid	Comprises 713 large reservoirs with storage capacities larger than 0.5 km^3
3	The World Register of Dams; ICOLD (2011)	Global; no geo-referencing information (location only indicated by name of river and nearest city)	Comprises 33,000 large dams; attributes include dam name, dam geometry, reservoir capacity and purpose of dam
4	Survey of the State of World Lakes; ILEC (1988-1993)	Global; point coordinates	Comprises 752 lakes and reservoirs, attributes include general information, physiographic, biological and socioeconomic data
5	Global Database and GIS WORLDLAKES; Ryanzhin *et al.* (2001)	Global; point coordinates	Currently comprises about 35,000 natural lakes, 5,000 reservoirs, and 220 wetlands; attributes include geography, morphometry, hydrology, meteorology, chemistry and biology
6	Ramsar Database - RDB; Wetlands International (2002)	Global; representative point coordinates	Currently comprises 1,200 wetlands; attributes include site names, area, designation date and wetland characteristics
7	Global Lakes and Wetlands Database - GLWD; Lehner and Doll (2004)	Global vector map	Comprises 654 largest reservoirs, 3,067 largest lakes and about 250,000 smaller lakes
8	Global Reservoir and Dam database - GRanD; Lehner *et al.* (2011)	Global vector map	Comprises 6,862 largest reservoirs

and knowledge over a longer period of time. The polygon maps can thus be assumed to incorporate, at least to some extent, historic conditions and may tend towards representing lakes or reservoirs as known in their maximum recorded extents. The inadequate data at regional and global scales have hindered the advancement of new and rigorous studies, although scientific research has provided critical assessments of the impacts caused by reservoirs. Therefore, the development of a parsimonious approach that can rapidly delineate reservoirs in developing countries is extremely urgent for reservoir-related studies.

The assessments of the cumulative impacts of dams on water regulation based on the above discussed data have been performed by researchers, such as, Graf (1999) Downing et al. (2006), Lehner et al (2011). Since there are numerous small reservoirs that are not included in these datasets, the assessment of the impact of water regulation for smaller rivers may be severely skewed by the omission of small reservoirs. Also, although they may contribute less to the overall alteration of flow regimes as a result of their limited storage capacities, small dams can still have a profound effect on river fragmentation at a regional scale (Lehner et al. 2011).

2.3 Cumulative impacts on sediment trapping

Extensive research on water-sediment regulation has propelled researchers to look into various aspects of dam effects in the hydrological system. Sedimentation behind dams is still a general area of focus. Over past decades, large number of methods and

models (Table 2.3) were proposed to estimate reservoir sedimentation. Each model differs greatly in terms of their complexity, inputs and other requirements. In the simplest way, the amount of sediment deposit in the reservoir can be estimated using empirical models based on its trapping efficiency (TE) (Jothiprakash and Garg, 2008). The models relate trapping efficiency to a capacity/watershed ratio (C/W), a capacity/annual inflow ratio (C/I) or a sedimentation index (SI) (Verstraeten and Poesen, 2000). Today, these models are the most widely used models to predict reservoir sedimentation, even for reservoirs that have totally different characteristics from the reservoirs used in these models. However, it should be noted that, for small reservoirs, these empirical models seem to less appropriate. They also cannot be used for predicting trapping efficiency for a single event. To overcome these restrictions, different theoretical models have been developed based on sedimentation principles. Differences between the developed models are: 1) whether they are for quiescent flow conditions in a pond or turbulent flow; and 2) whether they are for steady discharge conditions or variable discharge conditions (Haan *et al.*, 1994). On the consumption of steady discharge conditions, Camp (1945) studied sedimentation in an ideal rectangular continuous flow basin by simulating particles' settling velocity which is dependent on the water depth and the time that the water needs to flow through the reservoir. After that, Chen (1975) proposed a model with respect to the changing inflow and outflow. He simulated the total distance of a particle has to travel before being deposited with changing inflow and outflow. The both theoretical models are

Table 2.3 A summary of the existing models for reservoir sedimentation prediction

Model	Study area	References	Notes
Trap efficiency for individual reservoirs			
Capacity–watershed area ratio	Small scale or individual reservoirs	Brown, 1944	Empirical model
capacity–annual inflow ratio	Small scale or individual reservoirs	Brune, 1953	Empirical model; hydrological data required
Sedimentation index	Small scale or individual reservoirs	Churchill, 1948	Empirical model; hydrological data required
Theoretical models	Small scale or individual reservoirs	Camp, 1945 Ward et al., 1977	Based on sedimentation principles and variable discharge conditions
Trap efficiency for multiple reservoirs			
Basin-wide trap efficiency	Global/basin-wide scale	Vörösmarty et al., 2003; Kummu et al., 2010; Ran et al., 2013	Measurement of the interception of global or basin-wide sediment flux by large reservoirs; hydrological data required
Sedimentation rate for multiple reservoirs			
Semi-quantitative model	National scale	de Vente et al., 2005	Less data required
Spreadsheet-based model	State-wide scale	Minear and Kondolf, 2009	accounting for the effect of upstream traps but massive sedimentation survey data required
Other black box models			
Computer models	Multi-reservoir systems	Labadie, 2004; Garg et al., 2010	The drawback of the "black box" nature

developed to incorporate variable discharge conditions. Likewise, similar models were proposed other researchers, such as, variable flow models (Ward *et al.*, 1977), modified overflow rate model (Haan *et al.*, 1994), mathematical process model (Sundborg, 1992).

As a result of the improvements in computer technology, some computer models based on artificial neural networks or Genetic programming have been introduced to estimate sedimentation in reservoirs (Labadie, 2004; Garg *et al.*, 2010). These models offer a number of advantages, including requiring less formal statistical training, ability to implicitly detect complex nonlinear relationships between dependent and independent variables, ability to detect all possible interactions between predictor variables, and the availability of multiple training algorithms. However, one of the issues of these models is its 'black box' nature and they hence have limited ability to explicitly identify possible causal relationships. From this point, empirical- and theoretical-based models are superior to computer models. All in all, theoretical-based models usually operate at small spatial scales and require data such as yearly or daily hydrologic records, detailed reservoir bathymetry and sediment grain size distributions; but empirical-based models are suitable at large spatial scales, although these also need hydrologic records.

In a more sophisticated way, reservoir sedimentation in a multi-reservoir system can be estimated through basin-scale trap efficiency (Vörösmarty *et al.*, 2003; Kummu *et*

al., 2010; Ran *et al.*, 2013), or GIS models (de Vente and Poesen, 2005; Minear and Kondolf, 2009) on the basis of land use and hydrological data at a large scale. However, the applications of existing reservoir sedimentation models at a large scale are limited by some factors, such as, lack of reliable hydrological records and the complexity of the interaction between dams depending on local sediment supplies, geomorphic constraints, climate, dam structure and operation. Reliable hydrological records accompanying reservoir construction history are important to predict sediment trapped in reservoirs, but they are usually absent for reservoirs of interest. In addition, in a huge basin, the models based on basin-scale trapping efficiency can predict decreased sediment load at the catchment outlet, but sometimes the amount of reservoir sedimentation is not directly equivalent to the reduction in sediment load at its outlet due to the considerable distance of dams from the outlet and the interaction of different drivers (Walling, 2006). It should also be noted that existing models do not account for the effect of trapping by upstream reservoirs in a multi-dam system. As upstream reservoirs are built, they can significantly reduce sediment yield to downstream reservoirs. This effect is particularly important in areas with numerous reservoirs within the same watershed (Minear and Kondolf, 2009). These points are probably the most important gaps in the research of reservoir sedimentation estimation.Estimating sediment retention in a multi-dam system remains a daunting challenge.

2.4 Cumulative impacts on river connectivity and river landscape fragmentation

To quantify river fragmentation caused by dams, various models have been proposed over the past decades in global- or catchment-scale studies (Table 2.4). Serving as a first-level approximation of the potential impact on flow regulation, Dynesius and Nilsson (1994; 2005) used flow regulation ratio or degree of regulation and concluded that 77% of the total water discharge of the 139 largest river systems in North America and north Mexico, Europe and the republics of the former Soviet Union is strongly or moderately affected by fragmentation of the river channels by dams. Liermann et al. (2012) also measured the length of the longest undammed stretch of the five largest rivers in each 'freshwater ecoregion' to derive the percentage of free-flowing rivers; however these two studies are just a very rough assessment for flow regulation because no operating rules or reservoir locations were considered.

Meanwhile, graph-theoretic models were also presented. So-called graph-theoretic models combine a network of links and nodes, which represent river reaches and confluences, respectively, into a network. A simple yet elegant example in this category is the dendritic connectivity index (DCI) (Cote *et al.*, 2009). It is based on the proportion of the length of the disconnected network fragments in relation to the entire network, and it can be applied to river networks of different scales. A disadvantage of the approach, however, is that it can lead to the same index if a barrier is

Table 2.4 Metrics used in the literature to assess river connectivity and fragmentation

Metrics	Abbreviation	Formula	Description
A. Hydrological metrics			
Degree of regulation (Dynesius and Nilsson 1994; Nilsson et al. 2005; Lehner et al. 2011)	DOR	$DOR = \dfrac{\sum_{i=1}^{n} V_i}{Q} \times 100\%$	Where V_i is the reservoir storage capacity in km³, n is number of upstream reservoirs, Q is the river's annual flow volume in km³.
River regulation index (Grill et al. 2014)	RRI	$RRI = \sum_{i=1}^{n} DOR_i \dfrac{rv_i}{RV}$	Where n is the number of reaches in the network; DOR_i is the DOR values of river reach i; rv_i is the river volume of reach i; and RV is the total river volume of the entire river network.
Ratio of capacity to catchment area (Graf, 1999)	RCA	$DOA = \dfrac{\sum_{i=1}^{n} V_i}{A}$	Where V_i is the reservoir storage capacity in km³, n is number of upstream reservoirs, A is the river's catchment area in km².
Ratio of catchment area to number of reservoirs (Graf, 1999)	RAN	$RAN = \dfrac{A}{n}$	Where n is number of upstream reservoirs, A is the river's catchment area in km².
Percentage of free-flowing river (Liermann et al. 2012)	PFF	$RAN = \dfrac{\sum_{i=1}^{n} \dfrac{l_i}{L}}{n} \times 100\%$	Where l_i is the longest undammed distance of each of an ecoregion's n connected pathways, regardless of stream order; RAN is the average of the n undammed percentages, which ranges between 0% and 100%, where 100% denotes a free-flowing ecoregion, and a value less than 50% is referred to a heavily obstructed ecoregion.
Change in river flows (Döll et al. 2009)	CRF	$CRF = \dfrac{NAT - ANT}{NAT} \times 100\%$	Where NAT is naturalized river discharge in km³ yr⁻¹; ANT is water volume impacted by water withdrawals and reservoirs; this index is to assess how long-term river are flows affected.

Indicator of change in seasonal amplitude (Döll et al. 2009)	ISA	$$CRF = \frac{Q_{max} - Q_{min}}{Q_{nat}} \times 100\%$$	Where Q_{max} and Q_{min} are maximum and minimum long-term average monthly river discharge under anthropogenic impacts; Q_{nat} is annual river discharge under naturalized conditions. This indicator is to evaluate how the seasonal amplitude is affected.
Indicator of impact on interannual variability of monthly flows (Döll et al. 2009)	IIV	$$IIV = N_i - N_d$$	Where N_i is the number of months (Jan, Feb, etc.) in which the coefficient of variation of monthly flows increases; N_d is the number of months in which it decreases ($-12, -10, -8, \ldots, +8, +10, 12$) under anthropogenically impacted conditions as compared to naturalized conditions. This indicator is to investigate how the interannual variability of monthly flows is affected.

B. Graph-theoretic metrics

Dendritic connectivity index (Cote et al. 2009)	DCI	$$DCI = \frac{\sum_{i=1}^{n} c_i \times s_i}{\sum_{i=1}^{n} s_i} \times 100\%$$	Where s_i is the length of section i; c_i is the cumulative passability depending on the number and passability (p) of dams in section i; Assuming the passability of multiple dams is independent, if there are m dams on a river, then c_i is defined as: $c_i = \prod_{m=1}^{m} p_m$. This index is to quantify longitudinal connectivity of river networks.
River landscape fragmentation index (Sindorf and Wickel, 2011)	RLFI	$$RLFI = \frac{\sum_{i=1}^{n}(e_i^2 - e_i) \times pl_i}{E^2 - E} \times 10$$	Where e_i is total number of distinct landscape classes in network section i; E is total number of landscape classes fund in the basin; pl_i is percentage of river length in network section i relative to the total river network length in the basin. This index quantifies ecosystem connectivity based a function of the number of ecosystems that remain connected combined with the length of river networks.
Moving-average spatial covariance model incorporating stream distance and flow (Hoef et al. 2006;		Equation omitted[a]	Incorporating flow, stream distance to develop a spatial statistical model to estimate an average or total in nutrient concentration for a stream or a steam segment

Peterson et al. 2007)

Model	Abbr.	Formula	Description
Habitat connectivity index for upstream passage (HICU) (McKay et al. 2013)	HICU	$HCIU = \dfrac{\sum\limits_{i=1}^{n} c_i \times r_i}{\sum\limits_{i=1}^{n} r_i} \times 100\%$	Where r_i is the number of immediately upstream notes for note i; c_i is the cumulative passability. The index uses a graph-theoretic algorithm for assess upstream habitat connectivity to investigate both basic and applied fish passage connectivity problems.
Index of longitudinal riverine connectivity (ILRC) (Crook et al. 2009)	ILRC	$ILRC = \Pr D_k \times \Pr UC_k$	Where $\Pr D_k$ is the probability of downstream larval passage of dam k; $\Pr$ UCk is the probability that juveniles migrate past multiple dams to a given point (cumulative upstream passage). This index quantifies the cumulative effect of individual water dams on longitudinal riverine connectivity
Patch-based spatial graph (Flitcroft 2007; Erős et al. 2012)		No formula available	This index tries to measure habitat connectivity of freshwater ecosystems by considering the branching river networks
C. Models incorporating behavioral elements			
Observational movement studies (Fu et al. 2003; Park 2003; Wu et al. 2004; Zhang et al. 2012)			The studies Demonstrate biodiversity loss or population variety with before and after dam construction based on actual observations.
D. Others			
inSTREAM model (Harvey et al. 2012; Railsback et al. 2009)	inSTREAM	No formula available	The model Explores the effects of dams or other barriers on fish population by assuming fish cannot move upstream past a barrier or dam and move downstream over a barrier.
Barrier Analysis Tool (BAT) (Martin and Apse 2011)	BAT	Computer program; no formula available	The tool Executes the weighted ranking process to facilitate several of river fragmentation assessment

[a]Many equations were used to establish the model; the equations therefore are not given here due to lack of space.

placed very far upstream river section in the river network or very far downstream river section, as long as the disconnected fragments have the same length. Yet in hydrological, environmental and ecological applications it is commonly argued that dams placed further downstream pose a higher threat than their counterparts in headwater reaches as the former disconnect large portions of the critical river systems of the main stem or the delta and the dams directly affect the generally crucial parts of large rivers (Gupta, 2008; Kanno *et al.*, 2012). Also, this measurement does not account for different river landscapes although different river landscapes may have different importance (e.g. delta systems, unique main-stem areas and headwater permafrost areas). To overcome the problem, Sindorf and Wickel (2011) developed the river landscape fragmentation index (RLFI) to measure the extent of river landscape fragmentation by measuring river length and the number of disconnected river landscapes based on a river-landscape classification map. As an alternative technique, Mckay et al. (2013) developed a model to assess upstream longitudinal river connectivity on the basis of dendritic network morphology, partial passage improvement and stochastic passage rates, but the two models still does not take river size and stream length into account. As a remedy, Grill *et al.* (2014) proposed the river connectivity index (RCI) by simply replacing the 'river length' measure with 'river volume', but the model is less generally applicable because exact river volume for each river section is often unknown.

Some researchers (Gupta, 1998; Fu *et al.*, 2003; Park *et al.*, 2003; Wu *et al.*, 2004; Zhang *et al.*, 2012a) also investigated the impacts of dams on river connectivity and fragmentation using data on migratory species based on observational movement studies, but spatially explicit and reliable data on migratory species are often unavailable for large rivers. A way that addresses the absence of species data is to use ecosystems or habitats as a proxy. There is general agreement within the conservation community that protecting representative ecosystems or 'coarse-filter' targets, should conserve common communities, the ecological processes that support them, and the environments in which they are evolved (Grill *et al.*, 2014). Coarse-filter targets can be derived through the development of river-landscape classifications based on river basin characteristics such as climate (e.g., precipitation, temperature), topography (e.g., slope, elevation) and geology (e.g., karst geology). The river-landscape classifications can then serve as a proxy for representative ecosystems (Gupta, 2009). The abundance and distribution of river landscapes within the river basin can act as a surrogate for the actual species distribution (Sindorf and Wickel, 2011). The River environment fragmentation index (RLFI) based river-system classification map was proposed by Sindorf and Wickel (2011) as an index to assess river landscape fragmentation in the Mekong River basin.

In terms of large Asian river basins, dam building still booms nowadays, although worldwide dam construction significantly reduced after the 1980s. Most of the large

38

Asian rivers are being dammed at a dazzling pace. There are even more than 10 cascade dams built on some large rivers and their major tributaries. Under this context, more detailed knowledge is required to quantify the degree of river fragmentation. This knowledge can also be essential to identify environmental risks associated with further impacts on river systems. Also, using this knowledge, it is possible to quantify the potential impacts of incremental dam development on river connectivity at the basin and sub-basin level in terms of environmental intactness.

2.5 The overlooked role of small reservoirs

Small dams are always built on smaller river systems, designed to divert small amounts of water. There has been little interest in small dams and reservoirs because of the assumption that such units have fewer severe environmental impacts than large ones. However, few comprehensive analyses of this assumption have been done.

A pioneer study to validate this assumption was executed by Gleick (1992). He compared the environmental and ecological impacts of small and large hydroelectric facilities, with a focus on land requirements, evaporative water losses, seepage, and sediment rates, suggesting that many of the environmental impacts of small dams are comparable to or even worse than conventional large dams when measured on a unit-energy basis. Like this study, Kibler and Tullos (2013) investigated the cumulative biophysical effects of small and large hydropower dams in China's Nu River basin, and

compared effects normalized per MW of power produced. They obtained similar conclusions that biophysical impacts of small hydropower may exceed those of large hydropower dams, particularly with regard to habitat and hydrologic change. However, there are many other important environmental impacts, including downstream flow alterations and impacts on terrestrial and aquatic biota, which are not addressed in the two studies.

Another representative study was carried out by Graf (1999) based on simple statistical analysis; but this study focuses an impact of 75,000 dams on water regulation in the continental United States. Some simple metrics, such as, the ratio of area to number of dams, the ratio of storage capacity to area, and the ratio of storage to runoff were used to quantify the degree to which the continental United States is regulated by small dams. It suggested that water resource regions have experienced individualized histories of cumulative increases in reservoir storage and thus of downstream hydrologic and ecologic impacts. Unfortunately, the study did not compare the environmental and ecological impacts of small and large dams. The metrics proposed in this study were also used by other researchers (Smith *et al.*, 2002; Renwick *et al.*, 2006; Chin *et al.*, 2008), indicating that the impacts of small dams and reservoirs on hydrology, sedimentology, geochemistry, and ecology are apparently large in proportion to their area. Nevertheless, most of the conclusions were given based on simple statistical analysis. No new observational data were used in these studies.

Alternatively, Investigations based on observational movement studies on the impact of small dams on aquatic species have been increasingly documented in recent years (Lessard and Hayes, 2003; Almeida *et al.*, 2009; Czerniawski *et al.*, 2010; Mantel *et al.*, 2010; Gangloff *et al.*, 2011; Singer and Gangloff, 2011; Thoni *et al.*, 2014) due to widespread concerns over biodiversity conservation. These studies often compare fish assemblage composition and aquatic habitat directly upstream and downstream of dams, or before and after dam construction, to illustrate the effects of small dams on river ecosystems. One of the pioneer studies shows that there is circumstantial evidence that the distributions of aquatic species are limited by small dams in the investigated river systems (Watters, 1996). This statement was then supported by Anderson *et al.* (2006); but the study by Anderson et al. emphasized that one of the primary causes of change in river ecosystem is flow reduction after the construction of several dams. Reductions in stream flow are a substantial ecological impact frequently associated with dams. Flow reductions affect the physical characteristics of a stream (e.g. water velocity, sediment and nutrient transport, water temperature) and alter the quantity and quality of aquatic habitat (Tiessen *et al.*, 2011), with cascading impacts on stream biota. Hence, investigating the quantity of flow reduction after the construction of small dams is an important measure to examine the impacts led by small dams.

3 Description of the Yangtze River basin

The Yangtze River, known in China as the Changjiang, flows for 6,300 km from the glaciers on the Tibet Plateau in Qinghai Province eastward across southwest, central and eastern China before emptying into the East China Sea at Shanghai. In this chapter, a general description of the Yangtze River basin was presented for the aspects geographical characteristics, climate, hydrology, geology and major human impacts exerted during the past decades. As this PhD study tried to investigate the cumulative impacts of dams on water regulation, sediment retention river connectivity and river landscape fragmentation, it can be found that the study subjects were diverse although closely correlated. To carry out this study, datasets from different sources were utilized. Therefore, it is important to present necessary descriptions of the river basin at different aspects. In addition to the brief description given here, an additional description of corresponding datasets analyzed in each individual chapter was also presented.

3.1 Geography

The Yangtze River in southern China lies between 91°E and 122°E and 25°N and 35°N, has a basin area of approximately 1.8×10^6 km^2 and is the third largest river by river length and water discharge volume in the world (Figure 3.1). The river is generally divided into three parts: the upper, middle and lower reaches based hydrological processes and sediment transport mechanisms (sediment source zone, sediment
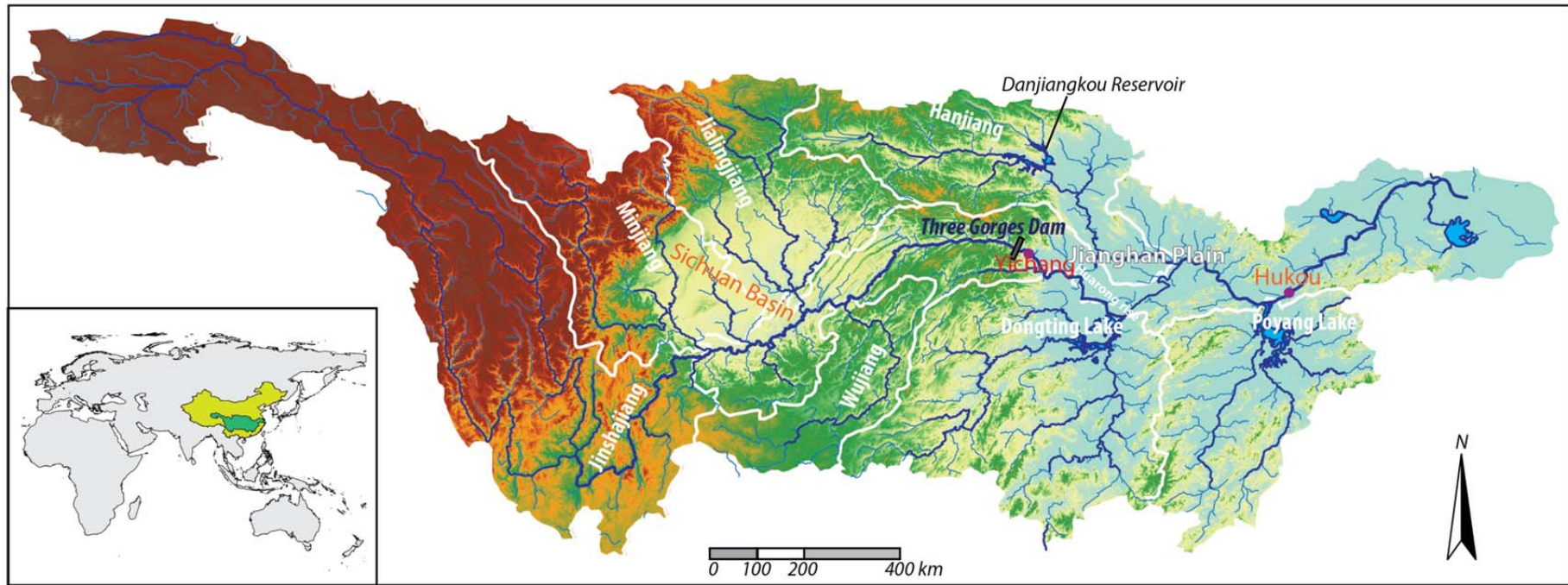
Figure 3.1 Geographical setting of the Yangtze River and its sub-basins.

Table 3.1 Basic information about the major tributaries and key hydrological stations on the Yangtze River

	Rivers	Stations	Area (10^4 km^2)	Water discharge[*] (km^3 yr^{-1})	Sediment load[*] (Mt yr^{-1})
Tributary	Jinsha	Pingshan	45.86	142.6	255
	Jialing	Beibei	15.61	66.54	120.1
	Min	Gaochang	13.54	50	26
	Tuo	Lijiawan	2.79	35.1	11.7
	Wu	Wulong	8.3	49.73	28.03
	Han	Huangzhuang	14.21	48.1	55.9
	Xiang	Xiangtan	8.16	65.9	10.3
	Zi	Tao	2.67	23.25	2.27
	Yuan	Taoyuan	8.52	64.65	12
	Lei	Shimen	1.53	14.97	6.05
	Gan	Waizhou	8.35	68.7	9.25
	Xiu	Qiujin	1.48	10.8	1.53
	Fu	Lijiadu	1.6	14.7	1.4
	Xin	Meigang	1.55	17.8	2.61
Mainstem		Zhutuo	69.47	269	302
	Upper	Cuntan	86.66	339.7	418
		Yichang	100.55	438.2	501
	Middle	Hankou	148.8	711.2	404
	Lower	Datong	170.54	905.1	433

*Values are multi-year averages of water discharge and sediment load (1950s-2000); data from (CWRC, 2002a).

transfer zone and sediment deposition zone). The upper reach, including four major tributaries — the Jinsha, Min, Jialing and Wu rivers, extends approximately 4,512 km to Yichang from the headwaters in the Himalayan Mountains (Saito *et al.*, 2001), with a drainage area of approximately 1.0 x 10^6 km^2. High plateaus, mountains, deep river valleys, and large intermontane basins characterize the landforms in the upper Yangtze River basin. The channels are about 0.5-1.5 km wide, 5-20 m deep, and vary in slope from 10 - 40 x 10^{-5}, reaching a maximum of 450 x 10^{-5} (Chen *et al.*, 2001b). Meltwater from glaciers and snow, rainfall and groundwater are important sources of

water supply to the river (Chen *et al.*, 2001a).

The Jinsha, the Min, the Jialing and the Wu tributaries are the four large tributaries in the upper basin (Figure 3.1), with catchment areas of 3.4 x 10^5, 1.33 x 10^5, 1.6 x 10^5 and 8.7 10^4 km^2, respectively. Of these four tributaries, the Jialing tributary basin is the most exploited by dam construction, land cover change (deforestation and reforestation), and urbanization. The Wu River is 1,037 km long, a rainwater-supplied river, with an annual water discharge of 53 km^3 yr^{-1}. The vegetation cover in this is up to 18.7% including shrubs (Mo, 1988).

At Yichang, the Yangtze River exits the Three Gorges Dam (TGD) and enters the 950-km middle reach (Yichang to Hukou). It receives more water from three large water bodies in this section: the Dongting Lake, the Han River and the Poyang Lake. The 930-km lower reach extends from Hukou to the river mouth approximately 20 km north of Shanghai and has a drainage area of 1.2 x 10^5 km^2. The Poyang Lake receives water from four major rivers: the Gan, Fu, Xin and Xiu rivers. The Dongting Lake has four major tributaries: the Xiang, Zi, Yuan and Lei rivers. The 1,756 km long Han River has a catchment of 159 x10^3 km^2. In contrast to the upper reach, extensive floodplains, large lakes, low mountains and hills characterize the middle-lower reaches. The channel of the middle Yangtze is wider than the upper course, with the width between 1 and 2 km and the depth between 6 and 15 m. A typical meandering river pattern with many cutoffs prevails in this river reach, where the river exits from

the upper rock-confined valley into the Jingjiang floodplain.

Downstream from Datong to the estuary, no large tributary flows into the Yangtze River; thus, the additional input of water into this part of river is small. The tidal fluctuations, however, can influence the water level at Datong. Therefore, the water discharge at Datong is commonly used to represent the total discharge from the Yangtze to the sea, although it is still 680 km from the sea. This segment of the river wanders among plains and hills, on which a high-stage water level about 8 m above mean water level, is clearly marked. The slope of the riverbed decreases to $0.5 - 1.0 \times 10^{-5}$, and the channel widens to 2 - 4 km and deepens to 10 - 20 m (Chen *et al.*, 2001b). The river channel can however, be wider than 15 km and as shallow as 6 m in its estuarine region. The lower Yangtze drainage basin, including its large estuarine system, benefits largely from upstream discharge and sediment accumulation.

The Yangtze River basin includes a complex variety of geomorphological units. The headwater drainage basins of the Yangtze, covering an area of 1.1×10^4 km^2, are situated at an elevation of about 4,900 m in the Tanggula Mountains. Fed by glaciers on the roof of the world, most of this river basin is far away from influences of anthropogenic activities (e.g. pollution, dams). The upper Yangtze, with elevation ranging from 1,100 m to 4,900 m, is primarily located in a mountainous region. In this region, the Yangtze River also passes through a mountain-girt basin, namely, the Sichuan Basin (Figure 3.1). Due to its relative flatness and fertile grounds, it

demonstrates a unique geomorphological feature in the upper Yangtze reach. The middle reach is made up of a series of floodplains along the Yangtze River and its major tributaries. The floodplains are somewhat swampy, made up of a large number of lakes and small streams, making it suitable for freshwater fishes. It is therefore known as the "land of fish and rice". The Lower Yangtze is an area of anabranching rivers with constricted floodplains and early to late Pleistocene terraces along the valley (Chen *et al.*, 2008b). The various geomorphological units provide downstream a wealth of freshwater, sediment, nutrients and other resources.

3.2 Climate

Subtropical monsoon climate prevails over most of the Yangtze River basin. The spatial and temporal variations of precipitation in the Yangtze River basin are closely related to summer monsoon activities that transport a huge amount of atmospheric moisture from the East and South China Sea to the basin (Jiang *et al.*, 2007). Normally, the summer monsoon starts to influence the Yangtze River basin in April decreasing in October. Summer rainfall from June to August, accounts for 45% of the annual total of about 1,100 mm (CWRC, 2002b).

The long-term mean annual precipitation in the Yangtze River basin is approximately 1,070 mm but the spatial and temporal distribution of rainfall is highly uneven (Yang *et al.*, 2002; Xu and Milliman, 2009). Annual precipitation ranges from < 400 mm in the west to > 1,600 mm in the southeast (Figure 3.2). Because most of the basin is affected

by the southeast monsoon in the summer season, most precipitation occurs from May to October.
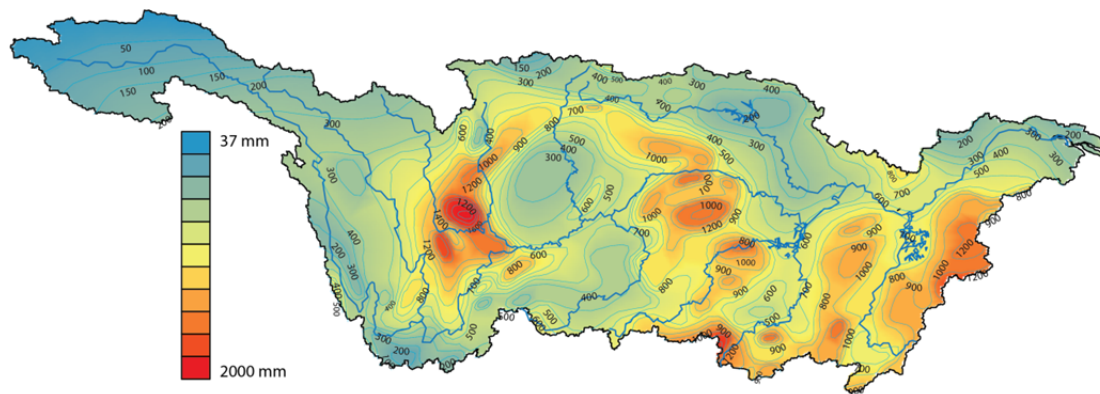
Figure 3.2 Annual mean precipitation in the Yangtze River basin; the raster map was outputted using Kriging spatial interpolation based on precipitation collected at meteorological stations in the Yangtze River basin.

It should be emphasized that, during the five decades from 1951 to 2010 annual precipitation increased in the south-east (> 100 mm) while it decreased in the upper reaches (-200 mm), particularly in the Jialing and Min tributary basins (Xu *et al.*, 2007) (Figure 3.3). The sub-basins of the Jinsha River, Dongting Lake and Poyang Lake showed a slight increase in precipitation, whereas a striking decrease in precipitation occurred in the Jialing and Min tributary basins and a slight decline in the Han tributary basin. Correspondingly, runoff (water discharge per unit area) also increased in the sub-basins of the Jinsha River, Dongting Lake and Poyang Lake but decreased in the tributary basins of the Jialing, Min and Han rivers.

Despite these sub-basin changes, water discharges along the mainstem in upper,

middle and lower reaches of the Yangtze have varied little since 1950, reflecting increases in some sub-basins being offset by decreases in others. Basin-wide runoff measured at Datong correlated well with precipitation, but neither showed a significant change over time (Yang *et al.*, 2005a) (Figure 3.4).
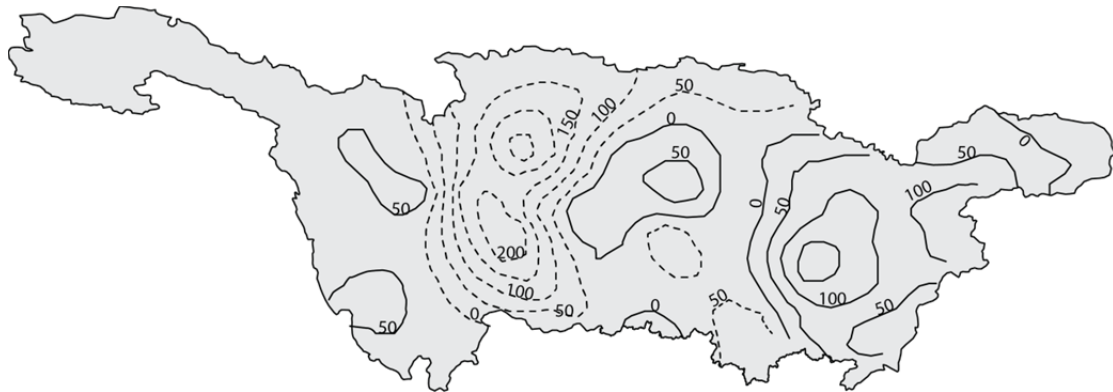
Figure 3.3 Precipitation change (mm) in the Yangtze River basin, 1951 to 2000. Solid and dashed lines correspond to increased or decreased precipitation, respectively. Figure was modified after Xu *et al.* (2007) and Dai and Tan (1996).

3.3 Hydrology

Hydrological records covering a 60-year period from the upper, middle and lower Yangtze River were collected to examine the temporal and spatial distribution of discharge and sediment load in the basin. The Yangtze discharge, as expected, increases from the upper drainage basin downstream. Only an estimated 50% of the discharge is derived from the upper Yangtze, with the rest being derived from the numerous tributaries of the middle-lower reaches (Chen *et al.*, 2001a). However, the distribution of sediment load along the Yangtze is the reverse of that observed for water discharge, with most of the sediment being derived from the upper reach. A

dramatic reduction in sediment load happens in the middle Yangtze as a result of a marked decrease in slope and the change to a meandering pattern from the upper Yangtze rock sections. Considerable siltation also occurs in the middle Yangtze reach as the river cuts through a large interior Dongting Lake system. Sediment load in the lower Yangtze, while significantly less than that of the upper river, is somewhat higher than the middle Yangtze due to additional load contributed by adjacent tributaries. A strong correlation exists between the discharge and sediment load along the Yangtze River basin during the dry season as lower flows carry lower sediment concentration. During the wet season, a strong correlation is also present in the upper Yangtze owing to the high flow velocity that suspends sand on the bed. However, a negative to poor correlation occurs in the middle and lower Yangtze because the flow velocity in these reaches is unable to keep sand in suspension, transporting only fine-grained particles downstream(Chen *et al.*, 2008b).

About half of the river water and nearly all its sediment originate from the upper reach upstream from Yichang (Lu *et al.*, 2003b), which has a catchment area of about 55.6% of the whole river basin. The annual water discharge and sediment load from the upper Yangtze River, recorded at the Yichang station, averaged 451 km^3 yr^{-1} and 516 Mt yr^{-1} between 1955 and 1965, amounting to approximately 50 and 116% of those at Datong (Chen *et al.*, 2002; Yang *et al.*, 2002). The main sources of sediment load at Yichang are the Jinsha and Jialing rivers, totally accounting for 73-90% of the total sediment load (Wang *et al.*, 2007c). Most of the sediment is from the area between the

confluence of the Yalong River and the Jinsha River down to Pingshan (Zhou *et al.*, 2002).
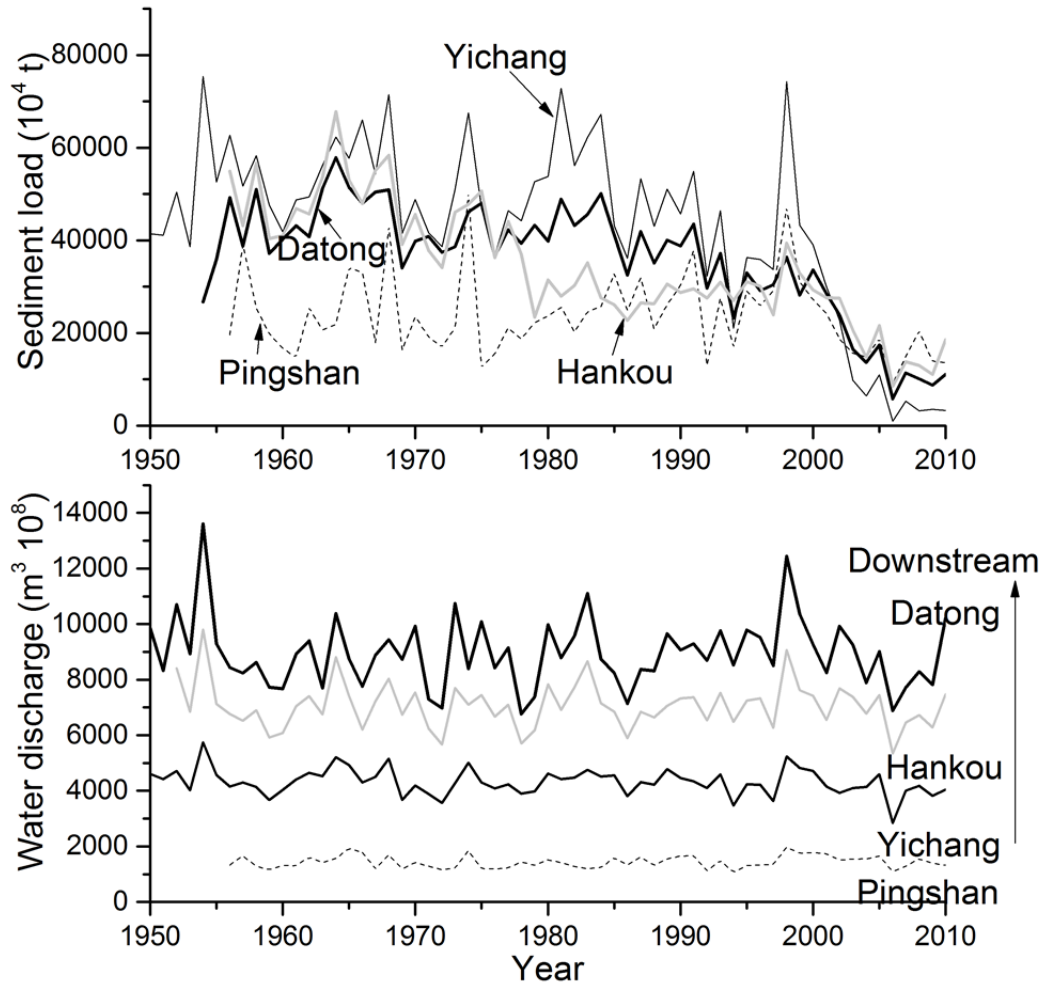
Figure 3.4 Temporal variations of runoff and sediment load along the main stem of the Yangtze River from 1950 to 2010.

The Dongting Lake plays a key in sediment transport processes in the Yangtze River basin. Previous studies (Shi *et al.*, 1999; Xiang *et al.*, 2002) demonstrated that the inflow from the four tributaries of the Dongting Lake contributes approximately 58% of the total water into the lake, while the runoff from the Yangtze River via four intakes occupies 34%. However, among the sediment transported into the lake, 80% is

from the Yangtze River, comparing to 18% provided by the four tributaries. Up to 74% of the sediment into the lake is deposited in the lake, with the rest carried out of the lake to the Yangtze River again. By comparing the sediment import and export, it is estimated that the sediment deposition rate of Lake Dongting was 111 Mt yr^{-1} from 1956 to 2003 (Dai *et al.*, 2005). Siltation and raised embankments decreased the size and its capacity to accommodate floods. However the construction of the TGD has significantly reduced the sediment deposition in the Dongting Lake. For instance, in 2003, the deposition in the lake dropped to 25 — 18% of the annual average in the period 1956 — 2002. The influence of the sediment deposited in the Dongting Lake on the sediment transport process has fallen since the completion of the TGD, and will be further decreased in future due to completion of more large dams.

Over the past 60 years, annual sediment discharges in all parts of the Yangtze River basin have varied considerably more than water discharges, and have declined markedly since the 1980s (Figure 3.4). As a result of several major decreases, annual discharges of sediment from upper (as measured at Yichang) and lower (as measured at Datong) reaches during the 2003–2005 period after the closure of TGD were approximately 50 and 100 Mt, respectively, only 10% and 33% of their 1950–1960s averages.

Figure 3.4 shows that sediment discharge data from the upper, middle, and lower reaches of the river indicate that the reduction of the Yangtze sediment load has

occurred in three phases: following the closure of the Danjiangkou Reservoir on the Han tributary in 1968, following the closure of numerous reservoirs after 1970 and following the closure of the TGR in 2003 (Yang, Z. et al., 2006; Wang, Z.Y. et al., 2007). However, up to now, the exact reservoir sedimentation rate has been unclear.

It may be noted that previous studies principally reported the decreased sediment loads at hydrological stations as a result of reservoir development; but sometimes the amount of reservoir sedimentation is not directly equivalent to the reduction in the sediment load at its outlet due to the considerable distance of dams from the sea and the interaction of different drivers (Walling, 2006). Therefore, up to now, the exact reservoir sedimentation rate and impact on storage loss has been unknown.

It should be highlighted that, the bed load proportion in the Yangtze River is very low compared to other large rivers in the world where bed load usually contributes 5—10% of the total sediment load (Eisma, 1998). On average, bed load represented only 0.044% of the total sediment load (Yang *et al.*, 2002). In other words, the sediment flux in the Yangtze River was dominated by suspended load. For example, for the same period at Yichang station, suspended load and bed load were 530 x Mt yr^{-1} and 8.45 Mt yr^{-1}, respectively (Xiang and Zhou, 1986), suggesting that suspended load was 98.4% of the total sediment load. Thus, bed load was not considered in this study in light of the negligible role in sediment transport processes of the Yangtze River.
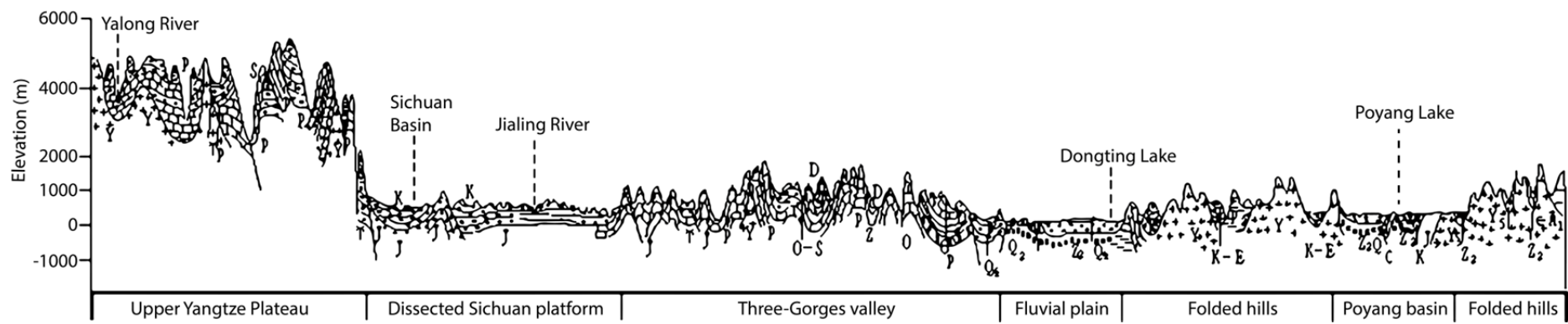
Figure 3.5 Geological transect from the upper to lower Yangtze River, modified after Chen *et al.* (2008b).

3.4 Geology

The Yangtze River basin includes a complex variety of geological units, primarily sedimentary rocks of different ages. The geological transect (Figure 3.5) from the upper to lower Yangtze summarizes the geological characteristics of the basin. Limestone and terrigenous sedimentary rocks of Palaeozoic age with granite NW–SE across the east-central basin highlight the alternate anticlines and synclines of Permian and Triassic age (Chen *et al.*, 2008b). The Yangtze River cuts through these geological structures to enter the Three Gorges.

Figure 3.6 Pre- and post-landslide aerial-image comparison on the landslide occurred on August 8, 2010 in the upper reach of the Jialing River; images were provided by the National Administration of Surveying, Mapping and Geoinformation of China. The arrow in the left panel indicates the residential area, which has destroyed and

moved down to the shore of the Bailong River (arrow in the right panel).

constitute the upper Yangtze River basin (Chen *et al.*, 2008b). The sedimentary strata have been highly fractured due to the Himalayan uplift and erode easily. Cretaceous to Jurassic sandstone forms the Sichuan Basin, connecting the upstream Yangtze Plateau with the downstream Three Gorges Valley (Figure 3.5). The Sichuan Basin is surrounded by a complex of mountains framed by distinctive tectonic units (Tang and Xie, 1994). The alignment of highlands in the western and eastern basin are controlled by sets of major faults trending approximately NW–SE, and those in the northern and southern basin by faults running southwest. A set of linear faults running NW–SE across the east-central basin highlight the alternate anticlines and synclines of Permian and Triassic age (Chen *et al.*, 2008b). The Yangtze River cuts through these geological structures to enter the Three Gorges.

The upper reach of the Jialing River and the lower reach of the Jinsha River are underlain by a wide variety of sedimentary and metamorphic rock and unconsolidated sedimentary deposits and exposed strata of Cambrian, Silurian, Devonian, Carboniferous, Triassic, and Jurassic age and Quaternary high erodible deposits (Tang *et al.*, 2009). The rocks include Cambrian metavolcanite, metasandstone and slate, Silurian phyllite, and Devonian and Carboniferous limestone, Triassic quartzitic sandstone and shale, Jurassic sandy gravel and Sandshale; Quaternary high erodible deposits are widely distributed in the terraces and alluvial fans. These rocks are typically poorly or moderately indurated, structurally deformed by pervasive folding

and faulting, and covered by residual and colluvial soils as much as several meters deep. Sediment contribution to the Jialing, lower Jinsha rivers is periodically accelerated by seismic events such as the landslide occurred on August 8, 2010 (Figure 3.6).

Downstream of the Three Gorges, the geological framework of the Middle Yangtze River basin is primarily delineated by the two large tectonically-controlled subsidence basins: Jianghan and Dongting. The basins subsided since the late Cretaceous to the early Tertiary time (Huang *et al.*, 1965). The Huarong Rise separates the two basins. An earlier Yangtze channel flowed across the Jianghan floodplain to the north when the subsidence rate was higher there than in the Dongting Lake drainage area (Chen *et al.*, 2008b). The river channel migrated southward to Dongting Lake drainage area following a subsequent shift in the location of rapid subsidence.

Figure 3.7 Spatial distribution of karst areas in the Yangtze River basin

The distribution of Karstic rocks is widespread in the Yangtze River basin (Figure 3.7). Karstic rocks are primarily distributed in the Wu tributary basin, Dongting Lake

drainage area, main-stem area of the middle Yangtze, and a small part of the Han tributary basin. Soils in the karst areas are relatively thin and scattered, because of the low soil-forming capability of soluble bedrock and the highly weathered, leached, and impoverished soil nutrients in tropical and subtropical regions (Yuan, 1997). Streams and tributaries form a particular river system as a result of the special geological setting.

3.5 Major anthropogenic activities

Anthropogenic activities in the Yangtze River basin have been a long history. The Yangtze River supports more than 30% of China's population and help to produce about 40% of the county's industrial and agricultural value (Dai *et al.*, 2010). The upper Yangtze River basin is sparsely populated (i.e. < 100 person km^{-2}) but rich in hydropower resources; the middle-lower reaches are characterized by quite high population density (up to 800 people km^{-2}) (Zhang *et al.*, 2003). The unevenly distributed population has resulted in different anthropogenic activities to water resources, for example, deforestation, water withdraw, water diversion, water and soil conservation, dam construction, land reclamation, embankment of lakes, and land cover change (e.g. agriculture, urban development, road construction).

3.5.1 Deforestation in the upper Yangtze reach

Before the mid-1980s, there was no specific law protecting forests in China. Forest

coverage in the Sichuan Basin, which is one of the agricultural and industrial centers in China, with a population of about 100 million, declined from 20% in the 1950s to 12% in the 1980s as a result of increasing demand for timber and forest clearance for grain production. For the same period, forest coverage within the catchments of Min and Jialing rivers was also reduced from 1.3×10^6 hectares to 0.47×10^6 hectares (Lu and Higgitt, 1999; Zong and Chen, 2000).

Apart from the Jialing and the Min tributary basins, deforestation also occurred with varying intensity in other tributary basins. The hillside forests along the tributary rivers have almost disappeared as a result of excessive exploitation. The basin of 1,757 km long Yalong River used to be covered by natural forest due to the difficulty of access and the extremely low population. However, deforestation has reached even this remote area. The turbidity of river water has increased rapidly over the past decades according to the local residents (Zong and Chen, 2000; Lu et al., 2003a), but detailed information is currently not available.

The obvious consequences of deforestation are soil erosion and the reduction in water storage capacity of surface soil and reservoirs. As estimated by the Chongqing Municipal Government, in the areas around Chongqing, about 4.33×10^6 hectares of land is under severe soil erosion, producing about 200×10^6 tons of sediment each year, i.e., approximately 46 tons of sediment per hectare is lost annually. About 2/3 of this sediment is deposited in local reservoirs, ponds and river networks, and the other

1/3 is transported into the main channel of the Yangtze (Zong and Chen, 2000). At the end of the 1970s, forest coverage reached to its lowest point. After 1980, great efforts have been made to construct a shelter forest system in southwestern China. Vegetation has gradually recovered in the upper Yangtze valley. Forest coverage ratio has risen from 13 % in 1978, to the current 21 % for the Sichuan Basin (Cheng, 1999), which is slightly higher than the historical level of 20% in the 1950s.

3.5.2 Soil and water conservation in the upper Yangtze reach

As stated in the climate section, the upper Yangtze Reach has a variety of physiographic features in its different parts and is characterized by diversity of erosion patterns. In general the basic patterns of surface erosion involve water erosion, gravitational erosion and a combination of the two in most regions (Walling and Fang, 2003), except in the Qinghai-Tibet Plateau with its higher elevation and severe cold climate, where glacial and freeze-thaw processes are also an important pattern of surface erosion (Wang *et al.*, 2007a; Wang *et al.*, 2009a).

Water erosion, including sheet erosion and gully erosion, is the main type of surface erosion in the basin. Hillslope erosion (sheet and rill erosion) is the most important contributor to soil loss from the basin. It occurs over the widespread cultivated slope land, and on crop-rotation land and wasteland, which constitute a large proportion of the farmland in the basin. In the upper Jialing basin, for example, 70 % of farmland is found on slopes of 20-30°. In the mountain and hill areas of the Lower Jinsha basin,

cultivated slope land accounts for 50-90% of the total farmland, and one third of the cultivated land has slopes of over 25° (Dai and Tan, 1996; Lu *et al.*, 2003a). When heavy rainfall occurs over the area, the topsoil, being characterized by steep slopes, thin soil layers and sparse vegetation in many places, is easily eroded by rain splash and overland flow.
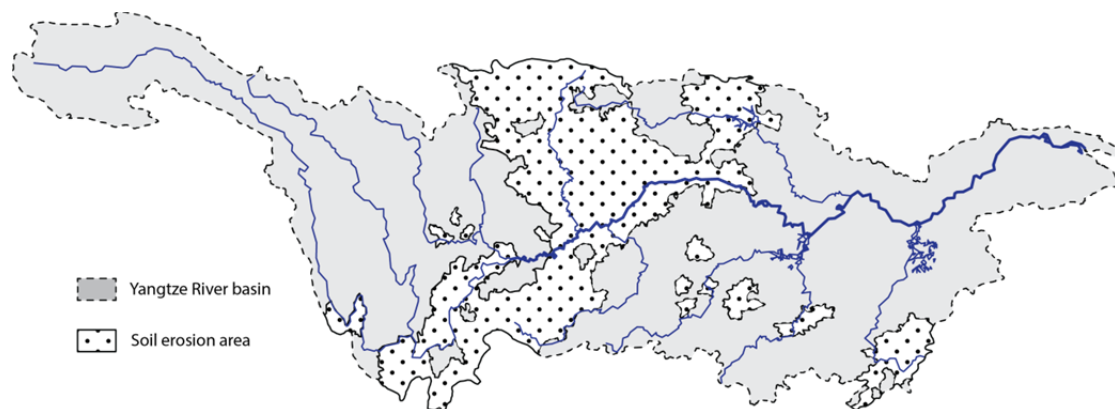
Figure 3.8 Map of soil erosion in the Yangtze River basin

Water conservancy plans, focusing on irrigation and water-soil conservation, had been proposed as early as in the 1950s, while substantial work, the Changzhi Project, inaugurated in 1989 (Xu, 2004). Four regions with severe water and soil loss have been selected in the first phase: the lower Jinsha River, the upper and middle reaches of the Jialing River and the Three Gorges Reservoir region. The total soil-loss area in the Yangtze River basin is 531,000 km^2, of which affects 524,000 km^2 (Figure 3.8). The percentages of regions where erosion is extremely severe to severe, moderate and slight levels are 3.2%, 14.5%, 40.5% and 41.8%, respectively (CWRC, 2007b).

The Changzhi Project has involved terracing, afforestation and small hydraulic

engineering measures over 700 watersheds, controlling sediment production from 150,000 km^2 (Dai *et al.*, 2002). As a result of the Changzhi Project, the sediment yield in upper Yangtze reach decreased gradually, especially in two high-yield regions: the Jialing River and the lower Jinsha River (Xu *et al.*, 2006).

The soil and water conservation has complicated the assessment of the cumulative impacts of reservoirs on sediment retention because decreased sediment loads are a joint result of the above discussed factors and reservoir retention. For example, despite the evidence for increased precipitation in the lower Jinsha tributary basin, sediment load at Yichang station has decreased. In such a large river basin as the Yangtze River, the effects of increased sediment fluxes from some tributary basins could be 'averaged out' and, equally, some increases could be offset by decreases elsewhere (Walling and Fang, 2003). Therefore, it is challenging to distinguish the impact of reservoir sediment trapping from the effects of other factors.

3.5.3 Dam and reservoir construction

In the Yangtze River basin, rapid economic growth has increased the pressure for greater hydropower production and other water-related developments, such as large-scale irrigation. Before 1949, there were only several small hydroelectric dams in the Yangtze River basin. Since the 1950s, the reservoir construction experienced fast development; numerous reservoirs have been constructed in the river basin. The development of reservoirs can be divided into three phases (Yang and Lu, 2013a). The

first phase (from the 1950s to the 1970s) was set for a dramatic development of the country's hydropower industry. From the 1950s and 1970s, China experienced a "great leap forward" in terms of hydraulic engineering projects, leading to the construction of most of China's reservoirs. By the end of the 1970s, the state-organized campaigns for electricity, irrigation, and flood control succeeded in building nearly 80,000 reservoirs, more than half of which were located in the Yangtze River basin (National Bureau of Statistics of China, 1993). During the second phase (from the 1980s to 1990s), Less than 4,000 reservoirs were built in the Yangtze River basin; but the growth rate of large reservoirs maintained a higher level than in the first phase, indicating that the government principally focused on large reservoir projects. The same trend continued in the next phase after the 1990s. By 1992, when the Three Gorges Project was approved for construction, China already had 369 large reservoirs, 125 of which are in the Yangtze River basin. By 2009, when the Three Gorges project was completed, the number of large reservoirs in the Yangtze River basin increased to 190 (Yang and Lu, 2014a).

Despite the economic benefits, such as energy generation, construction of these reservoirs has also caused severe environmental and ecological problems (Yang and Lu, 2013b). For example, after the construction of the Three Gorges Dam, the riparian ecosystem has been significantly disrupted (Wu *et al.*, 2003). For example, stagnant water in the tributaries has elevated pollution levels — an existing concern for populations along the Yangtze River. The dam has blocked approximately ten million

tons of plastic bags, bottles, animal corpses, trees, and other detritus that would have otherwise flowed out to sea (Yang and Lu, 2013b). Since 2004, algal blooms caused mainly by dinoflagellates have occurred each February in 22 Yangtze tributaries including the Xiangxi, Pengxi, and Daning rivers (Fu *et al.*, 2010). Water impoundment has also resulted in lower water levels in the downstream channel and less water storage in the adjoining riparian lakes (e.g., Dongting and Poyang lakes), which contributed to extreme drought conditions in 2011 when precipitation was low (Lu *et al.*, 2011). Additionally, the delta front has shifted from sediment accumulation during the 1960s to an erosion rate of approximately 100×10^6 m^3 $year^{-1}$ in recent years (Yang *et al.*, 2011), exacerbating saltwater intrusion in the Yangtze estuary.

As stated above, the direct and indirect impacts of a certain dam (e.g. the TGD) have been widely reported; but few studies have addressed the cumulative impacts by multiple dams because these impacts manifest in a cumulative manner over broad temporal and spatial scales. Given the development of contiguous cascade dams on the major tributaries of the Yangtze River, it is an excellent to opportunity to integrate a large amount of existing information in a cumulative impact context.

3.5.4 Land reclamation and lake shrinkage

Another important factor affecting fluvial processes is lake shrinkage caused by land reclamation in the middle and lower Yangtze reaches. Previous studies (Shi and Wang, 1989; MWR, 1998; Wang and Dou, 1998) have reported that the sharp decrease in the

number and surface area of lakes occurred from the 1950s to the 1970s due to land reclamation. Since when I delineated reservoirs, natural lakes were also extracted in this study, a more detailed discussion on lake shrinkage is given later in Chapter 4. On this point, there is no longer discussion here.

4 Reservoir delineation and water regulation assessment

4.1 Introduction

It is estimated that today 8 million lake larger than 1 ha (Meybeck, 1995) and 304 million small ones (Downing *et al.*, 2006), approximately 45,000 reservoirs with dam higher than 15 m (Lehner *et al.*, 2011) and some 800,000 smaller ones (McCully, 2001) exist worldwide. Due to the their basic ability to retain, store, clean, and evenly provide water, as well as their distinct characteristics as still-water bodies, lakes and reservoirs constitute essential components of the hydrological water cycle, and affect many aspects of environment, ecology, economy, and human welfare. Therefore, knowledge about the distributions of lakes, reservoirs and wetlands is therefore of great interest in many scientific disciplines. Despite this regional significance, few comprehensive data sets exist which comprise information on location, extent and other basic characteristics of open water bodies and wetland areas on a global scale (Lehner and Doll, 2004).

However, the correct classification (on aerial imagery) of an open water surface or a mixed vegetation area, say into 'lake', 'pond' or 'reservoir', is difficult. Misinterpretation of the spectral signal may lead to errors, and the provided raster-cell representation hinders a clear identification of separate lake pools, individual reservoirs or single components of braided river and lake systems. Despite their

individual limitations, the existing lake and reservoir registers, maps and databases are highly valuable sources of information, focusing on different geographic regions or aspects.

As an alternative to the above data sources, recent developments in the field of remote sensing, including increases in data quality and resolution, promise large-scale land cover images making it possible to monitor spatio-temporal changes in lake and reservoir extent. For example, Landsat Thematic Mapper (TM)/Enhanced Thematic Mapper Plus (ETM+) imagery has been employed in recent studies to delineate water bodies in Zimbabwe (Sawunyama *et al.*, 2006), India (Mialhe *et al.*, 2008), Ghana (Annor *et al.*, 2009) and the Yellow River of China (Ran and Lu, 2012). This chapter presents a parsimonious approach to rapidly delineate reservoirs, which combines information of both categories i and ii introduced in section 2.2 in a consistent manner. The specific aims of this chapter are to: (a) explore the advantages of using remote sensing techniques to delineate water bodies across the entire Yangtze River basin, (b) establish empirical formulas to quantify the storage capacity of reservoirs and lakes and (c) assess the magnitude and distribution of the potential impacts of reservoirs on water regulation at a basin-wide scale.

4.2 Data and methods

4.2.1 Data sources and data preprocessing

Remotely-sensed data provide a means of delineating water body boundaries over a

large area at a given point in time. The Landsat program is the longest running enterprise for acquisition of satellite imagery of Earth. Its Landsat Thematic Mapper (TM) and Enhanced Thematic Mapper Plus (ETM+), which acquired digital-format imagery with 30 m spatial resolution in seven spectral channels, have become a unique resource in the study of albedo and its relationship to water scape change. Landsat TM/ETM+ images, mainly acquired after the monsoon season (September–October) in the period 2005 to 2008, were used in this study. A total of 104 images, including 94 TM images and 10 ETM+ images, were used (Figure 4.1). On 31 May 2003, the ETM+ Scan Line Corrector (SLC) failed, causing the scanning pattern to exhibit wedge-shaped scan-to-scan gaps. Images acquired after the SLC failure are referred to as SLC-off images. In this study only SLC-off images were used. An approach (Scaramuzza *et al.*, 2004) was used to fill gaps in Landsat ETM+ SLC-off images.

Ideally, contemporary data for the same year were used, but the limited availability of cloud-free data necessitated the use of data from multiple years (from 2005-2008). Even then, cloud-free images covering the entire Yangtze River basin could not be found. Haze correction and cloud removal for some images was used in image pre-processing. Five images with clouds were used. For images with thin clouds or haze, the approach proposed by Martinuzzi et al. (2007) was used for haze correction. For images with thick clouds, this study have developed a program based on thresholding that segments an image into two categories (cloud, non-cloud) defined by a single DN (digital number) threshold. The detected thick clouds were then replaced with a suitable

value by looking into the next or previous available images. After that, the images could be used in this study. All the images were acquired from the United States Geological Survey (USGS) (http://glovis.usgs.gov/, last accessed in October 2013).

Additionally, the very high-resolution satellite data IKONOS and QuickBird images from the Google Earth mapping service were used for selected areas to improve and validate the classification of water bodies. DEMs (digital elevation models) with a spatial resolution of 90 m were downloaded from the Consultative Group on International Agricultural Research (CGIAR) (http://srtm.csi.cgiar.org, last accessed in October 2013) and used to determine the backwater region of each reservoir.
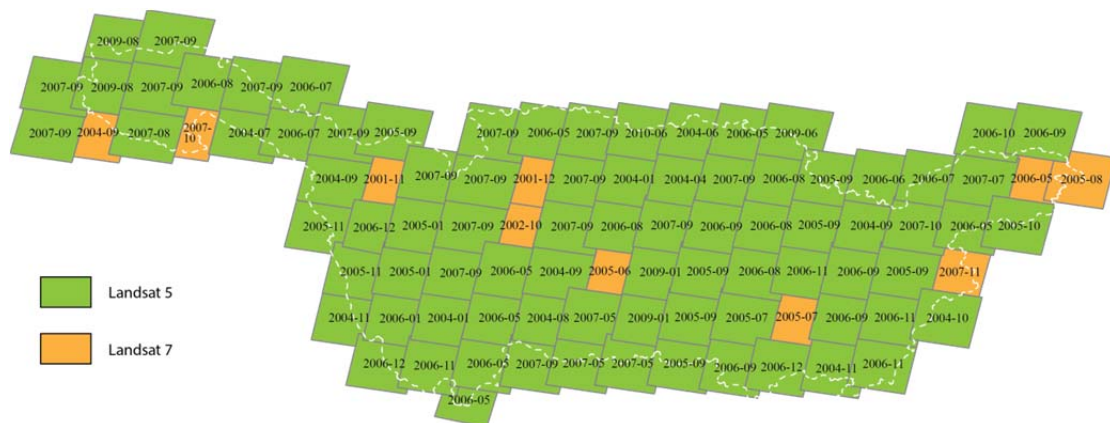
Figure 4.1 Landsat TM/ETM+ images used in this study.

4.2.2 Water body detection and classification

The overall procedure of image processing can be summarized into two phases, namely, water body detection and water body classification (Figure 4.2). Because processing approximately 100 satellite images would have been time-consuming and

labor-intensive, this study developed an automated procedure that employs multiple thresholds, generating the DN magnitudes normalized difference vegetation index (NDVI)(Tucker, 1979) and normalized difference water index (NDWI) (Gao, 1996) and differences in the spectral characteristics of different land cover types (e.g., water, snow, bare land and vegetation) in visible, near infrared and mid-infrared bands. An automated computer program has been developed, which employs multiple thresholds to generate the DN magnitudes NDVI and NDWI and differences in the spectral characteristics of different land cover types (e.g., water, snow, bare land and vegetation) in visible (band 3), near infrared (band 4) and mid-infrared bands (band 5). The normalized difference snow index (NDSI)(Sidjak, 1999) threshold was also used to remove the impact of snow on the Tibetan Plateau. Also, Digital elevation model (DEM) data was integrated in this program to remove the impact of shadows in mountainous areas (Figure 4.3). However, it should be noted that no specific thresholds for the parameters were set because I could manually adjust the threshold to achieve the best overall result for each image. In this step, satellite images were classified into two categories: water and non-water. The results were then converted into polygons with contiguous pixels and stored in a shapefile. Subsequently, as a result of filtering, any object smaller than 4 pixels or 0.0036 km^2 was automatically removed from the data to remove image noises. The removed water bodies are insignificant in size; therefore, they had an insignificant effect on the total area.
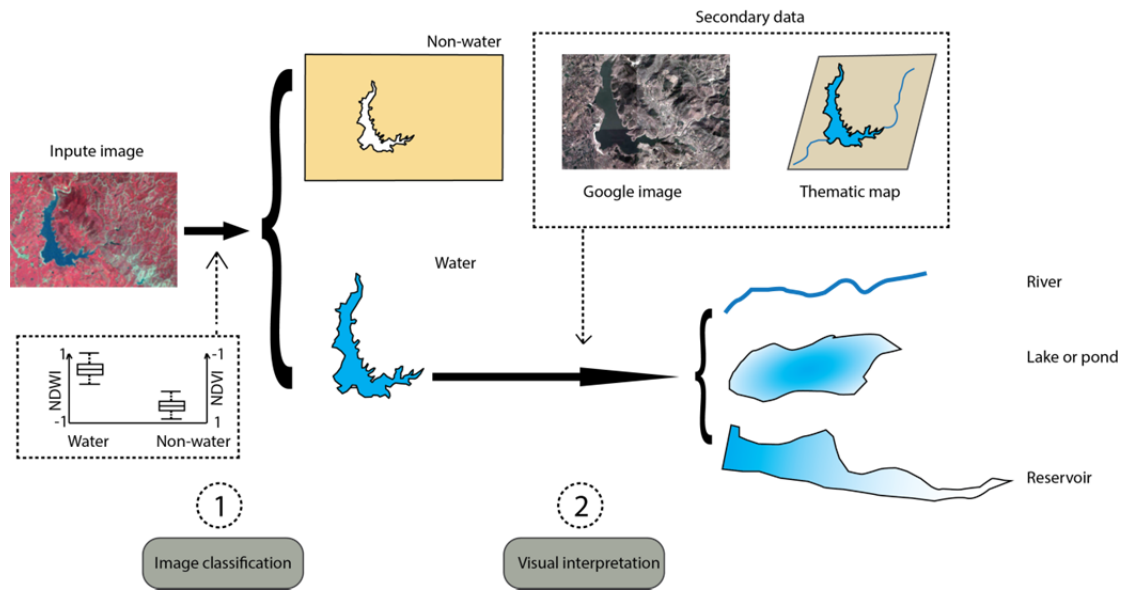
Figure 4.2 Flow chart of water body detection and classification using remote sensing techniques. NDWI is the normalized difference water index derived from Landsat TM bands 4 and 5, (TM4 - TM5)/(TM4 + TM5) (Gao, 1996); NDVI is the normalized difference vegetation index derived from Landsat TM bands 4 and 3, (TM4 – TM3) / (TM4 + TM3) (Tucker, 1979).
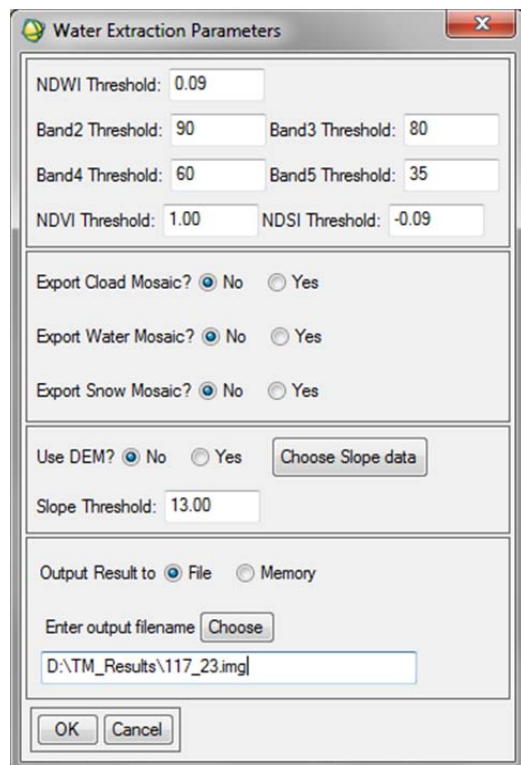
Figure 4.3 A computer program developed by me for water discrimination, the program was integrated into the software of ENVI 4.7.
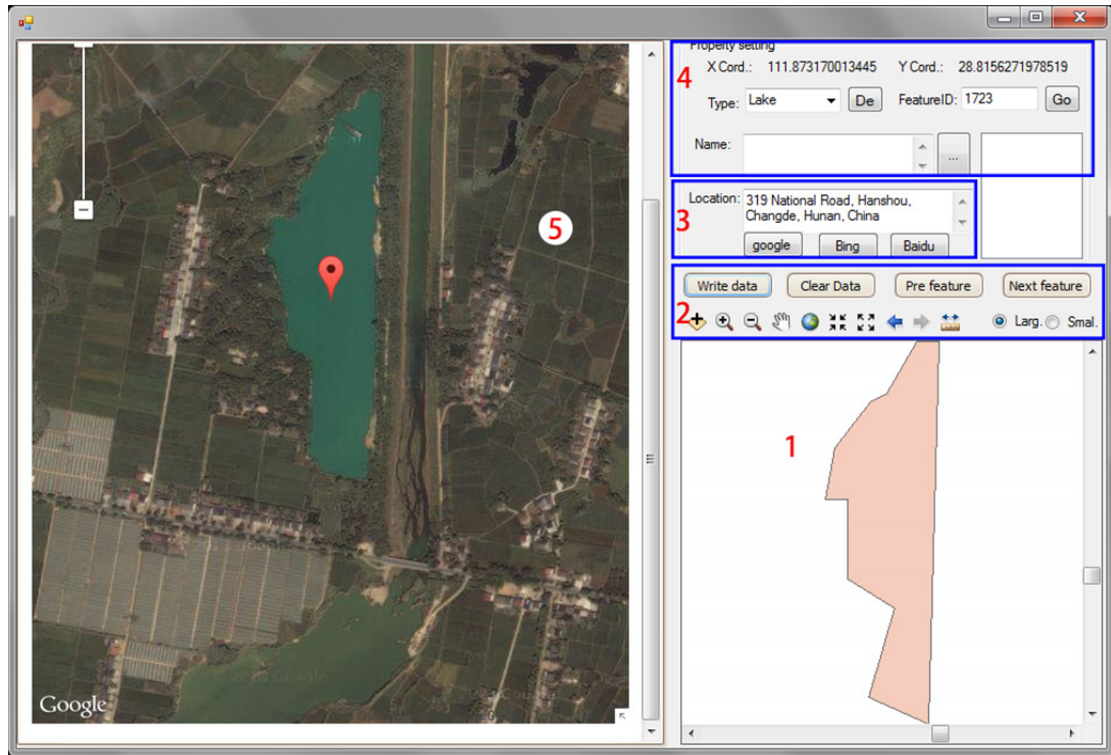
Figure 4.4 The tool kit used for visual interpretation. 1. Polygon to be classified; 2. Tools to operate map (zoom in, zoom out, pan, etc.) (the "Write data" button is used to save information such as water types, locations and names); 3. Electronic maps/images (shown in left panel) used as auxiliary data; 4. Real-time data request from GeoNames geographical database based on the polygon's coordinates. Using visual cues, such as tone, texture, shape, pattern, and relationship to other objects, I could easily classify polygons into different types. The auxiliary data were automatically extracted by the tool kit; it could be carried out the classification efficiently.

In the second step, based on secondary data and high-resolution satellite data from Google Earth, the polygons were visually interpreted to classify water bodies into three classes: lakes (lakes and ponds), artificial reservoirs and rivers. One of the major impediments to the classification was that there are numerous paddy fields and aquacultural farms which have similar spectral characteristics to natural lakes in the lower reaches of the Yangtze and Pearl rivers. To reduce misclassification error, this

study used ancillary data, visual interpretation and expert knowledge of the area

through GIS to visually interpret the images. Using visual cues, such as tone, texture,

shape, pattern, and relationship to other objects (a reservoir has an associated dam), an

observer can identify many features on high-resolution images (such as Google Earth

image). This study has also developed a computer program to assist me visually classify

each polygon into different water-body types. I could easily and efficiently classify

each polygon into different water-body types. After classification, other features of the

water bodies such as surface area, names and administrative divisions were also added

to the dataset.
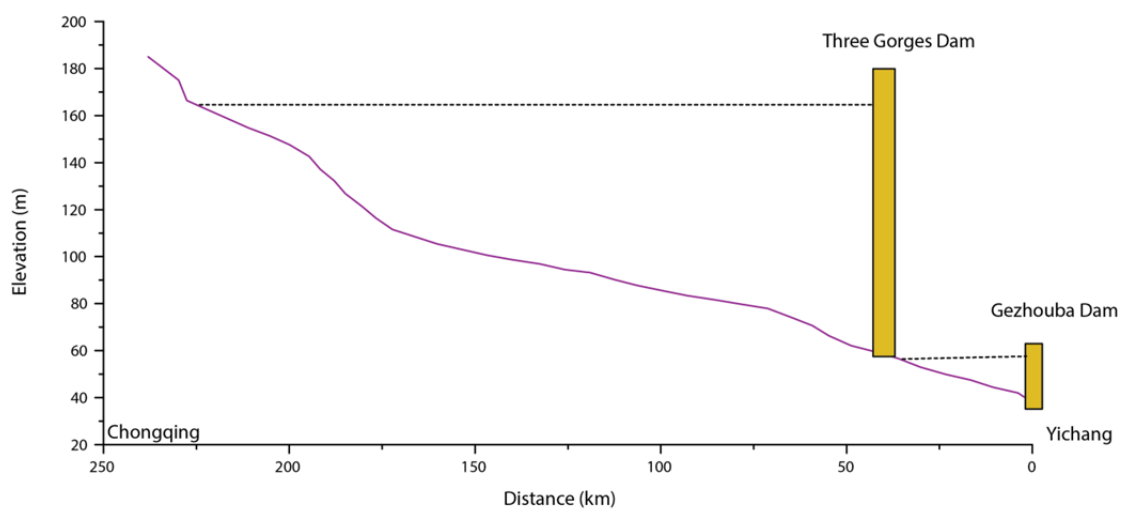
Figure 4.5 Identification of the backwater region of cascade hydropower reservoirs to identify reservoir boundary using the Three Gorges Reservoir as an example.

The cascade reservoirs were identified by the dam locations identified in the

high-resolution Google Earth images, which was necessitated by the lack of data on

backwater curves. The shape of each reservoir was determined based on the assumption

that the water surface within the reservoir was flat. The Three Gorges Reservoir (TGR)

73

as an example (Figure 4.5). First, the Yangtze River polygon was divided into two parts at the location of the Three Gorges Dam (TGD). The section behind the TGD was then superimposed on the DEM. If a pixel near the dam intersected the polygon boundary, the pixel was marked and the water surface level at that point was determined from the DEM. The average elevation of all marked pixels was used to estimate the water surface level in the TGR. Second, for each cell located inside or partially inside the Yangtze River polygon, the height difference between the DEM value for that cell and the water level was calculated. The boundary of the TGR was delineated by connecting the cells for which the difference between the elevation for the cell and water level for the dam was zero. Figure 4.5 shows the water level at 165 m, with the area delineated as backwater reaching almost to Chongqing.

4.2.3 Estimating reservoir and lake storage capacity

Many studies have demonstrated the existence of a robust relationship between the surface area and storage capacity of reservoirs at both regional and global scales (Lehner *et al.*, 2011; Ran and Lu, 2012). This relationship was used to develop a method for area-based estimation of reservoir storage capacities. Meigh (1995) first developed a formula for the power relationship between capacity (C; 10^6 m^3) of a reservoir and its surface area (A; km^2):

$$C = \mathrm{a}A^{\mathrm{b}} \tag{4.1}$$

where a and b are constants.

To build the regression equation, data on the storage capacities of 1,185 reservoirs ($0.01–10$ km^3) and 1,118 large lakes (surface area ≥ 1 km^2) were collected from official documents of the Chinese government, particularly a series of reports on reservoir development from the Yangtze (Changjiang) Water Resources Commission (CWRC). A number of other ancillary data sources as well as information from previous studies (MWR, 1998; Wang and Dou, 1998) were also used. This study adopted a very conservative approach to data collection; i.e., only storage capacity values that appeared in multiple sources were used in order to guarantee data quality.

The equations established for reservoirs and lakes in the Yangtze River basin were as follows:

$$\text{Large reservoirs (A} \geq 3.3 \text{ km}^2\text{):} \quad C = 28.386 \times A^{1.0516} \quad (R^2 = 0.8438) \tag{4.2}$$

$$\text{Small reservoirs (A} < 3.3 \text{ km}^2\text{):} \quad C = 30.382 \times A^{0.9859} \quad (R^2 = 0.8801) \tag{4.3}$$

$$\text{Large lakes (A} \geq 10 \text{ km}^2\text{):} \quad C = 1.5018 \times A^{1.1104} \quad (R^2 = 0.9236) \tag{4.4}$$

$$\text{Small lakes (A} < 10 \text{ km}^2\text{):} \quad C = 1.625 \times A^{1.0611} \quad (R^2 = 0.7374) \tag{4.5}$$

In China, reservoirs are classified based on volume into the categories of large ($C \geq 0.1$ km^3 or $A \geq 3.3$ km^2), medium ($0.1 > C \geq 0.001$ km^3) and small ($C < 0.001$ km^3), whereas the lake classification is based on surface area, with small, medium and large

lakes having a surface area of < 1.0, 1–10, and > 10 km^2, respectively. Based on these two physical characteristics of reservoirs and lakes, this study divided the reservoirs into two groups (large and small) to obtain better regression equations (Eqs. 4.2 – 4.5).

Because of the relatively low resolution of Landsat TM/ETM+ images and the effects of mixed pixels and shadow removal, it was not possible to accurately identify smaller water bodies (< 3,600 m^2) using the Landsat images. Therefore, this study estimated their surface area and volume based on previous studies that have suggested that the global distribution of natural lakes and their surface area can by described by a power law distribution (Lehner and Doll, 2004) and a similar distribution has been proposed for artificial reservoirs at global and regional scales (Downing *et al.*, 2006). By fitting such a statistical distribution to the data, the number of lakes in the Yangtze River basin can be expressed as a power function of their area as follows:

$$N_{A \geq A_t} = 581 \times A^{-0.768} \quad (R^2 = 0.9985) \tag{4.6}$$

and the number of reservoirs can be expressed as:

$$N_{A \geq A_t} = 871 \times A^{-0.796} \quad (R^2 = 0.9884) \tag{4.7}$$

where $N_{A \geq A_t}$ is the number of reservoirs or lakes with an area greater than or equal to a threshold area (A_t ; km^2). Using Eqs. (4.6) and (4.7), this study estimated the total number and surface area of the small lakes and reservoirs in the basin.

4.3 Results

4.3.1 Quantity and surface area of delineated lakes and reservoirs

This study delineated 43,602 reservoirs and 42,708 lakes, covering approximately 8,606 km^2 and 16,236 km^2, respectively, of the territorial land surface. The surface area distribution for lakes and reservoirs are shown in Figure 4.6. When the surface area data were transformed to a log scale, a linear regression could not be fit to either the reservoir or the lake data. It reveals that while most lakes and reservoirs in the Yangtze River basin are small, large lakes and reservoirs account for most of the basin's water surface area. For example, small lakes (< 1 km^2) are the largest in number (~99%), but their total surface area is only 1,419 km^2. Medium and large lakes (>1 km^2), of which there are 573, make up approximately 1% of the total number of lakes and represent 91.2% of the total surface area (Table 4.1). The relatively large contribution of large lakes to total surface area is consistent with previous reports (Wetzel, 1990; Kalff, 2001). Similarly, large reservoirs ($C \geq 0.1$ km^3 or $A \geq 3.3$ km^2) with a capacity of approximately 189.6 km^3, account for only 0.7% of the total number of reservoirs, yet they provide 65.8% of the total storage capacity (Table 4.2). Therefore, large reservoirs are most likely to have the greatest impact on downstream river systems. Global proportions are similar, with the 633 world largest reservoirs (storage capacity > 0.5 km^3) representing 60% of the total global capacity

(Vörösmarty *et al.*, 1997). Small reservoirs are numerous, but their aggregate effect is likely to be small except in highly localized contexts (Graf, 1999). The results shown in Tables 4.1 and 4.2 show that artificial reservoirs have overtaken natural lakes in terms of total number and storage capacity and have become the dominant water bodies in the Yangtze River basin.
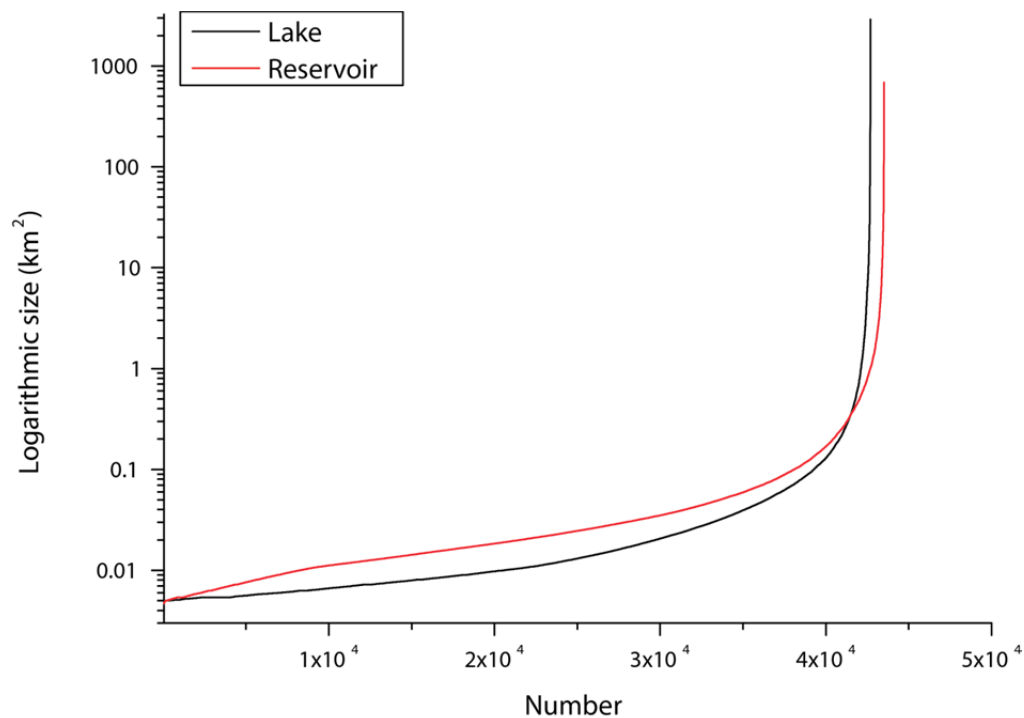
Figure 4.6 Lake and reservoir size distributions in the Yangtze River basin.

The frequency distributions for lake and reservoir surface area closely follow a power law distribution (Tables 4.1 and 4.2). The smallest reservoirs occur at the highest frequency (> 95%) and the frequency of reservoirs descends exponentially with increasing surface area. The distributions are roughly consistent with certain general laws in stream morphometry, such as Horton's law of stream numbers (Horton, 1945).

This law refers to the expected number of streams in a certain stream order, where lower-order stream segments are more frequent than higher-order stream segments. Thus, the two frequency distributions of lake and reservoir surface area closely mirror Honton's law, which is applied to and derived from stream morphometry. The surface area frequency distributions of lakes and reservoirs in the Yangtze River basin, according to Horton's law, are presumably indicative of their fractal nature.
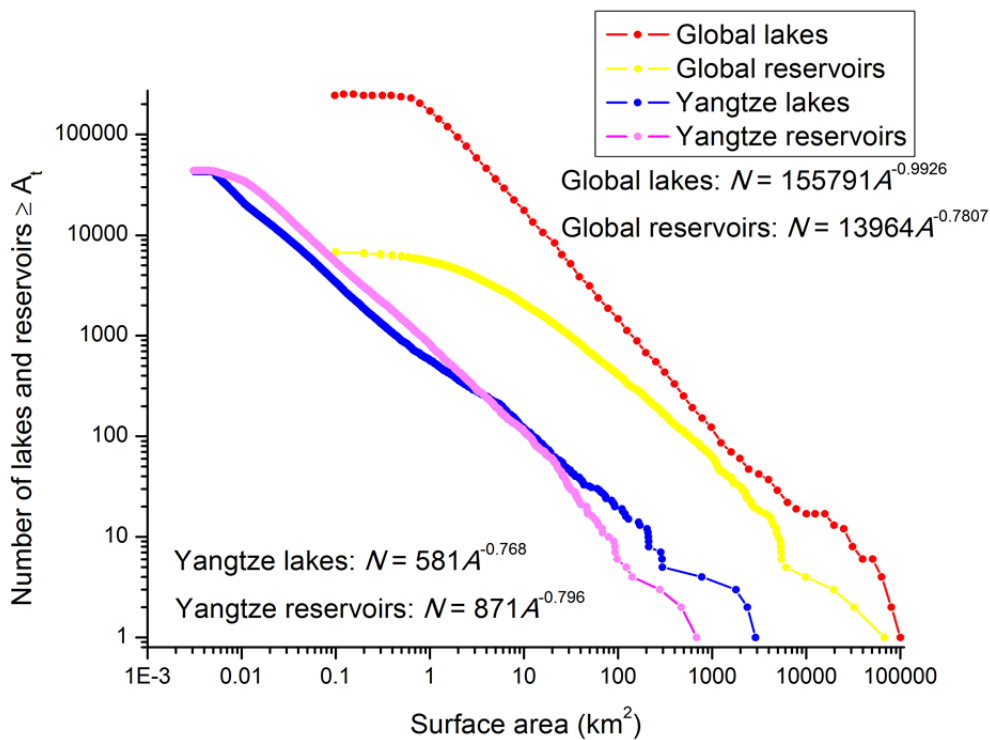
Figure 4.7 Number of reservoirs and lakes (y axis) exceeding increasing surface areas (x axis), based on remotely sensed results and data presented by Lehner *et al.* (2011). For global lakes and reservoirs, they assume that the reservoirs (> 10 km^2) and lakes (> 1 km^2) surface are complete records, and trend lines (not shown) were fitted for lakes and reservoirs, respectively.

In addition, the results of the integral distributions of lake and reservoir surface area (total number N of lakes larger than area A_t) are interesting from a statistical

79

Table 4.1 Number of lakes from remote sensing and estimation using Eq. (4.6).

Lake area (km²)		Extracted results				Predicted results			
Min	Max	Num. of lakes	Avg area (km²)	Total area (km²)	Volume (km³)	Num. of lakes	Avg area (km²)	Total area (km²)	Volume (km³)
0.0001	0.001					461,342	0.00028	129	0.1
0.001	0.0036					59,855	0.00183	109	0.1
0.0036	0.01	20,571	0.007	143	0.17				
0.01	0.1	18,715	0.029	536	0.71				
0.1	1	2,849	0.26	740	1.12				
1	10	453	3.2	1,451	2.57				
10	100	101	26.7	2,695	5.98				
100	1,000	16	226.7	3,627	10.1				
1,000	10,000	3	2348	7,044	25				
Total		42,708		16,236	45.65	521,197		238	0.2

The results include both completely natural lakes and regulated natural lakes.

Table 4.2 Number of reservoirs from remote sensing and estimation using Eq. (4.7).

Reservoir area (km^2)		Values based on remote sensing				Estimated values			
Min	Max	Num. of reservoirs	Avg area (km^2)	Total area (km^2)	Volume (km^3)	Num. of reservoirs	Avg area (km^2)	Total area (km^2)	Volume (km^3)
0.0001	0.001					609,448	0.000278	169	3.2
0.001	0.0036					74,958	0.001823	137	2.9
0.0036	0.01	8,358	0.0071	59.8	1.9				
0.01	0.1	29,825	0.029	877	27.9				
0.1	1	4,597	0.28	1,282	39.6				
1	10	711	2.6	1,875	57.4				
10	100	105	25.6	2,697	91.5				
100	1000	6	302.48	1,815	70				
Total		43,602		8,606	288.3	684,406		306	6.1

The minimum reservoir area (0.0001 km^2) corresponds to the smallest reservoirs practically recognizable (Downing *et al*. 2004). Reservoirs do not include regulated natural lakes which occupy because more than 80% of natural lakes in the middle and lower Yangtze watersheds.

perspective. Lehner et al. (2004; 2011) reported that the most striking statistical feature of global lakes and reservoirs is the linearity of their distributions when drawn on a double logarithmic scale. A similar trend was also observed in the Yangtze River basin (Figure 4.7). Compared to the global reservoir distribution, the distribution of Yangtze reservoirs has an even steeper rise and thus has a relatively higher total number of small reservoirs (derived from Eq. 4.7). This result suggests that reservoir density in the Yangtze River basin is greater than the global average and therefore, the basin has experienced a relatively high density of anthropogenic impacts. However, the lake surface area distribution has a much flatter rise than that of global lakes. This curve suggests that the average density of lakes in the Yangtze River basin is lower than the global average. For a formerly glaciated area such as Canada, the lake distribution curve is much steeper than the global average distribution (Lehner and Doll, 2004).

4.3.2 Spatial distribution of lakes and reservoirs

Reservoir density in the Yangtze River basin (Figure 4.8) shows a clear east-to-west gradient except in the Sichuan Basin. The reservoirs are mainly distributed in the middle and lower reaches. The highest density of dams occurs on the Poyang Lake floodplain, which has a density of 0.71 reservoirs km^{-2}. The high reservoir density reflects the legacy of this region's long history of mill dams for irrigation and aquaculture. In addition, Figure 4.8 shows that more than half of the large reservoirs
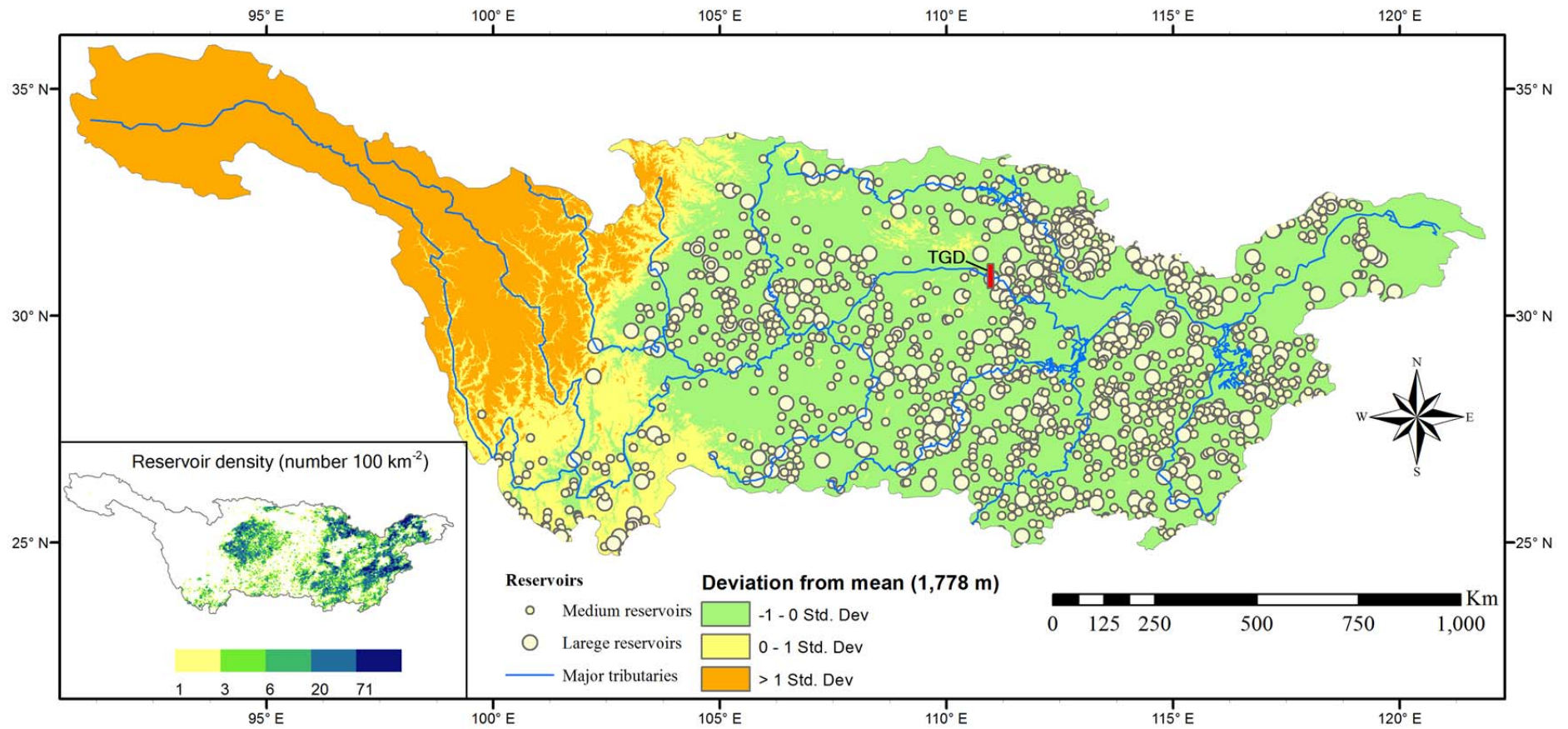
Figure 4.8 Spatial distribution of reservoirs with respect to topography. The reservoirs are mainly located in the middle and lower reaches in low-relief areas (within -1 to 1 standard deviation from the main elevation of 1,778 m.
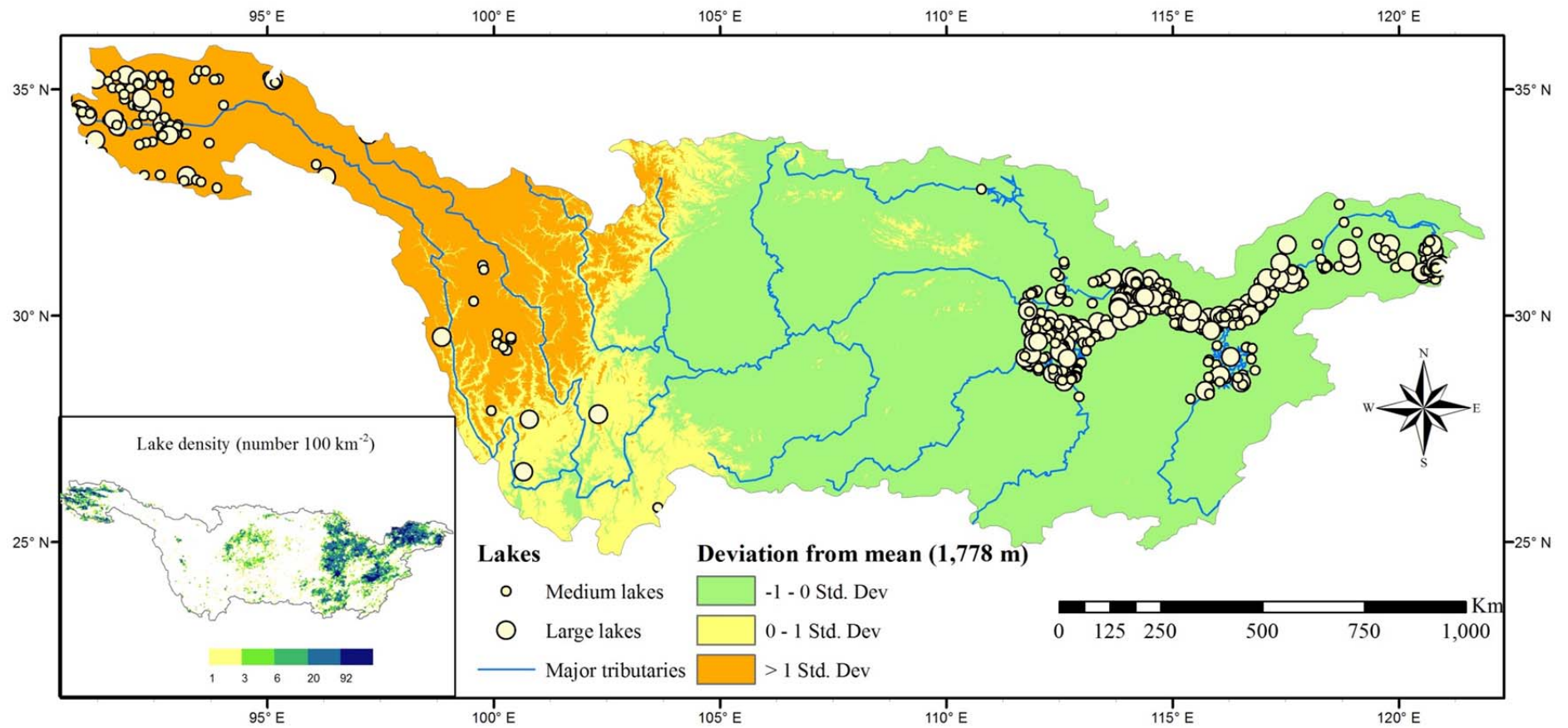
Figure 4.9 Spatial distribution of lakes with respect to topography. Most lakes are distributed in the middle and lower reaches, but many lakes also occur in the upper reaches.

are built along the mainstream channel and major tributaries, indicating that reservoir construction is the combined result of naturally occurring stream morphometry phenomena and man-made features that have anthropogenic impacts. Additionally, the higher frequency of lower-order segments shown in Table 4.2 indicates a greater number of opportunities for dam construction, and vice-versa. The dimensions of reservoirs on lower-order segments are comparably small, but the construction is easier and cheaper, which again addresses a large number of potential needs.

Figure 4.9 shows the density of lakes in the Yangtze River basin. Most lakes are located in the middle and lower reaches, especially in the areas near Poyang, Dongting, Chaohu and Taihu Lakes. The highest density occurs in the lower reaches around Chaohu Lake at 0.92 lakes km^{-2}. However, many lakes also occur in the upper reaches in areas such as the Qinghai-Tibet Plateau. The density of lakes in the Sichuan Basin is relatively low compared to the density of reservoirs (Figure 4.8). Most large lakes in the middle and lower Yangtze River basin are located along the main trunk stream and major tributaries, which feed into or drain the lakes. However, many large lakes in the Qinghai-Tibet Plateau do not follow this pattern because they are glacial lakes (Chen et al., 2007).

Topography helps explain why the spatial distributions of quantity and surface area of artificial reservoirs differ from those of natural lakes. The maps in Figure 4.8 and Figure 4.9 show the steps of standard deviation (1,782 m) of the mean elevation

(1,778 m) against the distributions of lakes and reservoirs. Figure 4.8 indicates that the reservoirs are mainly located in low-relief areas (within -1 to 1 standard deviations of the mean) and there are no reservoirs outside of 1 standard deviation of the mean elevation. In contrast, the distribution of natural lakes corresponds to the full range of standard deviation values, although most of the lakes are located in the lower-elevation range. These results suggest that, despite the natural topographic constraints, the distribution of artificial reservoirs is determined to a great extent by human needs.

4.3.3 Estimated volume of lakes and reservoirs

The total estimated reservoir storage capacity is approximately 288 km^3, representing approximately 28% of the annual discharge of the Yangtze River (Table 4.2) but only 46 km^3 of the total estimated lake volume (Table 4.1). The total reservoir storage capacity is slightly higher than the 250 km^3 value reported by MWR (2011). This difference in capacity is mainly due to changes that have occurred between the two periods of data collection, given that reservoir construction has progressed rapidly in recent years.

This study estimated a total of 684,406 small impoundments and 521,197 small lakes of <3,600 m^2 in size, with a total capacity of approximately 6.1 km^3 and 0.2 km^3, respectively (Tables 4.1 and 4.2). The total capacity of all reservoirs is approximately 294 km^3 and their total area is approximately 8,910 km^2. Nevertheless, it should be

highlighted that the total area of natural lakes (> 0.0036 km^2) is 16,236 km^2, which is much less than the 21,000 km^2 previously reported by Wang et al. (2006) using data produced in the 1980s. although some of the difference could be a result of different measurement methods (e.g., field survey and remote sensing), the difference should be much low because the results reported Wang et al. (2006) was based on topographic maps and thus the accuracy could be guaranteed. The lakes in the Yangtze River basin have experienced dramatic shrinkage in recent years due to land reclamation and urbanization.

The results for quantity, surface area, and storage capacity of smaller reservoirs and natural lakes also differ considerably from some previous studies (Lehner and Doll, 2004; Downing *et al.*, 2006; Lehner *et al.*, 2011). First, previous studies indicate that natural lakes are much more abundant than reservoirs. However, this study found the opposite result in the Yangtze River basin. Second, at the global scale, the average area of small reservoirs (Lehner *et al.*, 2011) is larger than the average area of small reservoirs in the Yangtze River basin (Table 4.1), indicating that the waterscape in the Yangtze watershed is more fragmented. The differences between these results and the results of previous studies indicate that there have been strong anthropogenic impacts in the Yangtze River basin.

4.4   Discussion

4.4.1   Accuracy assessment

Errors occurred at the three stages, i.e., the extraction of water bodies, the classification of water bodies into reservoirs and lakes and the estimation of storage capacity. The accuracy of the identification and extraction of water bodies was mainly influenced by aspects of image quality such as resolution, cloud cover, shadows and sedimentation in the tail-water of reservoirs. First, the mixed pixels made some small water bodies, including small reservoirs, difficult to extract. Based on my experience, reservoirs with a width of less than two pixels cannot be extracted because both sides of the feature are affected by the mixed pixels. Thus, delineated water bodies that were smaller than 2x2 pixels or 0.0036 km^2 were removed to ensure that the delineated features were real water bodies. In addition, in rugged mountainous areas such as the upper Yangtze River basin, shadows may block solar radiation in narrow river valleys, making the identification of smaller water bodies difficult. However, these small reservoirs have a minimal effect on total surface area and storage capacity.

Smaller reservoirs and lakes were also difficult to distinguish from paddy fields and aquacultural farms because natural lakes, paddy fields and aquacultural farms share similar spectral characteristics. In fact, many aquacultural farmlands are reclaimed natural lakes. Visual interpretation can partly solve this problem. Based on my measurements, the accuracy for lakes with a surface area > 1 km^2 was 96% but the accuracy for small lakes was somewhat low (85%) because of misclassification of aquacultural farms and natural lakes. Some small lakes were misclassified as aquacultural farms because parts of the lakes were used for fish farming. Because of

these misclassifications and the results of my field measurements, the lake classification was double-checked and updated. However, it should also be noted that small lakes represent only 8.8% of the total surface area of lakes and thus the relatively low accuracy in the classification of small lakes has negligible impacts on the study results.
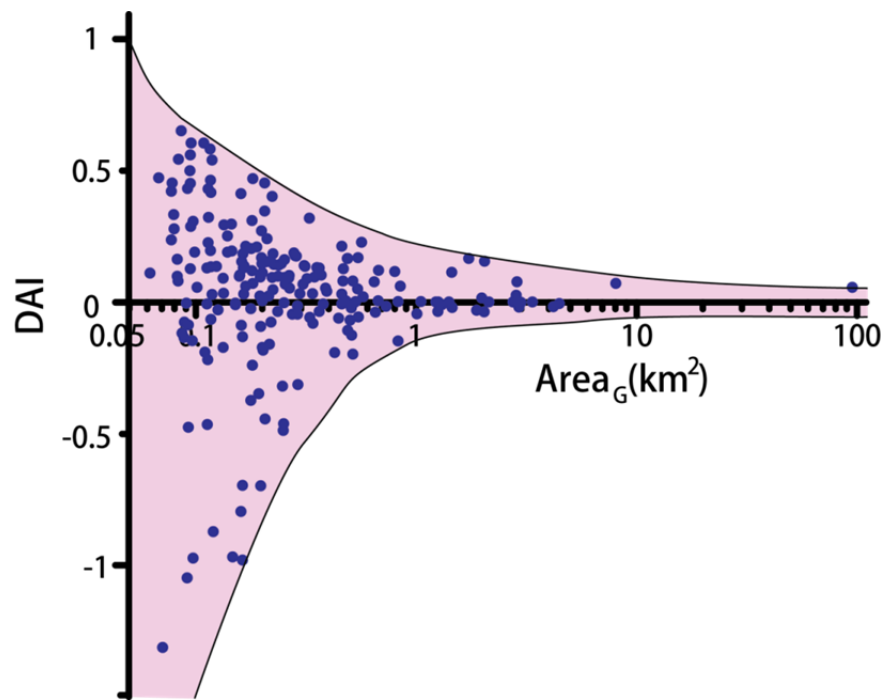
Figure 4.10 DAI distribution against area of lakes and reservoirs delineated in high resolution images using Google Earth[TM] polygon tool

In addition, sediments accumulate in the backwater of reservoirs, making the reservoir surfaces appear smaller than they are. Using remote sensing images that are acquired when the reservoirs are fully regulated is a possible solution, but some reservoir capacities were still underestimated due to the lack of available data for the study period.

Because image acquisition mainly took place in 2005 and 2008 and there was no field work during this period, there was no possible comparison between water body found in the field and in the images. The deviation area index (DAI) was therefore used to quantify the difference between the surface area derived from Landsat TM/ETM+ images and the area delineated in high resolution images provided by Google Earth in the similar period. Nevertheless, it should be noted that the slight discrepancy between Landsat TM/ETM+ images and high-resolution images provided by Google Earth is an objective phenomenon due to different acquisition time. Thus, the method based on DAI is just a rough assessment. The DAI is defined as follows:

$$DAI = (Area_G - Area_S)/Area_G$$

(4.8)

where $Area_G$ is the surface area of lakes and reservoirs delineated in high resolution images using Google Earth^{TM} polygon tool; $Area_S$ is the surface area derived from Landsat TM/ETM+ images. The DAI values obtained from this equation range from $-\infty$ to 1. Water bodies with values close to zero have the best match between $Area_G$ and $Area_S$ while moving to extremes indicates increasing deviations between the two areas (Liebe *et al.*, 2005).

Manual digitizing of high-resolution images is extremely laborious, especially for large water bodies because the accuracy of manual digitizing depends on how accurate a water-body boundary is duplicated on a computer by hand. To get an accurate water-body boundary, one had to pick as many points as possible. Two

hundred randomly selected water bodies with an area range of 0.05 km^2—100 km^2, including 100 reservoirs and 100 lakes, were used to assess the accuracy. The 200 water bodies are randomly distributed in all the large river basins.

The *DAI* distribution is shown in Figure 4.10. It can be seen that most DAI values range between -0.3 and 0.3 and, with the increase of the surface area, the absolute values of *DAI* close to zero, indicating that the larger are the water bodies, the better match of the surface areas. Figure 4.10 also shows that more DAI values for small water bodies are greater than zero, indicating small water bodies delineated in high-resolution images are slightly larger than their corresponding areas extracted from Landsat TM/ETM+ images. On average, the satellite based areas were found to be 8.1% smaller than the Google Earth^{TM} image based area estimates. This is not surprising because in Landsat TM/ETM+ images, reservoir and lake inlets could be identified until the width of the inlet/arm/peninsula is larger than 30 m due to the coarse resolution. This phenomenon was more common for small water bodies as it is more difficult to extract their boundaries on the coarse-resolution TM/ETM+ images. Although the accuracy for small water bodies (< 1 km^2) is relatively low, lakes and reservoirs with area greater than 1 km^2 contribute respectively 92% and 81% of the total surface area. Therefore, the relatively low accuracy for small water bodies has insignificant impact on further area-based analysis.

In the second stage, the classification of water bodies into lakes, reservoirs and rivers

was initially based on the GeoNames database and thematic map of water resources. This study used the center coordinates of the classified features on the thematic map and in the GeoNames database to facilitate the classification. Each water body was matched by its center coordinates to the corresponding feature on the thematic map and in the GeoNames database. For the water bodies without corresponding features on the thematic map and in the GeoNames database, visual interpretation using high-resolution Google Earth images was performed. A water body with the striking mark of a dam on the high-resolution images was classified as a reservoir and other bodies of water were classified as natural lakes. Thus, in this stage, accuracy depended largely on the accuracy of the GeoNames database and the thematic map. However, the reservoirs that did not have corresponding features on the thematic maps and in the GeoNames database could have been misclassified as natural lakes if their dams were not easily identified through visual interpretation. This was the major impediment to obtaining a high accuracy in the classification of water bodies.

The errors in the third stage, i.e., the estimation of storage capacity, were due to the shape of the terrain and topography. Most of the large reservoirs are constructed in valleys and rely on the natural topography to supply most of the reservoir basin, whereas most small reservoirs are bank-side reservoirs that are constructed to store the water pumped or siphoned from a river. This study used the area-capacity model introduced by Liebe et al. (2005) to develop area-capacity relationships for large ($C \geq$ 0.1 km^3) and small reservoirs ($C <$ 0.1 km^3):

$$C = \frac{1}{6} Ad \qquad\qquad (4.9)$$

where *d* is the depth of water stored behind the dam in meters (m) (Figure 4.11A). The value of *d* for valley-dammed reservoirs is slightly higher than for bank-side reservoirs within the same size range. To eliminate this influence, this study established two different area-capacity curves and fitted them separately to large and small reservoir data. The established empirical equations (Eqs. 4.2 and 4.3) also help to address this issue.
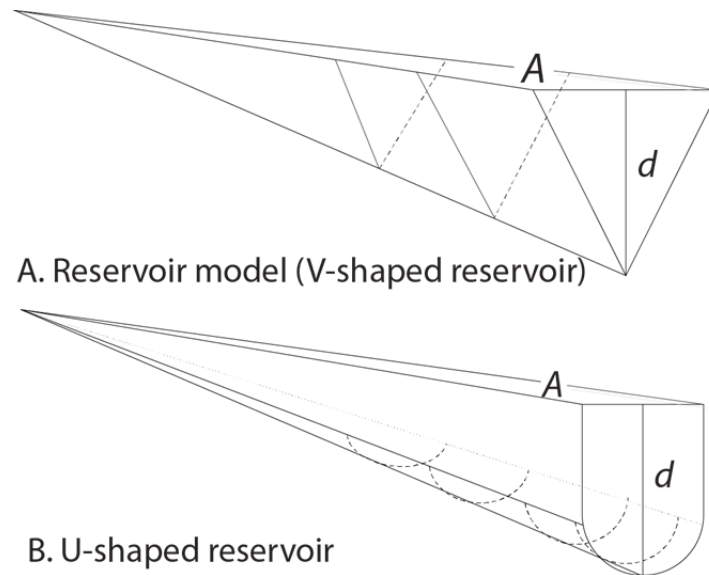
Figure 4.11 Reservoir model and reservoir shape examples. The theoretical derivation of this relationship starts with a cut V-shaped valley in order to approximately represent the shape and volume of a reservoir. The U-shaped reservoirs, built on U-shaped valleys formed by the process of glaciation, are observed in few regions of the Qinghai-Tibet Plateau.

In addition, the model used in this study is mainly based on the V-shaped reservoirs and arc-shaped lakes that are dominant in the study area. The established equations may not be a good fit for deep U-shaped reservoirs (Figure 4.11B) with very steep

sides because the area-capacity relationship of these reservoirs differs slightly from that of V-shaped reservoirs. However, there are few deep U-shaped reservoirs in the Yangtze River basin. Thus, the effect of reservoir shape seems to be fairly small in this study.

4.4.2 Changes in the lakes and reservoirs

Before the founding of the People's Republic of China in 1949, there were few reservoirs in the Yangtze River basin. However, when the Three Gorges project was completed in 2009, the number of large reservoirs was greater than 190 (MWR, 2009). The growth in both the number and storage capacity of the reservoirs in the Yangtze River basin has occurred during several periods of rapid growth (Yang *et al.*, 2005b).

A more detailed examination of decade-by-decade increases in the total storage capacity of reservoirs with capacity of >0.01 km^3 shows that the greatest rate of increase was from the late 1940s to the late 1970s Figure 4.12A). By the end of the 1970s, nearly 80% of the 1,358 reservoirs (capacity $\geq$ 0.01 km^3) had been built, but their total capacity was only 89.3 km^3. Only 12 reservoirs with a capacity > 1 km^3 (e.g., Danjiangkou Reservoir at 20.8 km^3, Zhelin Reservoir at 7.9 km^3) had been built by the end of the 1970s (Yin *et al.*, 2011). After 1980, the growth in reservoir construction slowed down (Xu, 2005); however, total capacity experienced a sharp increase (Zhang *et al.*, 2009). This trend can be explained by a shift to large reservoir projects after the 1980s.
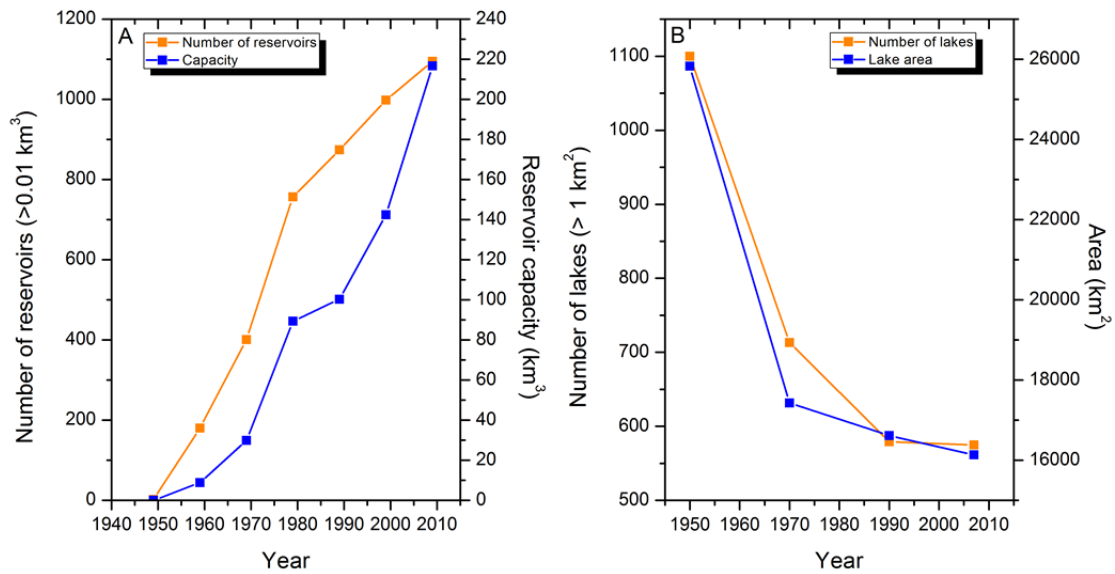
Figure 4.12 Fast increase in both the number and capacity of reservoirs (capacity $\geq$ 0.01 km^3) and dramatic decrease in the number and surface area of natural lakes over the past 60 years. Reservoir construction time was mainly obtained from (ICOLD, 2011). Although this study identified 1,358 reservoirs, only 1,120 reservoirs are presented in this figure due to unknown reservoir construction time. Lake data are mainly from Shi and Wang (1989), Zhao *et al.* (1991), Wang and Dou (1998) and Ma *et al.* (2010).

As a result of reservoir impoundment, the spatial distribution of water resources in the Yangtze River basin has undergone dramatic changes. Before 1949, water resources in the middle and lower reaches were sufficient to meet water requirements, especially in the Jianghan Floodplain, which is known as the "water bag" because of its abundance of lakes (Gemmer, 2003). These lakes held nearly 30 km^3 of water that was used for agriculture and aquaculture (Fang *et al.*, 2005). Based on this study, the total capacity of the 11,000 reservoirs in the upper reaches is approximately 85 km^3. With the construction of numerous large reservoirs in the upper reaches, much water was impounded upstream and the natural water supply to the lakes in the middle-to-lower reaches was severely impacted.

Table 4.3 Status of some large lakes (> 10 km^2) in the middle and lower reaches of the Yangtze River

Name	Isolation time	Causes	Name	Isolation time	Causes
Dong Lake	1930	Land reclamation	Wang Lake	1975	Levee construction
Caisang Lake	1958	Levee construction and land reclamation	Chi Lake	1963	Levee construction
Taibai Lake	1742	Levee construction	Sai Lake	1983	Levee construction
Dadong Lake	1951	Levee construction and land reclamation	Junshan Lake		Sluice construction
Huanggai Lake	1959	Levee construction	Wuchang Lake	1959	Sluice construction
Hong Lake	1955	Levee construction	Huangda Lake	1950s	Sluice construction
Xiliang Lake	1935	Sluice construction	Shengjin Lake	1962	Sluice construction
Liangzi Lake	1956	Sluice construction	Caizi Lake		Sluice construction
Zhangdu Lake	1964	Sluice construction	Chao Lake		Sluice construction
Daye Lake	1970	Sluice construction	Gucheng Lake		Sluice construction

Other causes of waterscape change are land reclamation and lake isolation in the middle and lower reaches. From the late 1950s to the 1970s, sluice gates were constructed for water conservation projects in almost all large lakes, except for Dongting Lake and Poyang Lake (Liu and Wang, 2010) (Table 4.3 and Figure 4.13). The sluice gates blocked the interchanges of water, sediment and nutrients in the river-lakes ecosystem, which further led to severance of species exchange and the decrease in species richness and abundance of migratory fishes (Xie and Chen, 1999). For example, migratory fish abundance of Lake Bohu in the lower reaches decreased

from 56% of the total catch before the building of sluice gates in 1956 to 20% of the total catch after the building of sluice gates (Fu *et al.*, 2003).
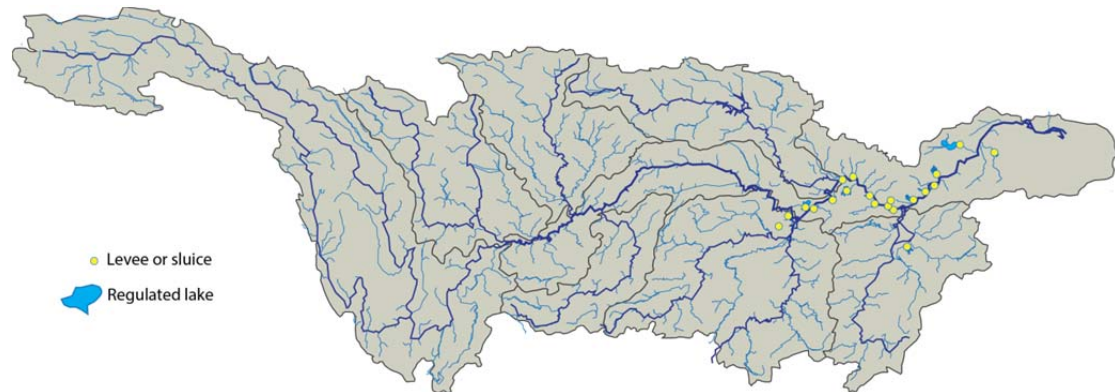
Figure 4.13 Spatial distribution of 20 regulated lakes in the middle and lower reaches of the Yangtze River

A comparison of the results with the results of previous studies (Figure 4.12B) (Shi and Wang, 1989; MWR, 1998; Wang and Dou, 1998) shows that the sharp decrease in the number and surface area of lakes occurred from the 1950s to the 1970s due to land reclamation. Half of the lakes > 1 km^2 have disappeared during the past six decades and their total surface area has shrunk by nearly 9,000 km^2. After 1990, the rate of decrease of the number and area of lakes was reduced (Fang *et al.*, 2005). The dramatic decrease in lake surface area reflects the severe anthropogenic impacts in the Yangtze River basin. The Dongting and Poyang lakes are the two key examples showing the rapid decrease in lake surface area since 1950s. The surface area of the Dongting Lake has decreased by 37%, from 2,825 km^2 in 1950s to 1,785 km^2 in 2008 primarily due to human activity, such as littoral land reclamation (Figure 4.14). Du *et al.* (2011) indicated that human activities may have contributed to the decrease in lake area

because the decrease in total lake area appears to coincide with periods of rapid land reclamation in the middle reaches of the Yangtze River. The area of the Poyang Lake has also decreased significantly as a result of land reclamation (Shankman and Liang, 2003). Total reclaimed land from 1949 to 2007 measured 2,300 km^2 and resulted in a decrease in surface lake area from 5,200 km^2 to 2,900 km^2, indicating a 45-percent decrease in the sixty-year period (Figure 4.15).
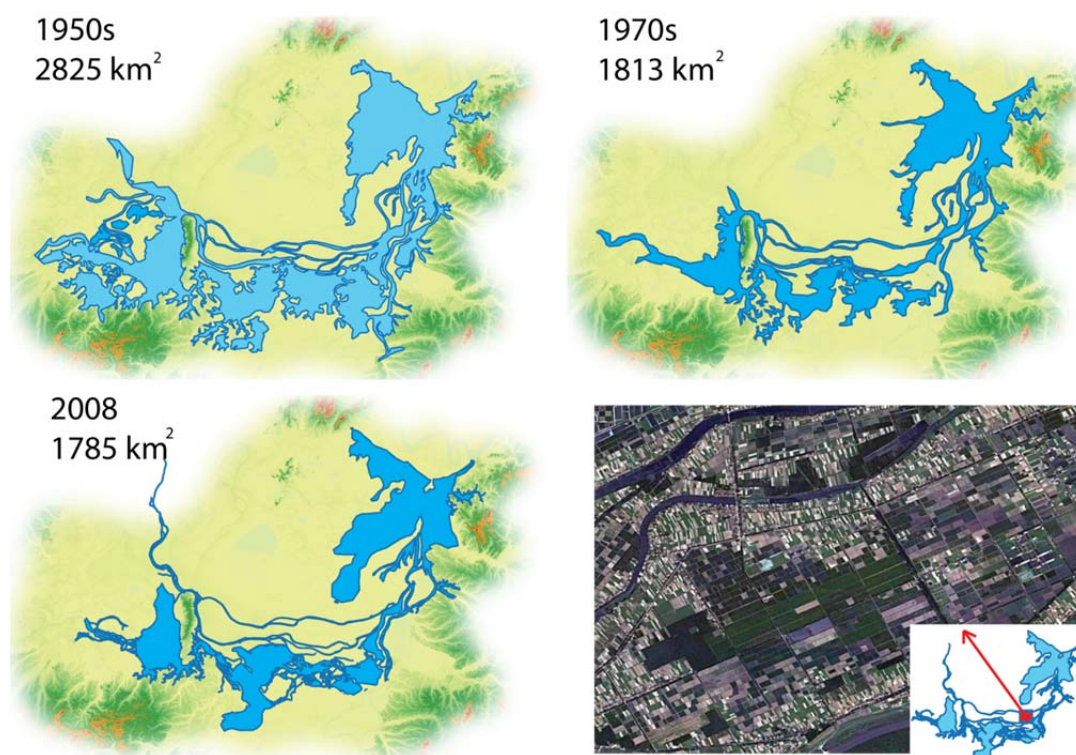
Figure 4.14 Area changes of the Dongting Lake in the 1950s, 1970s and 2008 based on the historical maps released by the Department of Land and Natural Resources (DLNR) of Hunan Province (DLNR, 2011) and Landsat images used in this study. The enlarged remote image shows that previous lake surface area has been replaced by cropland.
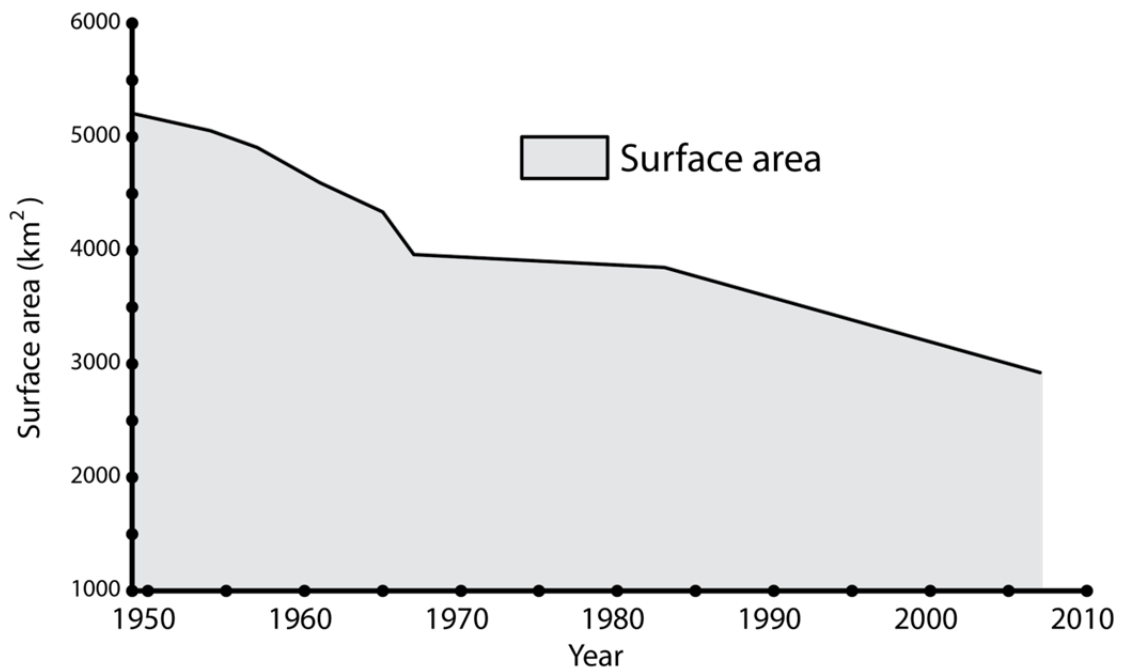
Figure 4.15 Decrease in area of the Poyang Lake in the middle Yangtze River basin since the 1950s (data based on this study result and Chen *et al*. 2001).

4.4.3 Potential impacts of the lakes and reservoirs

The ratio of reservoir storage capacity to watershed area is a gross measure of the magnitude of potential change in river flows and the consequent water flow disruption and river fragmentation caused by reservoir construction (Milliman and Meade, 1983; Graf, 1999). Regions with high storage capacity-to-drainage area ratios show the greatest potential changes. Table 4.4 shows a comparison of the ratios among global large rivers. With the exception of the Nile, Colorado and Columbia rivers in arid and semi-arid regions, the highest ratios and thus the greatest potential changes correspond to the Mississippi and Yangtze rivers because of the numerous large

99

Table 4.4 Comparison of general characteristics, capacity-area and capacity-runoff ratios for some large world rivers

River	Drainage area (10^6 km^2)	Runoff[a] (km^3 yr^{-1})	Reservoir capacity [b] (km^3)	Capacity/Area (10^3 m^3 km^{-2})	Capacity/runoff[c] (yr)
Amazon	6.16	6,300	22	3.6	0.003
Congo	3.68	1,293	< 1	< 0.27	< 0.001
Mississippi	3.27	580	331	177	0.57
Nile	2.96	30	379	128	12.6
Yenisey	2.58	631	113.6	44	0.18
Río de la Plata	2.58	662	185.4	71.9	0.28
Niger	2.09	192	29	13.9	0.15
Yangtze	1.8	1,035	250	138	0.27
Murray	1.06	24	16.1	15.2	0.67
Indus	0.96	207	27	28	0.13
Mekong	0.79	470	19	24	0.04
Yellow	0.745	66	65	87.2	0.98
Colorado	0.64	17	74	115.6	4.3
Columbia	0.42	236	56.6	135	0.24

[a] Data source: (Milliman, 1993).

[b] Data source: (Nilsson *et al*. 2005; ICOLD 2011); data were updated based on the current status of the hydropower plants; this reservoir capacities exclude reservoirs with dams less than 15m.

[c] Capacity/runoff ratio = water discharge/total reservoir capacity.

Table 4.5 Sub-basins, their general characteristics, reservoir capacity data and information on capacity-area and capacity-runoff ratios

	Sub-basin	Drainage area (10^6 km^2)	Runoff (km^3 yr^{-1})	No. of reservoirs	Reservoir capacity (km^3)	Area/reservoir[b] (km^2)	Capacity/area (10^3 m^3 km^{-2})	Capacity/runoff (yr)
	Jinsha	0.5	135.1	1,817	11.3	275	22.6	0.08
	Min	0.16	87.5	2,683	11.2	59.6	70.0	0.13
Upper reaches	Jialing	0.16	72.7	3,531	17.1	45.3	106.9	0.24
	Wu	0.08	42.9	1,086	11.6	73.7	145.0	0.27
	Mainstem area	0.13		1,719	33.9[a]	75.6		
	Upper Yangtze River	**1.03**	**405.8**	**10,836**	**85.1**	**95**	**82.6**	**0.21**
	Han	0.15	55.3	3,461	49.8	43.3	332	0.90
Middle reaches	Poyang Lake Region	0.16	184.4	10,476	55.6	15.3	347.5	0.3
	Dongting Lake Region	0.27	389.6	7,731	49.7	34.9	184.1	0.13
	Main stream area & lower reach	0.19		11,098	48.1	17.12		
Basin-wide		**1.8**	**1035.1**	**43,602**	**288.3**	**41.3**	**160.2**	**0.28**

[a] The Three Gorges Reservoir is located in this area; however it was not fully regulated from 2005 to 2008 when the remote sensing image were acquired. Thus the estimated capacity is far much less than its contemporary capacity.

[b] Area/reservoir ratio = drainage area/number of reservoirs

reservoirs in these basins (total reservoir capacities of 331 and 250 km^3 for the Mississippi and Yangtze, respectively). In contrast, there are few potential changes predicted for the Congo, Mekong and Amazon River basins. At the sub-basin scale, the highest ratios of 332,000 and 347,500 m^3 km^{-2} are for the Han tributary and the Poyang Lake Region, respectively. Reservoirs partition the two regions into units averaging only 43.3 and 15.4 km^2 for the Han River and Poyang Lake, respectively (Table 4.5). Thus, these two areas may have experienced flow alteration. However, in the Han tributary basin, this is due to limited runoff (only 55.3 km^3 yr^{-1}), whereas for the Poyang Lake Region, this is partly due to the numerous impoundments located in this low-relief region that give the region the highest dam concentration in the entire Yangtze River basin.

Perhaps a more informative measure of the potential impact of reservoirs is a comparison of the amount of reservoir capacity to the mean annual runoff. Although runoff varies from year to year, long-term averages provide a basis for a general analysis (Leeden *et al.*, 1990). The basin-wide total storage capacity of approximately 288 km^3 for the Yangtze River, largely from large and medium reservoirs, is nearly 30% of the mean annual runoff of 1,000 km^3 (Table 4.5). The ratios of storage to annual runoff are less than 0.1 years for the Amazon and Mekong, 0.57 years for the Mississippi, and 13 years for the Nile. In terms of individual sub-basins, in the upper Yangtze reaches the ratios of capacity to runoff range from 0.08 to 0.27 years (Table 4.5). At the opposite extreme is the Han tributary, for which the constructed reservoirs

store approximately 90% of the mean annual runoff.

The impoundment of river channels regulates discharge downstream, potentially affecting flooding patterns, flow regimes, and nutrient transport (Lu, 2005; Wellmeyer *et al.*, 2005; Graf *et al.*, 2010). It is likely that with increases in the average time that water is retained in reservoirs (increases in the capacity-runoff ratio), the impacts will become more evident. For example, an average ratio of 0.27 years indicates the reservoirs in the Wu tributary have a large capacity to absorb flows, and thus the downstream channel would experience a diminished flow regime; conversely, an average ratio of 0.08 years indicates that the reservoirs in the Jinsha tributary would have little impact on the flow regime downstream of the reservoirs. Evidence of this idea has been reported in the Yangtze River basin by many researchers (Lu *et al.*, 2003b; Xu *et al.*, 2008; Hassan *et al.*, 2010). As a case in point, a severe drought that occurred in the middle and lower reaches, from April to June 2011, exposed the impacts from reservoir construction and lake shrinkage. When water was released from the Three Gorges Reservoir in response to the water shortage, over 50 km^3 of water, which is more than the maximum storage of the Three Gorges Reservoirs, remained impounded and available for power generation in the many large reservoirs in the upper reach. The cumulative effect of these reservoirs on the Yangtze's large-scale hydrologic regime are evident (Lu *et al.*, 2011).

4.5 Summary and conclusions

Compared with conventional methods such as hydrographic surveys, which are expensive, time-consuming and laborious, remote sensing techniques are a rapid and cost effective approach to information acquisition for short time intervals and large spatial scales. Using Landsat TM/ETM+ imagery and a variety of free data and information, this study created a new basin-wide lake and reservoir dataset. The application of GIS to data obtained from the best available free sources for lake and reservoir data at the basin-wide scale enabled the generation of a dataset that included all natural lakes and artificial reservoirs with a surface area larger than 0.0036 km^2. This is the first time such a dataset has been created across such a large river basin. The following conclusions can be drawn from this study.

This study delineated nearly 43,600 reservoirs and 42,700 lakes, and based on these results this study estimated a quantity of nearly 0.7 million smaller (< 0.0036 km^2) reservoirs and approximately 0.5 million smaller lakes. The study's estimates are consistent with published inventories in terms of the number and total storage capacity of lakes and reservoirs in the Yangtze River basin, indicating that remote sensing is an effective application for the quantification of water bodies. Cloud cover, shadows (in the upper reach) and paddy fields (in the middle and lower reaches) are unavoidable interferences in the identification of small lakes and reservoirs because the shadows and paddy fields are sometimes misinterpreted as water bodies. Visual

interpretation of auxiliary data (from sources such as Google image service, GeoNames and thematic maps) and the collection of field data are useful methods for differentiating among shadows, water bodies and paddy fields.

The analyses of the remote sensing results revealed that the Yangtze River basin, while previously dominated by natural lakes, has become reservoir-dominated due to anthropogenic impacts, especially reservoir construction and lake shrinkage. However, there is considerable geographic variation in the potential surface water impacts of the reservoirs. The greatest impacts to water discharge, environmental destruction and river fragmentation may occur in the Poyang Lake Region, which have the greatest capacity-area ratio. Future anthropogenic impacts could worsen the situation as additional large hydropower projects are completed in the upper reaches of the basin (MWR, 2011), potentially affecting the water cycle in the entire basin.

5 Estimate of cumulative sediment retention by multiple reservoirs

5.1 Introduction

There are around 45,000 large reservoirs worldwide used for water supply, power generation, flood control, and navigation (Vörösmarty *et al.*, 2003). For example, about 20% or 3 million km^2 of cultivated land worldwide is irrigated by reservoirs; about 20% of the worldwide generation of electricity is attributable to hydroelectric projects, equating to about 7% of worldwide energy usage (White, 2001). Reservoir construction currently represents the most important anthropogenic influence on land-ocean sediment fluxes (Syvitski *et al.*, 2005; Kummu and Varis, 2007). However, due to dramatic reservoir sedimentation, it has dramatically decreased sediment loads of many rivers thereby triggering erosion of many deltas (Milliman, 1997; Syvitski *et al.*, 2009), including those of the Nile (Stanley and Warne, 1993), Colorado (Topping *et al.*, 2000), Mississippi (Blum and Roberts, 2009), and Yellow (Wang *et al.*, 2007b) rivers. Inadequate investigations of these and other rivers, unfortunately, have limited the extent to which changes in sediment discharge and their impacts could be identified, let alone adequately quantified.

Dams hold back sediments that would naturally replenish downstream river systems, leading the flow to become sediment-starved and prone to erode the channel bed and banks, producing channel incision (downcutting), coarsening of bed material, and loss

106

of spawning gravels for fish species (Kondolf, 1997). Half of all discharge entering large reservoirs shows a local sediment trapping efficiency of 80% or more. Several large basins such as the Colorado and Nile show nearly complete trapping due to large reservoir construction and flow diversion (Vörösmarty *et al.*, 2003).

Numerous previous studies have focused on the impacts of individual dams and reservoirs on sediment retention; yet literature is rare concerning the cumulative impacts of reservoirs on sediment retention in a multi-reservoir system. Modeling the impacts in such a multi-reservoir system is still a great challenge at present. There are two research challenges: First, the estimation of surface erosion and sediment yield from a large catchment has large uncertainty due to the spatial variation of rainfall and to great heterogeneity in relief, slope and soil (Williams, 1975); second, in a multi-reservoir system, trapping efficiency is insufficient to explain the true sediment retention of a dam, because sediment trapping by upstream reservoirs is also important. By considering the effect of trapping by upstream reservoirs in a multi-reservoir system, the rate of sediment retention in each individual reservoir could be significantly different.

In terms of the two research challenges, the specific aims of this chapter are to (a) develop a model to estimate reservoir sedimentation in a multi-reservoir system by integrating the effect of upstream traps; (b) estimate the current impact of sediment retention by reservoirs in the Yangtze River basin; and (c) analyze the variation in the

rates of storage loss in different tributary basins.

5.2 Data and methods

5.2.1 Data sources and data processing

An extensive hydrological and sediment monitoring program over the entire basin was established in the 1950s by the Changjiang (Yangtze) Water Resources Commission (CWRC). The monitoring program includes discharge, suspended sediment concentration, and suspended load, in accordance with national data standards. The original records for each station provide information on station coordinates (latitude and longitude), catchment area, mean monthly and annual water discharge and sediment load, and the magnitude and date of occurrence of the maximum daily discharge. Suspended sediment is measured daily, with an estimated daily error of 16% (Yan *et al.*, 2011).

Sediment load data used in this study were primarily obtained from the CWRC. In this study, the data of 223 sites were used to study the variation in sediment yield with a number of climatic and topographic variables (Figure 5.1). Here this study only used the data between 1950 and 1965 because most large reservoirs were put into operation after 1965 and this could lead to sharp reductions in sediment yield at corresponding hydrological stations. Each station was examined in order to identify any disturbance
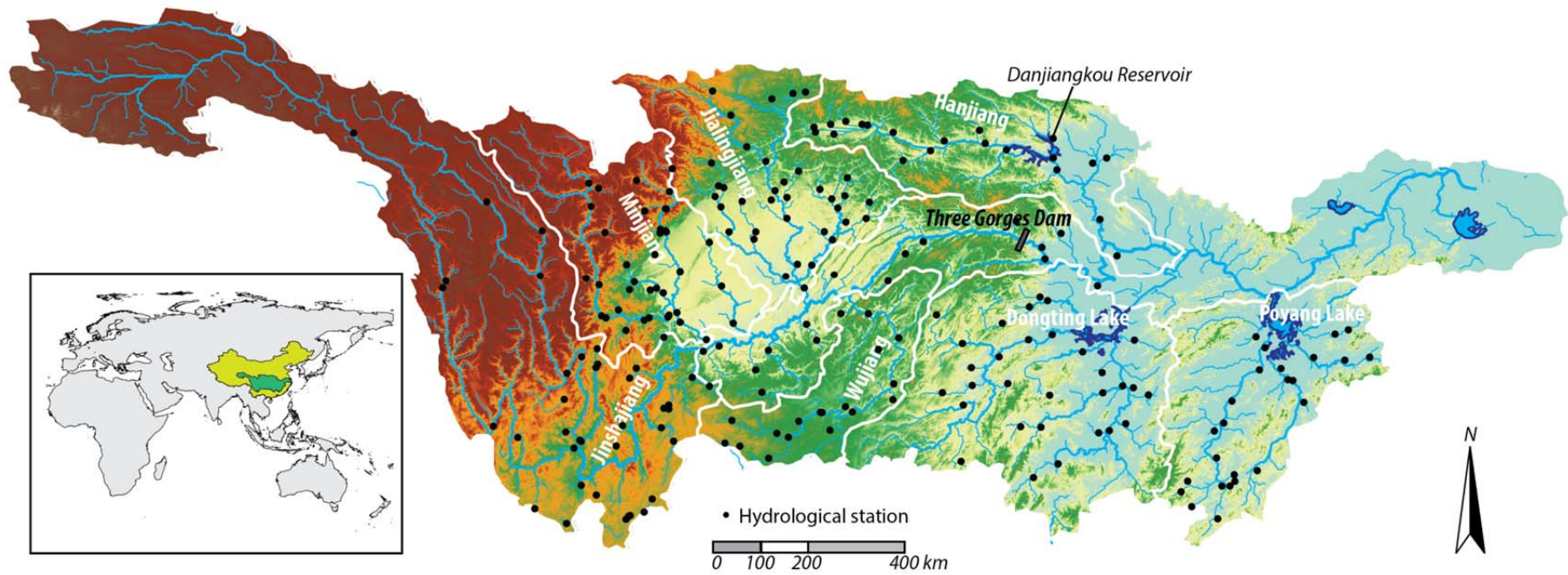
Figure 5.1 Spatial distribution of hydrological stations which were used to establish empirical relationships for sediment yield prediction.

(e.g. dams, sand mining) that might obscure regional trends: such stations were removed from the analysis. There are some inconsistencies in the original data set (Lu and Higgitt, 1999); it took considerable time to correct those errors during the conversion from paper to digital format. The drainage areas and locations for many stations are not consistent throughout the time series. This may reflect correction of previous measurement of drainage area or a slight change of station location.

It should be highlighted that large-scale deforestation and land reclamation primarily occurred at the end of the 1950s in response to the disastrous political campaign of Mao Zedong's "great leap forward". The compensatory measures of water and soil conservation did help to reduce soil erosion, but the measures were mainly taken in the Jialing River and lower Jinsha River, or only 3% of the basin area (Xu, 2007). Thus, the data covering the period 1950-65 can be used as a reasonable reference of sediment yield in the Yangtze River basin before large-scale reservoir construction.

In addition, long-term average precipitation data were collected from the national meteorological network in China for the same period from 1950 to 1965. The spatially explicit precipitation data for different drainage areas of reservoirs and hydrological stations were obtained using Kriging interpolation and were then used as a climatic variable to predict sediment yield. While terrain plays an important role for the process of soil erosion and sediment transport, in order to extract terrain variables, a DEM was obtained from the global topography database (http://srtm.csi.cgiar.org/,

last accessed in January 2013), which has a 90 x 90 m spatial resolution. The terrain variables were derived using ArcGIS.

According to the study results in Chapter 4, there are 1,358 reservoirs with storage capacity greater than 1×10^7 m^3 in the Yangtze River basin. Literature on dam construction and deposition in reservoir of the drainage basin were collected. The dam coordinates were marked in Google Earth and were calibrated using the river network extracted from DEM data so that all the dams are correctly located on the river network. Field trips were also carried out to investigate sediment trapped in some reservoirs. These materials were used to relate the human activities with variation in river sediment load.

5.2.2 Sediment yield prediction

It is believed that many factors influence sediment yield, and sediment yield will vary considerably unless all the factors are uniform from watershed to watershed (Walling, 1999). A number of studies have addressed the relationships between sediment yield and its controlling factors through correlation and regression analysis at the global and regional scales (Lu and Higgitt, 1999; Van Rompaey *et al.*, 2005; Restrepo *et al.*, 2006; Ali and de Boer, 2008). Some of these factors are the types of sediment sources, the magnitude of the sediment sources, climatic factors, texture of the materials, environments of deposition, and watershed characteristics. At a global scale, variables expressing basin relief characteristics and runoff magnitude tend to be most strongly

associated with sediment yields (Milliman and Syvitski, 1992; Syvitski and Milliman, 2007).

Based on differences in geomorphology, geology and climate, this study divided the Yangtze River basin into 6 sub-basins: Jinsha and upper reach along the mainstem, Min and Tuo, Wu, Jialing and Han, Poyang Lake Region and middle-lower reach along the mainstem, Dongting Lake Region. Because there is no sediment yield map available yet, this study used multiple regression analyses to develop models to predict sediment yields for each sub-basin. 17 catchment properties were analyzed in order to understand the variation in sediment yield. Stepwise regression analyses were used to obtain the best area-specific sediment yield (SSY in t km^{-2} yr^{-1}) model. Since these 17 variables may inter-correlated (multicollinearity), variance inflation factor (VIF) was used to detect if multicollinearity is significant in the regression models. VIF assesses how much the variance of an estimated regression coefficient increases if variables are correlated. If no factors are correlated, the VIFs will all be 1. If multicollinearity was detected, principal components analysis was used to cut the number of variables to a smaller set of uncorrelated components to establish a regression model again.

Based the regression models, the annual sediment yield (SY in t yr^{-1}) within the drainage area of a reservoir was calculated using the following equation:

$$SY = SSY \times A \qquad\qquad (5.1)$$

where *SSY* was estimated using the regression model in each reservoir's sub-basin; *A* is the reservoir's drainage area in km^2.

5.2.3 Estimating reservoir sedimentation for representative reservoirs

A representative reservoir is defined as the reservoir that has no upstream reservoirs in its drainage area. The single most informative attribute for a representative reservoir is its trap efficiency (*TE*) (Heinemann, 1981). This value is defined as the ratio of deposited sediment to the total sediment inflow for a given period. Here this study used the following equation from Brown (1944) to calculate trap efficiency:

$$TE = 100 \times (1 - \frac{1}{1 + D \times (\frac{C}{A})}) \tag{5.2}$$

where *C* is the reservoir storage capacity (m^3); *A* is the reservoir's drainage area (km^2) derived from DEM data; *D* is a coefficient (particle size) with values ranging from 0.046 to 1.0 and a mean value of 0.1 (Brown, 1944). Liu *et al.* (2010) investigated the frequency of grain size of suspended sediment delivered from the Yangtze River to the estuary. Their results show that medium-sized suspended sediment constitutes the largest part in the Yangtze River estuary. The study by Wang and Chen (2009) also indicated that medium-sized sediment constitutes a large part the middle-lower Yangtze riverbed. Gill (1979), Verstraeten and Poesen (2000) and Tesfahunegn and Vlek (2013) indicate that Values of *D* = 1.0, 0.1 and 0.046 may be used for coarse, medium and fine sediments, respectively. Since medium-sized sediment constitutes the largest part, this study used the value of *D* = 0.1 in this study to estimate all trap efficiencies. Here the Brown equation was used instead of the better known Brune curve (Brune, 1953)

because the Brune relation requires water inflow data, which were absent for most large reservoirs in the Yangtze River basin.

For a representative reservoir the annual sedimentation rate (S) was estimated using this equation:

$$S = SY \times TE \tag{5.3}$$

where SY is sediment yield in t yr^{-1} calculated from Eq. 5.1; TE is the reservoir's trap efficiency calculated from Eq. 5.2.

5.2.4 Estimating reservoir sedimentation in a multi-reservoir system

One problem of Eq. 5.3 is that this model does not account for the effect of upstream traps in a multi-reservoir system. As upstream reservoirs are built, they can dramatically reduce sediment yield to downstream reservoirs. This effect is particularly important in such an area as the Yangtze River basin with numerous reservoirs within the same watershed. Reservoirs can be roughly classified into three types in relation to other reservoirs (Figure 5.2): (1) a representative reservoir (reservoir *c*, *d* and *e*), which has no upstream traps; (2) a reservoir that has both upstream and downstream traps (reservoir *a* and *b*); (3) reservoirs that have only upstream reservoirs (reservoir *f*). To calculate the sediment yield from a basin with multiple reservoirs, this study constructed a model to calculate the weighted sediment yield for a reservoir of interest,

while taking into account the effect of upstream traps. Taking the reservoirs in Figure 5.2 as an example, corresponding to the three reservoir types, this study created a set of equations to calculate weighted sediment yield and annual rate of reservoir sedimentation:

Figure 5.2 Protocol for predicting reservoir sedimentation in a multi-reservoir system. Reservoir *f* is the farthest downstream; reservoirs *a*, *d*, and *e* are immediately upstream of *f* and they are direct sediment-contributing reservoirs to reservoir *f*. Reservoirs *c*, *d*, *e* are representative reservoirs that have no upstream reservoirs. *SY'* is weighted sediment yield for each reservoir, for example, sediment yield at reservoir *f* is the sediment yield in $SY_f^{'}$ plus the sediment released from its immediately upstream reservoirs *a*, *d* and *e*.

$$SY_c^{'} = \{(A_c)/A_c \times SY_c\} \tag{5.4}$$

$$SY_a^{'} = \{(A_a - A_b)/A_a \times SY_a\} \tag{5.5}$$

$$SY_f^{'} = \{(A_f - A_a - A_d - A_e)/A_f \times SY_f\} \tag{5.6}$$

$$S_c = TE_c \times \{SY_c^{'}\} \tag{5.7}$$

$$S_a = TE_a \times \{SY_a' + [\frac{S_b}{TE_b} - (S_b)]\} \qquad (5.8)$$

$$S_f = TE_f \times \{SY_f' + [\frac{S_a}{TE_a} + \frac{S_d}{TE_d} + \frac{S_e}{TE_e} - (S_a + S_d + S_e)]\} \qquad (5.9)$$

where SY' is the weighted sediment yield (t yr^{-1}); A is the catchment area (not sediment contributing area) (km^2), derived from DEM data; S is the annual amount of sediment (t) trapped by reservoirs; TE is trap efficiency, calculated from Eq. 5.2; [•] in Eqs. 5.7−5.9 is the sediment delivered downstream from immediately upstream reservoirs and (•) is the sediment trapped by immediately upstream reservoirs; subscripts a, b, c, d, e and f denote different reservoirs. In this case of Figure 5.2, reservoir f is the farthest downstream; Reservoirs a, d, and e are immediately upstream of f and they are directly sediment contributing reservoirs to reservoir f. Reservoirs c, d, e are representative reservoirs that have no upstream reservoirs; thus, the equations used for reservoirs d and e are similar to Eq. 5.4 and Eq. 5.7.

5.2.5 Estimating reservoir sedimentation in small reservoirs

Over the past 60 years, numerous small reservoirs with capacity less than 10^7 m^3 were constructed for domestic water supply, agricultural irrigation, livestock watering and aquaculture in the Yangtze River basin. Since a major proportion of the sediment input to a small reservoir actually could not previously reach its downstream large reservoir except in mountain catchments or during extreme floods, it could not become

sediment yield at its downstream large reservoir. Small reservoirs were therefore considered as representative reservoirs and the annual reservoir sedimentation can be calculated directly using Eq. 5.3.

The estimates of sedimentation rates for small reservoirs were fundamentally aspatial, necessitated by the difficulty in catchment area delineation due to the coarse resolution of the DEM data. This study used a statistical method proposed by Vörösmarty *et al.* (2003) to make the estimates. The strategy of this method used the statistical characteristics of the geographically referenced large and medium-sized reservoirs to predict the role of small reservoirs in sediment trapping.
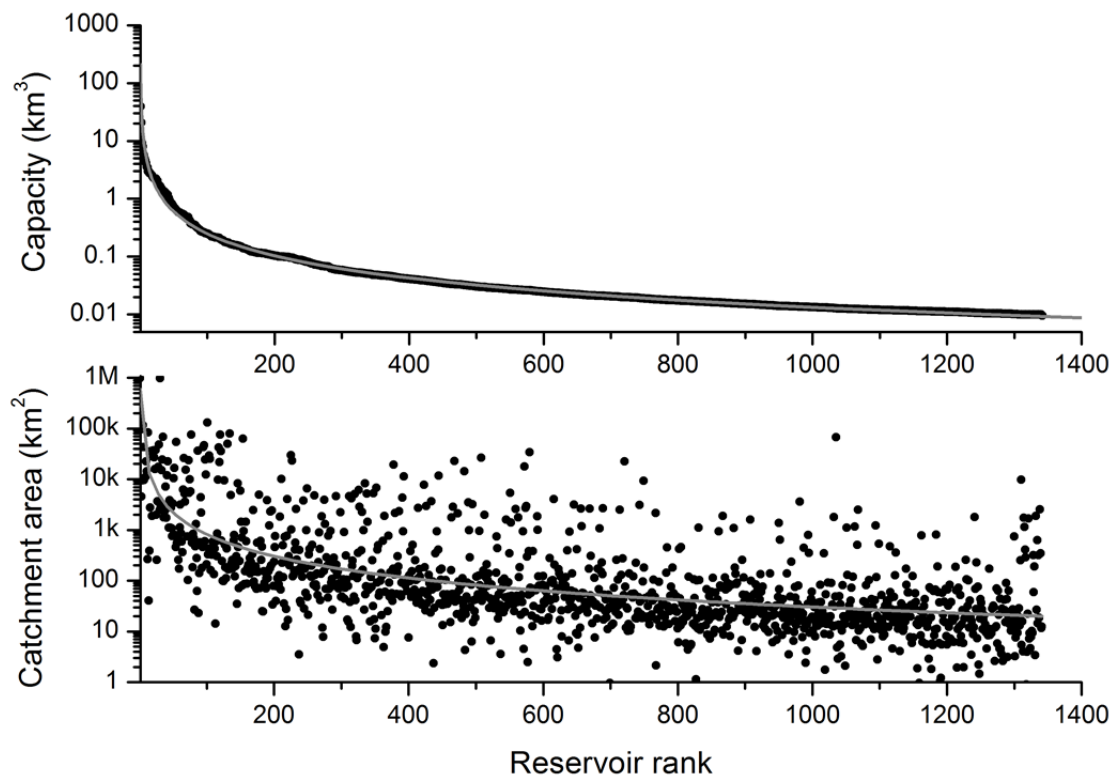
Figure 5.3 Statistical relationships of reservoir volume capacity (in km^3) and of reservoir catchment area (in km^2) to reservoir rank.

These computations require a characterization of the statistics of three key attributes of small reservoirs: storage capacity (C, in km^3), catchment area (A, in km^2) and trap efficiency (TE). This study examined cumulative distribution functions, ranked by storage capacity (R_r) for each of these variables (Figure 5.3). For the 1,358 large and medium-sized reservoirs, these curves were stable and predictable, and this study assumed that they are sufficient to extrapolate the cumulative behavior of the remaining 42,000 small reservoirs with capacity $\geq$ 0.1 million m^3. This study specifically fit three nonlinear functions:

$$A = 598001 \times R_r^{-1.431} \quad (R^2 = 0.4249) \tag{5.10}$$

$$C = 86.787 \times R_r^{-1.271} \quad (R^2 = 0.9957) \tag{5.11}$$

$$SSY = 278.86 \times A^{0.0071} \quad (R^2 = 0.762) \tag{5.12}$$

where R_r is reservoir rank which was defined according to reservoir capacity. Figure 5.3 presents these relationships represented by Eqs. 5.10 and 5.11, plus the observed distributions from large and medium-sized reservoirs.

5.3 Results

5.3.1 Established multiple regression models for each sub-basins

Table 5.1 shows the established multiple regression models along with model

assessment for each sub-basin. For the sub-basin of the Jinsha River and upper reach along the mainstem, this sub-basin is characterized by small basins, which drain directly into the main channel, a strong positive relationship between SSY and runoff (RO) was exhibited. The Min sub-basin is located in the transition zone between the Tibetan plateau and the Sichuan Basin. 42% of this sub-basin has slopes steeper than 25º, which accounts for 94% of the total erosion area (Yan *et al.*, 2011). The strong positive relationship between SSY and relief ratio (RR) implies the intensity of erosion processes operating on slopes of the sub-basin. For the sub-basin of the Jialing and Han, relating SSY to precipitation (P), slope (S_{mean}) and NDVI, a relationship implies the joint function of all the three relative factors. In terms of lithology, the Wu sub-basin is covered by limestone, shales, and sandstones. Most of the sediment comes from the highly erodible upper and middle sections, implying a positive relationship between SSY and mean elevation (H_{mean}) and slope (S_{mean}). Influenced by the East Asian summer monsoon in the Poyang Lake Region and middle-lower reach along the mainstem, the SSY shows a strong relationship to annual precipitation (P). The Dongting Lake Region and Poyang Lake Region are similar in terms of land surface characteristics and climate conditions (Yan *et al.*, 2011). However, part of this sub-basin is very steep implying a strong relationship with morphometric indices (e.g. hypsometric index and slope).

Table 5.1 Regression models predicting specific sediment yield in 6 sub-basins

Sub-basin	Regression model	R^2	Number of stations
Jinsha and upper reach along the mainstem	$LOG(SSY) = 5.1103 + 0.9785*LOG (R) - 2.4114*LOG(H_{mean}) + 0.9056*LOG(RO)$	0.7658	53
Min and Tuo	$LOG (SSY) = 1.1823 + 2.7896* LOG (R) - 3.5566* LOG (H_{max}) + 1.6979*LOG(RR) + 0.5283*LOG(SS)$	0.7597	37
Wu	$LOG (SSY) = -6.9044 + 2.0031* LOG (H_{mean}) + 2.8628*LOG(S_{mean})$	0.8334	19
Poyang Lake Region and middle-lower reach along the mainstem	$LOG (SSY) = 22.6648 - 13.0370* LOG (NDVI) + 2.5648* LOG (P)$	0.8074	25
Dongting Lake Region	$LOG (SSY) = 2.5282 + 0.9899* LOG (HI) + 0.3465* LOG (S_{mean})$	0.6721	32
Jialing and Han	$LOG(SSY) = 0.5751 + 1.5098*LOG(P) + 1.6797*LOG(S_{mean}) - 1.9546*LOG(NDVI)$	0.7780	57

[a] 17 catchment properties were analyzed in order to understand the variation in sediment yield; SSY: area-specific sediment yield (t km^{-2} yr^{-1}); A: drainage area (km^2); DL: drainage length (km); H_{mean}: mean elevation (m); H_{min}: minimum elevation (m); H_{max}: maximum elevation (m); HD: elevation difference (m); HI: hypsometric integral, given by: $(H_{mean}-H_{min})/(H_{max}-H_{min})$; R: basin relief (m); RR: ratio of the basin relief and the basin length; RG: index of basin ruggedness, given by $HD*A^{-0.5}$; SS: rate of change of elevation with respect to distance proxy to surface runoff velocity, given by HD/DL; DD: balance between erosive forces and surface resistance, degree of dissection of terrain, given by DL/A; S_{mean}: mean slope (degree); NDVI: normalized difference vegetation index, driven from remote sensing images; P: mean annual precipitation (mm yr^{-1}); P_{max}: Maximum monthly precipitation (mm month^{-1}); RO: mean annual runoff (mm).

[b] The global digital elevation model (DEM) provided by the Shuttle Radar Topographic Mission (SRTM) with a resolution of 90 m was used to derive drainage areas as well as basic topographic parameters.

[c] Landsat Multispectral Scanner (MSS) and Thematic Mapper (TM) images, acquired from the United States Geological Survey (USGS), were used to calculate normalized difference vegetation index (NDVI). These are earliest remote sensing data available from public access.

5.3.2 Quantity of cumulative sediment trapping by reservoirs

The mean estimated area-specific sediment yield in the Yangtze River is 384 t km^{-2} yr^{-1}, with the highest yield (2,080 t km^{-2} yr^{-1}) in the lower Jinsha sub-basin and the lowest (38 t km^{-2} yr^{-1}) in the central Poyang Lake Region. Walling (1983) indicated that area-specific yields tend to be lower for larger basins. The same trend was also observed in the Yangtze River basin. Based on the estimated sediment yield, this study predicted that the annual sediment accumulated in the Yangtze reservoirs is approximately 691 Mt, 669 Mt of which is trapped by 1,358 large and medium-sized reservoirs and only 22 Mt is trapped by smaller reservoirs, indicating that sediment is primarily trapped by large reservoirs with storage capacity greater than 0.01 km^3.

Considering a bulk density of 1.3 tons m^{-3} (Yang *et al.*, 2007), the reservoirs in the Yangtze River basin are losing their cumulative storage capacity at an average rate of approximately 5.3 x 10^8 m^3 yr^{-1}. Vörösmarty *et al.* (2003) found that the global annual sedimentation rate of all registered reservoirs was estimated to be on the order of 4,000-5,000 Mt yr^{-1}. This means that sediment trapped in the Yangtze River basin contributes approximately 14%–17% to the global reservoir sedimentation. In view of the Yangtze River's importance in global sediment transport and the continuing sediment retention efforts, the estimated annual sedimentation rate of 691 Mt is consistent with its contribution to global annual sedimentation rate. Figure 5.4 shows
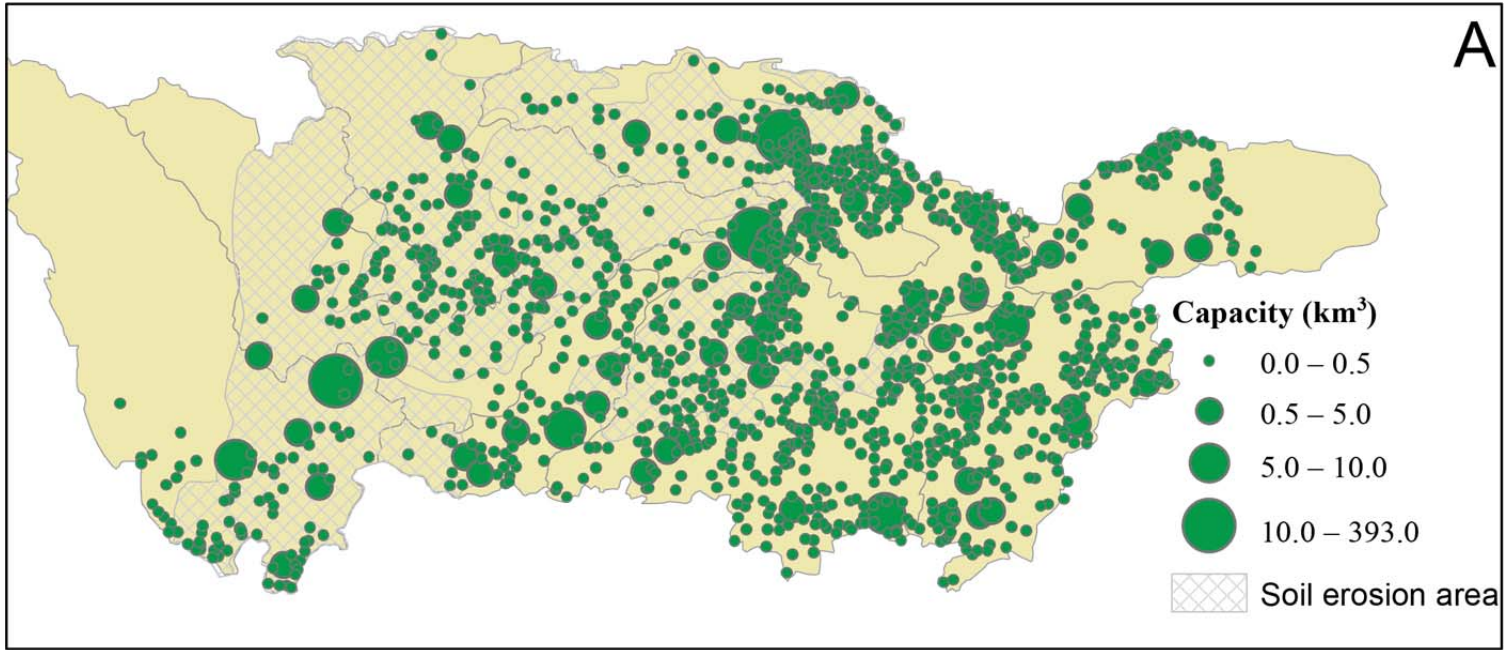
Figure 5.4A Geographical distribution of large reservoirs with storage capacity greater than 0.01 km^3 across the Yangtze River basin
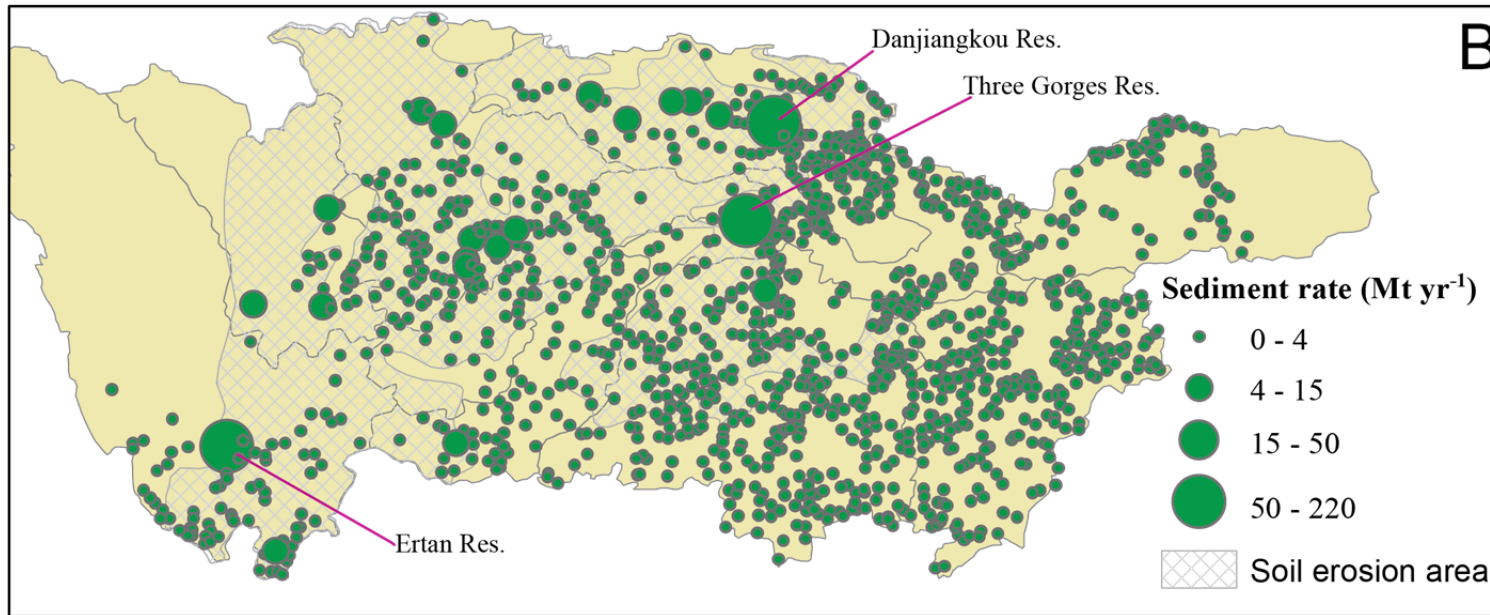
Figure 5.4B Spatial distribution of sedimentation rates of large reservoirs with storage capacity greater than 0.01 km^3 across the Yangtze River basin.

Table 5.2 Sub-basins, their general characteristics, reservoir capacities and sediment trapped in sub-basins

	Tributary basin	Drainage area (10^6 km^2)	No. of reservoirs	Reservoir capacity (km^3)	Trapped sediment[b] (Mt yr^{-1})
Upper reaches	Jinsha	0.5	1,817	11.3	86
	Min and Tuo	0.16	2,683	11.2	44
	Jialing	0.16	3,531	17.1	94
	Wu	0.08	1,086	11.6	26
	Mainstem area[a]	0.13	1,719	40.2	244
	Upper Yangtze River	1.03	10,836	91.4	494
Middle and lower reaches	Han	0.15	3,461	49.8	126
	Poyang Lake Region	0.16	10,476	55.6	16
	Dongting Lake region	0.27	7,731	49.7	36
	Mainstem and lower reaches	0.19	11,098	48.1	19
Basin-wide		1.8	43,602	294.6	691

[a] The Three Gorges Reservoir is located in this area.

[b] The reservoir sedimentation also includes the sediment trapped by small reservoirs, which was allocated in proportion to the number of reservoirs in each tributary basin.

the comparison between the capacities of the 1,358 reservoir and their sedimentation rates across the Yangtze River basin. In Figure 5.4A, reservoirs are almost uniformly located in all reaches except the headwater areas, but reservoirs with sedimentation rate greater than 4 Mt are primarily located in the severely eroded areas mapped by CWRC (2007a) (Figure 5.4B). The study predicted that, at present, over 23 reservoirs have the ability to trap sediment more than 4 Mt per year and 3 reservoirs can trap sediment more than 50 Mt per year, which are the Danjiangkou Reservoir (51 Mt yr^{-1}), the Ertan Reservoir (61 Mt yr^{-1}) and the Three Gorges Reservoir (217 Mt yr^{-1}), respectively. The total annual sediment accumulated in the 23 reservoirs is estimated to be 532 Mt per year. This indicates that these 23 reservoirs play a crucial role in sediment retention.

5.3.3 Cumulative sediment trapping in different reaches

Geographically, 494 Mt of sediment is annually trapped by the reservoirs in the upstream reaches, approximately 217 Mt of which is trapped by the TGR (Table 5.2). The reservoirs in the upper reaches are losing storage capacity at an average rate of 3.8 x 10^8 m^3 yr^{-1}, or 0.4% of the total capacity per year. The bathymetric surveys at the end of the 1980s by CWRC indicated the reservoir sedimentation rate in upper reaches was approximately 150 Mt yr^{-1}, the equivalent to 1.15 x 10^8 m^3 or 0.6% of the total capacity per year (CWRC, 1992). Xu (2007) estimated the total sediment trapped by reservoirs excluding the TGR in the upper reaches from 1991 to 2005 was

approximately 2,934 Mt, with an annual average of approximately 200 Mt. However, the sedimentation rate after 2000 was definitely higher than the average due to the closure of many large reservoirs after 2000. The two studies corroborate that the proposed model yielded a very modest estimate of the annual sediment trapped by reservoirs in the upper reaches. The amount of soil lost in the upper Yangtze reaches is approximately 1,570 Mt per year (Wang *et al.*, 2007c), indicating that 31% of the soil loss amount annually deposit in reservoirs. A reasonable explanation for the large amount of sediment trapped in the upstream reaches is that severe soil erosion happens in the upstream reaches and most large reservoirs were built on major tributaries, which intensifies the effect of reservoirs on sediment retention.

In the middle and lower reaches 197 Mt of sediment is trapped by reservoirs per year, although two-thirds of reservoirs are located in these areas, contributing to approximately 69% of the total capacity in the Yangtze River basin (Table 5.2). Due to relatively low soil erosion the amount of soil lost in the middle and lower Yangtze reaches is approximately 690 Mt per year (Xu, 2007), 29% of which is annually trapped by reservoirs. However, the spatial distribution of sediment trapped in middle and lower reaches is very non-uniform because of the extremely inhomogeneous distribution of soil erosion. For example, nearly two thirds of soil erosion occurs in the Han sub-basin, although its drainage area is only 15×10^4 km^2 (Table 5.2).

More specifically, the highest reservoir sedimentation rate (126 Mt yr^{-1}) occurs in the

126

Han tributary basin (Table 5.2). Although, 3,461 reservoirs have been built in this tributary basin over the last 60 years, the Danjiangkou Reservoir, constructed in the upper Han basin in the late 1960s, is responsible for approximately 40% of reservoir sedimentation. The second highest reservoir sedimentation rates happen in the Jialing and Jinsha sub-basins after the closure of a series of large reservoirs (e.g. Bikou Reservoir 1977, Ertan Reservoir in 1993 and Baozhusi Reservoir in 1998). Like the Danjiangkou Reservoir, the Ertan Reservoir annually traps approximately 61 Mt, or 71% of the total sediment impounded in the Jinsha tributary basin. The amounts of sediment trapped in the Wu tributary basin, Dongting and Poyang lake regions are relatively low (Table 5.2).
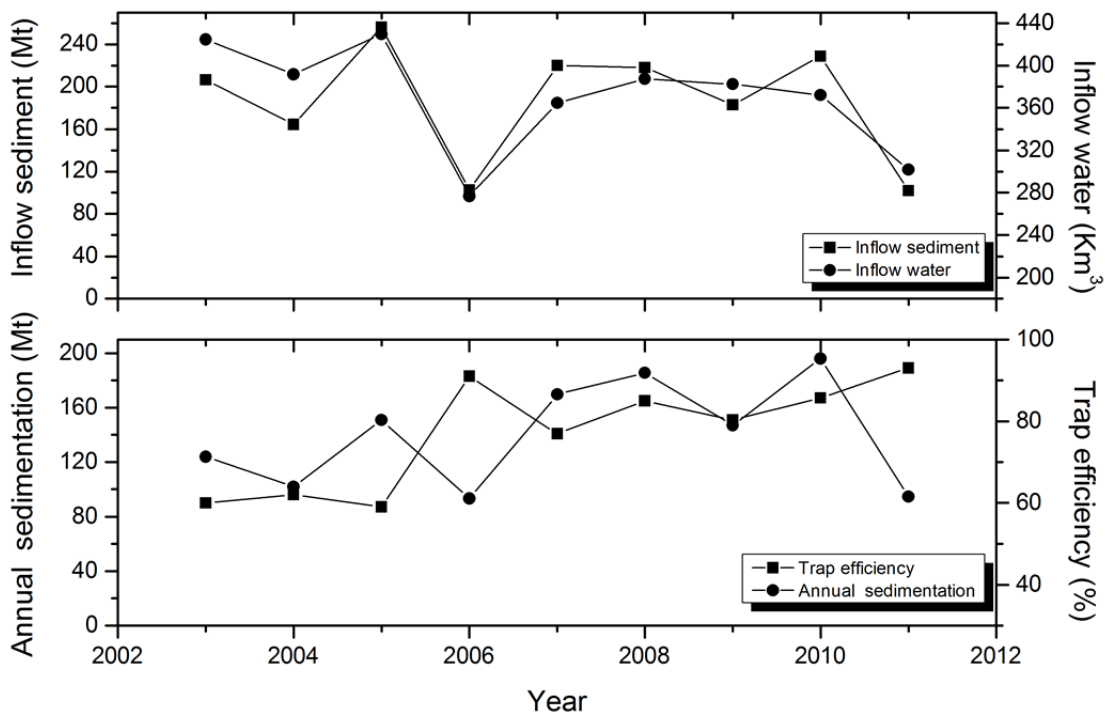
Figure 5.5 Observed water and sediment discharge to the TGR and annual sediment deposited in the TGR over the period 2003 − 2011.

The estimated annual sediment (217 Mt yr^{-1}) trapped in the TGR is somewhat higher than 160 Mt yr^{-1} observed over the period from 2003 to 2011 (Figure 5.5). The discrepancy is primarily attributable to two causes: first, the TGR was not fully regulated during the period 2003−2011 and thus the observed trap efficiencies in Figure 5.5 are much lower than predicted (89%); second, Yangtze's runoff and sediment load have distinct seasonal and secular variability as a result of climate change (Dai *et al.*, 2008; Liu *et al.*, 2008; Lu *et al.*, 2013). For example, the severe drought in the upper Yangtze River basin in 2006 was the worst in the last 50 years. The precipitation in the Yangtze River basin in 2006 was 15–25% lower than that in the years 2000–2005 (Dai *et al.*, 2011). A similar event also occurred in 2011 (Lu *et al.*, 2011). The combined influences of these factors caused sediment entering the TGR to be the lowest during the last 50 years (Dai and Liu, 2013).

5.4 Discussion

5.4.1 Uncertainty and limitations of the model

A validation dataset provided by CWRC was used to evaluate how well the model predicted reservoir sedimentation rates in terms of accuracy, consistency, and ease of application. At the end of the 1980s CWRC carried out a series of bathymetric surveys. A total of 221 reservoirs, including 12 large reservoirs, 25 medium-sized reservoirs and 184 small reservoirs, were investigated, which represented 100% of large reservoirs, 17% of medium-sized reservoirs and 2% of small reservoirs (CWRC,

1992). In addition, from June to August 2012, this study conducted more bathymetric and sedimentation surveys in 28 reservoirs (20 small and 8 medium-sized reservoirs) using a dual frequency (83/200 kHz) echo sounder system (Hummingbird 798ci) with integrated GPS. Some sporadic bathymetric survey reports carried out by local governments in the middle Yangtze reaches after 2000 were also collected. The bathymetric surveys were primarily conducted in mega reservoirs, such as, the Danjiangkou, Wuqiangxi, Zhexi and Fengtan reservoirs. These reports were valuable for validation of the model. Based on the measured sedimentation rates this study also back calculated the true sediment yields.
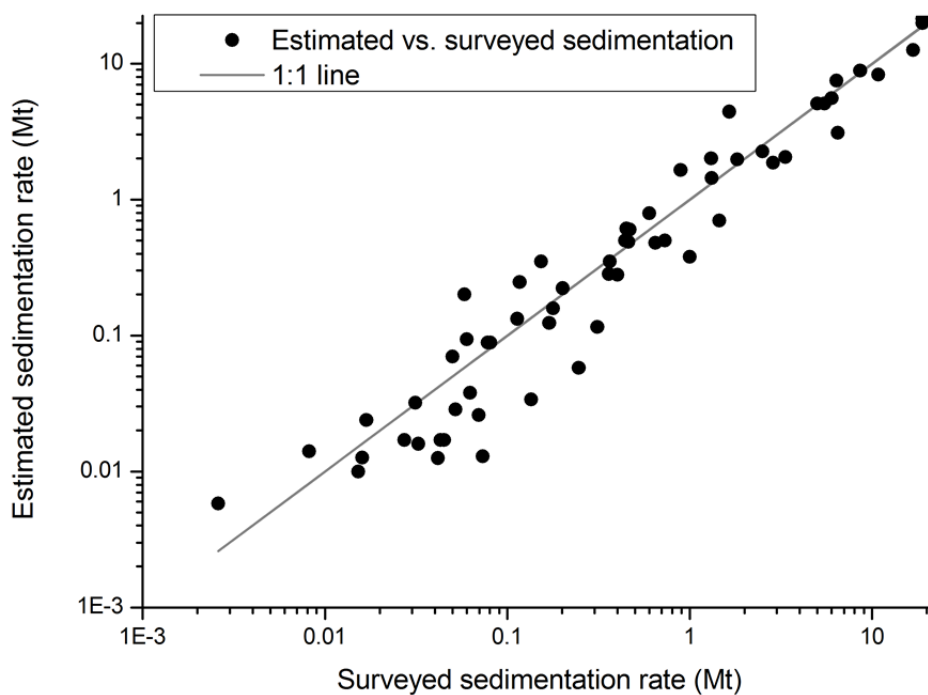
Figure 5.6 Comparison of estimated sedimentation rates to observed sedimentation rates by bathymetric surveys.

A comparison of the predicted sedimentation rates to the measured sedimentation rates

was used to evaluate each model (Figure 5.6). The comparison shows that the average uncertainty of *SY* for all the investigated reservoirs is relatively large (±12.4%) but the average uncertainty of *TE* is relatively low (±5%). If *SY* and *TE* have independent random errors δSY and δTE, according to the rule of error propagation the error in reservoir sedimentation *S* = *SY* x *TE* can be expressed as $\delta S/S = \sqrt{(\delta SY/SY)^2 + (\delta TE/TE)^2}$. The estimated uncertainty of *S* is ±13.4%; therefore, this study could calculate the total annual sediment trapped in the 1,358 reservoirs is 669 Mt yr^{-1} with an error estimate of ±13.4%, or 89.1 Mt. The uncertainty assessment for the smaller reservoirs shown that the total annual sediment trapped in smaller reservoirs is 22 Mt yr^{-1} with an error estimate of ±20.9%, or 4.6 Mt.

Given the complexity of sediment production in the large basin and the long duration of reservoir construction, the obtained estimates should be considered with caution. Other factors that could affect the sedimentation amount were not accounted for here. Downstream bank erosion after reservoir operation could be one of the most significant factors affecting downstream sediment transport because rivers tend to erode and lower their beds downstream of large reservoirs. However, in general, the response of bank erosion rates (and channel width) to upstream reservoir closure is very complex, with trends of widening, narrowing and no change reported for various rivers (Williams and Wolman, 1984). For example, on the Wu tributary with 10 cascade reservoirs end to end on the 900-km river, the impoundments have caused the velocity of the water behind the dams to drop dramatically and thus caused decreased

bank erosion in the 900-km river between dams. Little sediment is trapped in farthest downstream cascade reservoirs (e.g. Silin, Shatuo and Pengshui reservoirs), although their total capacity is nearly 3.6 km^3 (Chen *et al.*, 2008a). Relatively little work has been done on the effect of dam closure on bank erosion rates (Shields *et al.*, 2000). Given the complexity of the response of bank erosion rates to upstream reservoir closure, this study thus did not quantify this effect in this study.

Other variables may influence sediment deposition within a reservoir, including flow, relative pool depth, sediment supply from upstream, and sediment size and distribution, which vary regionally with geology, geomorphic delivery processes, land-use history, and climatic cycles (Minear and Kondolf, 2009). The proposed model assumed that similar processes occur within this basin which is a simplification necessary for computation. This model is appropriate for detecting a basin-wide trend and highlighting reservoirs potentially at risk of sedimentation but may not give accurate estimates of sedimentation rates within individual reservoirs.

Besides, the calculations for small reservoirs (< 0.01 km^3) were aspatial, necessitated by lack of high-resolution DEM data to delineate the reservoirs' drainage areas. It should be noted that these estimates are somewhat speculative because this is based on the assumption that reservoir data are a homogeneous distribution. However, the real reservoir density in the Yangtze River basin shows a clear east-to-west gradient. This means small reservoirs are primarily located in the middle and lower Yangtze

reaches, where sediment yield is relatively low, instead of a homogeneous distribution. Thus, the estimates for small reservoirs may need a more complete geographically referenced analysis. Nevertheless, small reservoirs only trap approximately 22 Mt of sediment per year; their effects on the overall predication are negligible.

5.4.2 Loss of reservoir storage

Reservoir capacity lost to sedimentation could pose a complex problem because many existing reservoirs in the Yangtze basin are irreplaceable due to their unique site characteristics. Figure 5.7 shows that the annual rates of storage loss for individual tributary basins vary greatly from 0.017% in the lower reach to 0.65% in the Tuo tributary basin. It suggests that the upper Yangtze reach (especially the Min and Jialing tributary basins) are a geographic singularity in the distribution of annual rates of loss for storage capacity in reservoirs: four of the five major tributary basins with the highest annual loss of storage capacity are in the upper Yangtze basin: Jinsha, Min, Tuo and Jialing. The annual rate of loss for storage capacity in the Tuo tributary basin (0.65%) is just slightly lower than that (0.75%) in the Yellow River basin (Ran *et al.*, 2013) which previously often was reported as a typical case in severe reservoir sedimentation. Thus, reservoirs in the upper Yangtze reaches probably experience localized sedimentation problems. Nevertheless, the sedimentation problem is not evident in the middle-lower reaches except the Han tributary basin, especially in the Poyang and Dongting lake regions with annual loss rates less than 0.1% (Figure 5.7).
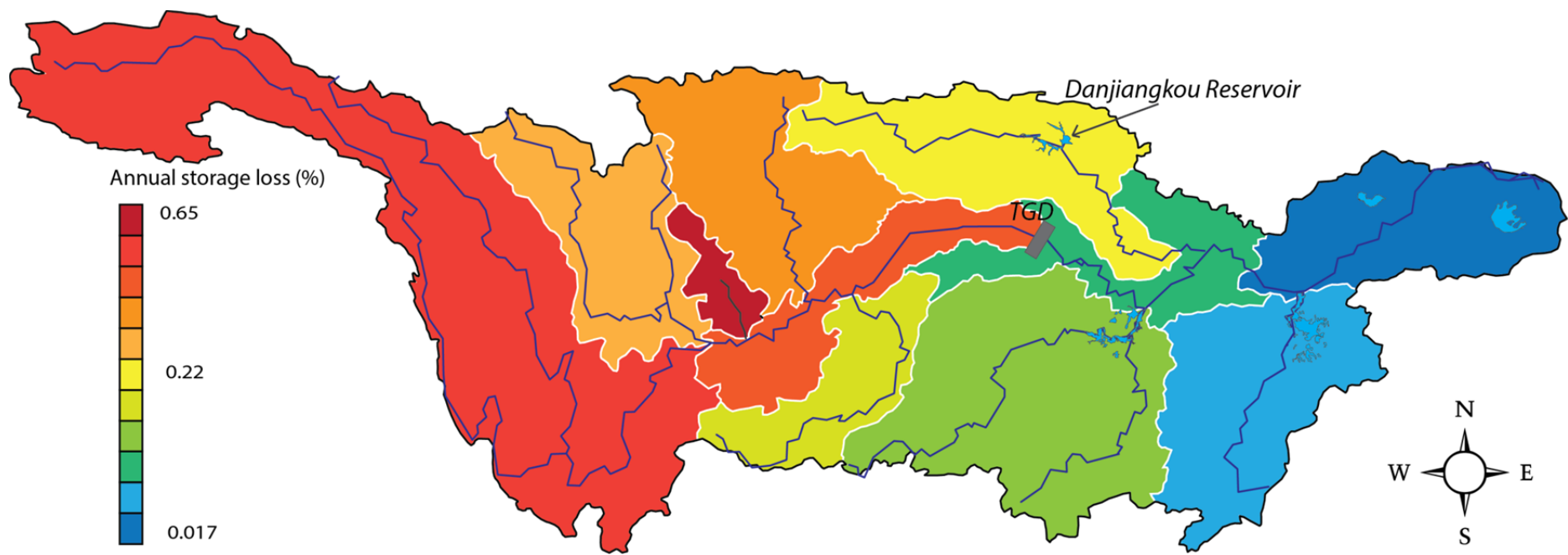
Figure 5.7 Distribution of mean annual loss of reservoir capacity in different Yangtze reaches; it shows a clear east-to-west gradient with a range from 0.017% in the lower Yangtze reach to 0.65% in the Tuo tributary basin.

Table 5.3 Regional sedimentation rates in different parts of the world

Region	Storage capacity (km^3)	Inventoried reservoirs	Annual storage loss (%)	Data source
China (Yellow River)	52.3	601	~1.0	MWR 2001
China (Yellow River)	60	3000	0.75	Ran et al. 2013
China (Upper Yangtze River)	19	10,000	0.6	CWRC 1992
China (Yangtze River)	294.6	43,602	0.02 − 0.65	This study
Asia excluding China	861	7,230	0.3 − 1.0	Basson 2008
North America	1,845	7,205	0.2	White 2001
Europe	1,083	5,497	0.17 – 0.2	White 2001
South and Central America	1,039	1,498	0.1	White 2001
North Africa	188	280	0.08 – 1.5	White 2001
Middle East	224	895	1.5	Basson 2008
Worldwide	6,325	45,571	0.5 − 1	White 2001

The world's reservoirs are currently losing their storage capacity to sedimentation at an estimated rate of 0.5–1% per year (Morris and Fan, 1998; White, 2001; Walling, 2012). Some distinctive features can be obtained by comparison with the rates of storage loss in other parts of the world (Table 5.3). First, the sedimentation problem is highly site specific. In general, the average rate of storage loss in the Yangtze River basin is higher than in North America and Europe, but lower than in some arid and semi-arid regions such as Middle East and the Yellow River basin in China. Second, the world is now losing reservoir capacity much faster than new capacity being constructed (Morris *et al.*, 2008), but the opposite trend is observed in the Yangtze River basin. The mean annual loss of reservoir capacity in upper reaches was approximately 1.15×10^8 m^3 yr^{-1} at the end of the 1980s (CWRC, 1992), increasing to approximately 1.5×10^8 m^3 yr^{-1} by 2003 (Xu, 2007) and peaking at 3.8×10^8 m^3 yr^{-1} at present; but the total reservoir capacity increased about fivefold from only 19 km^3 in 1990 to 294 km^3 over the same period. Despite that, it seems this trend will continue throughout the first half of the twenty-first century because the construction of hydroelectric dams, especially in the upper Yangtze River basin with vast exploitable hydroelectric resources, is the first option to help the Chinese government boost the share of non-fossil fuels in national energy consumption caused by tremendous economic boost (MWR, 1990).

5.4.3 Complexities in river response to sediment trapping

In many large river basins, reservoir sedimentation as the key driver of changing sediment load will interact with other drivers and the resultant signal, as reflected by the sediment load at the catchment outlet, could show little evidence of the changes occurring in the upstream basin (Walling, 2006). Despite the estimated annual reservoir sedimentation rate of 691 ($\pm$ 94) Mt yr^{-1}, sediment load reduction at Datong, closer to the outlet of the basin, was merely 305 Mt over the last 60 years (Yang *et al.*, 2006; CWRC, 2012). Some of this difference may reflect uncertainties discussed above. However, it also indicates that the discrepancy between the estimate of the current rate of sediment sequestration in reservoirs and the estimate of the reduction in the land-ocean sediment flux. The former represents the total amount of sediment trapped behind dams and the latter represents the reduction in downstream sediment flux resulting from sediment trapping by dams (Gupta and Krishnan, 1994; Walling, 2012).

The inconsistency between the estimate of annual reservoir sedimentation and the reduction in sediment load at the outlet also suggests the interaction between reservoir sedimentation and other drivers of changing sediment load, including reduced precipitation and runoff in the Jialing tributary basin, the impact of soil conservation programs in the Lower Jinsha and Jialing tributary basins, as well as sediment trapped

Table 5.4 Annual water discharge, sediment load change and key drivers of changing sediment load at hydrological stations in the upper Yangtze reaches

Station	Before 1990s		1991-2010		Key drivers of changing sediment load [a]			
	Runoff (km^3)	Sediment (Mt)	Runoff (km^3)	Sediment (Mt)	Climate change (Mt)	Reservoir sedimentation (Mt)	Water and soil conservation (Mt)	Others (Mt)
Jinsha (Pingshan)	144.0	246.0	144.7	152.0	0	-86	-28.8	-23
Min (Gaochang)	88.2	52.6	80.0	33.0	-3.5	-33	N/A [b]	-2.6
Tuo (Lijiawan)	12.56	11.7	10.7	1.6	-3.2	-11	N/A	-3.1
Jialing (Beibei)	70.4	134.0	57.1	35.0	-40.6	-94	-54.5	-9.9
Wu (Wulong)	48.6	30.4	51.0	15.0	3.0	-26	-2.7	-2.3

[a] Data sources: (CWRC, 2001-2010; Xu 2007; Chen *et al*. 2008; Xu 2012).

[b] N/A: no data is available.

Table 5.5 Annual water discharge and sediment load to the Dongting Lake in different periods

Period	Four outfalls (inflow)[a]		Four rivers (inflow)[b]		Outflow		Trapped sediment
	Water (km^3)	Sediment (Mt)	Water (km^3)	Sediment (Mt)	Water (km^3)	Sediment (Mt)	(Mt)
Before 1990s	98.5	157.8	165	36	296.5	51.4	142.4
1991 − 2002	62.3	70.4	174	23	269.8	27.6	65.8
2003 − 2008	49.9	13.8	154	9.3	229.5	15.3	7.8

[a] Partial water of the Yangtze River flows into the Dongting Lake via the "Four Outfalls" (Songzi, Taiping, Ouchi and Diaoxian outfalls) on the southern bank of the Yangtze River with four tributaries (Songzi, Hudu, Ouchi and Huarong rivers). The Diaoxian Outfall was blocked in 1958, at present, which does not divert the water of the Yangtze River into Dongting Lake any more.
[b] Four major tributaries (Xiang, Zi, Yuan, and Lei rivers) discharge water into the lake from south, west and northwest, respectively.
[c] Data sources: (Chen et al., 2001; Dai et al., 2005; Xu, 2012)

by dams. For example, Lu and Higgitt (1998) suggest that in the upper Yangtze River increases in sediment load in some tributaries, caused by forest clearance and expansion of cultivated land, have been offset by reductions in the sediment load of other tributaries, as a result of programs of soil and water conservation. Table 5.4 shows the decreasing trend in sediment loads in the upper Yangtze reaches over past 60 years as a result of a combination of reservoir sedimentation, soil and water conservation, climate change and other effects (e.g. debris torrents, sand dredging, revegetation). Among the drivers, reservoir construction is the key driver of sediment reduction, although climate change is also an important cause in the Jialing tributary basin. Although drivers vary greatly in different tributary basins, the estimated cumulative reduction in sedimentation in each tributary basin is still much higher than the reduction in sediment load at its outlet. In the lower and middle Yangtze reaches, river floodplains and other sediment sinks, such as the Dongting Lake floodplain, an important driver to buffer changes in upstream sediment flux. The Dongting Lake received and supplied sediment from and to the Yangtze River. It annually retained approximately 142 Mt of sediment before the 1990s (Table 5.5). Because of the decrease in inflow sediment from its major tributaries (Xiang, Zi, Yuan and Lei rivers) and the four outfalls (Songzi, Taiping, Ouchi and Diaoxian outfalls), The annual sediment load carried down to the lower Yangtze River sharply decreased from 51.4 Mt before the 1990s to 15.3 Mt during the period 2003 − 2008 (Chen et al., 2001b; Dai et al., 2005; Xu, 2012), suggesting that the riverbed has changed from stable to

erosional since 2003 (Dai and Liu, 2013).

In brief, this opinion emphasizes that any attempt to assess the impact of reservoir sedimentation within the reaches of the Yangtze River on downstream land−ocean sediment flux must take account of the potential for buffering within the river system and for the downstream signal to reflect complex time-variant interactions between sediment supply and depositional losses.

5.5 Summary and conclusions

Sediment accumulated in reservoirs creates costly problems for dam operation and ultimate decommissioning. Many of the dams on the landscape can be viewed as future maintenance problems, which will become more urgent as they fill with sediment and lose capacity. Given the inefficient, expensive reservoir investigations for reservoir sedimentation, managers can benefit from an effective approach with which to identify at a large-scale level those reservoirs at higher risk of filling in the near future. The model introduced in this study is an effective model to estimate reservoir sedimentation in a multi-reservoir system while taking into account the effect of reduced sediment input due to upstream traps. The model could be applied equally well to other large river basins despite varying sediment yields.

The results indicate that the cumulative sedimentation rate in the Yangtze River basin is approximately 691 ($\pm$ 94) Mt yr^{-1}, but sedimentation rates vary greatly in different

sub-basins. In the upper Yangtze reaches, especially the TGR and the reservoirs in the Jinsha and Jialing sub-basins are the major contributors to the sedimentation rate of approximately 494 Mt per year, while in the lower and middle reaches reservoirs in the Han tributary basin are another major contributor to sedimentation rate of approximately 197 Mt per year. Despite the large amount of sediment trapped by reservoirs, the reduction in sediment load at outlet (Datong station) was merely 305 Mt over the last 60 years. The difference indicates the important discrepancy between the estimate of the current rate of sediment sequestration in reservoirs and the estimate of the reduction in the land-ocean sediment flux. Despite the high sedimentation rate, numerous reservoirs are under construction or being planned driven by tremendous economic boost and growing energy shortages. Accordingly, the magnitude of sediment retention by reservoirs will be further increased. The resultant changes in downstream channel morphology near the estuary require more efforts to elucidate.

6 Assessing the cumulative impacts of large dams on river connectivity and river landscape fragmentation

6.1 Introduction

At present, there are approximately 45,000 large reservoirs worldwide used for water supply, power generation, flood control, etc. (Vörösmarty *et al.*, 2003). They have exerted severe influence on land-ocean processes thereby triggering various adverse, often unwanted consequences both locally and regionally, such as, loss of floodplains and adjacent wetlands (Rosenberg *et al.*, 2000), and deterioration and loss of river deltas and ocean estuaries (Milliman, 1997; Syvitski *et al.*, 2009) in the Nile (Stanley and Warne, 1993), Colorado (Topping *et al.*, 2000), Mississippi (Blum and Roberts, 2009), and Yellow (Wang *et al.*, 2007b) river basins.

A prominent example of the challenging trade-offs between benefits and risks related to dam construction is apparent in the Yangtze River basin. In the Yangtze River basin, rapid economic growth has increased the pressure for greater hydropower production and other water-related developments, such as large-scale irrigation. The mainstream and its tributaries are being dammed at a dazzling pace. Since the 1950s, numerous reservoirs have been constructed in the river basin. There are 43,600 reservoirs of different sizes in the Yangtze River basin with a total storage capacity of approximately

290 km^3, among which 1,358 reservoirs with storage capacity greater than 0.01 km^3 (Yang and Lu, 2013a). As a result of reservoir construction, the Yangtze River has been strongly fragmented, impeding not only the movement of species but also the delivery of sediments and other nutrients downstream. For example, after the construction of the Three Gorges Dam, the riparian ecosystem has also been significantly disrupted (Wu *et al.*, 2003). The latest investigation in 2012 shows that the population of finless porpoises in the Yangtze River basin has declined to approximately 1,000, making them even rarer than giant pandas in the wild (Qiu, 2012). On the hand, the international conservation community pays close attention to the issues caused by dam developments. For example, the World Wide Fund for Nature (WWF) and Chinese government have implemented more than one-hundred conservation projects which focus on species, forest, freshwater, climate change and adaptation, capacity building, policy advocacy as well as environmental education.

As both the plans for the economic development and the goal to conserve the integrity of the Yangtze River system are implemented on large scales, a sustainable hydropower strategy to reduce environmental impacts is required for the Yangtze River basin in which the risks of dam development is assessed for the entire basin. This chapter first investigated the impacts of the 1,358 'large' dams with storage capacity greater than 0.01 km^3; detailed analysis on small dams with storage capacity less than 0.01 km^3 are given later. Focusing on the Yangtze River's 14 major tributaries (Figure 6.1), this chapter therefore tries, (a) to set up a basic framework for assessing the
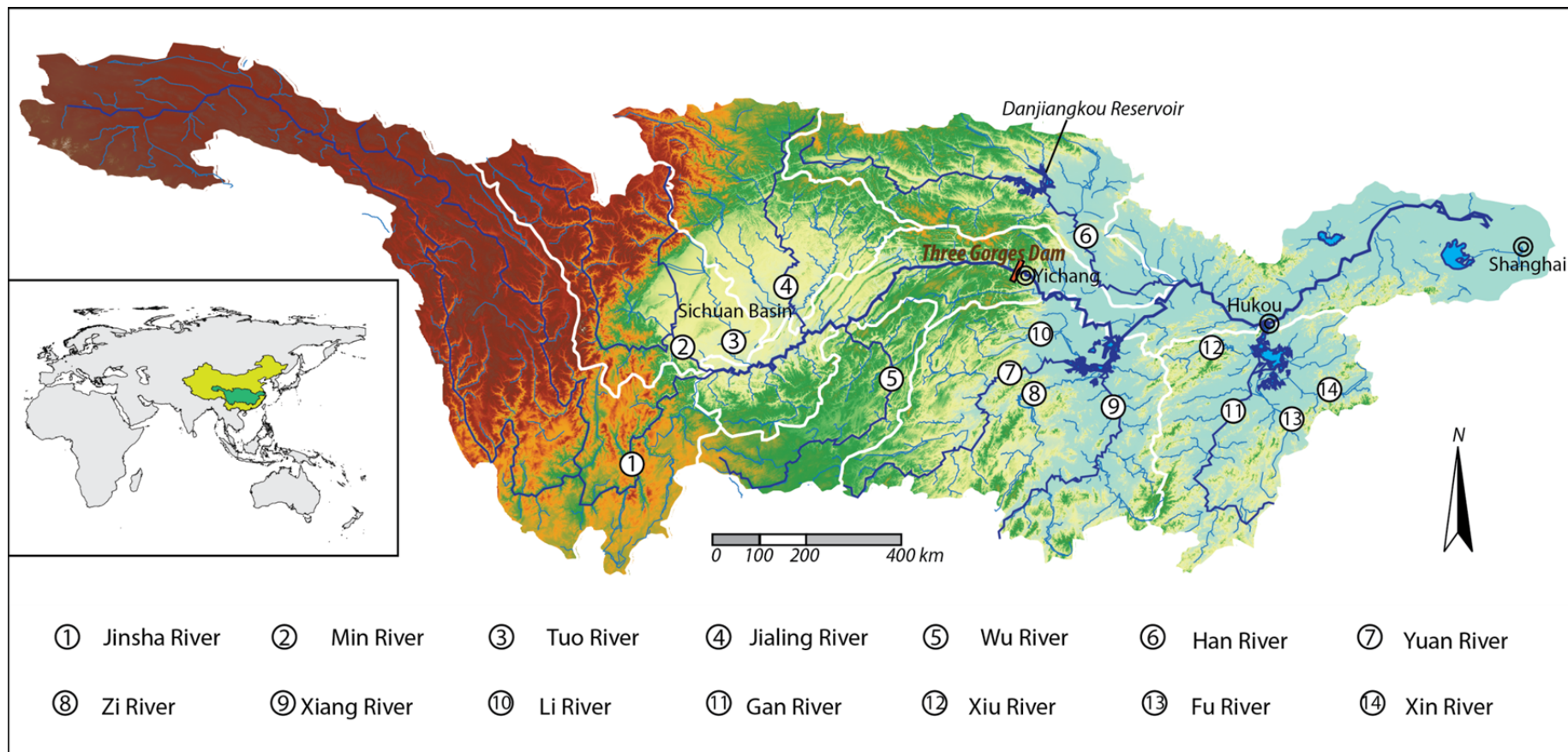
Figure 6.1 Geographical setting of the Yangtze River and its 14 major tributaries. Four tributaries including the Xiang, Zi, Yuan, and the Li rivers, flow into the Dongting Lake which converges into the Yangtze at Chenglingji; the Gan, Fu, Xiu and Xin rivers are the four major tributaries of the Poyang Lake which drains into the Yangtze at Hukou.

impacts of dams on river connectivity and river landscape fragmentation, which can be

considered as an initial attempt to investigate what can be done with simple, but

powerful analyses in river connectivity and river landscape fragmentation; (b) to

investigate the current condition of the Yangtze River and provide an important

reference for policy makers for future dam development in the Yangtze River basin.

6.2 Data and methods

6.2.1 Data sources and data processing

Data used in this chapter included dam information obtained in Chapter 4, digital

elevation model (DEM) data which was used to derive river network, reservoir

catchments, and catchment properties, such as, mean slope, mean elevation,

hydrological data providing water discharge for each tributary, thematic maps for river

landscape classification and visualization.

The DEM data were downloaded from the Consortium for Spatial Information of the

Consultative Group on International Agricultural Research (CGIAR – CSI,

http://srtm.csi.cgiar.org/). The data are available on a global scale through the C-Band

synthetic aperture radars imagery of the Shuttle Radar Topographic Mission (SRTM).

The spaceborne SRTM circled the globe over a wide swath generating radar data that

allowed for the digital reconstruction of the surface relief, producing the DEM data.

The DEM data, with a horizontal resolution of 3'' (~90 m near equator) and a vertical

resolution of 1 m, constitutes the finest resolution and most accurate topographic data available for most of the globe. The river network and catchment properties were derived using ArcGIS 10 with integrated ArcHydro tools.

The hydrological data were provided by an extensive hydrological monitoring program cross the entire Yangtze River basin, which was established in the 1950s by the CWRC. The monitoring program includes discharge and suspended load in accordance with national data standards. The original records for each station provide information on station coordinates (latitude and longitude), catchment area, mean monthly and annual water discharge, and the magnitude and date of occurrence of the maximum and minimum daily discharges (Yan *et al.*, 2011).

The 1,358 reservoirs with storage capacity greater than 1×10^7 m^3 in the Yangtze River basin were delineated in Chapter 4. Except their surface area and estimated storage capacity, other attributes (i.e. construction date) were collected from various sources, including government reports and the Internet, but only construction date that appeared in multiple sources were used in order to guarantee data quality. The dam coordinates were marked on Google Earth and were calibrated using river network extracted from DEM data so that all the dams are correctly located on the river network.

6.2.2 Theoretical framework and definition of geospatial metrics

Considerable obstacles need to be overcome to achieve the monitoring of the extent and condition of river systems, but the major drivers affecting their condition are quite clear and, for the most part, easier to assess and monitor. This is especially true in those areas lacking sufficient resources for extensive fieldwork (Revenga *et al.*, 2005). For example, using data on the size and location of dams, this study can derive some basic conclusions about the relative degree of alteration or stress affecting a river system. These geospatial metrics are often called proxies or surrogates because they are indicators of current threat and give only indirect information about the actual integrity of a river system. The geospatial metrics employed here are a series of quantitative indices representing the degree of alteration or stress exerted by large dams. In this chapter, three metrics were proposed to assess the impacts from different angles. This study employed these metrics using geospatial datasets and geographic information system (GIS), which allows us to analyze the spatial relationships between anthropogenic dam construction and river systems.

6.2.2.1 Weighted dendritic connectivity index (WDCI)

Cote et al. (2009) proposed the dendritic connectivity index (DCI) to assess river connectivity in terms of coincidence probability which is the probability that species can move between two randomly chosen points in a river network. Hence,

connectivity depends on how many dams are built between the two points, and the passability of these dams. Here, passability refers to the probability of species being able to cross a dam in the upstream direction. An obvious difference between riverine and terrestrial systems is the effect of the unidirectional water flow on movement. Specifically, this translates into dams that are potentially more likely to impede upstream than downstream movement. Thus, this conceptual view of connectivity can be simplified by considering upstream movement only (Figure 6.2).

The DCI can be calculated for any size of stream network, or portion of a stream network. For example, the DCI could be calculated for the entire Yangtze River, by choosing the estuary as the furthest downstream point, or for any tributary of the watershed, by choosing the intersection of the tributary with the main stem as the furthest downstream point. However, this model does not consider different river sizes in different sections. For example, the main-stem section of a river can usually sustain more species than its tributaries, even though they have similar channel lengths. Therefore, before calculating DCI values, each stream section can be assigned a weight to indicate the relative stream size. Stream order (Strahler, 1952) is a well-accepted way to define the size of a stream, thus it was used as the weight of the stream. The new index thereafter is termed "weighted dendritic connectivity index (WDCI)" in this study:

$$WDCI = \frac{\sum\limits_{i=1}^{n} w_i \times c_i \times s_i}{\sum\limits_{i=1}^{n} w_i \times s_i} \times 100\% \qquad (6.1)$$

Where s_i is the length of section i; w_i is the weight or Strahler number of section i; c_i is the cumulative passability depending on the number and passability (p) of dams in section i; Assuming the passability of multiple dams is independent, if there are M dams on a river, then c_i is defined as:

$$c_i = \prod_{m=1}^{M} p_m \qquad (6.2)$$

Where p_m is the upstream passability of the mth dam.

One of the obstacles for WDCI is how to define the passability p for each dam. Passability can be assessed as a binary outcome, i.e., a dam meets designated fish passability criteria ($p = 1$) or does not ($p = 0$) (e.g. Clarkin et al. 2005). However, it is almost impossible to obtain the passability for each dam in such a large-scale river basin as the Yangtze River basin with numerous dams. Alternatively, a uniform passability of 0.5 to all dams could be applied (e.g. Cote et al. 2009; Mckay et al. 2013) for the sake of expediency. In this study, a uniform passability of 0.5 was used for the calculations due to lack of passability data. It should be emphasized that these calculations are somewhat speculative because this assignment is arbitrary. If possible, passability data should be preferred.
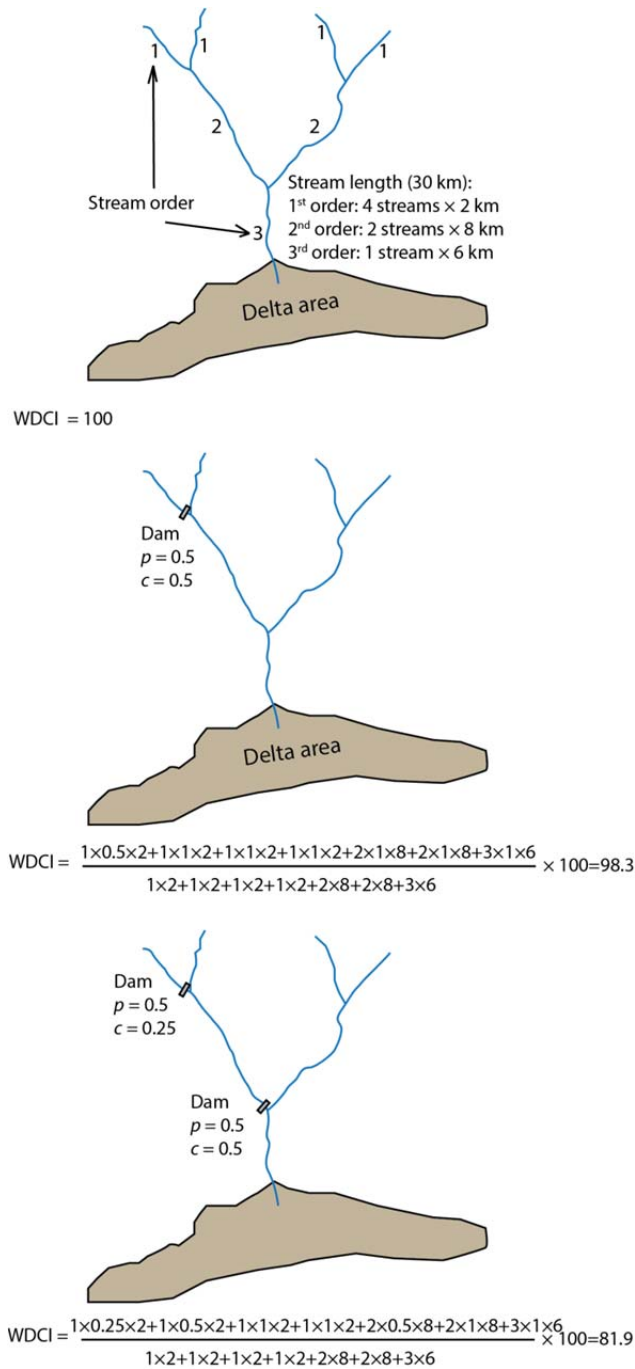
Figure 6.2 Illustration of the WDCI model based on channel lengths, river sizes (indicated by stream order) and passabilities for dams in upstream direction. In a river system without dam (A), the system is fully connected and the WDCI has the maximum value of 100; when a dam is constructed on its small tributary (B), the WDCI decreases slightly to 98.3; when another dam is constructed on its major tributary (C), the WDCI plunges to 81.9. Refer to the *data and methods* section for additional description about this index.

6.2.2.2   Weighted habitat connectivity index for upstream passage (WHCIU)

The index of WDCI measures river connectivity primarily on the base of stream length. This is reasonable because river length is one of the most important properties for a river. However, this index does not consider number of branches of a stream, although different branches may provide various high-quality river habitats in a dendritic river network (Urban and Keitt, 2001; Grant *et al.*, 2007). River confluences, which correspond to the nodes on a dendritic river network, are known to exhibit particular hydrodynamic traits (Rhoads and Kenworthy, 1995; Benda *et al.*, 2004a; Rice *et al.*, 2008). For example, Benda *et al.* (2004a) investigated several cases of river ecosystems created by confluences, e.g., the formation of fans and erosion-resistant deposits, which may influence ecosystem diversity.

In terms of the important of confluences, Mckay et al. (2013) developed the habitat connectivity index for upstream passage (HCIU) to assess river connectivity. This model initially constructed a river network with nodes at locations along the longitudinal dimension where dams are constructed and edges as river system between these nodes. Applying this assumption, the topology of a river network may be represented as a series of nodes and edges summarizing connectivity (Figure 6.3). However, one of the major criticisms of this model is that all nodes in this model, no matter on main stem or small streams, are of equal importance. Obviously, this is not appropriate because the main stem or major tributaries are usually able to sustain more species than the small streams. Like the WDCI, each node can be assigned a

weight to indicate the carrying capacity based on stream order(Strahler, 1952). The new index is thus termed "Weighted habitat connectivity index upstream passage (WHCIU)" in this study:

$$WHCIU = \frac{\sum\limits_{i=1}^{n} w_i \times c_i \times r_i}{\sum\limits_{i=1}^{n} w_i \times r_i} \times 100\%$$

(6.3)

Where w_i is the weight or stream order of section i; r_i is the number of immediately upstream notes for note i; c_i is the cumulative passability.
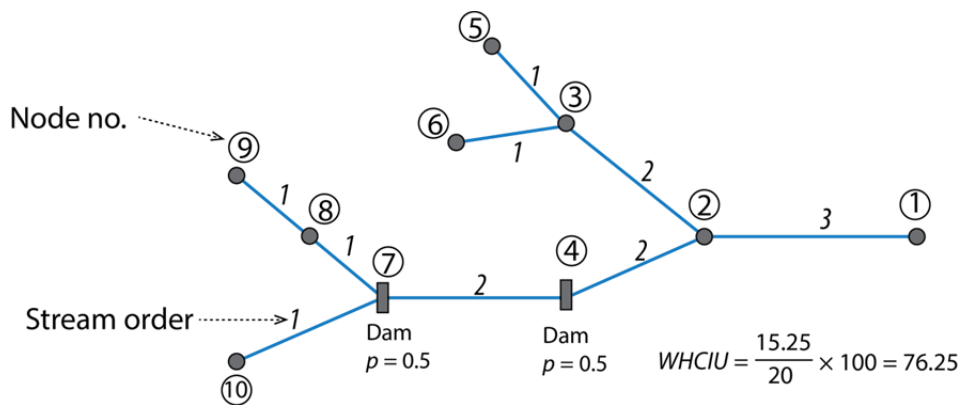
Node no.	Nodal passability	Cumulative passability (c)	No. of upstream nodes (r)	Stream order (w)	$w \times c \times r$	$w \times r$
1	1	1	1	3	3	3
2	1	1	2	3	6	6
3	1	1	2	2	4	4
4	0.5	0.5	1	2	1	2
5	1	1	0	1	0	0
6	1	1	0	1	0	0
7	0.5	0.25	2	2	1	4
8	1	0.25	1	1	0.25	1
9	1	0.25	0	1	0	0
10	1	0.25	0	1	0	0
Total					15.25	20

Figure 6.3 Illustration of the WHCIU model based on number of river confluences (nodes in the figure), river sizes (indicated by stream order) and passabilities for dams in upstream direction. Refer to the *data and methods* section for additional description

about this index.

It should be highlighted that, unlike WDCI which is on the basis of river length, WHCIU is based on the number of nodes; thus, the two indices were used in this study to complement, not to substitute for.

6.2.2.3 Weighted river landscape fragmentation index (WRLFI)

Observation-based investigations can obtain exact insights in how fragmented a river has become under river development, but spatially explicit and reliable data on migratory species are often unavailable for large rivers. A way that addresses the absence of species data is to use representative ecosystems or habitats as a proxy. There is general agreement within the conservation community that protecting representative ecosystem types, or 'coarse-filter' targets, should conserve common communities, the ecological processes that support them, and the river landscapes in which they are evolved (Grill *et al.*, 2014). Coarse-filter targets can be derived through the development of river-landscape classifications based on river basin characteristics such as climate (precipitation, temperature), topography (slope, altitude) and geology (karst geology). The river-landscape classifications can then serve as a proxy for representative ecosystems. The abundance and distribution of river landscapes within the river basin can therefore act as a surrogate for the actual species distribution (Sindorf and Wickel, 2011).

River landscapes are often defined as stream networks that share distinct

geomorphology and similar environmental characteristics (Groves *et al.*, 2002; Higgins *et al.*, 2005; Johnson and Host, 2010). This study specifically approaches river-landscape classification as an important input to evaluate river landscape fragmentation of the Yangtze River. The classification framework proposed by Snelder et al. (2004), using climate, topography, geology and network structure as classification variables, was used for the river-landscape classification. The premise of this approach is that by conserving representative river systems and the hydrological processes that maintain the environments in which river landscape integrity are conserved. Nevertheless, it should be emphasized that this method is not intended to capture stream-level nuances, but aims to capture the specifically relevant characteristics that shape the integrity of river systems as a whole.

Using the river-landscape classification map as an input, this study redefined the river landscape fragmentation index (RLFI) (Sindorf and Wickel, 2011) to measure how fragmented the Yangtze River has become under dam development by considering stream size based on Stream order (Strahler, 1952) (Figure 6.4):

$$WRLFI = \frac{\sum_{i=1}^{n}(e_i^2 - e_i) \times wp_i}{E^2 - E} \times 100\%$$

(6.4)

Where e_i is total number of distinct river landscapes in network section i; E is total number of river landscape classes found in the basin; wp_i is weighted percentage of river length for section i relative to the total river network length, which is defined as:

$$wp_i = \frac{\sum_{j=1}^{m}(w_j \times l_j)}{\sum_{t=1}^{k}(w_t \times l_t)} \qquad (6.5)$$

Where w_i and l_i are the stream order and stream length for each stream in section i; m is number of streams in section i; k is total number of streams in the entire river basin.

The index is defined as a function of the number of distinct river landscapes that remain connected upstream or downstream of a dam combined with the length of river network upstream or downstream of a dam. The assumption that every representative river landscapes provides equal functional connectivity to any of the other river landscapes, allows us to lump those parts of the Yangtze's river network that offer connectivity by the amount of river landscapes, and attribute this by network length. The functional connectivity of a river system can therefore be quantified by summing the total number of connected river landscapes upstream of each dam and incorporating the total weighted length of the low network upstream of each dam relative to the total number of river landscapes and total weighted network length. In practice, it does not matter how many different river landscapes are identified for a river system. The method assesses river-landscape layouts, but increasing or decreasing the number of river-landscapes does not automatically increase the sensitivity of connectivity to dam development.
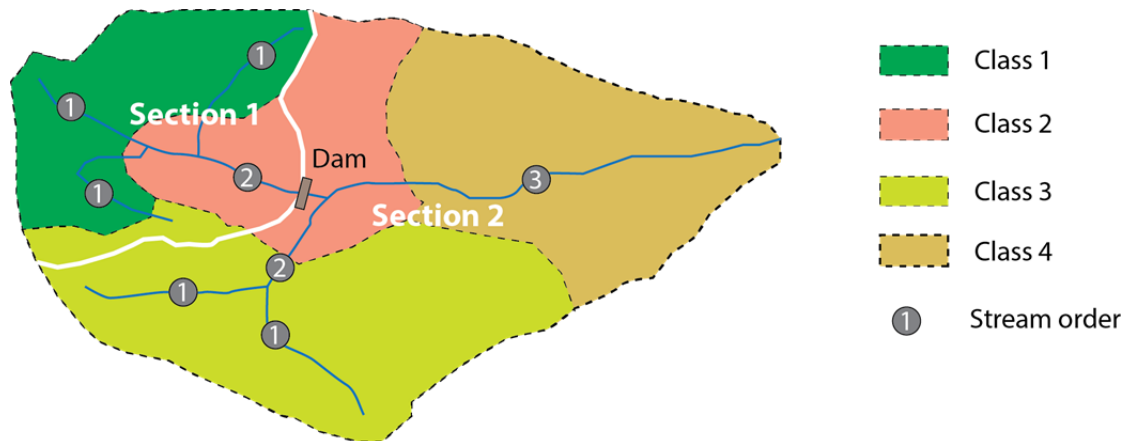
Total no. of river landscapes: 4
Total river length: 280 km: 125 km (order 1); 55 km (order 2); 100 km (order 3)
Section 1:
No. of connected river landscapes: 3
River length: 100 km: 75 km (order 1) ; 25 km (order 2)
Section 2:
No. of connected river landscapes: 3
River length: 180 km: 50km (order 1); 30 km (order 2);100 km (order 3)

$$wp_1 = \frac{75\times1+25\times2}{125\times1+55\times2+100\times3} = 0.23 \qquad wp_2 = \frac{50\times1+30\times2+100\times3}{125\times1+55\times2+100\times3} = 0.77$$

$$WRLFI = \frac{(3^2\text{-}3)\times0.23 +(3^2\text{-}3)\times0.77}{4^2\text{-}4} \times 100\% = 50.0\%$$

Figure 6.4 Illustration of the WREFI model based on channel lengths and river-landscape classification map. The river-ecosystem classification map is an important input to this model.

6.3 Results

6.3.1 Preliminary comparative assessment

Some basic metrics, such as the ratio of reservoir capacity to basin area and the ratio of reservoir capacity to river runoff, can serve as a first-level approximation of the potential impact on river systems. The ratio of reservoir storage capacity to basin area

is a gross measure of the magnitude of potential change in river flows and the consequent water flow disruption and river fragmentation caused by reservoir construction (Milliman and Meade, 1983; Graf, 1999). Regions with high storage capacity-to-area ratios show the greatest potential changes. At the tributary-basin scale, the highest ratio of 718,800 m^3 km^{-2} occurs in the Xiu tributary basin. This tributary basin may have experienced the greatest river regulation. The comparison of the amount of reservoir capacity to the mean annual runoff also reveals similar information. In terms of individual sub-basins, in the upper Yangtze reaches the ratios of capacity to runoff range from 0.08 year in the Jinsha tributary-basin to 0.49 year in the Tuo tributary-basin (Table 6.1). The opposite extreme are the Xiu, Han and Fu tributaries, for which the constructed reservoirs store 106%, 90% and 90% of their corresponding annual runoffs, suggesting that these tributary basins are likely to experience the greatest flow alternation.

The impoundment of river channels regulates discharge downstream, potentially affecting flooding patterns, flow regimes, and nutrient transport (Lu, 2005; Wellmeyer *et al.*, 2005; Graf *et al.*, 2010). It is likely that with increases in the average time that water is retained in reservoirs (increases in the capacity-runoff ratio), the impacts will become more evident. For example, an average ratio of 1.06 years indicates the reservoirs in the Xiu River have a large capacity to absorb flows, and thus the downstream channel would experience a diminished flow regime; conversely, an

Table 6.1 Tributaries, their general characteristics, reservoir capacity data and information on capacity-area and capacity-runoff ratios

	Sub-basin	Drainage area (10^4 km^2)	Runoff (km^3 yr^{-1})	Reservoir capacity (km^3)	Capacity/area (10^3 m^3 km^{-2})	Capacity/runoff (yr)
Upper reach	Jinsha River	47	135.1	11.3	24.0	0.08
	Min River	13	87.5	3.9	30.0	0.04
	Tuo River	3	14.9	7.3	243.3	0.49
	Jialing River	15	72.7	17.1	114.0	0.24
	Wu River	9	42.9	11.6	128.9	0.27
Middle reach	Han	15	55.3	49.8	332.0	0.90
	Dongting Lake Region					
	Li River	2.7	13.1	3.7	137.0	0.28
	Yuan River	9.4	64.3	15.5	164.9	0.24
	Zi River	3	21.7	5.9	196.7	0.27
	Xiang River	9.8	72.2	17.4	177.6	0.24
	Poyang Lake Region					
	Xiu River	1.6	10.8	11.5	718.8	1.06
	Gan River	7.4	68.7	18.5	250.0	0.37
	Fu River	1.5	14.7	4.3	286.7	0.90
	Xin River	1.6	17.8	2.8	175.0	0.16

average ratio of 0.08 years indicates that the reservoirs in the Jinsha River would have little impact on the flow regime downstream of the reservoirs. Evidence of this idea has been reported in the Yangtze River basin by many researchers (Lu *et al.*, 2003b; Xu *et al.*, 2008; Hassan *et al.*, 2010).

6.3.2 Quantifying the impact of individual dams on river connectivity

To accurately measure variation in impact on river connectivity due to dam characteristics (e.g. location), it is essential to measure each dam's effect on river connectivity. Here the impact of individual dams on river connectivity was measured based on the index of WDCI. When calculating the WDCI value for a dam, this study assumed that this dam was one and the only one dam in the Yangtze River basin. Dams with low WDCI values show the greatest potential impact on river connectivity. The overall result is an index-based ranking for the individual dams, which may provide guidance for decision makers wishing to include basin wide effects into dam planning. The lowest WDCI values of 72.90 and 72.94 are for the Gezhouba Dam and TGD (Figure 6.5). These two dams, regulating about 1 million km^2, or 55% of the Yangtze River basin, were built at the outlet of the upper Yangtze reach, leading to a sharp decrease in WDCI.
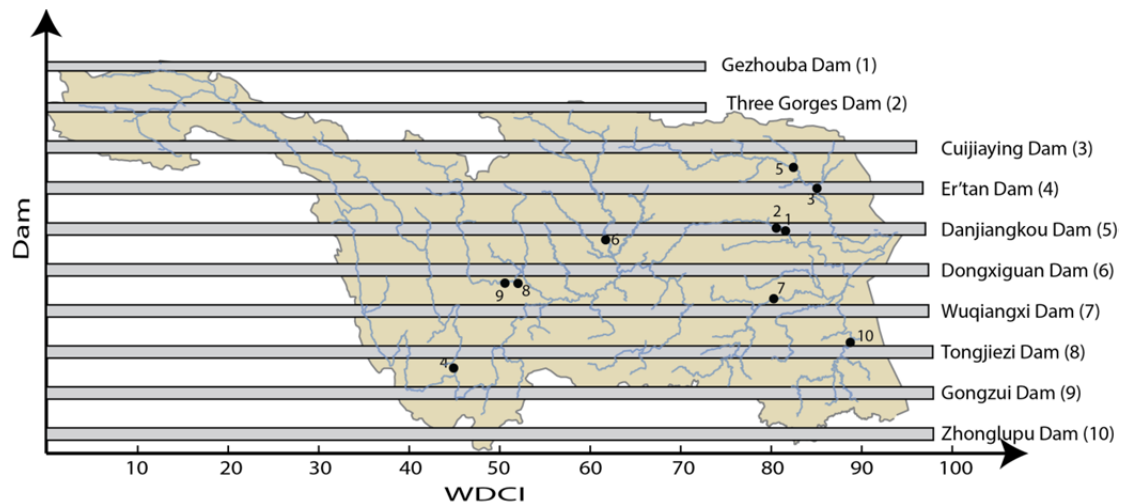
Figure 6.5 List of the dams with the lowest ten WDCI values. The Gezhouba and TGD dams are built on the main stem of the Yangtze River. Other eight dams are built on the major tributaries.

Ten dams with the lowest WDCI values are shown in Figure 6.5. The two dams with lowest WDCI values (Gezhouba and TGD) are all built on the main stem of the Yangtze River. The other eight dams were built on the major tributaries. Due to the construction of the Gezhouba and TGD, a large part of the 6,400-km free-flowing river was disconnected at the outlet of the upper Yangtze reach. This not surprising as it is inherent to any dam on the main stem, though it does add the perspective of subsidiarity. This assessment, both in disconnectivity status and in scale, illustrates that dam development shows a certain path of incremental degradation, but dam built on main stem can cause sharp degradation.

6.3.3 Quantifying the cumulative impacts of dams on river connectivity

In the assessment, The WDCI and WHCIU provided a mechanism for assessing

160

general trends in upstream connectivity. By calculating the two indices this study was able to consider the impacts of dam location and number of dams. This study calculated the cumulative impacts of 1,358 reservoirs/dams with storage capacity greater than 0.01 km^3 on river connectivity in the Yangtze River basin (Table 6.2). The results illustrate the importance of considering hydrological connectivity, expressed by the location of dams in relation to other already existing dams. The WDCI and WHCIU values for the whole Yangtze River have decreased from 100 to 43.97 and 44.00, respectively, indicating the Yangtze River has experienced strong alterations in river connectivity over the past decades, placing the basin among other heavily dammed rivers in the world.
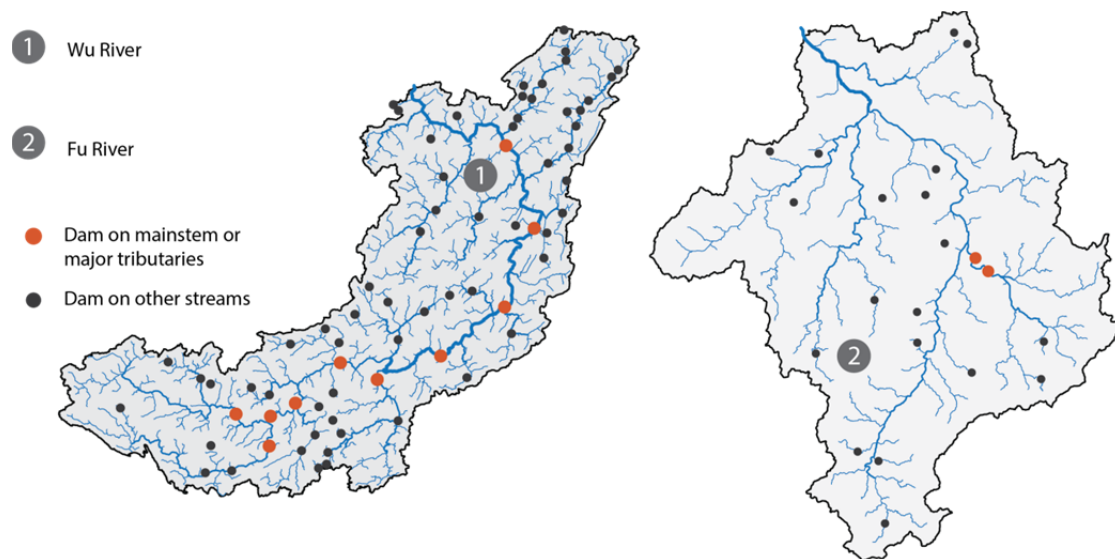
Figure 6.6 A comparison between the Wu River with WDCI value of 11.66 and the Fu River with WDCI value of 86.55: ten large dams are constructed on the Wu River and its major tributaries, while only two dams are constructed on the major tributary of the Fu River.

As anticipated, a single dam near the mouth of a tributary basin is sufficient for

Table 6.2 Summary of model parameterization and WDCI as well as WHCIU values for each tributary

	Tributary	Stream length (km)	No. of nodes	No. of dams	WDCI	WHCIU
	Jinsha River	51,453	5,613	82	42.60	42.64
	Min River	15,225	1,661	23	22.83	20.9
Upper reach	Tuo River	3,769	361	30	12.37	13.42
	Jialing River	20,550	1,851	91	15.83	15.32
	Wu River	10,140	1,089	71	11.66	12.89
	Han River	21,212	1,948	189	34.80	35.11
	Yuan River	11,567	1,062	110	17.55	19.56
	Li River	3,255	279	36	65.33	63.63
	Zi River	3,555	359	44	33.66	33.27
Middle reach	Xiang River	11,418	1,137	134	49.57	52.25
	Gan River	8,685	861	99	50.99	51.42
	Xiu River	1,835	178	15	54.10	58.6
	Fu River	1,892	199	21	86.55	89.64
	Xin River	2,007	188	34	59.90	62.08
Total	Overall Yangtze	211,527[a]	21,530	1,358	43.97	44.00

[a]This is the total length of streams in the Yangtze River basin; thus, it is not equivalent to the sum of the total length of streams in the 14 tributary basins.

reduction in river connectivity (McKay *et al.*, 2013), but the impact to river connectivity varies greatly with location due to differences in basin topology and the locations of dams. For example, the lowest WDCI and WHCIU are in the Wu tributary basin, which is mainly attributable to ten large cascade dams constructed on the main stem of the Wu River (Figure 6.6). Conversely, the Fu River, with the highest values of WDCI and WHCIU, still has no dams on its main stem. Collectively, rivers in the middle Yangtze reach obtained relatively higher WDCI and WHCIU values than their counterparts in the upper reach, indicating a sharp decline in river connectivity in the upper Yangtze reach. Indeed, the eco-system of the upper branches of the Yangtze has collapsed. For example, the fish species in the upper branches have declined dramatically in recent years (Zhang *et al.*, 2015).

It should also be highlighted that the rivers with low WDCI and WHCIU values are all the rivers with rich water power resources. The Min, Jinsha, Tuo, Wu rivers and the main stem of the upper Yangtze River have already disconnected due to dam construction. The Yuan and Zi rivers in the middle reach of the Yangtze River are also disconnected and fragmented. The rivers, such as the Fu River and Xin River with few hydropower resources, have narrowly escaped being disconnection.

These results show that the location of a dam determines its relative effect on river connectivity. The WDCI and WHCIU can demonstrate the magnitude of the cumulative impacts on river connectivity. As evidenced in the tributaries of the

Yangtze River, dams located at the headwaters or small streams can minimize loss of river connectivity (e.g. the Fu and Li rivers), while dams placed on main stem or a major tributary can lead to a noticeable impact on river connectivity.

6.3.4 Quantifying the cumulative impacts on river landscape fragmentation using WRLFI

There is general agreement within the conservation community that protecting representative ecosystems or 'coarse-filter' targets, should conserve common communities, the ecological processes that support them, and the river landscapes in which they are evolved. Coarse-filter targets can be derived through the development of river-landscape classifications based on river basin characteristics such as climate (precipitation, temperature), topography (slope, altitude) and geology (karst geology). The river-landscape classification was used as a proxy for ecosystem types. With careful consideration of the river basin characteristics, this study identified 12 distinct river landscapes (Figure 6.7A) based on the classification framework proposed by Snelder et al. (2004). It should be reiterated that this classification is only an interpretation of what are thought to be relevant variables based on data availability. It should also be noted that the final classification is never all encompassing and that the master factors of importance are basin-specific.
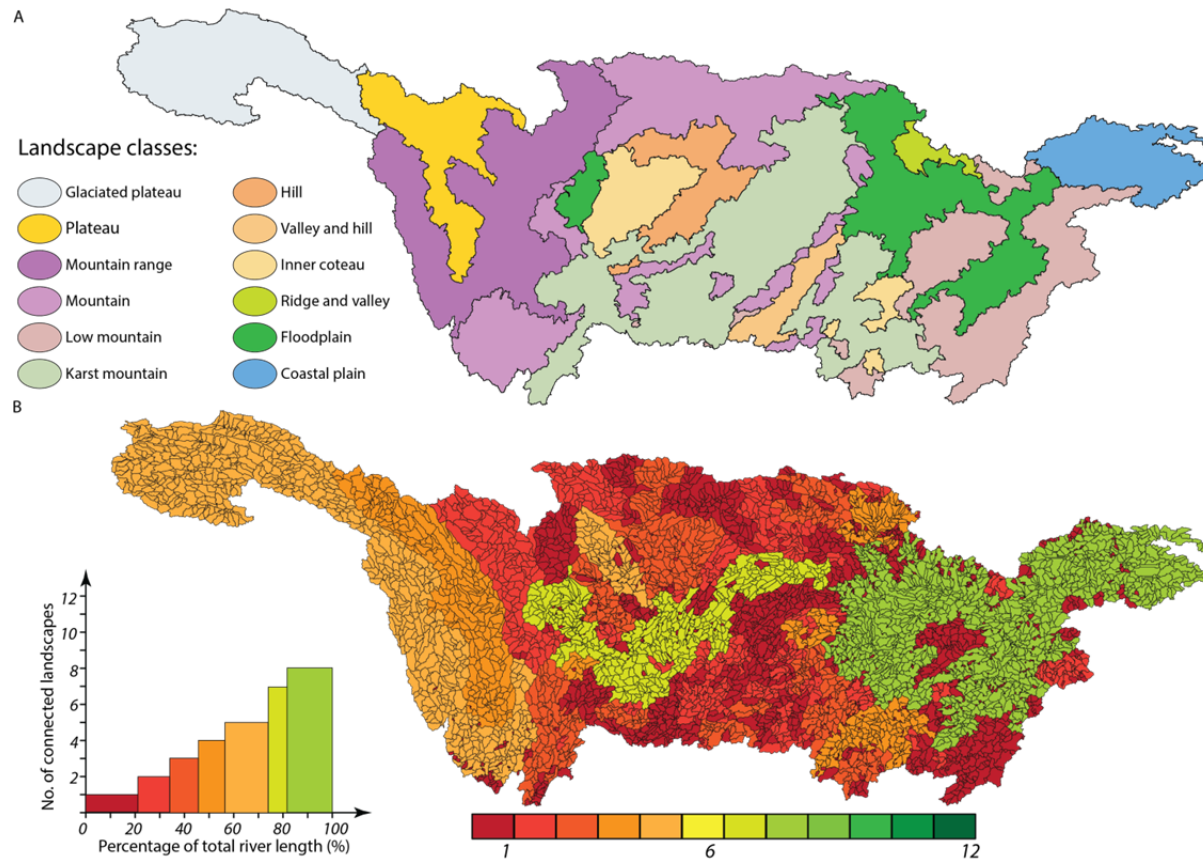
Figure 6.7 Results of river landscape fragmentation analysis based river-landscape classification map (A). The result (B) shows that substantial part of tributary basins, especially the Wu, Min, Jialing and the Yuan rivers, only maintain connectivity among one to three distinct river landscapes. Connectivity between different river landscapes in the middle and lower basin is the highest. Even so, only a small part of the system still maintains connectivity between seven out of twelve river landscapes.

165

Based on the basin-wide river-landscape classification map, the Yangtze River with 12 distinct river landscapes, and with full integrity, would have 100% connectivity. Nevertheless, the result in Figure 6.7B shows that the Yangtze River already shows a high degree of river fragmentation. In the upper Yangtze reach, with seven distinct river landscapes being locked behind the dams of the TGD, only six river landscapes remain connected in the main-stem area. What is even worse: a substantial part of tributary basins, especially the Jinsha, Wu, Min, Jialing and the Yuan rivers only maintain connectivity among one to three distinct river landscapes. The result shows that connectivity between different river landscapes in the middle and lower basin is the highest because no dams have been constructed on the middle-lower main stem. Even so, only a small part of the system still maintains connectivity between seven out of twelve river landscapes — no part of the Yangtze connects all twelve river landscapes.

From these results, it can be seen that a proposed dam on the Yangtze main stem or major tributary would significantly further fragment the river basin. The results show that the middle-lower main-stem area and some tributary basins in the Poyang Lake Region are relatively 'better' left without dams. The analysis on river landscape fragmentation provides insights into how different river landscapes are distributed across the Yangtze River basin and how they relate to each other in terms of spatial configuration. This allows the identification of links between different river landscapes and supporting processes where connectivity is a key variable (Sindorf and Wickel, 2011), such as, sediment transport and migratory processes.

6.4 Discussion

6.4.1 Uncertainty analysis

Because of data unavailability, universal passability standards were applied to all dams in the Yangtze River basin. Yet these calculations are somewhat speculative because this assignment is arbitrary. If possible, passability data should be collected. In practice, although passability will vary for each dam, all the large and most medium-sized dams are constructed, supervised and managed by the CWRC or its provincial agencies. However, few fish passes have been constructed at these dams (Lin *et al.*, 2013). For example, The Gezhouba Dam and the TGD have no fish pass facilities and thus totally block fish migration (passability ≈ 0) (Wei *et al.*, 1997; Gao *et al.*, 2010). Therefore, the situation may be more serious than predicted in this study. Another impediment is that current methods of estimating passability are often problematic as the estimates need to consider hydrologic factors, such as, water chemistry changes and other variables. In addition, the passability can fluctuate stochastically in a nonlinear pattern, which would vary spatially and temporally within a catchment (Spens *et al.*, 2007; Jones *et al.*, 2008). As an example of an approach to estimate passability of dams, the proposed metrics could be merged with hydrological models that estimate variations in water discharge and sediment load and relate these parameters to variation in passability as a function of flow for species with different swimming abilities (Cote *et al.*, 2009), but this approach may be

inoperable and impractical because it is very complicated.

A second challenge is identifying whether the probability of passing a dam is independent among nearby dams. Independence may not be appropriate in situations where passability is dependent on water discharge (which varies at large spatial scales). For example, because the Gezhouba Dam is close to the TGD (38 km), the water discharge at the Gezhouba Dam is significantly affected by the water discharged from the TGD. In this case, the probability of passing the Gezhouba Dam may not be independent. In addition, on such a river as the Wu tributary with ten cascade dams on the 900-km river, the impoundments have caused changes in physical condition; for example, the velocity of the water behind the dams dropped dramatically (Yang and Lu, 2014b). The changes in physical condition have complicated the estimation of passability for each cascade dam. Although the WDCI and WHCIU require estimates of passability at individual dams and better estimates of passability will serve to reduce uncertainty, designing an approach to estimate passability of dams is still a challenge to the academic community. Also the approach should be validated against observed connectivity patterns.

A third challenge is that each river landscape was considered to be equal relevance throughout the entire Yangtze River basin when this study analyzed river landscape fragmentation using the WRLFI based river-landscape classification map. In fact, more crucial information could be obtained if the individual river landscapes and their

association with specific processes, basin layout can be better geographically quantified. Besides, it is to be noted that the WRLFI value is extremely dependent on the river-landscape classification map. You may get slightly different results with different classification maps. Thus, an appropriate classification map is the fundamental determinant of the assessment based on the WRLFI.

Another limitation for the three metrics is that they may undervalue the impacts of small dams because the three metrics can only provide an overall assessment on the impacts of dams, but small dams may contribute less to the overall alteration of large-river flows as a result of their limited storage capacities. Therefore, a method which can provide not only overall results but also detailed regional results is needed. This method is demonstrated in the next chapter.

Despite the many current limitations related to the implementation of the metrics, results have to be judged against large-scale needs of water resources managers and policy makers. Many critical characteristics along the Yangtze River network, such as highly fragmented condition, disruptions in river connectivity are well represented using the current metrics. Major changes between the tributaries or within geographical reaches (upper, middle and lower reaches) can easily be mapped. These metrics provide valuable information on expected impacts, supporting large-scale decision making.

6.4.2 Comparison of different metrics

This study quantified the impacts of 1,358 dams on river connectivity and river landscape fragmentation in the Yangtze River basin using three different metrics. The WDCI facilitated the consideration of longitudinal connectivity in the Yangtze River network. An advantage of the index is that it allows the evaluation of the impacts of individual projects at the scale of the entire river network that encompasses cumulative impacts of many large and medium-sized dams (Cote *et al.*, 2009). Yet, the WHCIU, regardless of the length of streams, is a graph-theoretic model to assess river connectivity by incorporating both quantity of confluences accessed and the cumulative passage rate to that point (McKay *et al.*, 2013). Both metrics present similar fragmentation history for the Yangtze River indicating a steady loss of river connectivity.

However, if we compare the two metrics with WRLFI, we may find some meaningful findings. For example, when the Gongzui hydropower dam was built on the Dadu River (the major tributary of the Min River) in 1978, the values of WDCI and WHCIU decreased by 2.79% and 3.11% respectively, relative to a drop of 5.5% in WRLFI. The decrease in WRLFI was almost twice of the decrease in WDCI; but it did not mean that the WRLFI has exaggerated the impacts caused by the Gongzui dam. Before construction of the Gongzui dam, the Min River maintained connectivity between six river landscapes. After the dam was constructed in 1978, a large part of the Dadu

River was disconnected with connectivity between only three river landscapes, leading to a sharp drop in WRLFI. WRLFI heavily depends on the number of river landscapes blocked by dams and it is therefore an important indicator of river landscape fragmentation. When the TGD was closed in 2003, leading to sharp drops in WDCI, WHCIU and WRLFI (20.02%, 20.37% and 23.50%, respectively), the drops in the three metrics were consistent, although the decreases in WDCI and WHCIU are slightly lower than that of WRLFI. However, they also indicate the impact of the TGD on river landscape fragmentation is slightly greater than the impact on river connectivity.
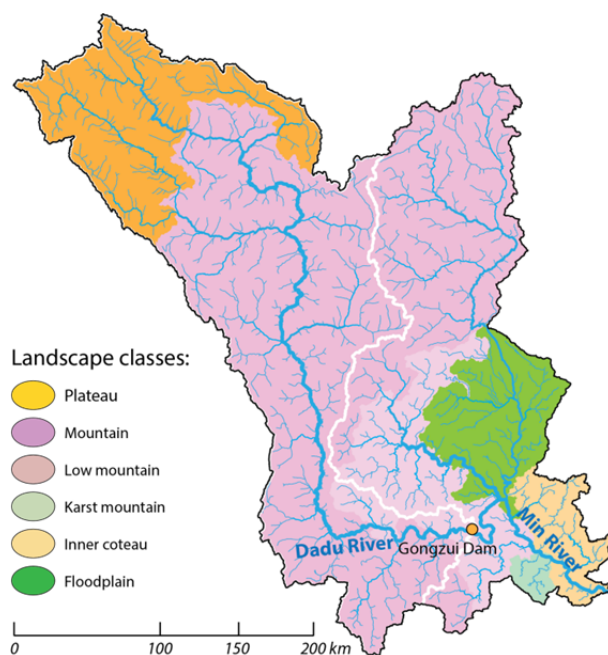
Figure 6.8 Location of the Gongzui Dam and its fragmented river landscapes in Min River basin. Before construction of the dam, the Min River maintained connectivity between six river landscapes. After the dam constructed in 1978, the large part of the Dadu River is now locked and maintains connectivity between only three landscapes, leading to a sharp drop in WRLFI.

In addition, the study results show that WDCI and WHCIU are more sensitive than

WRLFI in extreme circumstances. For example, in a specific river section, if the river already maintains connectivity among only one river landscape due to previous dam construction, WRLFI would not decrease any more even if more dams are constructed on the river. Conversely, WDCI and WHCIU can still reflect the variation in river connectivity.

6.4.3 Past and future trends

Figure 6.9 presents the year-by-year fragmentation history of the Yangtze River in comparison with the world's five largest rivers on the basis of the variation in DCI/WDCI. It illustrates that the indices decrease over time as dams are built on the rivers. Graf (1999) reported that, in North America, the greatest rate of increase was from the late 1950s to the late 1970s. The resulting value of DCI then decreased rapidly from the 1950s to 1970s, such as in the Columbia and Mississippi rivers. The oft-heard colloquial wisdom that "the nation's dam building era is over" was born out by the relatively minor increases in storage after 1980 in North America. This general history explains why the downstream environmental costs of dams have only recently captured the attention of scientists. The maximum potential for the downstream hydrologic disruptions through reservoir storage has been in place for less than three decades, and the effects have only recently become obvious (Graf, 1999). In Asia, however, dam construction still keeps a strong momentum, especially after the 1990s. Most of the large Asian rivers (such as the Mekong, Indus, Ganges and Yangtze) are

being dammed at a dazzling pace. Figure 6.9 shows that a sharp decrease in DCI/WDCI for the Mekong and Yangtze occurred since 1975. Moreover, the decreasing trend will remain in next 10 years based on the prediction. Although Asian rivers experienced river fragmentation later than their counterparts in North America, all the rivers ended up with quite low DCI/WDCI value or high river disconnectivity eventually.
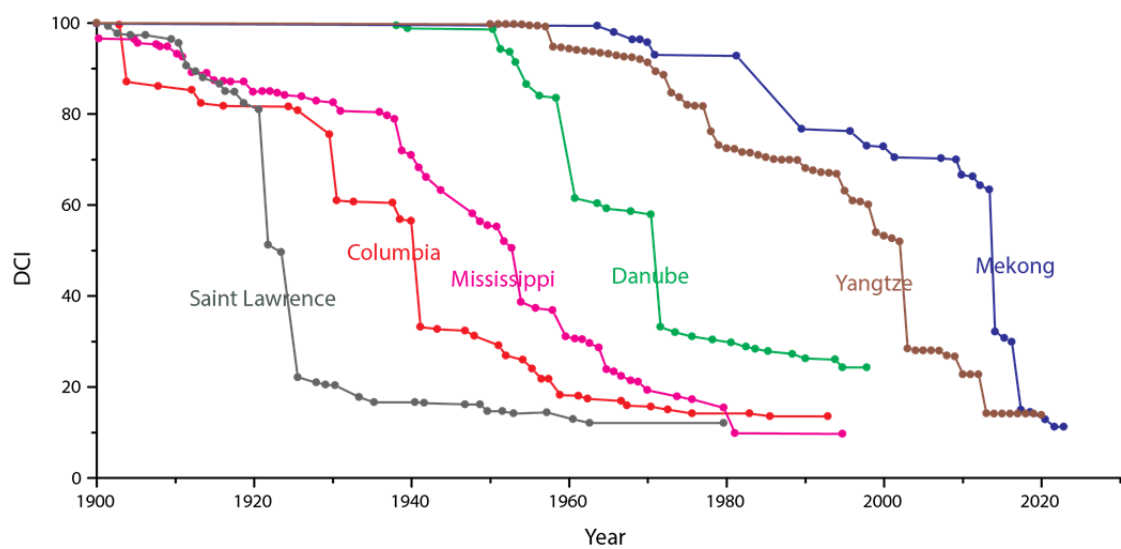
Figure 6.9 Fragmentation history for selected large rivers in the world. Data for the Yangtze was provided by this study; data for other rivers were provided by Grill et al. (2014). In North America, the greatest rate of increase in dams was from the late 1950s to the late 1970s leading to a nosedive in DCI, such as the Columbia and Mississippi rivers. The sharp decrease in DCI for Asian rivers (the Mekong and Yangtze) occurred since 1975, but the decreasing trend will remain in next 10 years based on the prediction.

6.5 Summary and conclusions

This study performed a pilot investigation in implementation of a basin-wide river fragmentation assessment in the Yangtze River basin. It provides environmental

insights to all major tributaries. The value of this study extends beyond the Yangtze River example in presenting an analytical approach that can be replicated on other river basins. The metrics provide insights into river connectivity and fragmentation as components of river integrity, thereby allowing resource managers to characterize watersheds and determine priorities for optimizing resource allocation and infrastructure plans (placement of dams).

For the Yangtze River, the results indicate that the Gezhouba Dam and the TGD have highest impact on river connectivity and fragmentation. The WDCI and WHCIU values for the whole Yangtze River have decreased from 100 to 43.97 and 44.00, respectively, indicating that the Yangtze has experienced strong alterations over the past decades. In terms of the major tributaries, the lowest WDCI and WHCIU values happen in the Wu tributary basin, which is mainly attributable to contiguous cascade dams on the main stem of the Wu River. The measurement of WRLFI provides more insights to river landscape fragmentation, which shows that the Yangtze River already has a high degree of river landscape fragmentation. A substantial part of tributary basins, especially the Wu, Min, Jialing and the Yuan tributaries only maintain connectivity among one to three river landscapes.

As demands on energy and water resources increase in the Yangtze River basin, the Chinese government is now engaged in a new expansion of dams in great staircases. This research can help address the environmental risks associated with further impacts

caused by newly constructed dams. For example, the metrics used in this study would allow aiming at different specific processes, such as, fish migration, dam design and operation (e.g., flood protection, environmental flows, or hydropower potential) and quantification of different issues at difference scales. Integrating the assessment into environmental impact assessments can also present a new framework to effectively integrate river connectivity and free-flowing functionality into dam planning and adds a basin-wide perspective to conventional environmental impacts assessments. Based on the assessments, dam projects which focus economic reward but may cause irretrievable environmental damage should be halted. Environment-friendly alternative programs should be prioritized to develop the Yangtze River basin with relatively lower environmental costs.

7 Assess the cumulative impacts of small dams on flow regulation and river landscape fragmentation

7.1 Introduction

Today about 800,000 dams operate worldwide, most of which are small (Keiser *et al.*, 2005; Richter and Thomas, 2007). According to Kucukali and Baris (2009), about 19,000 micro- and 19,606 mini-hydropower dams with total installed capacities of 687 and 7171 MW respectively were constructed between 1994 and 2004. Their benefits have been widely reported (Downing *et al.*, 2006; Marks, 2007): rainwater harvest, water table recharge, flood control, affordable energy, and more importantly, improved water availability for irrigation and domestic uses in rural communities. The global installed capacity of small hydropower dams is around 47,000 MW against an estimated potential of 180,000 MW. China has over half of the world's developed small hydropower capacity in about 42,000 stations with an installed capacity of over 35,000 MW (Ohunakin *et al.*, 2011).

A growing number of nations have recently highlighted development of small hydropower resources in national energy policies. In Sri Lanka, approximately 30 small hydropower projects are either in operation or planned for the country's rivers (Ljung *et al.*, 2000). Growth of the electricity industry in Zimbabwe is expected to result in a

significant increase in the number of small dams as the country looks toward developing chains of hydropower plants as a means to provide rural electrification (Mungwena, 2002; Kalitsi, 2003; Klunne, 2007). The Nigerian Government has also taken steps to diversify energy sources in order to promote small hydropower development by encouraging private investments in the energy sector through reforms (Ohunakin et al., 2011). India also added approximately 300 MW of small hydropower projects in 2011 for a cumulative small hydropower capacity of 3,200 MW; another 1,100 MW of small hydropower dams are under construction (Sharma et al., 2013). Likewise, total installed capacity at small hydropower plants in China had grown from 100 MW in 1949 to 59 GW be the end of 2011 at an annual growth rate of 29.6% (Zhai et al., 2013).

However, unlike single large dams, which have attracted the most attention from the environmental science and environmental advocacy communities because they often create enormous reservoirs, flood large land areas, displace large populations and form significant barriers to aquatic species and navigation, small dams may be built on smaller river systems, and be designed to divert small amounts of irrigation water. Small dams may be easier to manage than large dams that combine many stakeholders across many levels of society (Taylor et al., 2007); but their effects cannot be well quantified due to their huge number and lack of needed data. Therefore, the impacts of small dams are still unclear, although much has been written about the environmental impacts of large dams.

With respect to small dams and reservoirs, considerable uncertainty exists about the environmental impacts of single small dams or the cumulative impacts of many small dams on river systems (Anderson *et al.*, 2006; Kibler and Tullos, 2013). For example, in some cases, small dams actually dewater or fragment more kilometers of stream, flood more land area, or lose more water to evaporation per unit of energy produced than larger dams (Gleick, 1992; Kibler and Tullos, 2013). Despite their size, small hydropower dams almost always result in significant hydrologic alterations and losses in hydrologic connectivity. For example, small dam developments in tropical regions have been shown to affect movement patterns and persistence of migratory animals such as shrimps and fishes and to substantially alter physical habitat conditions (Anderson *et al.*, 2006). However, previous studies often evaluated the impacts at a basin-wide scale, which have considerably underestimated the impacts at a regional scale.

In addition, small dams also intercept the natural nutrient cycle in a river, which was initially delivered downstream where it is again available for ecosystems. Many small dams in developing countries are rapidly being constructed on previously unaltered systems draining rural areas. Consequently, the magnitude of environmental changes to water resources resulting from new small dam development may be much greater. Although they tend to avoid the more obvious environmental and social disruption of large projects, their cumulative impacts are still unknown to the public. Unfortunately, few comprehensive studies have been conducted to investigate the cumulative impacts

of small dams because information on small dams is especially limited in developing countries, where baseline environmental data, small-dam spatial information, and environmental assessments are less commonly available (Gleick, 1998). For example, in the report on the application of a hydrological modeling approach to investigate the uncertainty associated with simulating the impacts of small dams in several South African catchments, Hughes and Mantel (2010) concluded that the biggest source of uncertainty in South Africa appears to be associated with a lack of reliable information on volumes and patterns of water abstraction from the dams.

Fortunately, this study has obtained basic information about small dam distribution in the Yangtze River basin. Based on the data obtained in Chapter 4, the aims of this chapter is to: (a) develop a new model to quantify the cumulative impacts of small dams on water regulation in the Yangtze River basin; (b) propose a simple GIS model to measure the impact of small dams on river landscape fragmentation.

7.2 Data and methods

7.2.1 Data sources and data processing

Several datasets were used in this chapter, including spatial dataset of small dams and reservoirs delineated in Chapter 4 (Figure 7.1), DEM data which was used to derive river network and reservoir catchments, precipitation data used to estimate river runoff, various thematic maps for river landscape classification and visualization.

The dataset of small dams was obtained in Chapter 4 using remote sensing techniques. As stated in Chapter 4, this study only extracted dams with water surface area greater than 0.0036 km^2. Thus, further study based on this dataset could yield relatively conservative estimates of the impacts of small dams. Despite this limitation, it is nevertheless the best dataset available that provides basic spatial information on small dams in the Yangtze River basin, which gives valuable insight into cumulative impacts assessment and management implications. It thus enabled the calculation of indices to evaluate the impacts of small dams, as described later.

The DEM data were downloaded from (CGIAR – CSI, http://srtm.csi.cgiar.org/). The data are available on a global scale through the C-Band synthetic aperture radars imagery of SRTM. The DEM data, with a horizontal resolution of 3'' (~90 m near equator) and a vertical resolution of 1 m, constitutes the finest resolution and most accurate topographic data available for most of the globe. The river network and catchment properties were derived using ArcGIS 10 with integrated ArcHydro tools.

River runoff data from 223 gauging stations obtained primarily from the CWRC were collected to simulate runoff variation across the Yangtze River basin. The original records provided by CWRC for each station provide information on station coordinates (latitude and longitude), catchment area, mean monthly and annual water discharge, and the magnitude and date of occurrence of the maximum and minimum daily discharges (Yan *et al.*, 2011). Here runoff was calculated by dividing mean annual
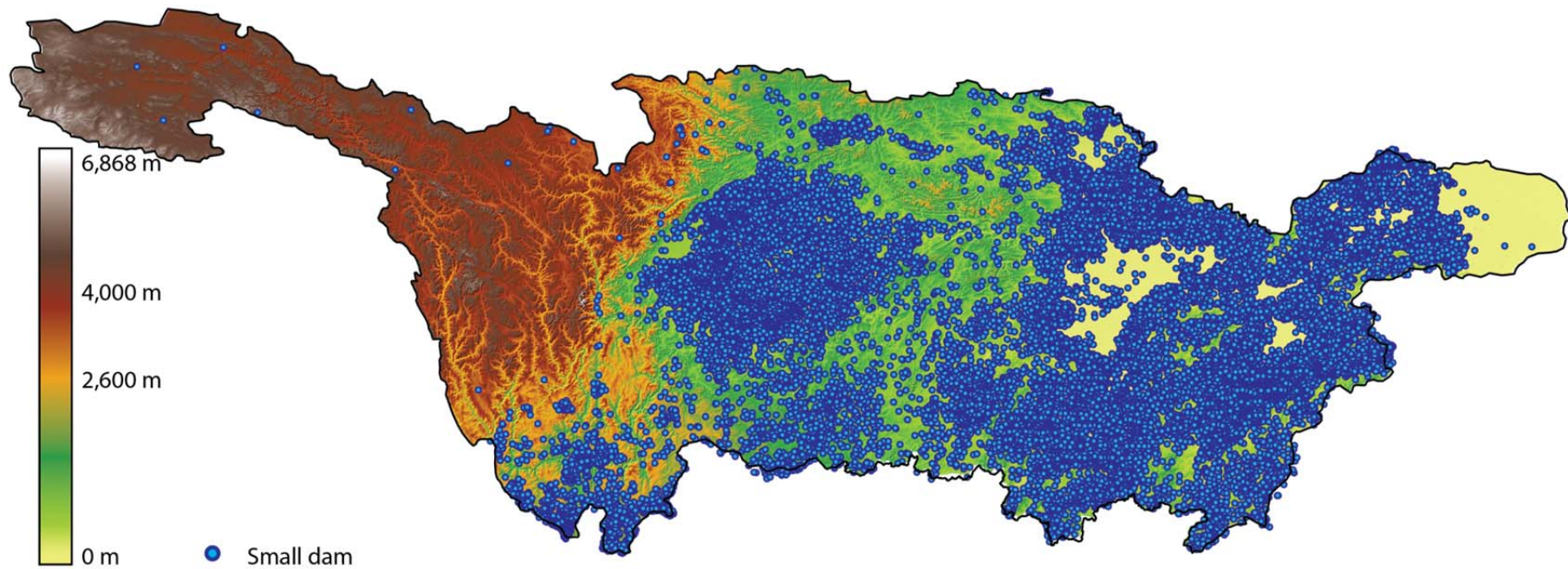
Figure 7.1 Spatial distribution of 43,600 dams in the Yangtze River basin. The reservoirs are mainly distributed in the middle and lower reaches. Dams are mainly located in low-relief areas; few dams located at high-relief (> 3,500m) areas.

water discharge by its corresponding drainage basin area upstream from the station. Annual precipitation data (1955-2008) from 220 meteorological stations (163 stations located in the Yangtze River basin, 57 stations located outside the basin but in the vicinity of the basin) were extracted from a 728-station precipitation dataset released by the China Meteorological Data Sharing Service System (http://cdc.cma.gov.cn/). Since these stations are not evenly distributed in space, basin-wide and sub-basin annual average precipitation was predicted using spatial interpolation by Kriging tool within ArcGIS 10.0.

7.2.2 Methods

The analysis was carried in two aspects: flow regulation and river landscape fragmentation. Flow regulation based on the ratio of reservoir storage capacity to runoff represents the potential degree to which the river section is affected by its upstream small dams; thus, it is a primary indicator of the magnitude of potential disruption to the hydrologic cycle.

However, one hindrance is that the runoff for each river section is often unknown. Even in highly monitored areas, only a fraction of catchments possess a stream gauge; all other stream sections are ungauged (Viglione et al., 2013). Besides, in terms of the huge number of small dams, collection and analysis of dam would be very expensive and time consuming. The only recourse is therefore to predict runoff in these catchments or locations using alternative data or information (Sivapalan, 2005; Hrachowitz et al.,

2013). Various methods have been proposed to estimate runoff in ungauged basins, such as regression methods (Omang and Parrett, 1984; Driver and Troutman, 1989; Viglione *et al.*, 2013), index methods (Budyko, 1974; Choudhury, 1999; Zhang *et al.*, 2001; Arora, 2002), geostatistical and proximity methods (Storm *et al.*, 1989; Sauquet, 2006) and computer models (Hsu *et al.*, 1995; Smith and Eli, 1995; Freer *et al.*, 1996; Tokar and Johnson, 1999). The regression method was used in this study as some results in Chapter 4 can be used as variables in the regression model.

The river landscape fragmentation, on the other hand, indicates the extent of fragmentation in the river network. Dams pose physical barriers to the flow of water, regardless of their size or reservoir storage capacity, so that dammed river networks are composed of disconnected channel segments between dams (Chin *et al.*, 2008). Therefore, it is a primary indicator of potential environmental impacts with many associated implications.

7.2.2.1 Estimating annual runoff for each river section

The regression method was used in this study, where the specific runoff (SR) is estimated based on relationships with catchment and climatic attributes via some analytical expression. Hawley and McCuen (1982) and Vogel *et al.* (1999) cited numerous advantages to the use of regression approaches for estimating annual stream flow. Regression approaches produce objective equations that are easily programmed into comprehensive watershed planning procedures. Regression equations that relate

annual average stream flow to geomorphic, land use, and climatic basin characteristics are easily integrated into and implemented using GIS. Regression approaches offer the opportunity to document the accuracy and uncertainty associated with water yield estimates, including estimation of confidence intervals and information content. Perhaps the most important advantage documented in the two studies may be developed to quantify both the mean and variance of annual stream flow for any watershed in a region. This was exactly what the study in this chapter needed.

Vogel and Wilson (1996) found that lognormal distributions provide a good fit to the distribution of annual stream flow throughout the continental United States based on multivariate relationships among annual stream flow and the basin characteristics, which is expressed as flows:

$$ SR = e^{\beta_0} \bullet X_1^{\beta_1} \bullet X_2^{\beta_2} \cdots X_m^{\beta_m} \qquad (7.1) $$

Where $X_i^{\beta i}$, $i = 1, \cdots m$ are basin characteristics; β_i $i = 1, \cdots m$ are model parameters. The model in Eq. 7.1 termed a log-linear model because taking natural logarithms yields

$$ Ln\, SR = \beta_0 + \beta_0 \bullet Ln(X_1) + \beta_0 \bullet Ln(X_2) + \cdots + \beta_m \bullet Ln(X_m) \qquad (7.2) $$

The goals in this model development were to, first, maximize the adjusted R^2, and second, include both geomorphic and climate characteristics while keeping the

number of basin characteristics used to a minimum. Thirteen catchment properties were analyzed in order to understand the variation in runoff. Stepwise regression analyses were then used to obtain the best specific runoff (SR in $km^3\ km^{-2}\ yr^{-1}$) model.

The annual river flow (Q in $km^3\ yr^{-1}$) within the drainage area of a river section was calculated using the following equation:

$$Q = SR \times A \qquad\qquad (7.3)$$

where SR was estimated using the regression model; A is the river section's drainage area in km^2.
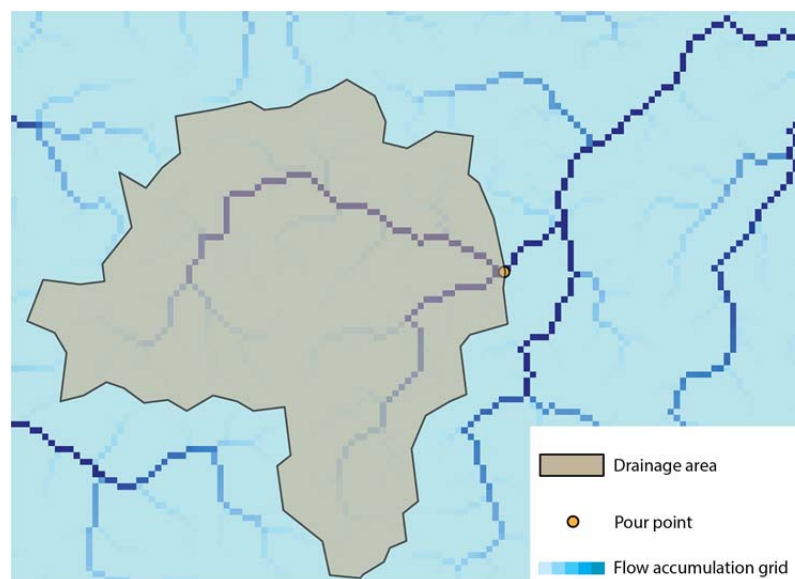
Figure 7.2 An illustrative example to show the approach to delineate drainage area for each river section using ArcGIS 10.

The drainage area for each river section was delineated using ArcGIS 10.0. Firstly, based on the DEM data, the river flow direction and flow accumulation grids were

185

created using an eight-direction (D8) flow model which follows an approach presented in Greenlee (1987). The flow accumulation data has a value for each pixel; that value represents the number of pixels upstream from that pixel. Apparently, pixels with higher values would tend to be located in drainage channels, based on which the software could snap the watershed outlets to the nearest pixel of highest accumulation. Catchment areas were then delineated based on the snapped pour points (Figure 7.2).

7.2.2.2 Calculating flow regulation for river sections

Smaller dams are often built on smaller river systems which have relatively limited river flow. When the small dams are designed to divert some amounts of water from these river systems, they would significantly affect aquatic species by disrupting the life cycles of aquatic species due to decreased river flow or volume. The effect of dams on the regulation of downstream flows can only be fully assessed if the operation rules of the reservoirs are known; yet it is rarely available at large scales. To quantify flow regulation, Lehner *et al.* (2011) used the degree of regulation (DOR) to assess the potential effect of dams on the natural flow regime. Likewise, this study defined the degree of regulation for each river section (DOR_s) as:

$$DOR_s = \frac{\sum_{i=1}^{n} C_i}{Q} \times 100\% \tag{7.4}$$

Where C_i is the reservoir storage capacity in km^3, n is number of upstream reservoirs, Q is the river section's annual runoff in km^3, which was calculated using Eq. 7.3. A high

DOR_s value indicates an increased probability that substantial discharge volumes can be stored throughout a given year and released at later times (Figure 7.3). For example, 10% is used as a threshold by Lehner *et al.* (2011) to mark the possibility of substantial changes in the natural flow regime to occur. However, unlike the DOR model proposed by Lehner *et al.* (2011), this index is derived for each individual river section and therefore does not capture the effect of dams on the entire network in one single value.

River section	River runoff ($10^4 m^3$)	Upstream dams	Total regulated volume ($10^4 m^3$)	DOR_s
1	10	1	5	50.0%
2	15	2	12	80.0%
3	10	- -	0	0.0%
4	10	- -	0	0.0%
5	15	3	10	66.7%
6	45	1, 2	17	37.8%
7	45	- -	0	0.0%
8	150	1, 2	17	11.3%
9	190	1, 2, 3	27	14.2%
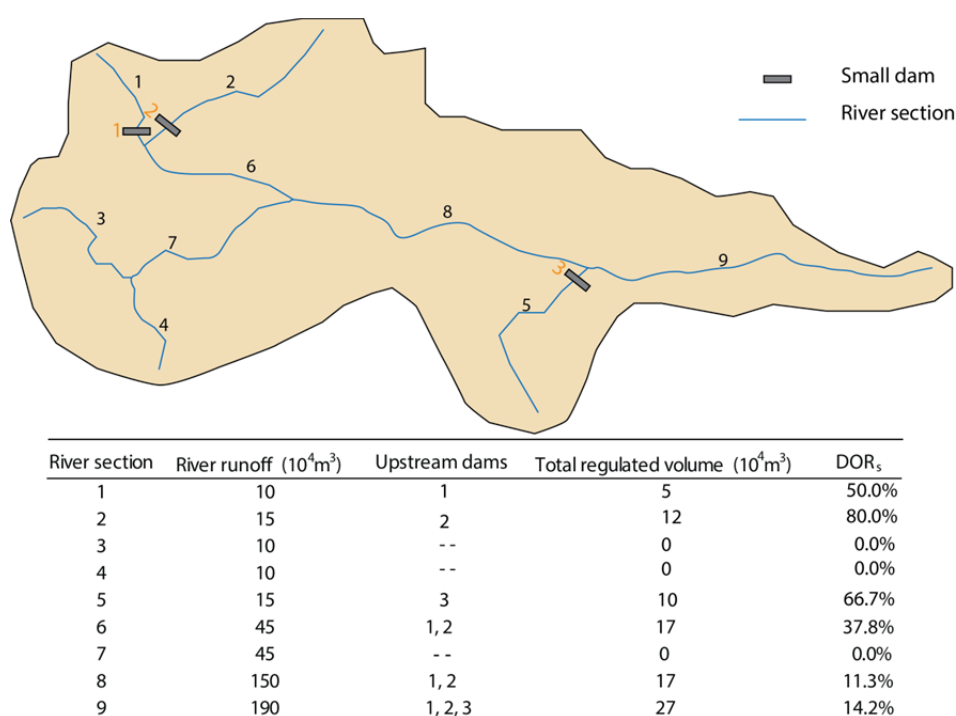
Figure 7.3 Simplified river network to demonstrate computation of DOR_s. For a river section with no upstream dams (section 7), the river is not regulated and has a minimum DOR_s value of 0.0%; when two dams are constructed on the headwater rivers, they have a relatively small effect on mainstem river sections 8 and 9 but very significant effect on their immediately downstream river section 6. Refer to the *Methods* section for additional description of the DOR_s computational algorithm.

7.2.2.3 Estimating the impact on river landscape fragmentation

Rivers originate from different river landscapes (e.g., glacial, mountain, and karst)

which work as functioning systems, exhibiting continual movements of materials, energy, and biota, which in turn constrain the natural processes and balances of the river environment (Moore and Archdekin, 1980). For example, karst landscape develops an overall calcium-rich riverine environment, while steep mountains with large gradients create fast-flowing rivers. Investigations on the impact of small dams on river landscape fragmentation can help us identify severely affected river landscapes and propose remedies based on the landscape characteristics.

This study employed area-weighted dam density (AWDD) as a proxy to quantify the impact on river landscape fragmentation. The formula to calculate AWDD is expressed as:

$$AWDD = \sum_{i=1}^{n} \left(D_i \times \frac{a_i}{A} \right) \tag{7.5}$$

Where n is the total number of river landscapes in a large river basin; a_i is the area of river landscape i in km^2; A is the total area of the whole river basin in km^2; D_i is the dam density (number of dams per 100 km^2) in river landscape i, which is defined as:

$$D_i = \frac{N_i}{a_i} \times 100 \tag{7.6}$$

Where N_i is the number of dams in river landscape i. The number of dams in each river landscape was obtained based on river-landscape classification map given in the previous chapter.

The model was proposed based on the assumption that a single river landscape provides equal function to any of the other river landscapes, allowing us to combine those parts of the river network that offer materials, energy, and biota by the amount of river landscapes, and attribute this by river network. It indicates the extent of fragmentation in the river network because dams pose physical barriers to the flow where they occur, regardless of their size or reservoir storage capacity, so that dammed river networks are composed of disconnected channel segments in between dams. A higher value of AWDD indicates a more severe degree of river landscape fragmentation.

7.3 Results

7.3.1 Established multiple regression model for predicting steam flows

The linkages between river landscape characteristics and runoff at gauging station revealed multivariate controls on runoff in the Yangtze River basin. Therefore, stepwise multivariate regression analysis was employed to examine these multiple controls on runoff variation at both the basin and catchment scales. This research examined runoff at 130 long-term gauging stations across Yangtze River basin. Twelve catchment properties listed in Table 7.1 were analyzed in order to understand the variation in runoff. It shows that precipitation alone explains 60.86% of the observed variance in runoff for the whole Yangtze River basin, but the remaining independent variables

show relatively poor linkages with runoff at the basin scale. The five variables showing the strongest linkages with runoff at the basin scale are P (precipitation) > T (temperature) > NDVI > H_{mean} (mean elevation) > DL (drainage length).

Stepwise regression analysis tested the addition of each variable using a chosen model comparison criterion, adding the variable (if any) that improves the model the most, and repeating this process until none improves the model. Table 7.2 summarizes the procedure and significance of independent variables in each chosen model. Finally, a combination of precipitation (P), relief (R), drainage length (DL), mean elevation (H_{mean}) temperature (T), and maximum elevation (H_{max}) explain 89.1% of the variance in runoff (Q). Therefore, a multiple regression model including the six factors was established to predict area-specific runoff (SR) in the Yangtze River basin:

$$Ln\,SR = -7.664 + 1.852\,Ln\,P + 1.147\,Ln\,R - 0.165\,Ln\,DL - 0.95\,Ln\,H_{max} - 0.154\,Ln\,T + 0.323\,LnH_{mean}$$

$$(7.7)$$

For the log-linear model developed here, the coefficients for P and T represent the elasticity of runoff to precipitation and temperature: the precipitation elasticity is positive and is quite large, indicating the highly nonlinear response of runoff to precipitation. As expected, the coefficient for the temperature term is negative, indicating that an increase in temperature tends to increase evapotranspiration, leading to a decrease in runoff.

Table 7.1 Correlation matrix between log-transformed catchment properties and river runoff

	A	R	DL	NDVI	HI	H_{mean}	H_{max}	H_{min}	HD	RR	S_{mean}	P	T	Runoff
A	1.00													
R	0.62	1.00												
DL	0.98	0.63	1.00											
NDVI	-0.33	-0.25	-0.35	1.00										
HI	0.15	0.42	0.19	-0.31	1.00									
H_{mean}	0.32	0.73	0.35	-0.51	0.84	1.00								
H_{max}	0.54	0.94	0.55	-0.44	0.55	0.88	1.00							
H_{min}	-0.28	0.09	-0.26	-0.27	0.46	0.50	0.26	1.00						
HD	0.62	1.00	0.63	-0.25	0.42	0.72	0.94	0.09	1.00					
RR	-0.83	-0.11	-0.84	0.27	0.05	0.06	-0.05	0.39	-0.11	1.00				
S_{mean}	0.16	0.26	0.19	-0.12	0.21	0.27	0.27	0.07	0.26	-0.06	1.00			
P	-0.39	-0.59	-0.43	0.46	-0.66	-0.82	-0.73	-0.46	-0.59	0.14	-0.33	1.00		
T	-0.45	-0.62	-0.49	0.52	-0.62	-0.73	-0.69	-0.31	-0.62	0.20	-0.25	0.78	1.00	
Runoff	-0.34	-0.16	-0.38	0.47	-0.34	-0.44	-0.32	-0.29	-0.16	0.38	-0.26	0.78	0.49	1.00

[a] DA: drainage area (km^2); DL: drainage length (km); H_{mean}: mean elevation (m); H_{min}: minimum elevation (m); H_{max}: maximum elevation (m); HD: elevation difference (m); HI: hypsometric integral, given by: $(H_{mean}-H_{min})/(H_{max}-H_{min})$; R: basin relief (m); RR: ratio of the basin relief and the basin length; S_{mean}: mean slope (degree); NDVI: normalized difference vegetation index, driven from remote sensing images; P: mean annual precipitation (mm yr^{-1}); T: annual mean temperature (^{o}C).

The river flow for each river section was predicted by multiplying the output of the equation by its drainage area (A in km^2). It should be emphasized that the precipitation was predicted using spatial interpolation by Kriging method. The accuracy of flow prediction is therefore heavily dependent on the accuracy of precipitation prediction. A large sample size of meteorological stations and the 'best' semivariogram model are the prerequisites of a high-accuracy precipitation prediction.

Table 7.2 Summary of models and significance of independent variables in stepwise multiple regression analysis

No.	Model Predictors[a]	Coefficients	t	Sig.	R^2	Adjusted R^2
1	(Constant)	-1.863	0.583		-3.196	0.002
	P	1.185	0.083	0.785	14.279	0
2	(Constant)	-8.222	0.856		-9.599	0
	P	1.612	0.082	1.068	19.768	0
	R	0.432	0.049	0.476	8.805	0
3	(Constant)	-7.086	0.716		-9.901	0
	P	1.561	0.067	1.034	23.268	0
	R	0.62	0.047	0.683	13.295	0
	DL	-0.178	0.022	-0.364	-7.934	0
4	(Constant)	-8.359	0.694		-12.041	0
	P	1.784	0.074	1.182	23.999	0
	R	0.589	0.043	0.649	13.768	0
	DL	-0.158	0.021	-0.321	-7.578	0
	HI	0.231	0.044	0.228	5.238	0
5	(Constant)	-6.705	0.881		-7.608	0
	P	1.65	0.086	1.093	19.286	0
	R	0.88	0.108	0.97	8.14	0
	DL	-0.173	0.021	-0.353	-8.287	0
	HI	0.255	0.044	0.252	5.838	0
	H_{max}	-0.348	0.119	-0.385	-2.915	0.004
6	(Constant)	-6.908	0.87		-7.941	0
	P	1.758	0.096	1.164	18.356	0
	R	0.907	0.107	0.999	8.49	0

No.	Model Predictors[a]	Coefficients	t	Sig.	R^2	Adjusted R^2
	DL	-0.184	0.021	-0.376	-8.748	0
	HI	0.244	0.043	0.241	5.665	0
	H_{max}	-0.383	0.118	-0.423	-3.239	0.002
	T	-0.136	0.058	-0.124	-2.341	0.021
7	(Constant)	-7.972	0.93		-8.573	0
	P	1.885	0.104	1.248	18.138	0
	R	1.255	0.163	1.382	7.7	0
	DL	-0.157	0.023	-0.32	-6.917	0
	HI	-0.13	0.141	-0.129	-0.922	0.358
	H_{max}	-1.206	0.318	-1.334	-3.788	0
	T	-0.165	0.057	-0.151	-2.869	0.005
	H_{mean}	0.474	0.171	0.872	2.774	0.006
8	(Constant)	-7.664	0.868		-8.834	0
	P	1.852	0.097	1.226	19.017	0
	R	1.147	0.114	1.264	10.08	0
	DL	-0.165	0.021	-0.336	-7.816	0
	H_{max}	-0.95	0.156	-1.05	-6.108	0
	T	-0.154	0.056	-0.141	-2.74	0.007
	H_{mean}	0.323	0.051	0.595	6.383	0

(*Table continued*)

[a]Dependent Variable: Runoff

7.3.2 The impact of small dams on flow regulation

The result shows that approximately 170,000 km^2, or 9.4% of the Yangtze River basin is locked by small dams. Figure 7.4 shows the cumulative frequency of the number of small dams: dams with catchments less than 5 km^2 occur at the highest frequency, and with increasing catchment area, their frequency decreases sharply. It illustrates that most dam catchments are small: 84.06% of them are less than 5 km^2; small dams can therefore play a significant role in fragmenting river systems by their sheer number.
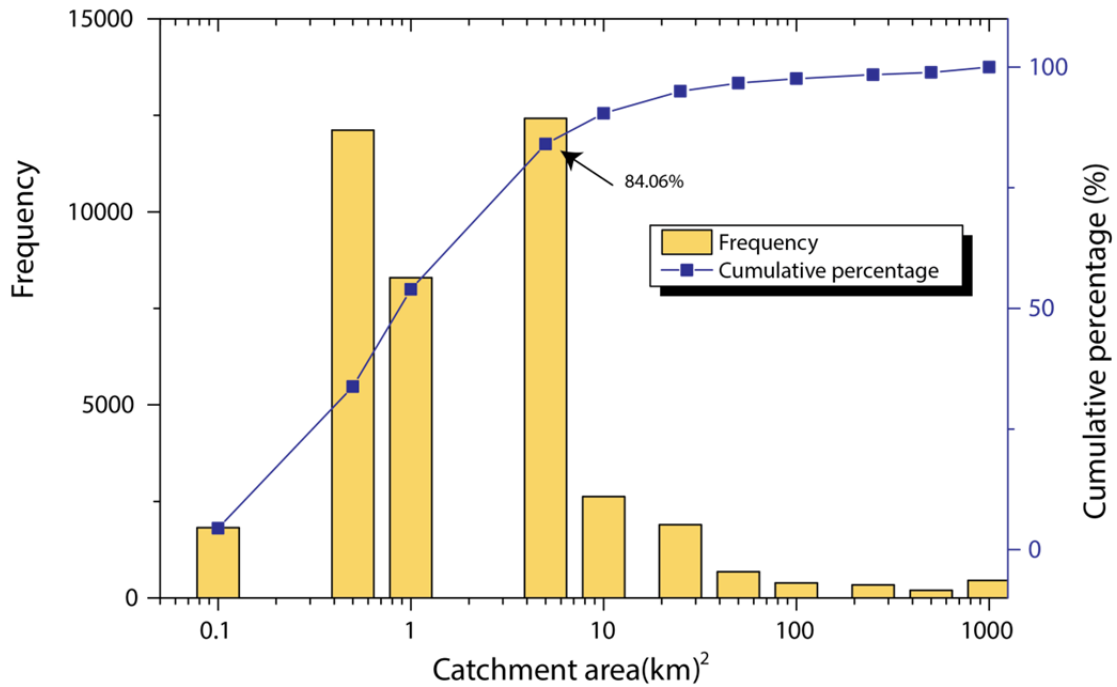
Figure 7.4 Cumulative frequency of number and catchment area of small dams. The dot line indicates that most dam catchment areas are small: 84.06% of all the dam catchments are less than 5 km^2.

The direct effect is reduction in downstream flow, which is a substantial impact frequently associated with small dams. Flow reductions affect the physical characteristics of a stream (e.g. water velocity, sediment transport, water temperature) and alter the quantity and quality of aquatic habitat, with cascading impacts on river systems (Anderson *et al.*, 2006). The statistics and map of the affected river sections are provided in Table 7.3 and Figure 7.5. They show that the relative impact increases slightly with river size peaking at fourth-order streams. Large stream sections show sharply reduced levels again because massive flows (e.g., the main stem and major tributaries) cannot easily be impacted by small dams. When adopting a DOR$_s$ threshold of 5%, it shows that 54, 977 km, or 26% of the streams are affected by upstream small

dams. Of these, 45,878 km are first-, second- and third-order streams, representing 25% of all streams in the three size classes. Approximately 771 km, or 11% of large streams with stream order greater than 5 are affected. Among the streams, the fourth-order streams are the most severely affected, 32% of which are affected.

Table 7.3 Summarized results for DOR_s analysis for small dams, tabulated by stream order and degree of regulation

Stream order	Total length (km)	Extent of affected river sections downstream small dams						Unit
		DOR_s(%)0-5%	5-10%	10-20%	20-30%	30-50%	>50%	
1	101,623	75,946	7,490	7,529	3,883	2,853	3,922	km
		74.7	7.4	7.4	3.8	2.8	3.9	%
2	52,592	38,148	4,316	4,381	2,198	1,749	1,801	km
		72.5	8.2	8.3	4.2	3.3	3.4	%
3	28,429	20,873	2,495	2,598	1,013	772	678	km
		73.4	8.8	9.1	3.6	2.7	2.4	%
4	13,991	9,476	2,203	1,292	647	289	84	km
		67.7	15.7	9.2	4.6	2.1	0.6	%
5	7,458	5,473	1,425	431	129	0	0	km
		73.4	19.1	5.8	1.7	0.0	0.0	%
6	4,634	3,920	661	53	0	0	0	km
		84.6	14.3	1.1	0.0	0.0	0.0	%
7	1,971	1,914	57	0	0	0	0	km
		97.1	2.9	0.0	0.0	0.0	0.0	%
8	674	674	0	0	0	0	0	km
		100.0	0.0	0.0	0.0	0.0	0.0	%
Total	211,372	156,424	18,674	16,285	7,870	5663	6,485	km
		74.0	8.8	7.7	3.7	2.7	3.1	%

Several tributaries stand out as being highly affected with many impacted river sections resulting from numerous small dams built on these river sections, such as , such as the Tuo River, Xin River, Zi River and Xiang River (Table 7.4). For example, More than 77% of the Tuo River is affected by small dams. Other three rivers are little
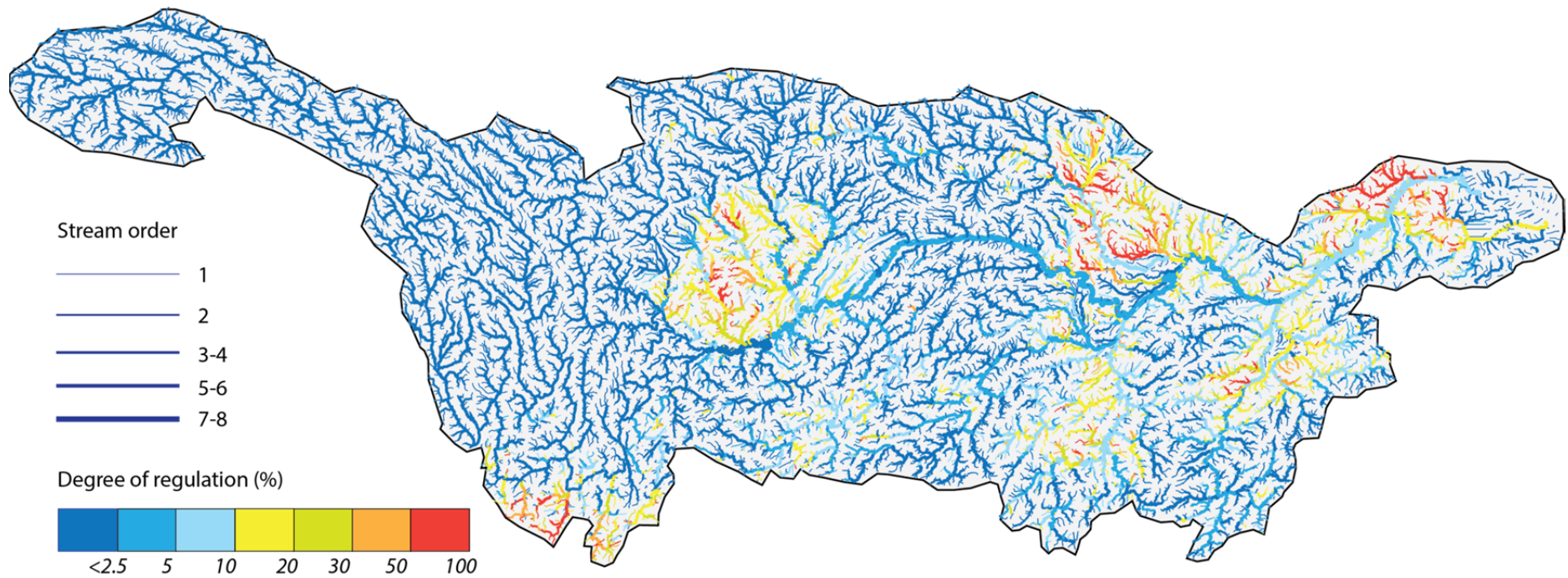
Figure 7.5 Affected river sections downstream of small dams. Different colors show an increasing degree of regulation, whereas line width is proportional to stream order.

Table 7.4 Total tributary length, number of dams, and extent of affected tributaries (in kilometers and percentages) downstream of small reservoirs for different tributaries in the Yangtze River basin, tabulated by river size and by DOR_s

Tributary	Total length (km)	No. of dams	Extent of affected river with a DORs >= 5% By stream order						Extent of affected rivers (all river sizes combined) By DORs				Unit
			1	2	3	4	5	6	>=5%	>= 10%	>=30%	>=50%	
Jinsha River	51,696	1,817	1975	1366	823	292	0	0	4457	3227	1468	733	km
			7.9	11.5	10.7	11.8	0.0	0.0	8.6	6.2	2.8	1.4	%
Min River	15,225	889	429	386	124	0	0	0	939	659	133	14	km
			5.8	10.7	5.4	0.0	0.0	0.0	6.2	4.3	0.9	0.1	%
Tuo River	3,769	1793	1322	729	426	459	0	0	2937	2563	1098	526	km
			79.0	66.3	85.2	100.0	0.0	0.0	77.9	68.0	29.1	14.0	%
Jialing River	20,550	3,531	3162	1638	1021	422	37	104	6385	4823	1208	466	km
			33.4	30.4	37.8	27.4	4.9	14.7	31.1	23.5	5.9	2.3	%
Wu River	10,148	1,086	1026	833	372	246	339	0	2817	1090	123	49	km
			20.5	33.0	25.1	41.3	63.1	0.0	27.8	10.7	1.2	0.5	%
Hanjiang	21,212	3,461	3067	2246	713	517	156	480	7179	5662	2908	1831	km
			50.0	38.0	29.1	39.6	18.0	100.0	33.8	26.7	13.7	8.6	%
Dongting Lake Region													
Lei River	3,255	500	184	168	11	153	0	0	517	285	83	15	km
			12.4	21.3	2.4	29.7	0.0	0.0	15.9	8.8	2.5	0.5	%
Yuan River	11,567	1,662	1836	573	200	51	0	0	1661	638	95	46	km
			32.4	20.8	15.6	4.0	0.0	0.0	14.4	5.5	0.8	0.4	%
Zi River	3,555	1,241	700	245	220	572	0	0	1736	648	122	3	km
			40.2	29.0	55.6	100.0	0.0	0.0	48.8	18.2	3.4	0.1	%

Tributary	Total length (km)	No. of dams	Extent of affected river with a DORs >= 5%						Extent of affected rivers (all river sizes combined)				Unit
			By stream order						*By DORs*				
			1	2	3	4	5	6	>=5%	>= 10%	>=30%	>=50%	
Xiang River	11,418	3,854	2302	1159	727	373	567	0	**5130**	2678	486	181	km
			41.7	40.8	48.4	39.0	100.0	0.0	**44.9**	23.5	4.3	1.6	%
Poyang Lake Region													
Xiu River	1,835	644	304	55	28	35	26	0	**449**	243	44	29	km
			34.2	9.0	38.4	15.1	100.0	0.0	**24.5**	13.2	2.4	1.6	%
Gan River	8,685	2,918	950	542	289	179	66	0	**2026**	981	215	151	km
			23.4	24.9	21.0	30.8	13.9	0.0	**23.3**	11.3	2.5	1.7	%
Fu River	1,892	1,125	293	154	86	8	42	0	**583**	407	88	20	km
			29.7	36.8	26.1	7.0	100.0	0.0	**29.4**	20.5	4.4	1.0	%
Xin River	2,007	1,862	533	142	76	235	0	0	**987**	551	20	2	km
			49.4	31.0	32.5	100.0	0.0	0.0	**49.2**	27.5	1.0	0.1	%

(*Table continued*)

[a] For the results "by stream order", the percent value refers to all river sections of the respective size class in the tributary basin; for the results "by DOR$_s$", the percent value refers to all rivers of all sizes in the tributary basin.

better, but still have more than 40% of stream sections affected by small dams. The four rivers are in the dam-dense areas, such as, the Sichuan Basin in the upper Yangtze reach, the Poyang Lake Region and the Dongting Lake Region in the middle Yangtze reach (Figure 7.1).

The analysis indicates that, although large dams can clearly exert a sizable impact on the hydrological cycle through the vast quantities of water that they can store, small dams can also significantly alter regional river flows through their sheer number. River basin development and management plans use approaches similar to this DOR_s assessment can inform decisions regarding the distribution of new dams and/or the operation of existing dams. Regional management schemes could also be "optimized" by prioritizing the siting of new small dams based on which locations would have the lowest estimated cumulative impacts downstream.

7.3.3 The impact of small dams on river landscape fragmentation

The AWDD analysis indicates that the density of dams and the extent of fragmentation in the hydrological system are decidedly unequal across the Yangtze River basin (Table 7.5). The greatest density of small dams occurs in the ridge-and-valley area in the middle Yangtze reach, with AWDD of approximately 9.1 dams per 100 km^2, especially on the plain side of the border between the plain and hills. This means that people can

find one small dam approximately every 11 km^2 of area on average. The floodplains in the middle reach, ranked second, are actually little better than the ridge-and-valley area: with an average partition area of 16 km^2. The AWDD is a gross measure of the extent of fragmentation in river networks. River networks in those river landscapes (ridge-and-valley area, floodplain and coastal plain) with highest AWDD values experience the greatest segmentation or fragmentation caused by small dams. The greatest density of dams occurs in plain areas, most of which are in the middle and lower Yangtze reaches, suggesting a large number of potential needs in these areas (Dai *et al.*, 1998). The primary reason is that dry-season agriculture and the pre-rainy season establishment of food and cash crops in these areas cannot be undertaken without large quantities of water. To rely upon precipitation in the dry season is unrealistic and risky. It is essential for a dam constructed on streams to allow for off-season storage of vital water supplies. Although primarily for irrigation, such dams can be used, either separately or combined, for fish farming, stock and domestic water purposes.

The results further show that, in the Yangtze River basin, the extent of river landscape fragmentation by small dams varies with river landscapes. It is lowest in the landforms of glaciated plateaus, plateaus and mountain ranges and increases generally to the east, where a large number of potential needs (irrigation, domestic uses and fish farming) encourage more farm ponds to be constructed. Unlike large dams which are often constructed in unfrequented river valleys with sufficient drop (height) to provide a hydropower opportunity, small dams are often built on rivers close to populated areas

(Yang *et al.*, 2006) and therefore have a more direct impact on human beings as a result of river landscape fragmentation.

Table 7.5 Summarized results from AWDD analysis for different landscapes

Landform type	Total area (km^2)	No. of dams	Average catchment area (km^2)	AWDD (Dams per 100 km^2)
Inner coteau	76,630	4377	14	5.7
Low mountain	197,089	7371	27	3.7
Mountain	272,540	2388	61	0.9
Valley and hill	31,826	535	58	1.7
Hill	63,564	2162	28	3.4
Ridge and valley	15,818	1435	7	9.1
Glaciated plateau	150,565	5	199	0.0
Karst mountain	356,884	6229	54	1.7
Floodplain	190,536	11782	9	6.2
Coastal plain	83,259	4846	4	5.8
Plateau	104,959	5	19	0.005
Mountain range	254,212	66	287	0.026
Overall	1,800,000	42,002	23	2.3

Another factor to the high fragmentation in those plains is that the dam catchment areas are relatively small due to relatively low relief. The small dams in those regions have relatively small average catchment area (less than 10 km^2) (Table 7.5), compared with their counterparts in the regions of glaciated plateau and mountain ranges with average catchment area of 199 and 287 km^2, respectively. The small reservoirs isolate their catchments, making the catchments "isolated islands". These isolations can often support only small river systems; thus, they are more sensitive to environmental fluctuations and stochastic perturbations of flow.

Previous studies (Dunham *et al.*, 1997; Jager *et al.*, 2001; Wofford *et al.*, 2005) have indicated that fragmentation of river landscapes changes migration patterns, and alters

riparian vegetation. The impacts of the small dams imply many ecological consequences. The river landscape fragmentation created by small dams might be similar to, although on a small scale, the habitat fragmentation caused by roads in forested environments (Reed *et al.*, 1996; Forman and Alexander, 1998; Benítez-López *et al.*, 2010). Thus, the impact could be most apparent in these isolated catchments.

7.4 Discussion

7.4.1 Accuracy and uncertainty analysis

The results of the DORs study need careful interpretation to avoid arriving at misleading generalizations. First, the impacts and consequences of flow regulation may vary for different river size classes. Sixth-, seventh- and eighth-order streams are more likely to be of high importance, including far-reaching environmental and socioeconomic aspects. Yet, first-, second-, third- and fourth-order streams can provide local ecosystem services, serve as ecological refuges, provide water resources for irrigation, or may represent headwater reaches for municipal water supply. When these streams are affected by small dams, the impacts are hidden at a basin-wide scale. Second, the DOR_s ratio is important. For river sections with high DOR_s values, major implications for the intra- and inter-annual flow regimes are to be expected. However, smaller values may indicate critical alterations as well, but of shorter duration or smaller amplitude. Third, it will largely depend on the individual reservoir operation scheme and additional impacts. For example, some small dams are operated as

run-of-the-river hydropower plants; thus they may not regulate river flows as expected. Finally, this study also recognized that environmental effects may vary and that some rivers may be threatened more than others by a certain level of regulation because the effects are the consequences of joint forces, such as, dam construction, deforestation, water diversion, land cover change and climate change. Undoubtedly, more research is required regarding the associated environmental consequences.

In addition, the DOR_s approach intrinsically is subject to various uncertainties. Beyond technical issues, such as flow estimation using multiple regression techniques, some aspects could be addressed because of a lack of data, such as high-resolution DEM data, the role of dam operation. River runoff is strongly related to precipitation, evaporation (temperature), soil moisture and geomorphic characteristics (Vogel *et al.*, 1999). Since the estimated river runoff was based on multi-year average records, we could simply assume that the change in soil moisture is insignificant and only consider precipitation, temperature and geomorphic characteristics. However, when predicting runoff for a single event or a short period, the omission of soil moisture may cause significant uncertainties. Besides, for small dams, the annual amount of water withdrawals and water transfers for various purposes (irrigation and domestic uses), plus the regulated volumes for energy generation, could be much larger than the total reservoir capacity. The impact of small dams could be underestimated based on Eq. 7.2. Besides, the DOR_s approach only accounted for impacts from upstream dams on downstream river sections; yet, for many additional upstream tributaries, connectivity and species

migration routes may be disrupted directly by the presence of downstream small dams or indirectly by downstream large dams. These impacts are not addressed in this study. Considering these impacts, it can be believed that the estimates of the extent of affected river sections are therefore conservative.

The river landscape fragmentation assessment was carried out based on a river landscape map. Therefore, this analysis is heavily dependent on how a researcher formulates criteria to classify river landscapes. Additionally, the river landscape fragmentation results should not be viewed in isolation; rather, this index should be used with other metrics (e.g., DOR_s) to evaluate the impact of small dams on the regional hydrological cycle. Also, the analyses in this study should never be considered as stand-alone; as they do not cover socioeconomic impacts, nor fully represent the spectrum of environmental impacts. However, this study does present a framework to effectively integrate river landscape fragmentation and free-flowing functionality into small dam planning and adds regional and basin-wide perspectives to conventional environmental impact assessments.

7.4.2 Comparative discussion and possible implications

To investigate the role of small and large dams in flow regulation based on DOR_s, a comparative analysis was carried out (Figure 7.6). Figure 7.6A and B reveal that small dams primarily affect streams at regional scale (steams with stream order < 5) while large dams principally affect large streams (stream order > 4). In terms of the impacts

on the fourth-order streams, small dams draw almost equal with large dams. For example, 26% of first-order streams are affected by small dams, while only approximately 4% of first-order streams are affected by large dams. The impacts on large streams (sixth-, seventh, eighth-order streams) is the reverse of that observed for the first-order streams, with most of the effects being caused by large dams. However, small dams have worsened the impacts on large streams. For example, excluding the impacts of small dams, no seventh- and eighth-order streams with $DOR_s > 30\%$ (Figure 7.6B and Figure 7.7). When small and large dams are all taken into account, 20% of seventh-order streams and 100% of eighth-order streams are affected with $DOR_s > 30\%$ (Figure 7.6C and Figure 7.8). Previous research has emphasized the impacts of large dams on river connectivity and fragmentation but believed that the impacts of small dams are marginal. This study revealed that the impacts of small dams are comparable to large dams for fourth-order streams, or even significantly exceed large dams for first-, second- and third-order streams.

Lehner *et al.* (2011) revealed that the relative impact by large dams increases with river size, peaking in large rivers (Figure 7.6D), although very large rivers show slightly reduced levels again, most likely because massive flows, such as those of the Amazon or Mississippi rivers, cannot easily be impounded in their entirety. However, as numerous small dams are not used in Lehner's study, the impacts by small dams are not really shown in Figure 7.6D. This study indicated that Lehner's study results are skewed by
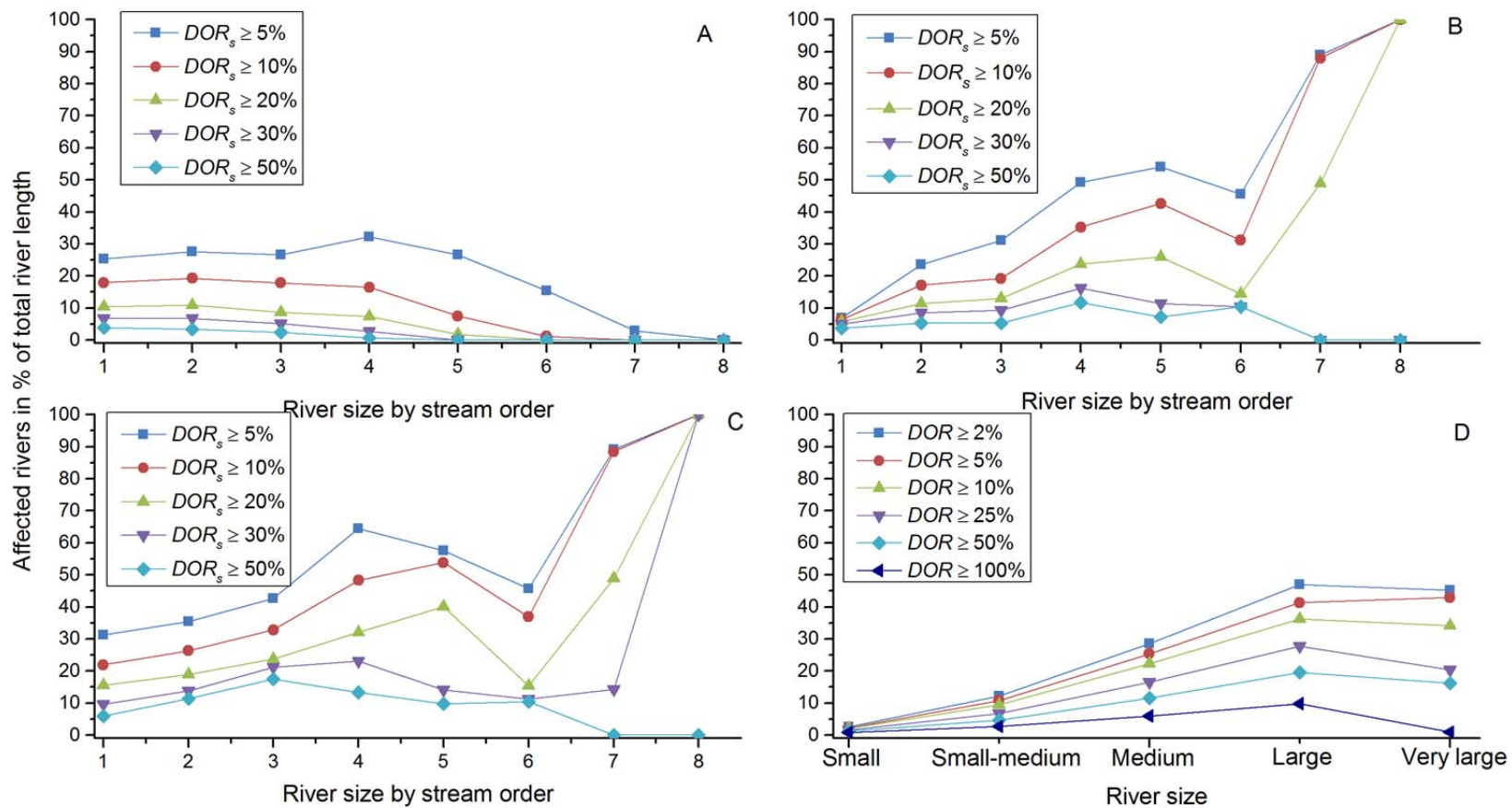
Figure 7.6 Comparison of the impacts caused by large dams and small dams based on DOR and DOR_s ratios; (A) DOR_s ratios for small dams in the Yangtze basin; (B) DOR_s ratios for large dams in the Yangtze basin; (C) DROs ratios for all dams in the Yangtze basin; (D) was modified after Lehner *et al.* (2011); (A-C) was drawn based this study results.
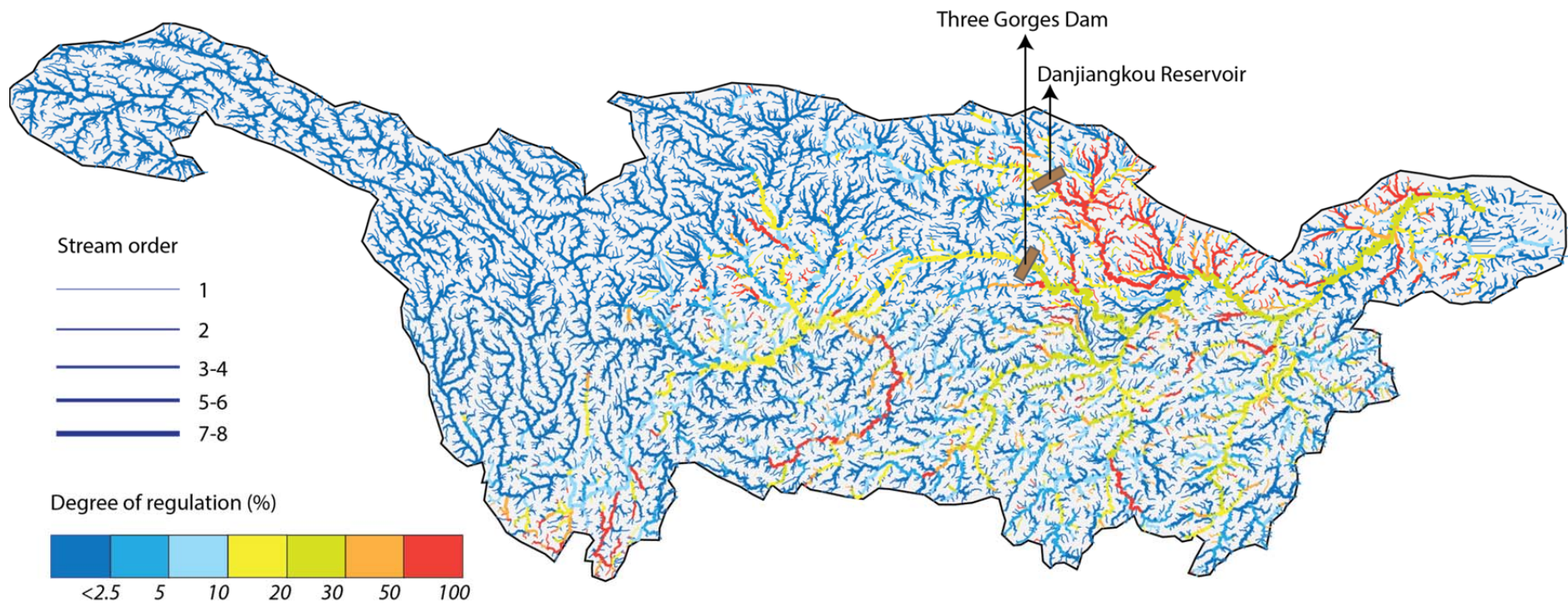
Figure 7.7 Affected river sections downstream of large dams in the Yangtze River basin. Different colors show an increasing degree of regulation, whereas line width is proportional to stream order.
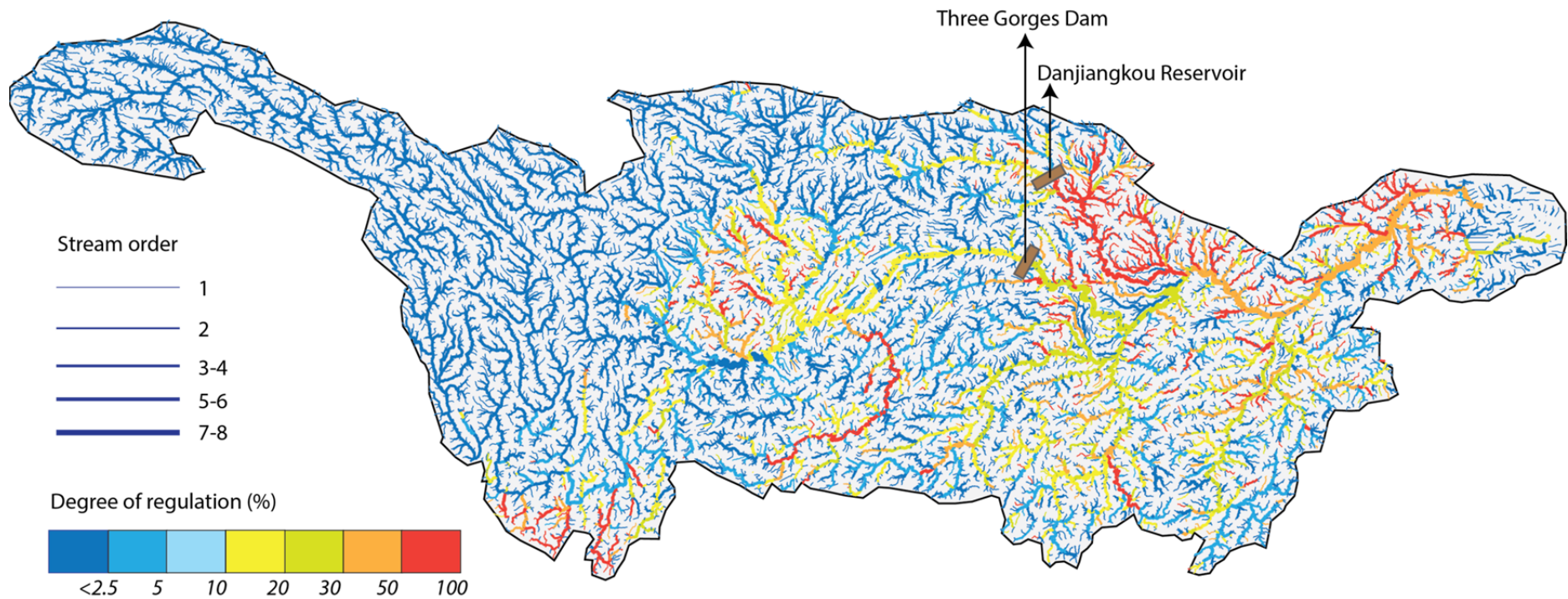
Figure 7.8 Affected river sections downstream of all dams (including large and small dams) in the Yangtze River basin. Different colors show an increasing degree of regulation, whereas line width is proportional to stream order.
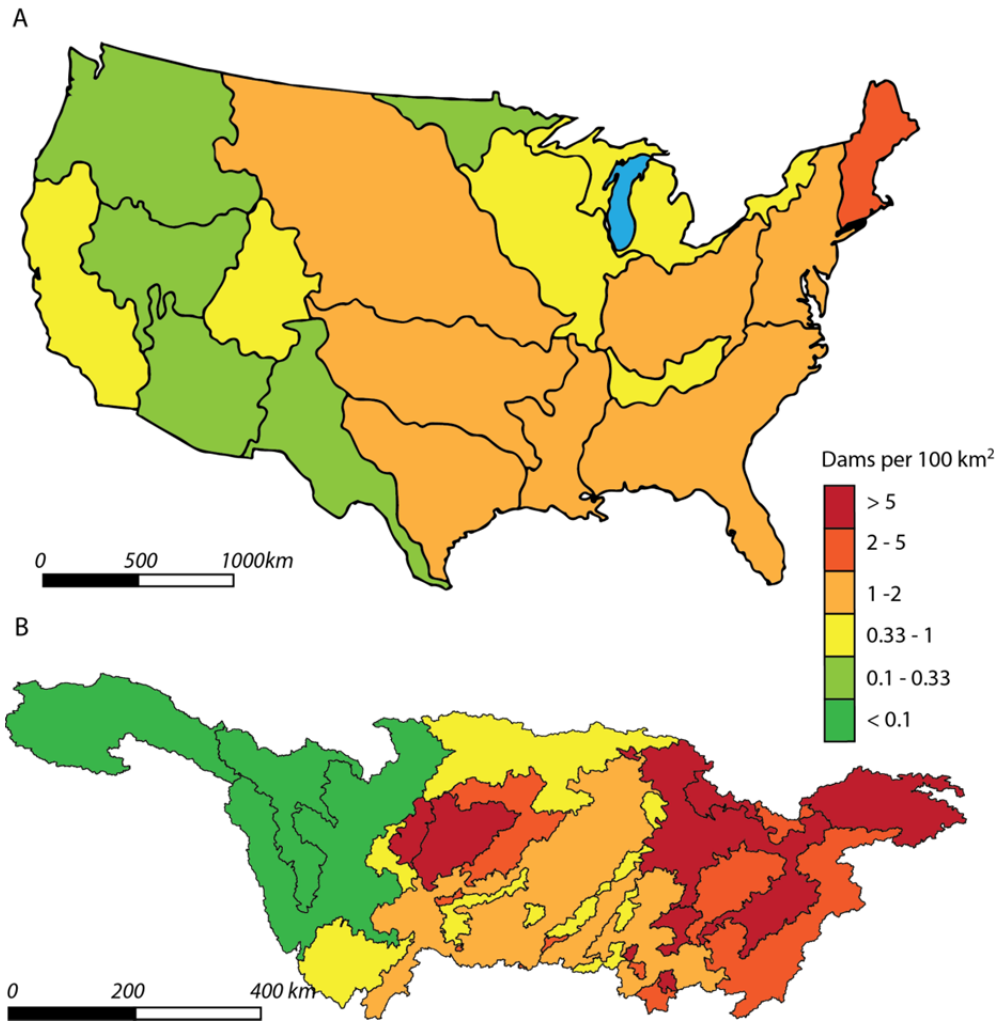
Figure 7.9 Comparison of dam distribution in the Yangtze River basin and the continental United States; (A) number of dams per 100 km^2 in the 18 water resource regions of the continental United States; (B) number of dams per 100 km^2 in the Yangtze River basin. Figure 7.9A was designed based on Graf (1999).

the omission of small reservoirs, which are typically located on smaller rivers.

Although small dams may contribute less to the overall alteration of large-river flows as a result of their limited storage capacities, small dams can still have a profound effect on regional flow regulation.

Some more interesting results can be found by comparing dam distribution in the

Yangtze River basin and the continental United States (Figure 7.9). On average, people can find 2.2 small dams every 100 km^2, compared to only 0.5 small dams in the continental United States (Graf, 1999), suggesting the significant role that small dams can play in fragmenting a river system by their sheer and number and density. In the Yangtze River basin, approximately 630,000 km^2, or one-third of the river basin is fragmented with dam density greater than 2 dams per 100 km^2, in contrast to only 2% of the continental United States. The results give an order of magnitude estimate of the extent of river landscape fragmented by small dams in the Yangtze River basin. One of the possible implications is that small dams should be emphasized in mitigating environmental impact associated with the fragmentation of river landscapes, including the degradation of aquatic habitat and the movement of nutrients as well as aquatic species.

7.5 Summary and conclusions

Based on small dam data obtained in Chapter 4, this chapter investigated the impacts of small dams on flow regulation and river landscape fragmentation. The study results revealed that 54, 977 km, or approximately 26% of the streams, are affected by upstream small dams. Of these, the first-, second-, third- and fourth-order streams are the worst-affected by small dams. The river landscape fragmentation analysis also revealed similar significant effects in regional areas such as the plain areas in the middle and lower Yangtze reaches. On average, one can find 2.2 small dams every 100

km^2; but the dam density can as high as 9.1 small dams per 100 km^2 in ridge-and-valley areas in the middle Yangtze reach.

Although previous research has emphasized the impacts of large dams on river connectivity and fragmentation, at least implying that the impacts of small dams are negligible, the analyses in this chapter revealed that small dams can also exert significant impacts in flow regulation and river landscape fragmentation on regional river systems through their sheer number and density. The implications of this study is that the effects of small dams should be fully emphasized in mitigating environmental impact associated with the fragmentation of river landscapes, including the degradation of aquatic habitat and the movement of nutrients. This DOR$_s$ assessment can also inform decisions regarding the distribution of new small dams and/or the operation of existing small dams. Regional management schemes could also be "optimized" by prioritizing the siting of new small dams based on which locations would have the lowest estimated cumulative impacts downstream. One of the real challenges facing decision-makers may prove to be balancing uncertain or largely unquantified ecological and environmental threats with the socio-economic benefits of additional small dam construction.

8 Possible projections of the future trends of the Yangtze River

8.1 Dam development

In the Yangtze River basin, the recent trend has been toward more and bigger dams (Dudgeon, 2000) because an increasing national demand for energy is being directed towards the installation of increasing numbers of hydropower facilities. For example, China intends to increase its hydropower capacity from 566×10^9 kW.h yr^{-1} in 2010 to $1,200 \times 10^9$ kW.h yr^{-1} in 2020. According to the distribution of hydropower resources, China has planned 13 hydropower bases, six of which are located in the Yangtze River basin (Figure 8.1) (Huang and Yan, 2009), namely the Jinsha River, Yalong River (one major tributary of the Jinsha River), Dadu River (one major tributary of the Min River), Wu River, main stem of the upper Yangtze River, and the Yuan River, although the Yangtze River has already been dramatically disconnected due to dam construction.

The lower Jinsha River is a very important river section in terms of water supply to the TGD. This stretch of the river is also ecologically important as it contains the greatest diversity of fish species found in the upper Yangtze basin (Lu *et al.*, 2010). The China Three Gorges Project Corporation (CTGPC), a state-authorized investment institution responsible for the construction of the TGD, began building a new dam on the Jinsha River in 2005. Now completed (but not yet operating), the Xiluodu Dam

(12.6 million kW; 278 m tall) ranks second in size to the TGD (Dudgeon, 2010).

Apart from the Xiluodu Dam, three more cascade dams (Wudongde, Baihetan, Xiangjiaba, Upper Hutiaoxia) have been under construction for the main stem of the lower Jinsha River. However, it will be part of a 12-dam cascade along the Jinsha River because construction is not proceeding in a coordinated fashion; the ultimate number of dams could exceed this number (Figure 8.1). The tail waters of each dam will extend backward to the dam wall of its upstream counterpart, so that the river will descend in a series of cascade dams with few or no free-flowing sections. The potential impacts of the dams will be highly significant.
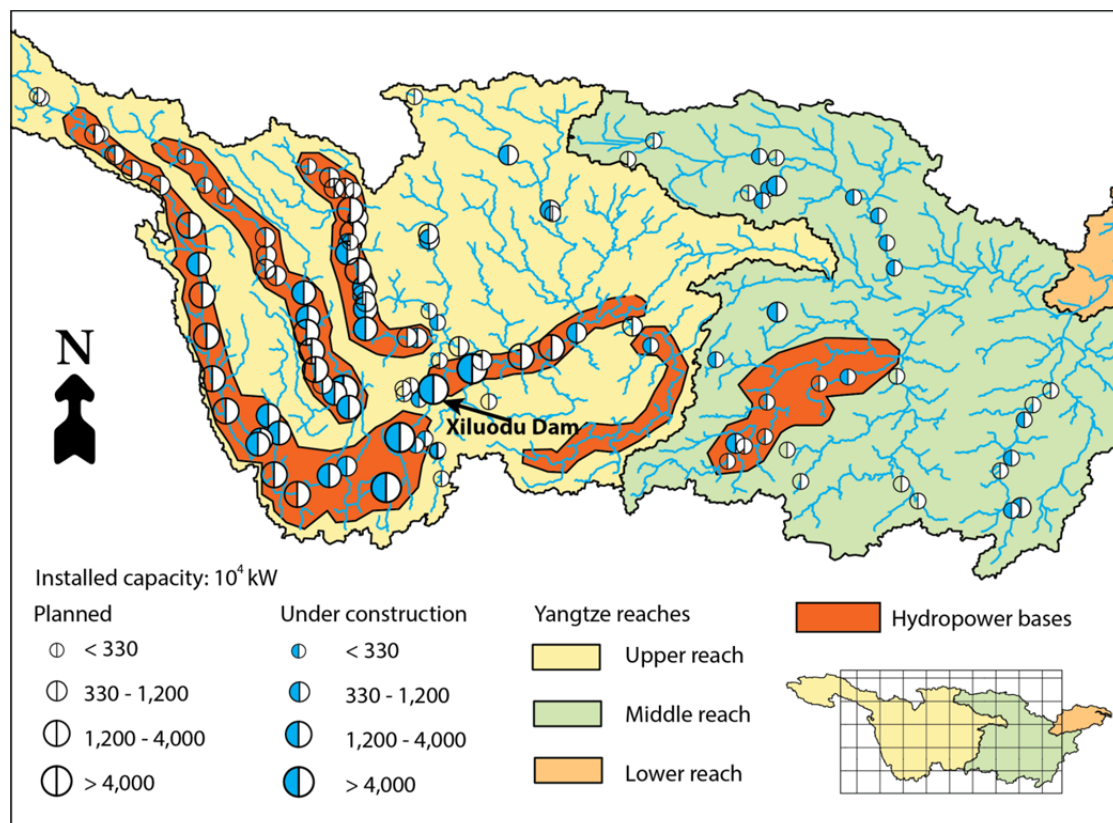
Figure 8.1 Map of hydropower development in the Yangtze River basin in future; data source: MWR (1982) updated with the latest information of dam status.

8.2 Water diversion from Yangtze to the north

Because of the large population, China suffers from water shortage in terms of a very low quantity of per capita water volume, only accounting for one-quarter of the world average. In particular, China's northern and northwestern regions mainly lie in vast semi-arid and arid zones, making up 44% of the total area of the country; but the annual runoff of those zones is less than 10% of the nation's total amount (Liu and Zheng, 2002). To cope with this problem, the South-to-North Water Diversion Project from the Yangtze to the more arid and industrialized North China was proposed in the 1950s when three broad alignments were described (the Western, Middle and Eastern Routes) (Figure 8.2).

The Western Route diverts water from the upper Yangtze tributaries in difficult and remote terrain in the Sichuan and Qinghai mountains to the upper reach of the Yellow River. The first stage will take water from a dam on the Yalong River via a 170 km tunnel to the upper Yellow River. Subsequent stages divert water from the Tongtian River to the Yalong River, and from the Zumuzu River to the Tongtian River, each stage dependent on completing the earlier works. Preliminary estimates suggest up to 20 km^3 could be diverted; but this project has not started yet.

The Central Route, starting at the Danjiangkou reservoir on the Han River, mainly serves domestic and industrial water uses in Beijing, Tianjin, and some cities in Hebei, Henan, and Hubei provinces. The first phase has just completed at the end of 2014. Its

total length is 1,230 km, with a branch to Tianjin of 142 km. The first stage will annually divert 9.5 km^3 yr^{-1} or 25–35% of Han flows at the Danjiangkou Reservoir.

Figure 8.2 Sketch map of the South–North Water Diversion Project

The Eastern Route diverts water from the lower reach of the Yangtze River to the north along roughly the ancient Beijing-Hangzhou Grand Canal. The first phase was completed in 2013, which can annually divert about 9 km^3 of water to the north, half of which is transferred to the north of the Huai River basin (Yang and Zehnder, 2005). The water is lifted 65 m by twelve pump stations to the Yellow River, crossed by tunnel. From there, water can flow north by gravity to Tianjin.

8.3 Possible impact on water regulation

Although there is no complete information (e.g., reservoir storage capacity) on the

planned dams on the Yangtze River, some future trends can also be obtained based on the available data. The total estimated reservoir storage capacity in the upper Yangtze reach is approximately 103 km^3, but the figure will jump to 133 km^3 if the water diverted to the north is considered. By combined the existing reservoirs with a total storage capacity of 85 km^3, the total regulated water volume will be 215 km^3, or 53% of the runoff of the upper Yangtze River. It means that the average time that water is retained in the reservoirs will be approximately 0.53 year. The impoundment of river channels regulates discharge downstream, potentially affecting flooding patterns, flow regimes, and nutrient transport (Lu, 2005; Wellmeyer *et al.*, 2005; Graf *et al.*, 2010). It is likely that with increases in the average time that water is retained in reservoirs (increases in the capacity-runoff ratio), the impacts will become more evident (Figure 8.3).

In the upper Yangtze reach, the Jinsha and Yalong rivers are the biggest victims of the dams currently under construction. For example, the DOR_s for the main stem of the Jinsha and Yalong rivers will jump to 62% and 47% respectively, when the under-construction dams are complete. The change for the Jinsha River is primarily caused by the construction of five large dams with mega storage capacity: Xiangjiaba (5.2 km^3), Xiluodu (12.7 km^3), Wudongde (7.6 km^3), Baihetan (18.8 km^3) and Upper Hutiaoxia (17.95 km^3). The tail waters of each dam will extend backward to the dam wall of its upstream counterpart, making the originally free-flowing Jinsha main stem into five connected artificial stagnant "lakes". Similarly, the degradation for the

216

Yalong River is led by the construction of the Lianghekou and Jinping-I dams with storage capacity of 10.7 km^3 and 7.76 km^3, respectively. However, unlike the five mega dams constructed on the Jinsha River, the two large dams are being constructed closer to the source of China's key large river systems (Yangtze, Yellow and Mekong rivers), and are operational in the valley. Operating with other four relatively small dams which are under construction, the dams are central to exacerbate the fragility of the area by affecting fragile river ecosystem stability. These projects can significantly endanger the fragile ecosystem and cultural heritage of the Qinghai-Tibetan Plateau due to high water regulation. In view of the planned dams, the Dadu River will become another victim of dam construction. The water regulation for the Dadu River is less than 3%, followed by an increase to 6.5% when the seven under-construction dams are complete, and a peak at 31.2% after the completion of 13 planned dams on the Dadu River (Figure 8.4). Eventually, all the major Yangtze tributaries in the upper reach will be highly regulated. The impacts on the river ecosystems are apparent.

There are also some dams under construction in the middle reach. The total storage capacity of the under-construction dams is 11.2 km^3. Although the total capacity is much less than their counterparts in the upper reach, it can also worsen the impact of the dams in the middle Yangtze reach on downstream water supply. As a case in point, a severe drought in the middle and lower reaches from April to June 2011 exposed the impacts from reservoirs in the middle Yangtze reach. When water was released from
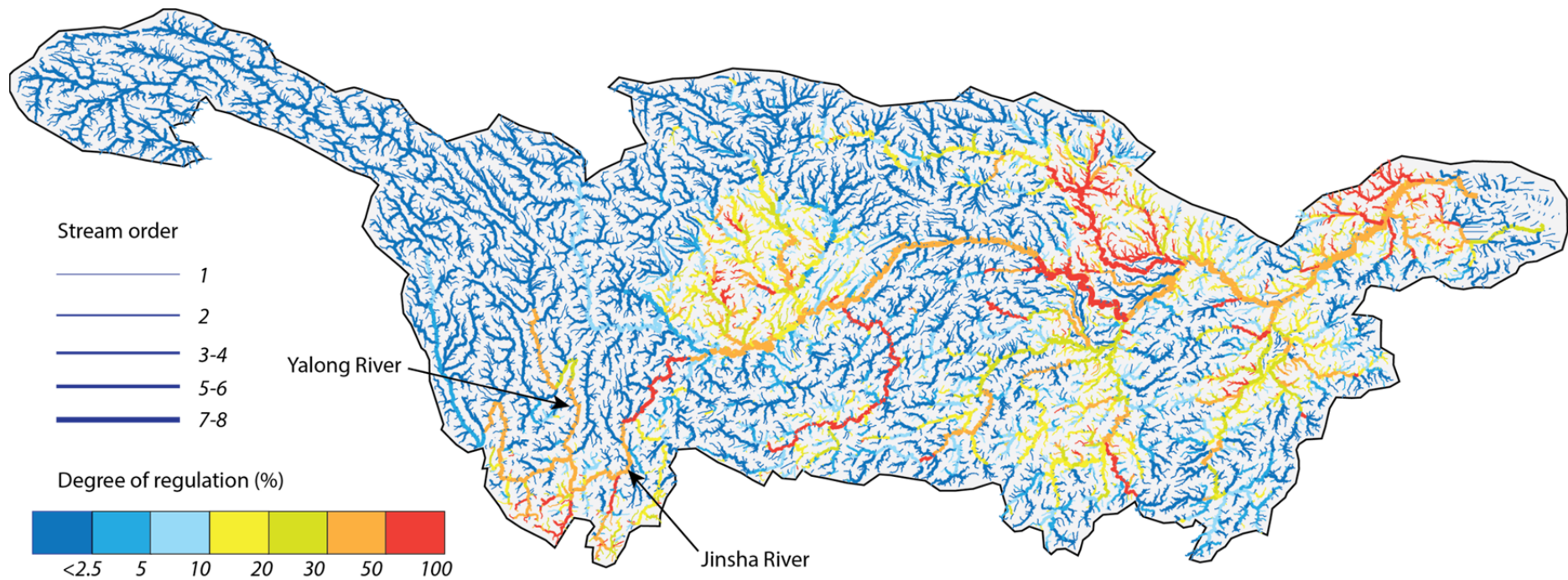
Figure 8.3 Predicted water regulation change based on DOR_s with respect to dams under construction. Different colors show an increasing degree of water regulation, whereas line width is proportional to stream order. Please note that this predicted result could be underestimated as a result of incomplete data on dam construction because many dams which are not being built on the major tributaries were excluded in the data.
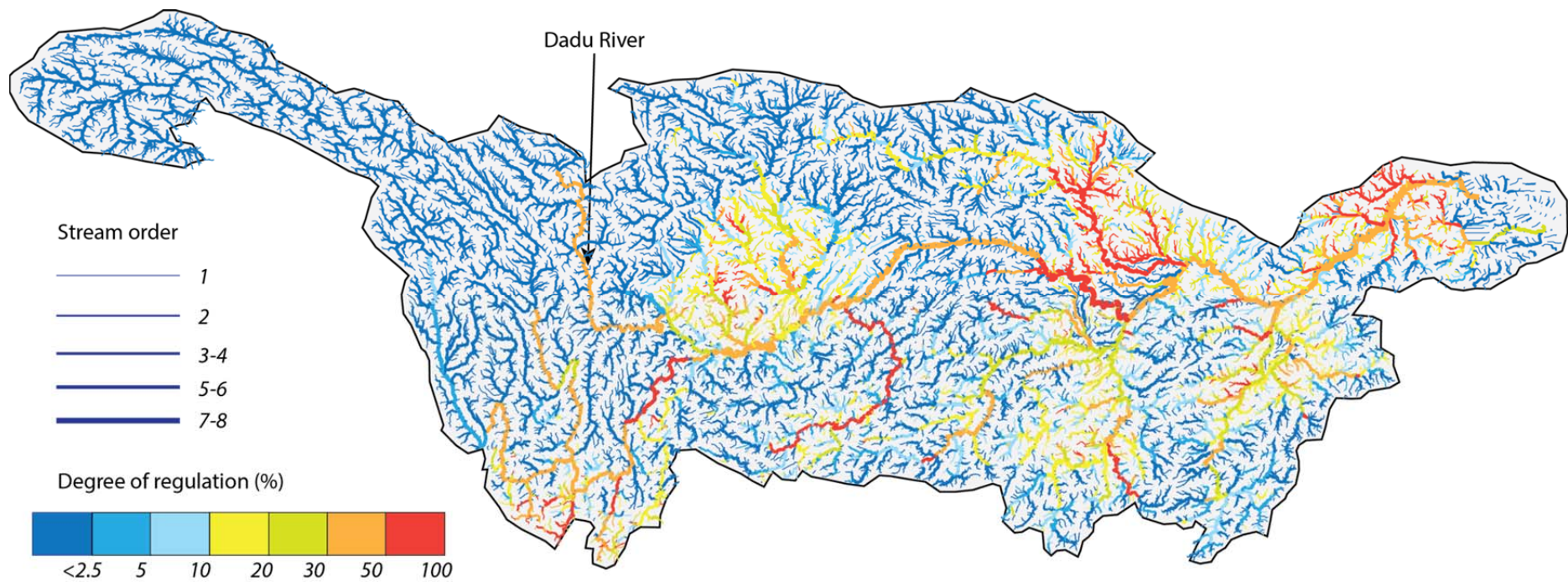
Figure 8.4 Predicted water regulation change based on *DOR$_s$* with respect to planned and under-construction dams. Different colors show an increasing degree of water regulation, whereas line width is proportional to stream order. This predicted result could be underestimated because some planned dams have no storage capacity data available.

Table 8.1 Comparison of water regulation change for different river sections based on DOR_s analysis, tabulated by stream order and degree of regulation

Stream order[a]	Dam status[b]	DOR_s(%)0-5%	5-10%	10-20%	20-30%	30-50%	>50%	Unit
		Extent of affected river sections downstream small dams						
4	A	4,841	2,174	2,139	1,317	1,525	1,994	km
		34.6	15.5	15.3	9.4	10.9	14.3	%
	B	4,719	2,061	2,324	1,274	1,619	1,994	km
		33.7	14.7	16.6	9.1	11.6	14.3	%
	C	4,719	2,045	2,340	1,274	1,619	1,994	km
		33.7	14.6	16.7	9.1	11.6	14.3	%
5	A	3,119	310	944	1,603	687	795	km
		41.8	4.2	12.7	21.5	9.2	10.7	%
	B	1,816	1,022	927	1,734	1,165	795	km
		24.4	13.7	12.4	23.2	15.6	10.7	%
	C	1,740	313	927	1,734	1,949	795	km
		23.3	4.2	12.4	23.2	26.1	10.7	%
6	A	2,515	239	1,055	304	40	480	km
		54.3	5.2	22.8	6.6	0.9	10.4	%
	B	1,818	126	237	344	1,320	789	km
		39.2	2.7	5.1	7.4	28.5	17.0	%
	C	1,656	126	237	501	1,325	789	km
		35.7	2.7	5.1	10.8	28.6	17.0	%
7	A	214	14	433	391	918	0	km
		10.9	0.7	22.0	19.9	46.6	0.0	%
	B	4	0	86	1	1,503	378	km
		0.2	0.0	4.4	0.0	76.2	19.2	%
	C	4	0	86	1	1,503	378	km
		0.2	0.0	4.4	0.0	76.3	19.2	%
8	A	0	0	0	0	674	0	km
		0.0	0.0	0.0	0.0	100.0	0.0	%
	B	0	0	0	0	674	0	km
		0.0	0.0	0.0	0.0	100.0	0.0	%
	C	0	0	0	0	0	674	km
		0.0	0.0	0.0	0.0	0.0	100.0	%

[a] Data for the first-, second- and third-order streams were not given here because this prediction was mainly based on under-construction and planned dams placed on large Yangtze tributaries;

[b] Dam status: A: only dams in operation were considered;

B: only dams in operation or under construction were considered;

C: all dams (in operation, under construction, planned) were considered.

the TGR in response to the water shortage, much of water remained impounded and available for power generation in the many large reservoirs in the middle reach. The cumulative impacts of these reservoirs on the Yangtze's large-scale hydrologic regime are evident.

Overall, the proportion of the unregulated or slightly regulated river sections will sharply drop with the completion of the under-construction and planned dams in coming decades (Table 8.1). For example, the total length of fifth-order streams with DOR_s less than 5% will be almost halved; approximately one third of the total length of sixth-order streams with DOR_s less than 5% will vanish; the seventh- and eighth-order streams with DOR_s less than 5% will even completely disappear. After the completion of the under-construction and planned dams, the main stem and major tributaries will be dominated by strongly regulated river sections. Although the condition for smaller river sections is a little 'better' than large ones, one should not be overly optimistic at the condition because real condition are still unclear due to lack of information about under-construction and planned small dams. As the degree of water regulation increases with the completion of more dams, the ecological risks associated with further impacts on river systems should be rigorously investigated.

It should also be emphasized the impact of the South-North Water Diversion Project on water regulation of the Han tributary. On the middle route of the South-to-North Water Diversion Project, the project transfers 14.7 km^3 of water to North China. This

amounts to approximately 2 per cent of the average flow at the Hankou Station and 1.5 per cent of that at the Datong Station. Although the regulating role of the large lakes will ensure that on the whole there will be no significant effect on the amount of water in the middle and lower reaches of the Yangtze River, the impact on shipping and irrigation in the lower reaches of the Han River should be carefully investigated. To investigate the impact, this study simulated annual runoff variation in coming decades and possible reduction in water discharge and water level due to water diversion. The simulation results indicated that the average precipitation may decrease by approximately 10% by 2030 due to climate change, leading to a decrease (35×10^8 m^3) in annual runoff entering the Danjiangkou Reservoir. As a result of reduced runoff, the water transfer would affect areas along both sides of the main channel of the middle and lower reaches of the Han River downstream from the reservoir. The main channel is 650 km long from Danjiangkou to Hankou; the nearly 79,000 km^2 in the middle and lower reaches is an important component of the commodity grain base of the Jianghan Plain. The simulation results indicate that the water level will decrease significantly. The most significant reduction happens at Xiantao station, which can change up to -2.25 m. Although the reduction at the Huangzhuang station is relatively low due to the wide and braided river channels between the Xiangfan and Xiantao stations. The decline in reservoir's downstream discharge will also cause water depth and the flow velocity to diminish further. This would not be favorable to river ecosystems.

8.4 Possible impact on sediment retention

Another significant impact could be reservoir sedimentation. The total estimated annual sediment trapped in the newly constructed reservoirs will be 160 Mt, which will cause a sharp decrease in sediment inflow to the TGR because a great of proportion of sediment will be trapped in the dams upstream of the TGR. In addition, the implementation of soil conservation projection can also decrease sediment yield in the area upstream of the TGR, which will cause a further decrease in sediment inflow to the TGR. Since more than half of the sediment entering the TGR comes from the Jinsha River, sediment inflow into the mega reservoir will decrease to approximately 90 Mt yr^{-1} due to upstream traps, assuming that sediment yield in tributary basins remains unchanged. As a result of low sediment inflow, the TGR should maintain approximately 34 km^3 of its storage capacity by the year of 2100. Accordingly, the reservoir will allow a high sediment retention rate and a low downstream sediment outflow (15 Mt yr^{-1}). In this way, the reservoir will keep approximately 20 km^3 of its storage capacity and a retention rate of 70% in 300 years after its closure. It should be highlighted that, sediment inflow from the ungauged areas surrounding the TGR will become increasingly important as upstream dams are constructed. After the construction of the cascade dams on the Jinsha, Yalong and Dadu rivers, the ungauged source of sediment supply may amount for approximately half of the gauged sediment discharge to the TGR.

Although this can significantly extend the life of the TGR for centuries, future downstream erosion and riverbed degradation will be much greater than expected, and the lower of the main channel will draw down and diminish the connected floodplain lakes. According to the prediction by Yang *et al.* (2014), the sediment discharge from the Yangtze to the sea will most likely decrease further to approximately 110 Mt yr^{-1} for the rest of this century and the next century, to about 20% of its level in the 1960s. The built dams have and will continue to cause dramatic impact on the sediment-water balance in coming decades. For example, if we take the mean annual sediment load between 1955 and 1960 to represent 100% of the baseline, then during the period from 2006 to 2010, the sediment load at Yichang station decreased to approximately 32Mt with a reduction of about 92%, followed by a further decrease in sediment load as a result of new dam construction (Figure 8.5). The downstream riverbed and delta erosion noted over the past decade undoubtedly will be intensified into the next century.

After further dam development, sediment load below Yichang is dramatically lower than the sediment-transport capacity of the flow and the dominant sediment transport processes have changed dramatically—the river has become sediment-starved and degradation has happened. The Yangtze River below Yichang will become a typical sediment-starved river. However, there is still a large quantity of erodible deposits in the middle-lower Yangtze River, where accretion had occurred for a long time until the sediment discharge from the upstream decreased below 250 Mt yr^{-1} because of

anthropogenic activities, especially dam construction (Yang *et al.*, 2011). The thickness of the unconsolidated Holocene sediments excluding the lowest gravel layer is < 20 m in the first 300 km reach, 20–30 m in the 300–700 km reach, and 30–40 m in the 700–1300 km reach downstream of the TGR; thus, the total estimated volume of the loose sediments in the middle-lower reaches is approximately 80 km^3 (Yang *et al.*, 2014).
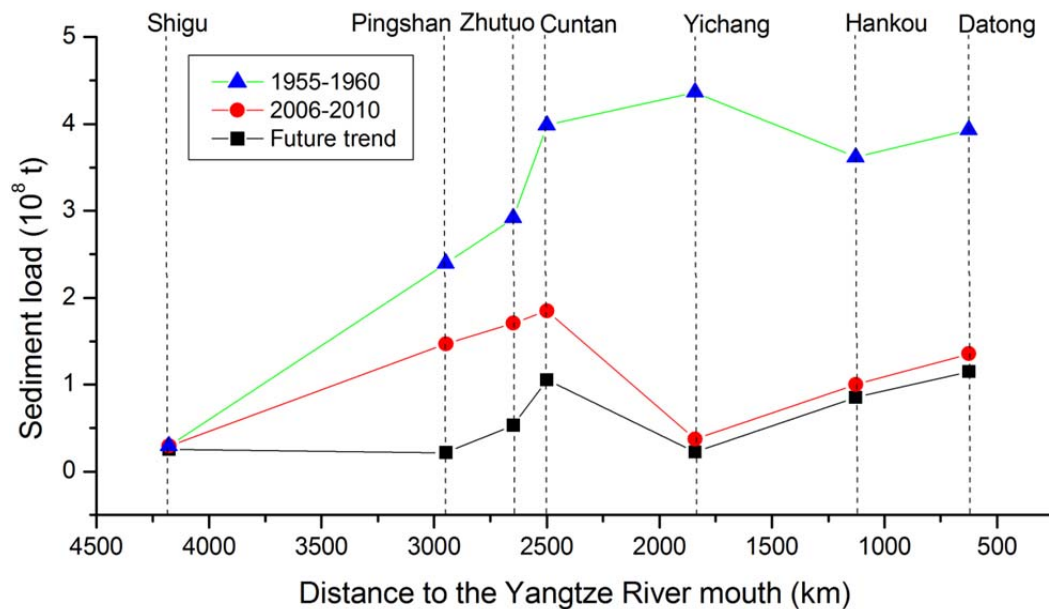
Figure 8.5 Sediment loads for 1956–1960, 2006–2010 and future after the completion of the Xiangjiaba, Wudongde, Xiluodu, Baihetan, Upper Hutiaoxia dams and other large dams.

In the late half of the 20th century, for example, nearly 4,000 Mt of sediment was deposited between Yichang and Datong. Considering such a large volume of erodible sediments, future channel erosion in the middle-lower reaches will be much greater than previously expected. Previous study (IWHR and YSRI, 1990) predicted that the erosion rate would a decreasing trend along with the reduction in the storage capacity

225

of the TGR and the increase in sediment outflow from the TGR. By the 2060s—2070s, the erosion between Yichang and Datong could reach a maximum of 4,200—4,500 Mt, or approximately 3 km^3, more than 90% of which could occur between Yichang and Hankou (Lu, 2002). However, because the construction of the large dams in the upper reach of the Yangtze River, the TGR sediment outflow will be lower than 15 Mt yr^{-1} in the coming decades and will most probably be less than 50 Mt yr^{-1} within the next century, i.e., erosion will occur through this century and the next. Yuan (2014) estimated that the riverbed erosion between Yichang and Hankou would be approximately 55 Mt yr^{-1} in the first 50 years after TGR operation and then would decrease to 50 Mt yr^{-1} by the end of this century. Taking the riverbed erosion between Hankou and Datong into account, this study roughly estimated that the total downstream erosion will probably amount to 7,000 Mt by the year of 2100, and to 12,000 Mt by 2200.

In addition, the South-to-North Water Diversion Project will transfer 45 km^3 yr^{-1} to North China, approximately 30 km^3 of which originally passes the Datong station. This would extract 2-4% of the sediment discharging to the sea; furthermore, the sediment-transport capacity of the flow could be reduced by 3-5% as a result of water diversion. Therefore, the erodibility of the riverbed sediments from Yichang to Datong may show a gradual reducing trend in coming decades. The combined impact of the TGR, the newly constructed large dams and the South-to-North Water Diversion Project can cause a significant decrease in sediment load to the sea in future decades.

It is estimated that the riverbed between Yichang and Datong will be deepened by approximately 2.3 m on average by the year of 2100, and by approximately 3.8 m by 2200 (Yuan, 2014). Although most erosion has occurred a few hundred kilometers immediately downstream of the TGR (Yang *et al.*, 2014), the section of maximum erosion is predicted to move downstream toward the Yangtze estuary in the future (Luo *et al.*, 2012).

The severe riverbed erosion and resultant water level reduction will threaten Lakes Dongting and Poyang, the two largest freshwater lakes in China, which are linked with the Yangtze River. In fact, the operation of the TGD has already modified the seasonal pattern of flow regimes in the Poyang Lake and significantly reduced the water level in the lower Yangtze River during the TGD impounding period from September to November. Although the impact of the recent droughts in the Poyang Lake and upper Yangtze reaches has played a crucial role in the low water level of Poyang Lake, more attention should be paid to its sensitivity to the influence of severe riverbed erosion and resultant water level reduction.

Using the Poyang Lake as a case study, based on the predicted water level reduction Yang *et al.* (2014), this study simulated the monthly variation in surface area of the Poyang Lake (Figure 8.6). The results show that a decrease in surface area have been observed in October, November and December due to water impoundment by the TGR after its closure in 2003, although the late water release from the dam can

significantly expand the lake's surface area in February, March, and April. However, with increasingly severe riverbed erosion and resultant channel downcutting, the water level in the middle-lower Yangtze reaches will decrease significantly, leading to a sharp decrease in water level of the Poyang Lake.
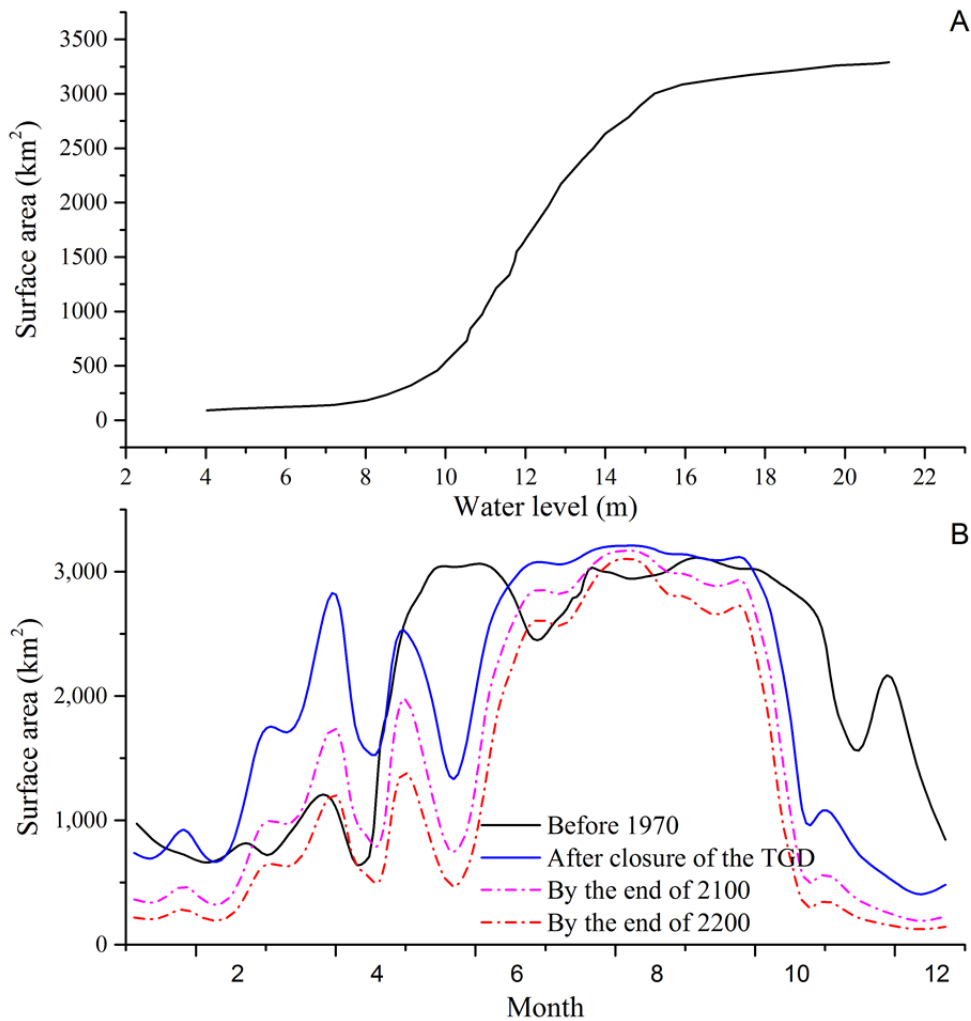
Figure 8.6 Prediction of the monthly variation in surface area of the Poyang Lake as a result of water level reduction in the middle-lower reaches of the Yangtze River; A: the relation curve for lake surface area (in km^2) and water level (in m); B: delineated and predicted monthly change in surface area of the Poyang Lake in different periods.

The lake surface area in the dry season will dramatically shrink further. The increase

in surface area due to late water release from February to April will also be offset by decrease caused by water level drop. The resultant lake surface area in February, March and April by the end of next century will even lower than it is now; but higher decrease in lake surface area will also happen in other months. However, it should be highlighted that the recent extremely low water levels were mainly because of the remarkable decline in inflows to the middle-lower reaches due to lack of precipitation and possible human activities (Lai *et al.*, 2014). Nevertheless, the effects of the TGD and many newly constructed dams on downstream rivers and lakes will be considerably intensified via riverbed erosion and resultant water level decrease in the foreseeable future.

In the delta area, the direct response to decreased sediment discharge could be estuary degradation. In fact, on the delta front, the salt marsh has significantly slowed progradation and the subaqueous slope has changed from accretion to erosion (Yang *et al.*, 2011). In coming decades, when the sediment discharge decrease to approximately 110 Mt yr^{-1}, further delta recession could be predicted. This has significant implications for coastal management around the metropolis of Shanghai. Another implication is the impact on suspended sediment concentration in the coastal area. In the upper Yangtze estuary, the suspended sediment concentration has decreased by 55% since the closure of the TGR. In the lower estuary, where sediment resuspension from seabed erosion has partly buffered the decreased suspended sediment concentration, a reduction of 20% of suspended sediment concentration has

been observed (Liu *et al.*, 2014). In the future, the estuarine suspended sediment concentration will most probably continue to decrease, which has great implications for wetland ecology and environmental management.

8.5 Possible impacts on river connectivity and river landscape fragmentation

As stated in Chapters 6 and 7, booming dam construction has already imposed dramatic stress on river ecosystems and the integrity of the river system via river disconnectivity and river fragmentation and new dams will further reduce connectivity. For instance, the TGD threatens 162 species of fishes in the main channel, 44 of which are endemic (Park *et al.*, 2003). As more large dams are constructed in the upper Yangtze reach, bigger environmental threads will be imposed on the distinctive river ecosystems developed in glaciated plateau, mountain ranges, Karst mountains and other river landscapes. For example, of the 361 native fish species in the whole Yangtze River basin, 267 can be found in the upper Yangtze reach, including 118 species that are endemic to the upper Yangtze reach (Heiner *et al.*, 2011), which will be dramatically affected by future dam construction.

Using the models proposed in Chapter 6, this study predicted the future trend of river landscape fragmentation based river-landscape classification map. The results are shown in Figure 8.7. By comparing with the current state in Figure 6.7B, it can be seen that the worst-affected areas are the main-stem area upstream of the TGD, the

Jinsha, Yalong and Min tributary basins. For example, most of the main-stem sections upstream of the TGD presently maintain connectivity among six river landscapes, whereas only three river landscapes will remain connected after a cascade of large dams are constructed in this area. The cascade dams also intercept the connection between the river landscapes in the upper Jinsha tributary basin and the river landscapes in the main-stem area, which would worsen the river fragmentation in the upper Jinsha tributary basin. Similar effects will also happen to the Yalong and Dadu rivers as a result of large dams built on the two rivers. For example, after the closure of all the under-construction and planned dams on the Yalong River, most of its river sections only keep connectivity among one to two different river landscapes. As a result of future dam construction, the percentage contribution of river sections with connectivity among one to two river landscapes will dramatically increase from approximately 33% at present to 52% after the completion of all the under-construction and planned dams. In contrast, the proportion of river sections with high connectivity (> 6 river landscapes) will dramatically shrink from 25% at present to only 16% in the future (Figure 8.7); but the shrinkage primarily happen in the middle-lower reaches downstream of Yichang, especially the main-stem area and the areas around the Poyang and Dongting lakes. The river fragmentation in the middle-lower reaches of the Yangtze River can also cause dramatic effects to the endemic species in this area. For example, The Yangtze finless porpoise is endemic to the middle-lower Yangtze reaches, which is now primarily restricted to the main-stem
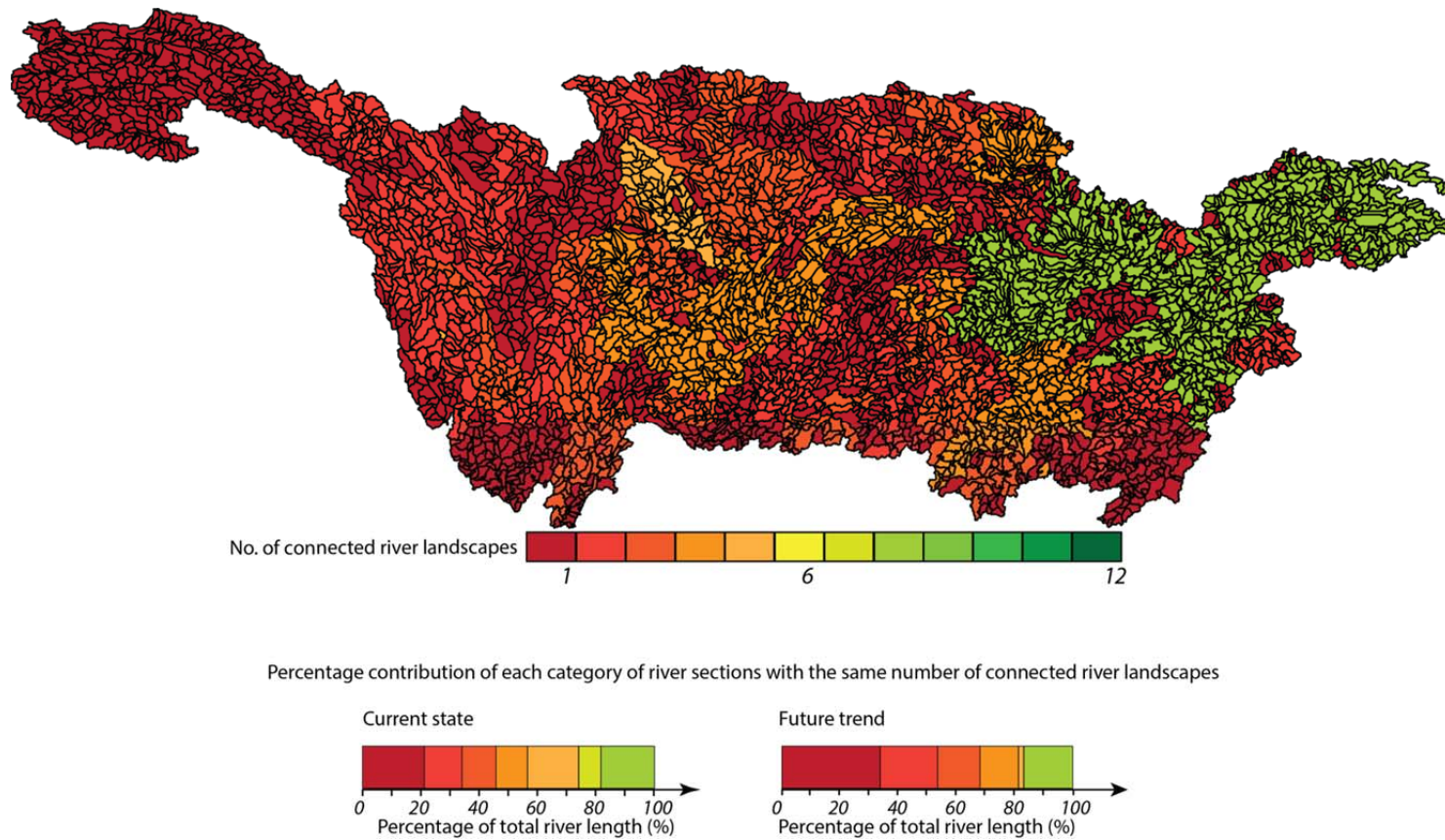
Figure 8.7 Predicted the future trend of river landscape fragmentation based river-landscape classification map in Figure 6.7A. Compared with Figure 6.7B, the predicted trend shows that future dam construction will cause further river landscape fragmentation, especially in the main-stem area upstream of the TGD, the Jinsha, Yalong and Min tributary basins.

area and its two largest appended lakes (Poyang and Dongting lakes) (Zhao *et al.*, 2008). Of the six extant species of porpoise, this is the only population found in fresh water. As a result of river landscape fragmentation, shrinkage in porpoise habitat could happen consequently, which could cause further alternations in ecological processes and the distribution of the Yangtze finless porpoise by blocking porpoise movements.
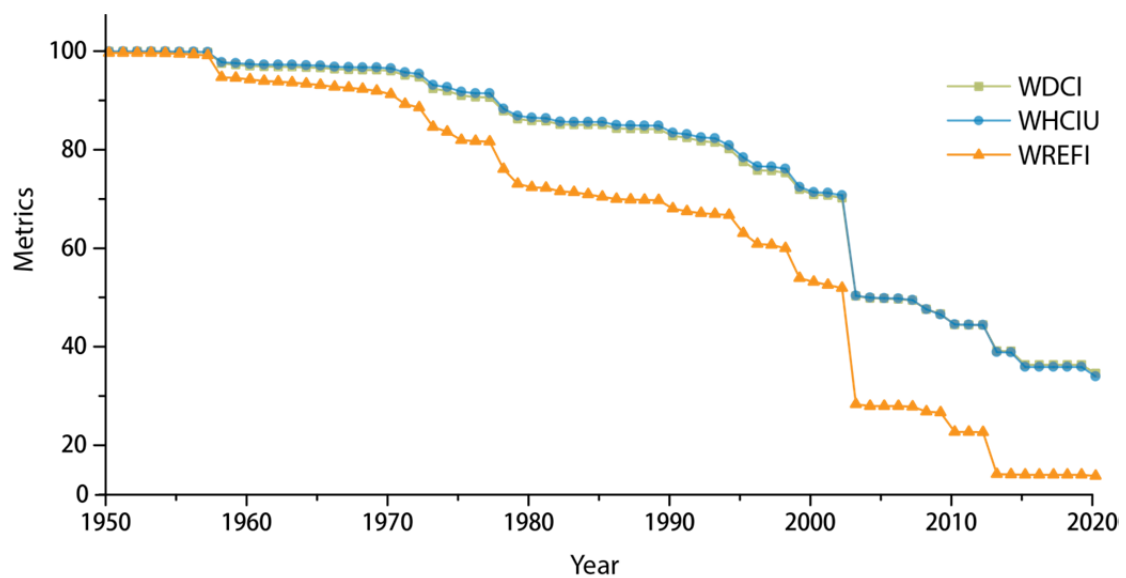
Figure 8.8 Variation of river connectivity and fragmentation for the Yangtze River represented by WDCI and WREFI from 1950 to 2020.

Except the river fragmentation assessment introduced above, the river connectivity assessment also reported a similar future trend of river system degradation. Figure 8.8 indicates a steady loss of river connectivity in future as a result of new dam construction. The steady decreases in WDCI and WHCIU reveal a steadily worsening crisis to the river system. The destruction of spawning sites and the obstruction of migration routes may result in sharp population decline of fish species and freshwater

animals. For example, after the closure of the TGD, the latest investigation in 2012 shows a total of only around 1,000 finless porpoises in the Yangtze River basin−making them even rarer than giant pandas in the wild (Qiu, 2012).

Another case in point is Chinese sturgeon, a kind of maricolous anadromous migratory fish. In 1981, the migratory route was disconnected by the Gezhouba Dam. The fish had to naturally reproduce at the downstream river of Gezhouba Dam, and a new spawning ground was formed. The length of the new spawning site became less than 1% of the historical sites (Zhou *et al.*, 2014). After water storage and power generation of the TGD in 2003, the propagation of Chinese sturgeon has been impacted dramatically. According to field surveys, the fish used to spawn twice a year before the closure of the TGD, but only once happened after that. Besides, the spawning scale is also declining with each passing year (Wang *et al.*, 2011). With more large dams constructed in the Yangtze River basin, the river will become more disconnected; more migratory fishes will be affected.

Additionally, it is particularly noteworthy that the Jiangxi Province has proposed a plan to dam the Poyang Lake to maintain the water levels in the lake. The dam would be built at the narrowest part of the channel that extends north from the Poyang Lake to enter into the Yangtze River at Hukou. The project was mainly stimulated by current severe situation that water is stored behind the TGD during the winter months for power generation, starving the Poyang Lake of supplies. Water levels in the

Poyang Lake have been dropping since 2003 and in December fell by a record low of 7.5 meters, although some researchers have argued that recent extremely low water levels were mainly caused by the remarkable decline in inflows to the middle-lower Yangtze reaches due to lack of precipitation and possible human activities (Lai *et al.*, 2014).

The huge dam on the Poyang Lake may cause dramatic river fragmentation and adverse effects to the river ecosystems in the middle-lower Yangtze reaches. The Poyang Lake and its tributaries would lose the connection with the Yangtze River. The disruption of the connection to the Yangtze River would dramatically affect the movements of the finless porpoise and fish. For example, 450 Yangtze finless porpoises, or 25% of the total in the Yangtze River, are distributed in the Poyang Lake (Zhao *et al.*, 2008). The density of porpoises in the Poyang Lake is the highest compared to all other river sections. The proposed dam may prevent the finless porpoises from movement between the Yangtze River and the Poyang Lake, and thus fragment their distribution. If fish paths could be designed for the passage of fish, the facility may not meet the requirements for this species. Even if the sluice gates are open, it is still unclear that if the porpoises will pass through. The dam could be fatal for this flagship species.

Despite the possible provision of fish paths, the dam would also impact fish species by blocking migrations and fragmenting their populations. According to a previous

study (Wu *et al.*, 2006), of 58 species of fish recorded at Nanjishan National Nature Reserve during 2003—2004, 20 species were migratory. Many fishes, including commercial fishes, utilize the sedge zone for spawning. After the damming of the Poyang Lake, the variations of water levels, which will affect distribution and abundance of the sedge communities, will have complex effects on fish spawning. In fact, populations for Chinese sturgeon, and other rare species initially found in the Poyang Lake, have already plunged across the Yangtze River basin (Dudgeon, 2010). The planned dam will worsen the current situation of natural ecosystems in the Poyang Lake drainage area. Given the intense negative pressures on many fish restricted to the Yangtze River basin, very thorough assessment of these impacts should be completed before a dam could be constructed.

8.6 Other possible impacts

Apart from the impacts discussed above, there are many possible impacts deserving deep discussion. The possible resultant signal of environmental impacts is favoring the reproduction of oncomelania snails downstream (McManus *et al.*, 2010). For example, the TGD increased the snail's habitat−and the infection risk. In endemic areas near lakes and wetlands in the middle reach, prevalence hovers around 5% (Stone, 2011). Although the health authorities are improving sanitation and implementing other measures to reduce the infection rate, for many of the villagers relocated to downstream schistosome-endemic areas, who have no immunity to

schistosomiasis, they will readily acquire a schistosome infection on exposure, and likely develop severe disease as a result (Gray *et al.*, 2012).

Also, as a result of the South–North Water Diversion Project, water pollution along the Eastern Route, limited water resources in the origin of the Han River and large displacement of 300,000 persons for the Central Route have also been concerned (Zhu *et al.*, 2008; Wang *et al.*, 2009b; Zhang, 2009; Liang *et al.*, 2012). Water transferred from the lower Yangtze reach will pass through and impound four lakes. The Eastern Route is laid on one of the most developed regions of China. Large amounts of untreated industrial wastewater are discharged to the lakes, which serves as water storage facilities along the route (Zhang, 2009). There are inadequate sewage treatment facilities for millions of people living in the rural areas. Although the government has been very active on pollution control in past decades, monitoring results suggest efforts are not very effective (Mao *et al.*, 2001). In addition, if the Poyang Lake is dammed and the water in the lake keeps stagnant in winter, the annual exchange rate would be greatly slowed. Water quality would decline. The aquatic vegetation of Poyang, highly important for fish and endangered waterbirds like the Siberian Crane, is sensitive to deterioration in water quality. Dongting and other lakes in the mid Yangtze basin have undergone a sudden transformation from macrophyte-dominated vegetation to a system dominated by phytoplankton, partially due to declined water quality (Harris and Zhuang, 2010). Such a change in the Poyang Lake area would be extremely expensive if not impossible to reverse.

8.7 Summary and conclusions

The expanded study reveals worsened impacts on water regulation, sediment retention, river connectivity, river landscape fragmentation and others due to future dam construction. By combining the existing reservoirs with a total storage capacity of 85 km^3, the total regulated water volume will be 215 km^3, or 53% of the runoff of the upper Yangtze River. The total estimated annual sediment trapped in the newly constructed reservoirs will be 150 Mt, which will cause a sharp decrease in sediment inflow to the TGR and further downstream erosion and riverbed degradation. The study also revealed a steady loss of river connectivity as a result of new dam construction. Thus, some countermeasures should be taken to preserve the Yangtze River and the associated river ecosystems. For example, better management of the existing reservoirs to recover the lost river connectivity. If necessary, the dams which can cause minor impacts on river connectivity and river landscape fragmentation should be prioritized. Where possible, hydropower projects should be built on tributaries, not on the main stem. If dams must be built on the mains tem, low-head dams sited as far from the estuary as possible should be preferred.

9 Conclusion

9.1 Introduction

In the Yangtze River basin, there are no places untouched by the consequences of dam development, although the extent and impact vary greatly across the river basin. These impacts can be seen directly through the inundation of land, crops, cities and villages by dam construction, flow regulation through water withdrawals and water transfers, fragmentation of river landscapes through river interception by the construction of small dams and weirs. Current efforts to assess the consequences, identify possible potential environmental risks and thereby control dam development, fits precisely with the goals of geographers who seek to explore spatial distribution patterns and hydrological processes related to dam development and the impacts on the physical river environment. This dissertation in place within the entire Yangtze basin includes exploring spatial distribution of dams, investigations of long-term impacts of dams on sediment retention and water regulation, developing metrics to quantify the impacts of dams on river connectivity and river landscape fragmentation, identification of vulnerable river sections to dam development. Without knowledge of the spatial patterns of dams and possible impacts related to dam development, it is impossible to comment on historical conditions or to speculate on the feasibility of the remediation efforts in the future.

Contributions to geography, fluvial geomorphology in both theoretical and applied

sense are an important component in any type of research in these fields. This dissertation adds to the numerous studies on anthropogenic impacts to the Earth and addresses the lack of detailed knowledge of the spatial patterns of dams and possible impacts related to dam development in the Yangtze River basin. The knowledge obtained in this study is essential to identify environmental risks associated with impacts on river systems. Also, using this knowledge, it has been possible to quantify the potential impacts of incremental dam development on river systems at basin and sub-basin levels in terms of environmental intactness. With this knowledge, it may be possible to develop the Yangtze River basin with a relatively lower environmental footprint, meeting local energy demands while conserving ecosystem processes basin-wide.

In the following sections, the major findings of this thesis and their implications are summarized, followed by the limitations and corresponding recommendations for future research.

9.2 Major findings and implications

In Chapter 4, this study used a parsimonious method based on remote sensing techniques to identify and extract water bodies in the Yangtze River basin and classify them into three main categories: natural lakes, artificial reservoirs and rivers. This method combined data from the best available free sources, resulting in higher data quality. This study delineated nearly 43,600 reservoirs and 42,700 lakes and estimated

a total quantity of 0.7 million smaller reservoirs and 0.5 million smaller lakes (surface area <0.0036 km^2). The combined surface area of the reservoirs is approximately 8,606 km^2 with a total storage capacity of approximately 288 km^3, and the total surface area of natural lakes is approximately 16,200 km^2, with a total storage capacity of only 46 km^3. These results indicate that the 43,600 reservoirs are capable of storing a volume of water equaling nearly 30% of the annual runoff of the Yangtze River. The results revealed that the Yangtze River basin, which was previously dominated by natural lakes, has become a reservoir-dominated basin due to anthropogenic impacts, especially reservoir construction and lake shrinkage. However, there is considerable geographic variation in the potential surface water impacts of the reservoirs. The greatest impacts to water regulation, environmental destruction and river fragmentation may occur in the Poyang Lake Region which has the greatest capacity-area ratio. Future dam construction could worsen the situation as additional large hydropower projects are closed in the upper reaches of the basin, potentially affecting the water cycle in the entire basin.

In Chapter 5, a framework on 1,358 of large and medium-sized reservoirs ($\geq 10^7$ maximum storage capacity) was developed and applied for calculating reservoir sedimentation rates in the multi-dam Yangtze River system while accounting for the effect of reduced sediment input due to upstream traps. Statistical inference was further used to assess the sedimentation rates of the remaining 42,000 smaller reservoirs. Given the inefficient, laborious reservoir investigations for reservoir

sedimentation, managers can benefit from an effective approach with which to identify at a large scale those reservoirs at higher risk of filling in the near future. The model is an effective approach to estimate reservoir sedimentation in a multi-reservoir system. The model could be applied equally well to other large river basins despite difference of sediment yields. The results indicate that annual sediment accumulated in the Yangtze reservoirs is approximately 691 (± 94) million tons (Mt), 669 (± 89) Mt of which is trapped by 1,358 large and medium-sized reservoirs. Only 22 (± 5) Mt is trapped by smaller reservoirs. The estimated mean annual rate of storage loss is 5.3 x 10^8 m^3 yr^{-1}; but against the world trend, the Yangtze River is now losing reservoir capacity much lower than new capacity being constructed.

Chapter 6 sets a pilot investigation in implementing a basin-wide assessment of river connectivity and river landscape fragmentation in the Yangtze River basin based proposed three metrics, WDCI, WHCIU and WRLFI. This study assessed the cumulative impacts caused by 1,358 large and medium-sized reservoirs at the scale of the entire Yangtze River basin. The overall result shows that the Gezhouba Dam and the TGD, have highest impact on river connectivity and fragmentation. The WDCI and WHCIU values for the whole Yangtze River have decreased from 100 to 34.12 and 33.96, respectively, indicating that the Yangtze has experienced strong alterations over the past decades. The measurement of WRLFI displays a substantial part of tributary basins, especially the Wu, Min and Jialing tributaries, only maintain connectivity among one to three river landscapes. Connectivity between different river landscapes in

the middle and lower basin is the highest. Even so, only a small part of the system still maintains connectivity between seven out of twelve river systems — no part of the Yangtze connects all twelve river landscapes.

Based on small dam data obtained in Chapter 4, Chapter 7 employed two metrics (DORs and AWDD) to investigate the impacts of small dams on flow regulation and river landscape fragmentation. The study revealed that 54, 977 km, or 26% of the streams are affected by upstream small dams. Of these, 45,878 km are first-, second- and third-order streams, representing 25% of all streams in the three size classes. Among the streams, the fourth -order streams are the most severely affected, 32% of which are affected. The AWDD analysis also revealed similar significant effects in regional areas such as the plain areas in the middle and lower Yangtze reaches. On average, people can find 2.3 small dams every 100 km^2; but the dam density can as high as 9.1 small dams per 100 km^2 in ridge-and-valley area in the middle Yangtze reach. The analyses in this chapter reveal that small dams can also exert significant impacts in river regulation and river landscape fragmentation on regional river systems through their sheer number and density. The results indicated that the impacts of small dams are comparable to large dams for fourth- and fifth-order streams, or even significantly exceed large dams for first-, second- and third-order streams. Therefore, small dams should be emphasized in mitigating environmental impact associated with the fragmentation of river landscapes, including the degradation of aquatic habitat and the movement of nutrients.

9.3 Limitations in this study

Being an exploratory study, this work made a preliminary assessment of the cumulative impacts of dams from three perspectives (sediment retention, river connectivity and river landscape fragmentation) in the Yangtze River basin. There are several limitations in this thesis and additional efforts are needed in future to obtain a more comprehensive understanding of the cumulative impacts caused by dams at basin and sub-basin scales.

9.3.1 Uncertainty in reservoir delineation

When the reservoir areas were delineated on remote sensing images, the accuracy was affected in three aspects: the extraction of water bodies, the classification of water bodies into reservoirs and lakes, and the estimation of storage capacity.

The accuracy of the identification and extraction of water bodies was mainly influenced by several aspects of image quality such as resolution, cloud cover, shadows and sediments in the tail-water of reservoirs. Thus, delineated water bodies that were smaller than 2x2 pixels or 0.0036 km^2 were removed to ensure that the delineated features were real water bodies. Smaller reservoirs and lakes were also difficult to distinguish from paddy fields and aquacultural farms because natural lakes, paddy fields and aquacultural farms share similar spectral characteristics. In addition, sediments accumulate in the backwater of reservoirs, making the reservoir surfaces

appear smaller than they are.

The classification of water bodies into lakes, reservoirs and rivers was initially based on the GeoNames database and thematic maps of water resources. For the water bodies without corresponding features on the thematic maps and in the GeoNames database, visual interpretation using high-resolution Google Earth images was performed. Therefore, in this stage, accuracy depended heavily on the accuracy of the GeoNames database and the thematic maps. However, the reservoirs that did not have corresponding features on the thematic maps and in the GeoNames database could have been misclassified as natural lakes if their dams were not easily identified.

The errors in the last stage, i.e., the estimation of storage capacity, were due to the shape of the terrain and topography. This study used the area-capacity model proposed by Liebe et al. (2005) to develop area-capacity relationships. The model is mainly based on the V-shaped reservoirs and arc-shaped lakes that are dominant in the study area. The established equations may not be a good fit for deep U-shaped reservoirs with very steep sides because the area-capacity relationship for these reservoirs differs slightly from that for V-shaped reservoirs.

9.3.2 Uncertainty in reservoir sediment estimation

When estimating sedimentation trapped in reservoirs, some factors that may affect the sedimentation amount were not accounted for here. First, downstream bank erosion

after reservoir operation could be one of the most significant factors affecting downstream sediment transport because rivers tend to erode and lower riverbed downstream from large reservoirs. However, in general, the response of bank erosion rates (and channel width) to upstream reservoir closure is very complex, with trends of widening, narrowing and no change reported for various rivers (Williams and Wolman, 1984). For example, on such a river as the Wu River with 10 cascade reservoirs end to end on the 900-km river, the impoundments have caused the velocity of the water behind the dams to drop dramatically and thus led to decrease in bank erosion between dams. Little sediment is trapped in farthest downstream cascade reservoirs (e.g. Silin, Shatuo and Pengshui reservoirs), although their total capacity is nearly 3.6 km^3 (Chen *et al.*, 2008a). Second, other variables, including flow, relative pool depth, sediment supply from upstream, and sediment size and distribution, may influence sediment deposition within a reservoir, as these variables vary regionally with geology, geomorphic delivery processes, land-use history, and climatic cycles (Minear and Kondolf, 2009). The proposed model assumed that similar processes occur within this basin which is a simplification necessary for computation. This model is appropriate for detecting a basin-wide trend and highlighting reservoirs potentially at risk of sedimentation but may not give accurate estimates of sedimentation rates within individual reservoirs. Finally, the calculations for small reservoirs (< 0.01 km^3) were aspatial. These estimates are somewhat speculative because this is based on the assumption that reservoir data are a

homogeneous distribution. However, the real reservoir density in the Yangtze River basin shows a clear east-to-west gradient except in the Sichuan Basin. Thus, the estimates for small reservoirs may need a more complete geographically referenced analysis.

9.3.3 Limitations in assessment of the impacts of dams on river connectivity and river landscape fragmentation

Three metrics were proposed in Chapter 6 to evaluate the cumulative impacts of dams on river connectivity and fragmentation. Because of data unavailability, universal passability standards were applied to the all dams. Yet these calculations may be problematic because this assignment is arbitrary. If possible, passability data should be collected. A second challenge is identifying whether the probability of passing a dam is independent among nearby dams. Independence may not be appropriate in situations where passability is dependent on water discharge (which varies at large spatial scales). For example, the Gezhouba Dam is close to the TGD (38 km), the water discharge at the Gezhouba Dam is significantly affected by the water released from the TGD. In this case, the probability of passing the Gezhouba Dam may not be independent. A third challenge is that each river landscape was considered to be of equal relevance throughout the entire Yangtze River basin when analyzing river landscape fragmentation using the WRLFI, but more crucial information could actually be obtained if the individual river landscapes and their associations with

specific processes and basin layout can be better geographically quantified. Besides, the WRLFI value is extremely dependent on the river-landscape classification map. Slightly different results may be obtained with a different classification map. Thus, an appropriate classification map is the fundamental determinant of the assessment based the index of the WRLFI.

Another limitation for the three metrics is that they may undervalue the impacts of small dams because the three metrics can only provide an overall assessment on the impacts of dams, but small dams may contribute less to the overall alteration of large-river flows as a result of their limited storage capacities. Therefore, a method which can provide not only overall results but also detailed regional results is demonstrated in chapter 7.

9.3.4 Limitations in assessment of the impacts of small dams on flow regulation and river landscape fragmentation

In Chapter 7, this study evaluated the impacts of 42,000 dams on flow regulation and river landscape fragmentation based the metrics of DORs and AWDD. The results of the DORs study need careful interpretation to avoid arriving at misleading generalizations. First, the impacts and consequences of flow regulation may vary for different river size classes. When the first-, second-, third- and fourth-order streams are affected by small dams, the impacts are more significant at a regional scale than at a basin-wide scale. Second, the DOR_s ratio is important. For river sections with high

DOR_s values, major implications for the intra- and inter-annual flow regimes are to be expected. However, smaller values may indicate critical alterations as well, but of shorter duration or smaller amplitude. Third, it will largely depend on the individual reservoir operation scheme and additional impacts. In addition, the DOR_s approach intrinsically is subject to various uncertainties due to the lack of data, such as high-resolution DEM data, the role of dam operation.

9.4 Recommendations for future work

Based on the study results obtained, the discussion presented in previous chapters and the conclusions drawn in this chapter, there are several important and intersecting perspectives for future work. Five major research subjects that should be targeted to address existing limitations were shortly stated below.

9.4.1 Reservoir storage estimation using multi-temporal remote sensing images

Water level in a reservoir often follows an annual cycle: trapping water after the wet season, releasing water in the dry season. For most reservoirs in the Yangtze River basin, impoundment starts at the end of the rainy season in September, peaking at the end of October. Reservoir capacity is strongly related to reservoir surface area. Thus, the surface area large enough is a prerequisite to the estimate of a reservoir's storage capacity. As stated previously, the Landsat images were obtained for September and

October from 2003 to 2008. Using images obtained in September and October is actually a compromise to obtain largest reservoir surface area. However, it should be highlighted that each water body was covered by only one image. Thus remote sensing has been unable to reflect the annual and inter-annual changes in reservoir surface area. Recent development and increased availability of satellite images (e.g., Landsat 8 launched in 2013) in the public domain has provided an opportunity for delineating reservoir surface area using multi-temporal remote sensing images. More accurate results could be obtained by analyzing multi-temporal remote sensing images; however, the image processing will be laborious and time-consuming, which will be another challenge to find a new approach to process the images efficiently.

In addition, when using multi-temporal remote sensing images, the available images differ in spatial and time scales, and give rise to compatibility issues in overlay analysis in a GIS environment. Moreover, there is a lack of information regarding the accuracy of the images as well. The inconsistency of the spatial and temporal scales in different satellite images and doubts regarding the accuracy of the images increase the uncertainty of the reservoir storage estimation based on these images.

9.4.2 More complex but accurate simulation of sediment retention in reservoirs

The proposed modeling framework has made satisfactory predictions of sediment yield and sediment trapped in reservoirs in the Yangtze River basin. This framework is

relatively simple and it is envisaged that the inclusion of additional processes of erosion and sediment yield would further improve the accuracy of predictions from the modeling framework. As a next step in this study, the modeling framework could be expanded to include bank and channel erosion processes, reservoir characteristics (e.g., flow, relative pool depth, sediment supply from upstream, and sediment size and distribution), and mass movements resulting from seismic activities.

In terms of the complexity of the modeling framework, model validation is another challenge, which is extremely important for the reliability of predictions. This, however, requires a comparison between the measured and predicted values from the model. The scarcity of sediment investigations in reservoirs is another source of uncertainty for the modeling results.

9.4.3 Developing new models to estimate passability for each dam for river connectivity assessment

When estimating passability for each dam, there are two future challenges. The first challenge is identifying whether the probability of passing a dam is independent of among nearby dams. Independence may not be appropriate in situations where passability is dependent on water discharge, which varies at large spatial scales. The second challenge is the changes in physical condition have complicated the estimation of passability for each cascade dam. Although the WDCI and WHCIU require estimates of passability at individual dams and better estimates of passability will

serve to reduce uncertainty, designing an approach to estimate passability of dams is still a challenge for the academic community. Also the approach should be validated against observed connectivity patterns.

9.4.4 Integrating the assessment of river connectivity and fragmentation into environmental impact assessment

An environmental impact assessment for dam construction is a formal process used to predict the environmental consequences (positive or negative); it proposes measures to adjust impacts to acceptable levels. Although an assessment may lead to difficult economic decisions and political and social concerns, environmental impact assessments protect the environment by providing a sound basis for effective and sustainable development to manage our water resources while taking into account the needs of present and future users. Thus, the assessment of river connectivity and fragmentation should not be viewed in isolation. It should be integrated into the formal environmental impact assessment to evaluate the impact of dams on river systems at basin-wide and regional scales because it does not cover socioeconomic impacts, not fully represent the spectrum of environmental impacts. Also, the assessment of river connectivity and river landscape fragmentation present a framework to effectively integrate river connectivity and free-flowing functionality into dam planning and adds regional and basin-wide perspectives to conventional environmental impact assessments.

In addition, it is commonly recognized that environmental effects may vary and that some rivers may be more threatened than others by a certain level of flow regulation because the effects are the consequences of joint forces, such as, dam construction, deforestation, water diversion, land cover change and climate change. Undoubtedly, regarding the associated environmental consequences, more research is required when carrying out formal environmental impact assessments.

9.4.5 Application of the developed models to other large river basins in the world

The developed models in this study for the large Yangtze River basin are mainly dependent on global datasets available in the public domain. Therefore, they can be repeatable to assess the cumulative impacts of dams on sediment retention, river connectivity and river landscape fragmentation for other large, data-sparse river basins in the world, such as, the Mekong, Indus, and Amazon. The resultant assessments can help identify, evaluate, and predict the environmental effects of new dam proposals prior to major decisions being taken and commitments made. However, the limitations introduced above on the models should also be noted to avoid misinterpretation.

Bibliography

Ali, K.F., de Boer, D.H., 2008. Factors controlling specific sediment yield in the upper

    Indus River basin, northern Pakistan. Hydrological Processes **22**, 3102-3114.

Almeida, E.F., Oliveira, R.B., Mugnai, R., Nessimian, J.L., Baptista, D.F., 2009.

    Effects of small dams on the benthic community of streams in an Atlantic

    forest area of Southeastern Brazil. International Review Of Hydrobiology **94**,

    179-193.

Anderson, E.P., Freeman, M.C., Pringle, C.M., 2006. Ecological consequences of

    hydropower development in Central America: impacts of small dams and

    water diversion on neotropical stream fish assemblages. River Research and

    Applications **22**, 397-411.

Annor, F.O., van de Giesen, N., Liebe, J., van de Zaag, P., Tilmant, A., Odai, S.N.,

    2009. Delineation of small reservoirs using radar imagery in a semi-arid

    environment: A case study in the upper east region of Ghana. Physics and

    Chemistry of the Earth **34**, 309-315.

Arora, V.K., 2002. The use of the aridity index to assess climate change effect on

    annual runoff. Journal of Hydrology **265**, 164-177.

Benda, L., Andras, K., Miller, D., Bigelow, P., 2004a. Confluence effects in rivers:

interactions of basin scale, network geometry, and disturbance regimes. Water Resources Research **40**, W05402.

Benda, L., Poff, N.L., Miller, D., Dunne, T., Reeves, G., Pess, G., Pollock, M., 2004b. The network dynamics hypothesis: how channel networks structure riverine habitats. Bioscience **54**, 413-427.

Benítez-López, A., Alkemade, R., Verweij, P.A., 2010. The impacts of roads and other infrastructure on mammal and bird populations: a meta-analysis. Biological Conservation **143**, 1307-1316.

Benstead, J.P., March, J.G., Pringle, C.M., Scatena, F.N., 1999. Effects of a low-head dam and water abstraction on migratory tropical stream biota. Ecological Applications **9**, 656-668.

Birkett, C.M., Mason, I.M., 1995. A new global lakes database for a remote-sensing program studying climatically sensitive large lakes. Journal Of Great Lakes Research **21**, 307-318.

Blum, M.D., Roberts, H.H., 2009. Drowning of the Mississippi Delta due to insufficient sediment supply and global sea-level rise. Nature Geoscience **2**, 488-491.

Brandt, S.A., 2000. Classification of geomorphological effects downstream of dams.

Catena **40**, 375-401.

Brown, C.B., 1944. Discussion of Sedimentation in reservoirs. In: J. Witzig (Ed.), Transactions of the American. Society of Civil Engineers, pp. 1493-1500.

Brune, G.M., 1953. Trap Efficiency of Reservoirs. Transactions of the American Geophysical Union **34**, 12.

Budyko, M., 1974. Climate and Life. Academic, San Diego, 508 pp.

Callow, J.N., Smettem, K.R.J., 2009. The effect of farm dams and constructed banks on hydrologic connectivity and runoff estimation in agricultural landscapes. Environmental Modelling & Software **24**, 959-968.

Camp, T.R., 1945. Sedimentation and the design of settling tanks Proceedings of the American Society of Civil Engineers 445-486.

Chao, B.F., Wu, Y.H., Li, Y.S., 2008. Impact of artificial reservoir water impoundment on global sea level. Science **320**, 212-214.

Charlton, R., 2007. Fundamentals of fluvial geomorphology. Routledge, Florence, Kentucky, 280 pp.

Chen, C., 1975. Design of sediment retention basins Proceedings, national symposium on urban hydrology and sediment control Lexington, KY: University of

Kentucky, pp. 285-298.

Chen, S., Xu, Q., Chen, Z., 2008a. Analysis on variation characteristics and influencing factors of runoff and sediment in the Wujiang River Basin. Journal of Sediment Research **34**, 43-48.

Chen, X., Cui, P., Li, Y., Yang, Z., Qi, Y., 2007. Changes in glacial lakes and glaciers of post-1986 in the Poiqu River basin, Nyalam, Xizang (Tibet). Geomorphology **88**, 298-311.

Chen, X.Q., Zhang, E.F., Xu, J.G., 2002. Large and episodic decrease of water discharge from the Yangtze River to the sea during the dry season. Hydrological Sciences Journal-journal Des Sciences Hydrologiques **47**, 41-48.

Chen, X.Q., Zong, Y.Q., Zhang, E.F., Xu, E.G., Li, S.J., 2001a. Human impacts on the Changjiang (Yangtze) River basin, China, with special reference to the impacts on the dry season water discharges into the sea. Geomorphology **41**, 111-123.

Chen, Z., Xu, K., Watanabe, M., 2008b. Dynamic hydrology and geomorphology of the Yangtze River. In: A. Gupta (Ed.), Large Rivers: Geomorphology and Management. John Wiley & Sons, Chichester, England, pp. 457-469.

Chen, Z.Y., Li, J.F., Shen, H.T., Wang, Z.H., 2001b. Yangtze River of China: historical analysis of discharge variability and sediment flux. Geomorphology **41**, 77-91.

Cheng, G.W., 1999. Forest change: Hydrological effects in the Upper Yangtze River valley. Ambio **28**, 457-459.

Chin, A., Laurencio, L.R., Martinez, A.E., 2008. The hydrologic importance of small- and medium-sized dams: Examples from Texas. Professional Geographer **60**, 238-251.

Choudhury, B., 1999. Evaluation of an empirical equation for annual evaporation using field observations and results from a biophysical model. Journal of Hydrology **216**, 99-110.

Churchill, M.A., 1948. Discussion of Analyses and use of reservoir sedimentation data by L.C.Gottschalk, In Proceedings of the federal interagency sedimentation conference. US Geological Survey, Denver, Colorado, pp. 139-140.

Clark, R., 1994. Cumulative effects assessment: a tool for sustainable development. Impact assessment **12**, 319-331.

Clarkin, K., Conner, A., Furniss, M., Gibernick, B., Love, M., Moynan, K., Wilson, S., 2005. National inventory and assessment procedure for identifying barriers to aquatic organism passage at road-stream crossings. No. 7700, San Dimas, CA.

Cooper, L.M., Sheate, W.R., 2002. Cumulative effects assessment: A review of UK

environmental impact statements. Environmental Impact Assessment Review **22**, 415-439.

Cote, D., Kehler, D.G., Bourne, C., Wiersma, Y.F., 2009. A new measure of longitudinal connectivity for stream networks. Landscape Ecology **24**, 101-113.

Coutant, C.C., Whitney, R.R., 2000. Fish behavior in relation to passage through hydropower turbines: a review. Transactions Of The American Fisheries Society **129**, 351-380.

Crook, K.E., Pringle, C.M., Freeman, M.C., 2009. A method to assess longitudinal riverine connectivity in tropical streams dominated by migratory biota. Aquatic Conservation: Marine and Freshwater Ecosystems **19**, 714-723.

CWRC, 1992. Study on water and sediment inflow condition in Three Gorges Reservoir symposium. Hubei Science and Technology Press, Wuhan, China, 246 pp.

CWRC, 2002a. Bulletin of Changjiang Sediment. Press of Ministry of Water Resources of the People's Republic of China, Beijing.

CWRC, 2002b. Floods and Droughts in the Yangtze River Catchment. Water Conservancy and Water Electricity Press, Beijing, 326 pp.

CWRC, 2007a. Bulletin of changjiang Sediment. Press of Ministry of Water Resources of the People's Republic of China, Beijing.

CWRC, 2007b. Bulletin of Changjiang water and soil conservation. Changjiang (Yangtze) Water Resources Commission, Beijing.

CWRC, 2012. Hydrological data of Changjiang River Basin. Annual hydrological report of P.R. China, 6. Changjiang Water Resources Commission, Beijing.

Czerniawski, R., Domagala, J., Pilecka-Rapacz, M., Krepski, T., 2010. Impact of Small Dam on Changes of Fish Fauna in Sitna Stream During Period of Nine Years (Buffer Zone of Drawienski National Park). Rocznik Ochrona Srodowiska **12**, 235-247.

Dade, W.B., Renshaw, C.E., Magilligan, F.J., 2011. Sediment transport constraints on river response to regulation. Geomorphology **126**, 245-251.

Dai, D., Tan, Y., 1996. Soil erosion and sediment yield in the Upper Yangtze River basin. IAHS Publications-Series of Proceedings and Reports-Intern Assoc Hydrological Sciences **236**, 191-204.

Dai, H., Lei, X., Cao, S., Dai, Y., 2002. Study on the Reducing Sediment Effect of "Changzhi Project" in the Hill of Sichuan Basin, Proceedings 12th International Soil Conservation Organization Conference-Process of Soil

Erosion and Its Environment Effect. Tsinghua University Press, Beijing, pp. 649-656.

Dai, Q., Thibodeau, J., Williams, P.B., 1998. The river dragon has come!: The three gorges dam and the fate of China's Yangtze River and its people. ME Sharpe, New York, 240 pp.

Dai, S.B., Lu, X.X., Yang, S.L., Cai, A.M., 2008. A preliminary estimate of human and natural contributions to the decline in sediment flux from the Yangtze River to the East China Sea. Quaternary International **186**, 43-54.

Dai, S.B., Yang, S.L., Zhu, J., Gao, A., Li, P., 2005. The role of Lake Dongting in regulating the sediment budget of the Yangtze River. Hydrology and Earth System Sciences **9**, 692-698.

Dai, Z.J., Chu, A., Du, J.Z., Stive, M., Hong, Y., 2010. Assessment of extreme drought and human interference on baseflow of the Yangtze River. Hydrological Processes **24**, 749-757.

Dai, Z.J., Chu, A., Stive, M., Du, J.Z., Li, J.F., 2011. Is the Three Gorges Dam the cause behind the extremely low suspended sediment discharge into the Yangtze (Changjiang) Estuary of 2006? Hydrological Sciences Journal-journal Des Sciences Hydrologiques **56**, 1280-1288.

Dai, Z.J., Liu, J.T., 2013. Impacts of large dams on downstream fluvial sedimentation: An example of the Three Gorges Dam (TGD) on the Changjiang (Yangtze River). Journal of Hydrology **480**, 10-18.

de Vente, J., Poesen, J., 2005. Predicting soil erosion and sediment yield at the basin scale: Scale issues and semi-quantitative models. Earth-science Reviews **71**, 95-125.

de Vente, J., Poesen, J., Verstraeten, G., 2005. The application of semi-quantitative methods and reservoir sedimentation rates for the prediction of basin sediment yield in Spain. Journal of Hydrology **305**, 63-86.

Department of Environment (DOE), 1989. Environmental assessment: a guide to the procedures. HMSO, London.

DLNR, 2011. Atlas of the historical changes of the Dongting Lake. Hunan map publishing house, Department of Land and Natural Resources of Hunan Province, Changsha, China, 313 pp.

Döll, P., Fiedler, K., Zhang, J., 2009. Global-scale analysis of river flow alterations due to water withdrawals and reservoirs. Hydrology and Earth System Sciences **13**, 2413-2432.

Downing, J.A., Prairie, Y.T., Cole, J.J., Duarte, C.M., Tranvik, L.J., Striegl, R.G.,

McDowell, W.H., Kortelainen, P., Caraco, N.F., Melack, J.M., Middelburg, J.J., 2006. The global abundance and size distribution of lakes, ponds, and impoundments. Limnology And Oceanography **51**, 2388-2397.

Draut, A.E., Logan, J.B., Mastin, M.C., 2011. Channel evolution on the dammed Elwha River, Washington, USA. Geomorphology **127**, 71-87.

Driver, N.E., Troutman, B.M., 1989. Regression models for estimating urban storm-runoff quality and quantity in the United States. Journal of Hydrology **109**, 221-236.

Du, Y., Xue, H.-p., Wu, S.-j., Ling, F., Xiao, F., Wei, X.-h., 2011. Lake area changes in the middle Yangtze region of China over the 20th century. Journal Of Environmental Management **92**, 1248-1255.

Dudgeon, D., 2000. Large-Scale Hydrological Changes in Tropical Asia: Prospects for Riverine Biodiversity The construction of large dams will have an impact on the biodiversity of tropical Asian rivers and their associated wetlands. Bioscience **50**, 793-806.

Dudgeon, D., 2010. Requiem for a river: extinctions, climate change and the last of the Yangtze. Aquatic Conservation: Marine and Freshwater Ecosystems **20**, 127-131.

Dugan, P.J., Barlow, C., Agostinho, A.A., Baran, E., Cada, G.F., Chen, D., Cowx, I.G., Ferguson, J.W., Jutagate, T., Mallen-Cooper, M., 2010. Fish migration, dams, and loss of ecosystem services in the Mekong basin. Ambio **39**, 344-348.

Duinker, P.N., Greig, L.A., 2006. The impotence of cumulative effects assessment in Canada: ailments and ideas for redeployment. Environmental Management **37**, 153-161.

Dunham, J.B., Vinyard, G.L., Rieman, B.E., 1997. Habitat fragmentation and extinction risk of Lahontan cutthroat trout. North American Journal of Fisheries Management **17**, 1126-1133.

Dynesius, M., Nilsson, C., 1994. Fragmentation and flow regulation of river systems in the northern 3rd of the world. Science **266**, 753-762.

Eisma, D., 1998. Intertidal deposits: river mouths, tidal flats, and coastal lagoons, 16. CRC Press, Boca Raton, Florida, 544 pp.

Erős, T., Olden, J.D., Schick, R.S., Schmera, D., Fortin, M.-J., 2012. Characterizing connectivity relationships in freshwaters using patch-based graphs. Landscape Ecology **27**, 303-317.

Erskine, W.D., 1985. Downstream geomorphic imapcts of large dams - the case of Glenbawn Dam, NSW. Applied Geography **5**, 195-210.

Fang, J.Y., Rao, S., Zhao, S.Q., 2005. Human-induced long-term changes in the lakes the Jianghan Plain, Central Yangtze. Frontiers in Ecology and the Environment **3**, 186-192.

Fearnside, P.M., 2006. Dams in the Amazon: Belo Monte and Brazil's hydroelectric development of the Xingu River basin. Environmental Management **38**, 16-27.

Flitcroft, R., 2007. Regions to streams: spatial and temporal variation in stream occupancy patterns of Coho Salmon (Oncorhynchus kisutch) on the Oregon coast. PhD, Oregon State University, Corvallis, Oregon, 206 pp.

Forman, R.T., Alexander, L.E., 1998. Roads and their major ecological effects. Annual Review Of Ecology And Systematics, 207-231.

Freer, J., Beven, K., Ambroise, B., 1996. Bayesian estimation of uncertainty in runoff prediction and the value of data: An application of the GLUE approach. Water Resources Research **32**, 2161-2173.

Fu, B.J., Wu, B.F., Lue, Y.H., Xu, Z.H., Cao, J.H., Niu, D., Yang, G.S., Zhou, Y.M., 2010. Three Gorges Project: Efforts and challenges for the environment. Progress in Physical Geography **34**, 741-754.

Fu, C.Z., Wu, J.H., Chen, J.K., Qu, Q.H., Lei, G.C., 2003. Freshwater fish biodiversity in the Yangtze River basin of China: patterns, threats and

conservation. Biodiversity And Conservation **12**, 1649-1685.

Gangloff, M.M., Hartfield, E.E., Werneke, D.C., Feminella, J.W., 2011. Associations between small dams and mollusk assemblages in Alabama streams. Journal Of The North American Benthological Society **30**, 1107-1116.

Gao, B.C., 1996. NDWI - A normalized difference water index for remote sensing of vegetation liquid water from space. Remote Sensing Of Environment **58**, 257-266.

Gao, X., Zeng, Y., Wang, J., Liu, H., 2010. Immediate impacts of the second impoundment on fish communities in the Three Gorges Reservoir. Environmental Biology Of Fishes **87**, 163-173.

Garg, V., Asce, S.M., Jothiprakash, V., 2010. Modeling the Time Variation of Reservoir Trap Efficiency. Journal of Hydrologic Engineering **15**, 1001-1015.

Gemmer, M., 2003. GIS/RS-based flood risk mapping for the eastern Honghu flood diversion area. Journal of Lake Sciences **15**, 166-170.

Gill, M.A., 1979. Sedimentation and useful life of reservoirs. Journal of Hydrology **44**, 89-95.

Gilpin, A., 1995. Environmental impact assessment (EIA): cutting edge for the twenty-first century. Cambridge University Press, 200 pp.

Gleick, P.H., 1992. Environmental consequences of hydroelectric development: the role of facility size and type. Energy **17**, 735-747.

Gleick, P.H., 1998. The World's Water: The Biennial Report on Freshwater Resources 1998-1999. Pacific Institute for Studies in Development, Environment, and Security, Washington DC, Covelo, California.

Gowans, A., Armstrong, J., Priede, I., 1999. Movements of adult Atlantic salmon in relation to a hydroelectric dam and fish ladder. Journal Of Fish Biology **54**, 713-726.

Graf, W.L., 1999. Dam nation: A geographic census of American dams and their large-scale hydrologic impacts. Water Resources Research **35**, 1305-1311.

Graf, W.L., 2006. Downstream hydrologic and geomorphic effects of large dams on American rivers. Geomorphology **79**, 336-360.

Graf, W.L., Wohl, E., Sinha, T., Sabo, J.L., 2010. Sedimentation and sustainability of western American reservoirs. Water Resources Research **46**, W12535.

Grant, C.E.H., Lowe, W.H., Fagan, W.F., 2007. Living in the branches: population dynamics and ecological processes in dendritic networks. Ecology Letters **10**, 165-175.

Gray, D.J., Thrift, A.P., Williams, G.M., Zheng, F., Li, Y.S., Guo, J.G., Chen, H.G.,

Wang, T.P., Xu, X.J., Zhu, R., Zhu, H.Q., Cao, C.L., Lin, D.D., Zhao, Z.Y., Li, R.S., Davis, G.M., McManus, D.P., 2012. Five-year longitudinal assessment of the downstream impact on schistosomiasis transmission following closure of the Three Gorges Dam. Plos Neglected Tropical Diseases **6**, e1588.

Greenlee, D.D., 1987. Raster and vector processing for scanned linework. Photogrammetric Engineering And Remote Sensing **53**, 1383-1387.

Grill, G., Ouellet Dallaire, C., Fluet Chouinard, E., Sindorf, N., Lehner, B., 2014. Development of new indicators to evaluate river fragmentation and flow regulation at large scales: A case study for the Mekong River Basin. Ecological Indicators **45**, 148-159.

Groves, C.R., Jensen, D.B., Valutis, L.L., Redford, K.H., Shaffer, M.L., Scott, J.M., Baumgartner, J.V., Higgins, J.V., Beck, M.W., Anderson, M.G., 2002. Planning for Biodiversity Conservation: Putting Conservation Science into Practice A seven-step framework for developing regional plans to conserve biological diversity, based upon principles of conservation biology and ecology, is being used extensively by the nature conservancy to identify priority areas for conservation. Bioscience **52**, 499-512.

Grumbine, R.E., Pandit, M.K., 2013. Threats from India's Himalaya dams. Science **339**, 36-37.

Grumbine, R.E., Xu, J., 2011. Mekong hydropower development. Science **332**, 178-179.

Gupta, A., 1998. Ecology and development in the Third World. Psychology Press, 125 pp.

Gupta, A., 2008. Large rivers: geomorphology and management. John Wiley & Sons, West Sussex, England, 712 pp.

Gupta, A., 2009. Geology and landforms of the Mekong Basin. In: I. Campbell (Ed.), The Mekong Biophysical Environment of an International River Basin. Academic Press, San Diego, CA, pp. 29-51.

Gupta, A., Hock, L., Xiaojing, H., Ping, C., 2002. Evaluation of part of the Mekong River using satellite imagery. Geomorphology **44**, 221-239.

Gupta, A., Krishnan, P., 1994. Spatial distribution of sediment discharge to the coastal waters of South and Southeast Asia. IAHS Publications-Series of Proceedings and Reports-Intern Assoc Hydrological Sciences **224**, 457-464.

Gupta, A., Liew, S.C., 2007. The Mekong from satellite imagery: a quick look at a large river. Geomorphology **85**, 259-274.

Haan, C.T., Barfield, B.J., Hayes, J.C., 1994. Design hydrology and sedimentology for small catchments Academic Press, San Diego, 588 pp.

Harris, J., Zhuang, H., 2010. An ecosystem approach to resolving conflicts among ecological and economic priorities for Poyang Lake wetlands, Wetlands International – IUCN SSC Crane Specialist Group, Gland, Switzerland.

Harvey, B., Railsback, S., 2012. Effects of passage barriers on demographics and stability properties of a virtual trout population. River Research and Applications **28**, 479-489.

Hassan, M.A., Church, M., Yan, Y., Slaymaker, O., 2010. Spatial and temporal variation of in-reach suspended sediment dynamics along the mainstem of Changjiang (Yangtze River), China. Water Resources Research **46**, W11551.

Hawley, M.E., McCuen, R.H., 1982. Water yield estimation in western United States. Journal of the irrigation and drainage division **108**, 25-34.

Heinemann, H.G., 1981. A new sediment trap efficiency curve for small reservoirs. Water Resources Bulletin **17**, 825-830.

Heiner, M., Higgins, J., Li, X., Baker, B., 2011. Identifying freshwater conservation priorities in the Upper Yangtze River Basin. Freshwater Biology **56**, 89-105.

Higgins, J.V., Bryer, M.T., Khoury, M.L., Fitzhugh, T.W., 2005. A freshwater classification approach for biodiversity conservation planning. Conservation Biology **19**, 432-445.

Hoef, J.M., Peterson, E., Theobald, D., 2006. Spatial statistical models that use flow and stream distance. Environmental And Ecological Statistics **13**, 449-464.

Horton, R.E., 1945. Erosional development of streams and their drainage basins: hydro-physical approach to quantitative morphology. Geological Society Of America Bulletin **56**, 275-310.

Hrachowitz, M., Savenije, H., Blöschl, G., McDonnell, J., Sivapalan, M., Pomeroy, J., Arheimer, B., Blume, T., Clark, M., Ehret, U., 2013. A decade of Predictions in Ungauged Basins (PUB)—a review. Hydrological sciences journal **58**, 1198-1255.

Hsu, K.l., Gupta, H.V., Sorooshian, S., 1995. Artificial Neural Network Modeling of the Rainfall‐Runoff Process. Water Resources Research **31**, 2517-2530.

Huang, D.F., Yang, S.Z., Liu, Z.Q., Mei, Z.Y., 1965. Geological studies of the formation and development of the three large freshwater lakes in the Lower Yangtze Valley. Oceanologia et Limnologia Sinica **7**, 396-423.

Huang, H., Yan, Z., 2009. Present situation and future prospect of hydropower in China. Renewable and Sustainable Energy Reviews **13**, 1652-1656.

Hughes, D., Mantel, S., 2010. Estimating the uncertainty in simulating the impacts of small farm dams on streamflow regimes in South Africa. Hydrological

Sciences Journal–Journal des Sciences Hydrologiques **55**, 578-592.

Hupp, C.R., Schenk, E.R., Richter, J.M., Peet, R.K., Townsend, P.A., 2009. Bank erosion along the dam-regulated lower Roanoke River, North Carolina. Geological Society of America Special Papers **451**, 97-108.

ICOLD, 2011. World register of dams. International Commission on Large Dams, Paris.

ILEC, 1988-1993. Survey of the State of World's Lakes. International Lake Environment Committee, Otsu, Japan.

IWHR, YSRI, 1990. Preliminary report on the bed erosion processes downstream of the Three Gorges Reservoir, Institute of Water Resources and Hydropower Research (IWHR) and Yangtze River Scientific Research Institute (YSRI), Beijing, China.

Jager, H.I., Chandler, J.A., Lepla, K.B., Van Winkle, W., 2001. A theoretical study of river fragmentation by dams and its effects on white sturgeon populations. Environmental Biology Of Fishes **60**, 347-361.

Jager, H.I., McManamay, R.A., 2014. Comment on "Cumulative biophysical impact of small and large hydropower development in Nu River, China". Water Resources Research **50**, WR014378.

Jiang, T., Su, B., Hartmann, H., 2007. Temporal and spatial trends of precipitation and river flow in the Yangtze River Basin, 1961–2000. Geomorphology **85**, 143-154.

Johnson, L.B., Host, G.E., 2010. Recent developments in landscape approaches for the study of aquatic ecosystems. Journal Of The North American Benthological Society **29**, 41-66.

Jones, K.L., Poole, G.C., O'Daniel, S.J., Mertes, L.A., Stanford, J.A., 2008. Surface hydrology of low-relief landscapes: Assessing surface water flow impedance using LIDAR-derived digital elevation models. Remote Sensing Of Environment **112**, 4148-4158.

Jothiprakash, V., Garg, V., 2008. Re-look to conventional techniques for trapping efficiency estimation of a reservoir. International Journal of Sediment Research **23**, 76-84.

Kalff, J., 2001. Limnology: Inland water ecosystems. Prentice Hall, New Jersey, 592 pp.

Kalitsi, E., 2003. Problems and prospects for hydropower development in Africa, Report prepared for the Workshop for African Energy Experts on Operationalizing the NEPAD Energy Initiative, pp. 2-4.

Kanno, Y., Russ, W.T., Sutherland, C.J., Cook, S.B., 2012. Prioritizing aquatic conservation areas using spatial patterns and partitioning of fish community diversity in a near‑natural temperate basin. Aquatic Conservation: Marine and Freshwater Ecosystems **22**, 799-812.

Keefer, M.L., Peery, C.A., Bjornn, T.C., Jepson, M.A., Stuehrenberg, L.C., 2004. Hydrosystem, dam, and reservoir passage rates of adult Chinook salmon and steelhead in the Columbia and Snake rivers. Transactions Of The American Fisheries Society **133**, 1413-1439.

Keiser, J., de Castro, M.C., Maltese, M.F., Bos, R., Tanner, M., Singer, B.H., Utzinger, J., 2005. Effect of irrigation and large dams on the burden of malaria on a global and regional scale. The American journal of tropical medicine and hygiene **72**, 392-406.

Kibler, K.M., Tullos, D.D., 2013. Cumulative biophysical impact of small and large hydropower development in Nu River, China. Water Resources Research **49**, 3104-3118.

King, J., Cambray, J.A., Impson, N.D., 1998. Linked effects of dam-released floods and water temperature on spawning of the Clanwilliam yellowfish Barbus capensis. Hydrobiologia **384**, 245-265.

Klunne, W.J., 2007. Small hydropower development in Africa. ESI Africa **2**, 36-37.

Kondolf, G.M., 1997. Hungry water: Effects of dams and gravel mining on river channels. Environmental Management **21**, 533-551.

Kondolf, G.M., Curry, R.R., 1986. Channel erosion along the Carmel River, Monterey County, California. Earth Surface Processes and Landforms **11**, 307-319.

Kucukali, S., Baris, K., 2009. Assessment of small hydropower (SHP) development in Turkey: Laws, regulations and EU policy perspective. Energy Policy **37**, 3872-3879.

Kummu, M., Lu, X.X., Wang, J.J., Varis, O., 2010. Basin-wide sediment trapping efficiency of emerging reservoirs along the Mekong. Geomorphology **119**, 181-197.

Kummu, M., Varis, O., 2007. Sediment-related impacts due to upstream reservoir trapping, the Lower Mekong River. Geomorphology **85**, 275-293.

Labadie, J.W., 2004. Optimal operation of multireservoir systems: State-of-the-art review. Journal Of Water Resources Planning And Management-asce **130**, 93-111.

Lai, X., Jiang, J., Yang, G., Lu, X., 2014. Should the Three Gorges Dam be blamed for the extremely low water levels in the middle–lower Yangtze River? Hydrological Processes **28**, 150-160.

Leeden, F., Torise, F., Todd, D., 1990. The Water Encyclopedia. CRC, Chelsea, Mich., 808 pp.

Lehner, B., Doll, P., 2004. Development and validation of a global database of lakes, reservoirs and wetlands. Journal of Hydrology **296**, 1-22.

Lehner, B., Liermann, C.R., Revenga, C., Voeroesmarty, C., Fekete, B., Crouzet, P., Doell, P., Endejan, M., Frenken, K., Magome, J., Nilsson, C., Robertson, J.C., Roedel, R., Sindorf, N., Wisser, D., 2011. High-resolution mapping of the world's reservoirs and dams for sustainable river-flow management. Frontiers in Ecology and the Environment **9**, 494-502.

Lessard, J.L., Hayes, D.B., 2003. Effects of elevated water temperature on fish and macroinvertebrate communities below small dams. River Research and Applications **19**, 721-732.

Liang, Y.-S., Wang, W., Li, H.-J., Shen, X.-H., Xu, Y.-L., Dai, J.-R., 2012. The South-to-North Water Diversion Project: effect of the water diversion pattern on transmission of Oncomelania hupensis, the intermediate host of Schistosoma japonicum in China. Parasit Vectors **5**, 52.

Liebe, J., van de Giesen, N., Andreini, M., 2005. Estimation of small reservoir storage capacities in a semi-arid environment - A case study in the Upper East Region of Ghana. Physics and Chemistry of the Earth **30**, 448-454.

Liermann, C.R., Nilsson, C., Robertson, J., Ng, R.Y., 2012. Implications of dam obstruction for global freshwater fish diversity. Bioscience **62**, 539-548.

Lin, P.C., Brosse, S., Gao, X., Liu, C.C., Liu, H.Z., 2013. Species composition and temporal pattern of fish passing through the navigation locks in the middle reach of Yangtze River: implications for fish conservation. Journal Of Applied Ichthyology **29**, 1441-1444.

Liu, C., Sui, J., Wang, Z.-Y., 2008. Sediment load reduction in Chinese rivers. International Journal of Sediment Research **23**, 44-55.

Liu, C., Zheng, H., 2002. South-to-north water transfer schemes for China. International Journal of Water Resources Development **18**, 453-471.

Liu, H., He, Q., Wang, Z.B., Weltje, G.J., Zhang, J., 2010. Dynamics and spatial variability of near-bottom sediment exchange in the Yangtze Estuary, China. Estuarine Coastal and Shelf Science **86**, 322-330.

Liu, J., Yang, S., Zhu, Q., Zhang, J., 2014. Controls on suspended sediment concentration profiles in the shallow and turbid Yangtze Estuary. Continental Shelf Research **90**, 96-108.

Liu, X., Wang, H., 2010. Estimation of minimum area requirement of river-connected lakes for fish diversity conservation in the Yangtze River floodplain. Diversity

and Distributions **16**, 932-940.

Ljung, P., Head, C., Sunman, H., 2000. Trends in the Financing of Water and Energy Resources Projects, World Commission on Dams, Cape Town, South Africa.

Lu, J.Y., 2002. Research on impact of downstream river channel scouring of TGP on bank revetment works. Yangtze River **33**, 23-25.

Lu, X.X., 2005. Spatial variability and temporal change of water discharge and sediment flux in the Lower Jinsha tributary: Impact of environmental changes. River Research and Applications **21**, 229-243.

Lu, X.X., Ashmore, P., Wang, J., 2003a. Sediment yield mapping in a large river basin: the Upper Yangtze, China. Environmental Modelling & Software **18**, 339-353.

Lu, X.X., Ashmore, P., Wang, J.F., 2003b. Seasonal water discharge and sediment load changes in the Upper Yangtze, China. Mountain Research and Development **23**, 56-64.

Lu, X.X., Higgitt, D.L., 1998. Recent changes of sediment yield in the Upper Yangtze, China. Environmental Management **22**, 697-709.

Lu, X.X., Higgitt, D.L., 1999. Sediment yield variability in the Upper Yangtze, China. Earth Surface Processes and Landforms **24**, 1077-1093.

Lu, X.X., Ran, L.S., Liu, S., Zhang, S.R., Wang, J.J., 2013. Sediment load response to climate change: A preliminary study of eight large Chinese rivers. International Journal of Sediment Research **28**, 1-14.

Lu, X.X., Siew, R.Y., 2006. Water discharge and sediment flux changes over the past decades in the Lower Mekong River: possible impacts of the Chinese dams. Hydrology and Earth System Sciences **10**, 181-195.

Lu, X.X., Yang, X.K., Li, S.Y., 2011. Dam not sole cause of Chinese drought. Nature **475**, 174-174.

Lu, X.X., Zhang, S.R., Jiang, T., Xiong, M., 2010. Sediment loads in the lower Jinshajiang of the Yangtze River: current status and potential impacts of the cascade dams. Sediment Dynamics for a Changing Future **337**, 113-120.

Luo, X., Yang, S., Zhang, J., 2012. The impact of the Three Gorges Dam on the downstream distribution and texture of sediments along the middle and lower Yangtze River (Changjiang) and its estuary, and subsequent sediment dispersal in the East China Sea. Geomorphology **179**, 126-140.

Ma, R., Duan, H., Hu, C., Feng, X., Li, A., Ju, W., Jiang, J., Yang, G., 2010. A half-century of changes in China's lakes: Global warming or human influence? Geophysical Research Letters **37**, L24106.

Ma, Z., Becker, D.R., Kilgore, M.A., 2009. Assessing cumulative impacts within state environmental review frameworks in the United States. Environmental Impact Assessment Review **29**, 390-398.

Magilligan, F.J., Nislow, K.H., 2005. Changes in hydrologic regime by dams. Geomorphology **71**, 61-78.

Mantel, S.K., Hughes, D.A., Muller, N.W., 2010. Ecological impacts of small dams on South African rivers Part 1: drivers of change-water quantity and quality. Water Sa **36**, 351-360.

Mao, W., Pang, Q., Fu, L., 2001. Effects and Countermeasures of Water Loss on Water Quality of Dongping Lake. Bulletin of Soil and Water Conservation **21**, 27-29.

Marks, J.C., 2007. Down go the dams. Scientific American **296**, 66-71.

Martin, E.H., Apse, C.D., 2011. Northeast aquatic connectivity an assessment of dams on northeastern rivers, The Nature Conservancy, Eastern Freshwater Program, Brunswick, Maine.

Martinuzzi, S., Gould, W.A., González, O.M.R., 2007. Creating Cloud-Free Landsat ETM+ Data Sets in Tropical Landscapes: Cloud and Cloud-Shadow Removal, United States Department of Agriculture, Rio Piedras.

McCully, P., 2001. Silenced Rivers: The Ecology and Politics of Large Dams. St. Martin's Press, New York, 416 pp.

McKay, S.K., Schramski, J.R., Conyngham, J.N., Fischenich, J.C., 2013. Assessing upstream fish passage connectivity with network analysis. Ecological Applications **23**, 1396-1409.

McManus, D.P., Gray, D.J., Li, Y.S., Feng, Z., Williams, G.M., Stewart, D., Rey-Ladino, J., Ross, A.G., 2010. Schistosomiasis in the People's Republic of China: the Era of the Three Gorges Dam. Clinical Microbiology Reviews **23**, 442-466.

Meigh, J., 1995. The impact of small farm reservoirs on urban water supplies in Botswana. Natural Resources Forum **19**, 71-83.

Meybeck, M., 1995. Global distribution of lakes. In: L. Abraham, M.I. Dieter, R.G. Joel (Eds.), Physics and chemistry of lakes. Springer, Berlin, pp. 1-35.

Mialhe, F., Gunnell, Y., Mering, C., 2008. Synoptic assessment of water resource variability in reservoirs by remote sensing: General approach and application to the runoff harvesting systems of south India. Water Resources Research **44**, W05411.

Milliman, J.D., 1993. Production and accumulation of calcium carbonate in the ocean:

Budget of a nonsteady state. Global Biogeochemical Cycles **7**, 927-957.

Milliman, J.D., 1997. Oceanography - Blessed dams or damned dams? Nature **386**, 325-325.

Milliman, J.D., Meade, R.H., 1983. World-wide delivery of river sediment to the oceans. Journal of Geology **91**, 1-21.

Milliman, J.D., Syvitski, J.P.M., 1992. Geomorphic tectonic control of sediment discharge to the ocean - the importance of small mountainous rivers. Journal of Geology **100**, 525-544.

Minear, J.T., Kondolf, G.M., 2009. Estimating reservoir sedimentation rates at large spatial and temporal scales: A case study of California. Water Resources Research **45**, W12502.

Mo, Y., 1988. Work narration about the Wujiang River basin planning. Quarterly of Changjiang River Annals **1**, 16-18.

Moore, M.K., Archdekin, G.C., 1980. Streamside Management: A Decision-making Procedure for South Coastal British Columbia. Land Management Handbook Volume 1. Information Services Branch, Ministry of Forests, Province of British Columbia, Victoria, BC, 689 pp.

Morris, G., Fan, J., 1998. Reservoir Sedimentation Handbook. McGraw-Hill, New

York, 805 pp.

Morris, G.L., Annandale, G., Hotchkiss, R., 2008. Reservoir sedimentation. Sedimentation Engineering: Processes, Measurements, Modeling, and Practice. ASCE Publications, 1132 pp.

MSSL, UNEP, W., 1998. Global Lake and Catchment Conservation Database. In: M.S.S. Laboratory (Ed.), Surrey, UK.

Mungwena, W., 2002. Hydropower development on Zimbabwe's major dams. Reneable Energy **25**, 455-462.

MWR, 1982. Map of spatial distribution of hydropower resources in China. China Water Power Press, Beijing.

MWR, 1990. China Water Statistical Yearbook. China Water Power Press, Beijing.

MWR, 1998. Standard of the People's Republic of China: Code for China Lake Name. China Water Power Press, Beijing.

MWR, 2009. China Water Statistical Yearbook. China Water Power Press, Beijing.

MWR, 2011. Yangtze River and regional development, The 4th Yangtze Forum. Changjiang Water Resources Commission, Nanjing, China.

National Bureau of Statistics of China, 1993. China Statistical Yearbook. China

Statistics Press, Beijing.

Neraas, L.P., Spruell, P., 2001. Fragmentation of riverine systems: the genetic effects of dams on bull trout (Salvelinus confluentus) in the Clark Fork River system. Molecular Ecology **10**, 1153-1164.

Nilsson, C., Reidy, C.A., Dynesius, M., Revenga, C., 2005. Fragmentation and flow regulation of the world's large river systems. Science **308**, 405-408.

Ohunakin, O.S., Ojolo, S.J., Ajayi, O.O., 2011. Small hydropower (SHP) development in Nigeria: An assessment. Renewable and Sustainable Energy Reviews **15**, 2006-2013.

Omang, R., Parrett, C., 1984. A method for estimating mean annual runoff of ungaged streams based on basin characteristics in central and eastern Montana. No. 84-4143, US Geological Survey.

Park, Y.S., Chang, J.B., Lek, S., Cao, W.X., Brosse, S., 2003. Conservation strategies for endemic fish species threatened by the Three Gorges Dam. Conservation Biology **17**, 1748-1758.

Peterson, E.E., Theobald, D.M., VER HOEF, J.M., 2007. Geostatistical modelling on stream networks: developing valid covariance matrices based on hydrologic distance and stream flow. Freshwater Biology **52**, 267-279.

Phillips, J.D., Slattery, M.C., Musselman, Z.A., 2005. Channel adjustments of the lower Trinity River, Texas, downstream of Livingston Dam. Earth Surface Processes and Landforms **30**, 1419-1439.

Poff, N.L., Olden, J.D., Merritt, D.M., Pepin, D.M., 2007. Homogenization of regional river dynamics by dams and global biodiversity implications. Proceedings of the National Academy of Sciences **104**, 5732-5737.

Power, M.E., Dietrich, W.E., Finlay, J.C., 1996. Dams and downstream aquatic biodiversity: potential food web consequences of hydrologic and geomorphic change. Environmental Management **20**, 887-895.

Qiu, J., 2012. Yangtze finless porpoises in peril. Nature, doi:10.1038/nature.2012.12125.

Radoane, M., Radoane, N., 2005. Dams, sediment sources and reservoir silting in Romania. Geomorphology **71**, 112-125.

Railsback, S.F., Harvey, B.C., Jackson, S.K., Lambersonm, R.H., 2009. InSTREAM: the individual-based stream trout research and environmental assessment model, California.

Ran, L.S., Lu, X.X., 2012. Delineation of reservoirs using remote sensing and their storage estimate: an example of the Yellow River basin, China. Hydrological

Processes **26**, 1215-1229.

Ran, L.S., Lu, X.X., Xin, Z.B., Yang, X.K., 2013. Cumulative sediment trapping by reservoirs in large river basins: A case study of the Yellow River basin. Global and Planetary Change **100**, 308-319.

Reed, R.A., Johnson, B.J., Baker, W.L., 1996. Contribution of roads to forest fragmentation in the Rocky Mountains. Conservation Biology **10**, 1098-1106.

Renwick, W.H., Sleezer, R.O., Buddemeier, R.W., Smith, S.V., 2006. Small artifical ponds in the United States: Impacts on sedimentation and carbon budget, Proceedings of the Eighth Federal Interagency Sedimentation Conference. USGS, Reno, NV, pp. 738-744.

Restrepo, J.D., Kjerfve, B., Hermelin, M., Restrepo, J.C., 2006. Factors controlling sediment yield in a major South American drainage basin: the Magdalena River, Colombia. Journal of Hydrology **316**, 213-232.

Revenga, C., Campbell, I., Abell, R., De Villiers, P., Bryer, M., 2005. Prospects for monitoring freshwater ecosystems towards the 2010 targets. Philosophical Transactions of the Royal Society B: Biological Sciences **360**, 397-413.

Rhoads, B.L., Kenworthy, S.T., 1995. Flow structure at an asymmetrical stream confluence. Geomorphology **11**, 273-293.

Rice, S., Roy, A., Rhoads, B., 2008. River confluences, tributaries and the fluvial network. John Wiley & Sons, West Sussex, England, 457 pp.

Richter, B.D., Thomas, G.A., 2007. Restoring environmental flows by modifying dam operations. Ecology and Society **12**, 12.

Rosenberg, D.M., McCully, P., Pringle, C.M., 2000. Global-scale environmental effects of hydrological alterations: introduction. Bioscience **50**, 746-751.

Ryanzhin, S.V., Straskraba, M., Geller, W., 2001. Developing WORLDLAKE: database and GIS for limnological studies, Proceedings of the Ninth International Conference on the Conservation and Management of Lakes. ILEC Publications, Otsu, Japan, pp. 25-28.

Saito, Y., Yang, Z.S., Hori, K., 2001. The Huanghe (Yellow River) and Changjiang (Yangtze River) deltas: a review on their characteristics, evolution and sediment discharge during the Holocene. Geomorphology **41**, 219-231.

Sauquet, E., 2006. Mapping mean annual river discharges: geostatistical developments for incorporating river network dependencies. Journal of Hydrology **331**, 300-314.

Sawunyama, T., Senzanje, A., Mhizha, A., 2006. Estimation of small reservoir storage capacities in Limpopo River Basin using geographical information systems

(GIS) and remotely sensed surface areas: Case of Mzingwane catchment. Physics and Chemistry of the Earth **31**, 935-943.

Scaramuzza, P., Micijevic, E., Chander, G., 2004. SLC gap-filled products phase one methodology. Landsat Technical Notes. U.S. Geological Survey.

Schilt, C.R., 2007. Developing fish passage and protection at hydropower dams. Applied Animal Behaviour Science **104**, 295-325.

Shankman, D., Liang, Q., 2003. Landscape changes and Increasing flood frequency in China's Poyang Lake region. The Professional Geographer **55**, 434-445.

Sharma, N.K., Tiwari, P.K., Sood, Y.R., 2013. A comprehensive analysis of strategies, policies and development of hydropower in India: Special emphasis on small hydro power. Renewable and Sustainable Energy Reviews **18**, 460-470.

Shi, C.X., Wang, X., 1989. Introduction to Chinese Lakes. Science Press, Beijing,China.

Shi, X., Xia, W., Yang, B., 1999. Sediment Deposition and Erosion in Dongting Lake (1956- 1995). Journal of Lake Sciences **11**, 205-211.

Shields, F.D., Simon, A., Steffen, L.J., 2000. Reservoir effects on downstream river channel migration. Environmental Conservation **27**, 54-66.

Sidjak, R., 1999. Glacier mapping of the Illecillewaet icefield, British Columbia, Canada, using Landsat TM and digital elevation data. International Journal Of Remote Sensing **20**, 273-284.

Sindorf, N., Wickel, A.J., 2011. Connectivity and fragmentation:Hydrospatial analysis of dam development in the Mekong River Basin, World Wildlife Fund, Washington DC.

Singer, E.E., Gangloff, M.M., 2011. Effects of a small dam on freshwater mussel growth in an Alabama (USA) stream. Freshwater Biology **56**, 1904-1915.

Sivapalan, M., 2005. Pattern, process and function: elements of a unified theory of hydrology at the catchment scale. In: M.G. Anderson (Ed.), Encyclopedia of hydrological sciences. John Wiley, Hoboken, N.J., pp. 193-219.

Smith, J., Eli, R.N., 1995. Neural-network models of rainfall-runoff process. Journal of water resources planning and management **121**, 499-508.

Smith, S.V., Renwick, W.H., Bartley, J.D., Buddemeier, R.W., 2002. Distribution and significance of small, artificial water bodies across the United States landscape. Science Of The Total Environment **299**, 21-36.

Snelder, T.H., Cattanéo, F., Suren, A.M., Biggs, B.J., 2004. Is the River Environment Classification an improved landscape-scale classification of rivers? Journal Of

The North American Benthological Society **23**, 580-598.

Spens, J., Englund, G., Lundqvist, H., 2007. Network connectivity and dispersal barriers: using geographical information system (GIS) tools to predict landscape scale distribution of a key predator (Esox lucius) among lakes. Journal Of Applied Ecology **44**, 1127-1137.

Stanley, D.J., Warne, A.G., 1993. Nile delta - recent geological evolution and human impact. Science **260**, 628-634.

Stone, R., 2011. The Legacy of the Three Gorges Dam. Science **333**, 817-817.

Storm, B., Høgh, J.K., Refsgaard, J., 1989. Estimation of catchment rainfall uncertainty and its influence on runoff prediction. Nordic Hydrology **19**, 77-88.

Strahler, A.N., 1952. Hypsometric (area-altitude) analysis of erosional topography. Geological Society Of America Bulletin **63**, 1117-1142.

Sundborg, A., 1992. Lake and reservoir sedimentation prediction and interpretation. Geografiska Annaler Series A-physical Geography **74**, 93-100.

Syvitski, J.P.M., Kettner, A.J., Overeem, I., Hutton, E.W.H., Hannon, M.T., Brakenridge, G.R., Day, J., Vörösmarty, C., Saito, Y., Giosan, L., Nicholls, R.J., 2009. Sinking deltas due to human activities. Nature Geoscience **2**,

681-686.

Syvitski, J.P.M., Milliman, J.D., 2007. Geology, geography, and humans battle for dominance over the delivery of fluvial sediment to the coastal ocean. Journal of Geology **115**, 1-19.

Syvitski, J.P.M., Vörösmarty, C.J., Kettner, A.J., Green, P., 2005. Impact of humans on the flux of terrestrial sediment to the global coastal ocean. Science **308**, 376-380.

Tang, C., Zhu, J., Liang, J., 2009. Emergency assessment of seismic landslide susceptibility: a case study of the 2008 Wenchuan earthquake affected area. Earthquake Engineering and Engineering Vibration **8**, 207-217.

Tang, S., Xie, X., 1994. The Exploration on the Causes of Geotectonic to Form the Regularity of Distribution of the Mountain Cal amity Landforms Surrounding Sichuan Basin. Journal of Soil Erosion and Soil and Water Conservation **8**, 76-84.

Taylor, W.W., Schechter, M.G., Wolfson, L.G., 2007. Globalization: Effects on fisheries resources. Cambridge University Press, Cambridge, UK, 574 pp.

Tesfahunegn, G.B., Vlek, P.L.G., 2013. Assessing Sediment-Nutrient Export Rate and Soil Degradation in Mai-Negus Catchment, Northern Ethiopia. ISRN Soil

Science **2013**, 748561.

Thoni, R., Holcomb, J., Nichols, R., Gangloff, M.M., 2014. Effects of Small Dams on Sunfish Assemblages in North Carolina Piedmont and Coastal Plain Streams. Transactions Of The American Fisheries Society **143**, 97-103.

Tiessen, K., Elliott, J., Stainton, M., Yarotski, J., Flaten, D., Lobb, D., 2011. The effectiveness of small-scale headwater storage dams and reservoirs on stream water quality and quantity in the Canadian Prairies. Journal Of Soil And Water Conservation **66**, 158-171.

Tokar, A.S., Johnson, P.A., 1999. Rainfall-runoff modeling using artificial neural networks. Journal of Hydrologic Engineering **4**, 232-239.

Topping, D.J., Rubin, D.M., Vierra, L.E., 2000. Colorado River sediment transport - 1. Natural sediment supply limitation and the influence of Glen Canyon Dam. Water Resources Research **36**, 515-542.

Tucker, C.J., 1979. Red and photographic infrared linear combinations for monitoring vegetation. Remote Sensing Of Environment **8**, 127-150.

Tullos, D., 2009. Assessing the influence of environmental impact assessments on science and policy: An analysis of the Three Gorges Project. Journal Of Environmental Management **90**, S208-S223.

Urban, D., Keitt, T., 2001. Landscape connectivity: a graph-theoretic perspective. Ecology **82**, 1205-1218.

Van Rompaey, A., Bazzoffi, P., Jones, R.J.A., Montanarella, L., 2005. Modeling sediment yields in Italian catchments. Geomorphology **65**, 157-169.

Verstraeten, G., Poesen, J., 2000. Estimating trap efficiency of small reservoirs and ponds: methods and implications for the assessment of sediment yield. Progress in Physical Geography **24**, 219-251.

Viglione, A., Parajka, J., Rogger, M., Salinas, J., Laaha, G., Sivapalan, M., Blöschl, G., 2013. Comparative assessment of predictions in ungauged basins–Part 3: Runoff signatures in Austria. Hydrology and Earth System Sciences **17**, 2263-2279.

Vinson, M.R., 2001. Long-term dynamics of an invertebrate assemblage downstream from a large dam. Ecological Applications **11**, 711-730.

Vogel, R.M., Wilson, I., 1996. Probability distribution of annual maximum, mean, and minimum streamflows in the united states. Journal of Hydrologic Engineering **1**, 69-76.

Vogel, R.M., Wilson, I., Daly, C., 1999. Regional regression models of annual streamflow for the United States. Journal of Irrigation and Drainage

Engineering **125**, 148-157.

Vörösmarty, C.J., Meybeck, M., Fekete, B., Sharma, K., Green, P., Syvitski, J.P.M., 2003. Anthropogenic sediment retention: major global impact from registered river impoundments. Global and Planetary Change **39**, 169-190.

Vörösmarty, C.J., Sharma, K.P., Fekete, B.M., Copeland, A.H., Holden, J., Marble, J., Lough, J.A., 1997. The storage and aging of continental runoff in large reservoir systems of the world. Ambio **26**, 210-219.

Walling, D., Fang, D., 2003. Recent trends in the suspended sediment loads of the world's rivers. Global and Planetary Change **39**, 111-126.

Walling, D.E., 1983. The sediment delivery problem. Journal of Hydrology **65**, 209-237.

Walling, D.E., 1999. Linking land use, erosion and sediment yields in river basins. Hydrobiologia **410**, 223-240.

Walling, D.E., 2006. Human impact on land-ocean sediment transfer by the world's rivers. Geomorphology **79**, 192-216.

Walling, D.E., 2012. The role of dams in the global sediment budget. Erosion and Sediment Yields in the Changing Environment **356**, 3-11.

Wang, D.-y., Ma, W., Niu, Y.-h., Chang, X.-x., Wen, Z., 2007a. Effects of cyclic freezing and thawing on mechanical properties of Qinghai–Tibet clay. Cold Regions Science And Technology **48**, 34-43.

Wang, G., Hu, H., Li, T., 2009a. The influence of freeze–thaw cycles of active soil layer on surface runoff in a permafrost watershed. Journal of Hydrology **375**, 438-449.

Wang, H., Yang, Z., Saito, Y., Liu, J.P., Sun, X., Wang, Y., 2007b. Stepwise decreases of the Huanghe (Yellow River) sediment load (1950-2005): Impacts of climate change and human activities. Global and Planetary Change **57**, 331-354.

Wang, S., Dou, H., 1998. Chinese Lake Catalogue. Science Press, Beijing.

Wang, S.R., Jin, X.C., Zhao, H.C., F.C., W., 2006. Phosphorus fractions and its release in the sediments from the shallow lakes in the middle and lower reaches of Yangtze River area in China. Colloids and Surface A **273**, 109-116.

Wang, W., Dai, J., Liang, Y., Huang, Y., Coles, G., 2009b. Impact of the South-to-North Water Diversion Project on the transmission of Schistosoma japonicum in China. Annals Of Tropical Medicine And Parasitology **103**, 17-29.

Wang, Y., Xia, Z., Wang, D., 2011. Assessing the effect of Separation Levee Project

on Chinese sturgeon (Acipensor sinensis) spawning habitat suitability in Yangtze River, China. Aquatic Ecology **45**, 255-266.

Wang, Z.J., Chen, Z.Y., 2009. Downstream Grain-Size Variation to Interpret River-Channel Process-Form in the Middle-Lower Yangtze River, China. Advances in Water Resources and Hydraulic Engineering **1-6**, 939-944.

Wang, Z.Y., Li, Y., He, Y., 2007c. Sediment budget of the Yangtze River. Water Resources Research **43**, W04401.

Ward, A.D., Haan, C.T., Barfield, B.J., 1977. The performance of sediment detention structures Proceedings of the international symposium on urban hydrology, hydraulics and sediment control Lexington, KY: University of Kentucky pp. 58-68.

Watters, G.T., 1996. Small dams as barriers to freshwater mussels (Bivalvia, Unionoida) and their hosts. Biological Conservation **75**, 79-85.

Wei, Q., Ke, F.e., Zhang, J., Zhuang, P., Luo, J., Zhou, R., Yang, W., 1997. Biology, fisheries, and conservation of sturgeons and paddlefish in China. Environmental Biology Of Fishes **48**, 241-255.

Wellmeyer, J.L., Slattery, M.C., Phillips, J.D., 2005. Quantifying downstream impacts of impoundment on flow regime and channel planform, lower Trinity River,

Texas. Geomorphology **69**, 1-13.

Wetlands International, 2002. Ramsar Database (RDB). In: W. International (Ed.), Wageningen, The Netherlands.

Wetzel, R.W., 1990. Land-water interfaces: Metabolic and limnological regulators. Verh Internat Verein Limnol **24**, 6-24.

White, W., 2001. Evacuation of Sediments from Reservoirs. Thomas Telford, London, 260 pp.

White, W.R., 2000. Flushing of sediments of reservoirs: Working Paper of the World Commission on Dams, Thematic Review: Operation, Monitoring and Decommissioning of Dams. World Commission on Dams, Vlaeberg, Cape Town, South Africa.

Williams, G.P., Wolman, M.G., 1984. Downstream effects of dams on alluvial rivers, US Geological Survey professional paper. US Government Printing Office, Washington DC, USA, pp. 83.

Williams, J.R., 1975. Sediment routing for agricultural watersheds. Journal Of The American Water Resources Association **11**, 965-974.

Willis, C.M., Griggs, G.B., 2003. Reductions in fluvial sediment discharge by coastal dams in California and implications for beach sustainability. The Journal of

Geology **111**, 167-182.

Wofford, J.E., Gresswell, R.E., Banks, M.A., 2005. Influence of barriers to movement on within-watershed genetic variation of coastal cutthroat trout. Ecological Applications **15**, 628-637.

Wright, S.A., Anderson, C.R., Voichick, N., 2009. A simplified water temperature model for the Colorado River below Glen Canyon Dam. River Research and Applications **25**, 675-686.

Wu, J.G., Huang, J.H., Han, X.G., Gao, X.M., He, F.L., Jiang, M.X., Jiang, Z.G., Primack, R.B., Shen, Z.H., 2004. The Three Gorges Dam: an ecological perspective. Frontiers in Ecology and the Environment **2**, 241-248.

Wu, J.G., Huang, J.H., Han, X.G., Xie, Z.Q., Gao, X.M., 2003. Three-Gorges Dam - Experiment in habitat fragmentation? Science **300**, 1239-1240.

Wu, Z., Hu, M., Zeng, W., Ding, X., 2006. Fish. In: X. Liu, S. Fan, H. Hu (Eds.), Comprehensive and scientific survey of Jiangxi Nanjishan Wetland Nature Reserve. China Forestry Publishing House, Beijing, pp. 109-125.

Xiang, L., Lu, X.X., Higgitt, D.L., Wang, S.M., 2002. Recent lake sedimentation in the middle and lower Yangtze basin inferred from (137)Cs and (210)Pb measurements. Journal Of Asian Earth Sciences **21**, 77-86.

Xiang, Z.A., Zhou, G.Y., 1986. An analysis of sediment transport in the Changjiang River. Sediment Information **22**, 8-13.

Xie, P., 2003. Three-Gorges Dam: Risk to ancient fish. Science **302**, 1149-1149.

Xie, P., Chen, Y., 1999. Threats to biodiversity in Chinese inland waters. Ambio, 674-681.

Xu, J., 2004. Response of Erosion and Sediment Producing Processes to Soil and Water Conservation Measures in the Wudinghe River Basin. Acta Geographica Sinica **59**, 972-981.

Xu, J., Yang, D., Yi, Y., Lei, Z., Chen, J., Yang, W., 2008. Spatial and temporal variation of runoff in the Yangtze River basin during the past 40 years. Quaternary International **186**, 32-42.

Xu, J.X., 2005. Variation in grain size of suspended load in upper Changjiang River and its tributaries by human activities Journal of Sediment Research **29**, 8-16.

Xu, K., Milliman, J.D., 2009. Seasonal variations of sediment discharge from the Yangtze River before and after impoundment of the Three Gorges Dam. Geomorphology **104**, 276-283.

Xu, K., Milliman, J.D., Yang, Z., Wang, H., 2006. Yangtze sediment decline partly

from Three Gorges Dam. EOS, Transactions, American Geophysical Union **87**, 185-196.

Xu, K.H., Milliman, J.D., Yang, Z.S., Xu, H., 2007. Climatic and Anthropogenic Impacts on the Water and Sediment Discharge from the Yangtze River (Changjiang), 1950-2005. In: A. Gupta (Ed.), Large Rivers: Geomorphology and Management. John Wiley & Sons, pp. 609-626.

Xu, Q.X., 2007. Research on the variation of sediment transport regularity and affecting factors in the upper Yangtze reaches. PhD thesis, Wuhan University, Wuhan, China, 265 pp.

Xu, Q.X., 2012. Research on reservoir sedimentation and downstream channel erosion of dam after impoundment of the Three Gorges Reservoir. The Yangtze River **43**, 1-6.

Yan, Y., Wang, S., Chen, J., 2011. Spatial patterns of scale effect on specific sediment yield in the Yangtze River basin. Geomorphology **130**, 29-39.

Yang, H., Zehnder, A.J., 2005. The south-north water transfer project in China: An analysis of water demand uncertainty and environmental objectives in decision making. Water International **30**, 339-349.

Yang, S., Milliman, J., Xu, K., Deng, B., Zhang, X., Luo, X., 2014. Downstream

sedimentary and geomorphic impacts of the Three Gorges Dam on the Yangtze River. Earth-science Reviews **138**, 469-486.

Yang, S.L., Gao, A., Hotz, H.M., Zhu, J., Dai, S.B., Li, M., 2005a. Trends in annual discharge from the Yangtze River to the sea (1865-2004). Hydrological Sciences Journal-journal Des Sciences Hydrologiques **50**, 825-836.

Yang, S.L., Milliman, J.D., Li, P., Xu, K., 2011. 50,000 dams later: Erosion of the Yangtze River and its delta. Global and Planetary Change **75**, 14-20.

Yang, S.L., Zhang, J., Xu, X.J., 2007. Influence of the Three Gorges Dam on downstream delivery of sediment and its environmental implications, Yangtze River. Geophysical Research Letters **34**, L10410.

Yang, S.L., Zhang, J., Zhu, J., Smith, J.P., Dai, S.B., Gao, A., Li, P., 2005b. Impact of dams on Yangtze River sediment supply to the sea and delta intertidal wetland response. Journal of Geophysical Research-Earth Surface **110**, F03006.

Yang, S.L., Zhao, Q.Y., Belkin, I.M., 2002. Temporal variation in the sediment load of the Yangtze river and the influences of human activities. Journal of Hydrology **263**, 56-71.

Yang, X.K., Lu, X.X., 2013a. Delineation of lakes and reservoirs in large river basins: an example of the Yangtze River Basin, China. Geomorphology **190**, 92-102.

Yang, X.K., Lu, X.X., 2013b. Ten years of the Three Gorges Dam: a call for policy overhaul. Environmental Research Letters **8**, 041006.

Yang, X.K., Lu, X.X., 2014a. Drastic change in China's lakes and reservoirs over the past decades. Scientific Reports **4**, 6041.

Yang, X.K., Lu, X.X., 2014b. Estimate of cumulative sediment trapping by multiple reservoirs in large river basins: An example of the Yangtze River basin. Geomorphology **227**, 49-59.

Yang, Z., Wang, H., Saito, Y., Milliman, J.D., Xu, K., Qiao, S., Shi, G., 2006. Dam impacts on the Changjiang (Yangtze) River sediment discharge to the sea: The past 55 years and after the Three Gorges Dam. Water Resources Research **42**, W04407.

Yin, Z.J., Huang, W., Chen, J., 2011. Research on ecological operation framework for large reservoirs in the Yangtze River Basin. Yangtze River **42**, 60-63.

Yuan, D., 1997. Rock desertification in the subtropical karst of south China. Gerbüder Borntraeger **108**, 81-90.

Yuan, W., 2014. The fluvial dynamic process and the river-channel evolution of the Middle Yangtze after 3-Gorges Dam closure: prediction of new sediment source to estuary. PhD, East China Normal University, Shanghai, China, 215

pp.

Zhai, Y.W., Liu, C.W., Zhai, X.X., 2013. Research on Main Problems and their
Countermeasures on Chinese Small Hydropower Development. Applied
Mechanics and Materials **295**, 1889-1893.

Zhang, G., Wu, L., Li, H., Liu, M., Cheng, F., Murphy, B.R., Xie, S., 2012a.
Preliminary evidence of delayed spawning and suppressed larval growth and
condition of the major carps in the Yangtze River below the Three Gorges
Dam. Environmental Biology Of Fishes **93**, 439-447.

Zhang, L., Dawes, W., Walker, G., 2001. Response of mean annual evapotranspiration
to vegetation changes at catchment scale. Water Resources Research **37**,
701-708.

Zhang, L.P., Xia, J., Hu, Z.F., 2009. Situation and problem analysis of water resources
security in China. Resources and Environment in the Yangtze Basin **18**,
116-120.

Zhang, Q., 2009. The South-to-North Water Transfer Project of China: Environmental
Implications and Monitoring Strategy1. JAWRA Journal of the American
Water Resources Association **45**, 1238-1247.

Zhang, Q., Zhou, Y., Singh, V.P., Chen, X., 2012b. The influence of dam and lakes on

the Yangtze River streamflow: long-range correlation and complexity analyses. Hydrological Processes **26**, 436-444.

Zhang, X., Gao, X., Wang, J.W., Cao, W.X., 2015. Extinction risk and conservation priority analyses for 64 endemic fishes in the Upper Yangtze River, China. Environmental Biology Of Fishes **98**, 261-272.

Zhang, X.B., Zhang, Y.Y., Wen, A.B., Feng, M.Y., 2003. Assessment of soil losses on cultivated land by using the Cs-137 technique in the Upper Yangtze River Basin of China. Soil & Tillage Research **69**, 99-106.

Zhao, R., Zhao, H., Yan, X.R., 1991. Structure and features of lake database of China. Journal of Lake Sciences **3**, 67-73.

Zhao, X., Barlow, J., Taylor, B.L., Pitman, R.L., Wang, K., Wei, Z., Stewart, B.S., Turvey, S.T., Akamatsu, T., Reeves, R.R., 2008. Abundance and conservation status of the Yangtze finless porpoise in the Yangtze River, China. Biological Conservation **141**, 3006-3018.

Zhou, G.Y., Goel, N.K., Bhatt, V.K., 2002. Stochastic modelling of the sediment load of the upper Yangtze River (China). Hydrological Sciences Journal-journal Des Sciences Hydrologiques **47**, 93-105.

Zhou, J., Zhao, Y., Song, L., Bi, S., Zhang, H., 2014. Assessing the effect of the Three

Gorges reservoir impoundment on spawning habitat suitability of Chinese sturgeon (Acipenser sinensis) in Yangtze River, China. Ecological Informatics **20**, 33-46.

Zhu, Y., Zhang, H., Chen, L., Zhao, J., 2008. Influence of the South–North Water Diversion Project and the mitigation projects on the water quality of Han River. Science Of The Total Environment **406**, 57-68.

Ziemer, R.R., 1994. Cumulative effects assessment impact thresholds: myths and realities. In: A.A.o.P. Biologists (Ed.), Proceedings: Cumulative Effects Assessments in Canada: From Concept to Practice, Edmonton, Canada, pp. 319-326.

Zong, Y., Chen, X., 2000. The 1998 flood on the Yangtze, China. Natural Hazards **22**, 165-184.

Appendix

List of publications

Journal papers

1. Lu, X.X., **Yang, X.K.**, Li, S.Y., 2011. Dam not sole cause of Chinese drought. Nature 475, 174-174.

2. Ran, L., Lu, X.X., **Yang, X.K.**, 2012. Mindset change needed for China's water crisis. AMBIO: A Journal of the Human Environment 41, 216-218.

3. Ran, L.S., Lu, X.X., Xin, Z.B., **Yang, X.K.**, 2013. Cumulative sediment trapping by reservoirs in large river basins: A case study of the Yellow River basin. Global and Planetary Change 100, 308-319.

4. **Yang, X.K.**, Lu, X.X., 2013. Delineation of lakes and reservoirs in large river basins: an example of the Yangtze River Basin, China. Geomorphology 190, 92-102.

5. **Yang, X.K.**, Lu, X.X., 2013. Estimate of cumulative sediment trapping by multiple reservoirs in large river basins: An example of the Yangtze River basin. Geomorphology 227, 49-59.

6. **Yang, X.K.**, Lu, X.X., 2013. Ten years of the Three Gorges Dam: a call for policy overhaul. Environmental Research Letters 8, 041006.

7. **Yang, X.K.**, Lu, X.X., 2014. Drastic change in China's lakes and reservoirs over the past decades. Scientific Reports 4, doi:10.1038/srep06041.

8. **Yang, X.K.**, Lu, X.X., 2014. Assessing the cumulative impacts of dams on river connectivity and fragmentation in the Yangtze River basin. Ecohydrology, under review.

Proceedings

1. **Yang, X.K.**, Lu, X.X., 2012. Model of water regulation in the Yangtze River Basin and its effects using remote sensing techniques. In: A.L. Collins, V. Golosov, A.J. Horowitz, X.X. Lu, M. Stone, D.E. Walling, X.B. Zhang (Eds.), Erosion and Sediment Yields in the Changing Environment. IAHS, Chengdu, China, pp. 235-243.

2. Lu, X.X., **Yang, X.K.**, Ran, L.S., 2012. Delineation of China's reservoirs and

lakes using remote sensing techniques. In: A.L. Collins, V. Golosov, A.J. Horowitz, X.X.L. Lu, M. Stone, D.E. Walling, X.B. Zhang (Eds.), Erosion and Sediment Yields in the Changing Environment. IAHS, Chengdu, China, pp. 20-28.